



This work is protected by copyright and other intellectual property rights and duplication or sale of all or part is not permitted, except that material may be duplicated by you for research, private study, criticism/review or educational purposes. Electronic or print copies are for your own personal, non-commercial use and shall not be passed to any other individual. No quotation may be published without proper acknowledgement. For any other use, or to quote extensively from the work, permission must be obtained from the copyright holder/s.

Comparison of Near-surface Geophysical Techniques in Forensic and Archaeological Investigations

James D. Hansen

Submitted for the degree of Doctor of Philosophy

Keele University

December 2016

This electronic version of the thesis has been edited solely to ensure compliance with copyright legislation and excluded material is referenced in the text. The full, final, examined and awarded version of the thesis is available for consultation in hard copy via the University Library

RE-SUBMISSION OF THESIS FOR A RESEARCH DEGREE**Part I. DECLARATION by the candidate for a research degree. To be bound in the thesis**Degree for which thesis being submitted **Doctor of Philosophy (PhD)**Title of thesis **Comparison of Near-surface Geophysical Techniques in Forensic and Archaeological Investigations****This thesis contains confidential information and is subject to the protocol set down for the submission and examination of such a thesis.****~~YES~~/NO [please delete as appropriate; if YES the box in Declaration Part II should be completed]**Date of submission **07/03/2016**

Original registration date

28/09/2009

(Date of submission must comply with Regulation 2D)

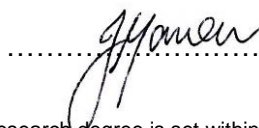
Name of candidate **James D Hansen**Research Institute **Faculty of Natural Sciences**Name of Lead Supervisor **Dr Jamie K Pringle**

I certify that:

- (a) The thesis being submitted for examination is my own account of my own research
- (b) My research has been conducted ethically. Where relevant a letter from the approving body confirming that ethical approval has been given has been bound in the thesis as an Annex
- (c) The data and results presented are the genuine data and results actually obtained by me during the conduct of the research
- (d) Where I have drawn on the work, ideas and results of others this has been appropriately acknowledged in the thesis
- (e) Where any collaboration has taken place with one or more other researchers, I have included within an 'Acknowledgments' section in the thesis a clear statement of their contributions, in line with the relevant statement in the Code of Practice (see Note overleaf).
- (f) The greater portion of the work described in the thesis has been undertaken subsequent to my registration for the higher degree for which I am submitting for examination
- (g) Where part of the work described in the thesis has previously been incorporated in another thesis submitted by me for a higher degree (if any), this has been identified and acknowledged in the thesis
- (h) The thesis submitted is within the required word limit as specified in the Regulations

Total words in submitted thesis (including text and footnotes, but excluding references and appendices)**41,854**

Signature of candidate

Date ...**02/06/2016**...**Note**

Extract from Code of Practice: If the research degree is set within a broader programme of work involving a group of investigators – particularly if this programme of work predates the candidate's registration – the candidate should provide an explicit statement (in an 'Acknowledgments' section) of the respective roles of the candidate and these other individuals in relevant aspects of the work reported in the thesis. For example, it should make clear, where relevant, the candidate's role in designing the study, developing data collection instruments, collecting primary data, analysing such data, and formulating conclusions from the analysis. Others involved in these aspects of the research should be named, and their contributions relative to that of the candidate should be specified (*this does not apply to the ordinary supervision, only if the supervisor or supervisory team has had greater than usual involvement*).

Abstract

Near-surface geophysical techniques should be routinely utilised by law enforcement agencies to detect and locate shallowly buried forensic objects, saving manpower and resources. However, there has been little published research on optimum geophysical detection method(s) and configurations beyond metal detectors and high frequency GPR.

This thesis firstly details systematic multi-frequency GPR surveys over simulated clandestine burials of murder victims in a semi-urban environment over a three year monitoring period. Wrapped burials could be detected throughout, though naked burials were more difficult to detect. It is suggested that detection of naked burials is possible within 18 months of presumed burial. 225 MHz frequency GPR antennae were deemed optimal for target detection and 2D profile analysis alone was deemed sufficient to target burials. Surveys conducted between winter and spring were deemed optimal for target detection.

This thesis next presents three U.K. case studies of church graveyards in contrasting burial environments, soil types, burial styles and ages. Geophysical survey results reveal that unmarked burials can be identified using 0.5 m spaced 2D GPR profiles using 225 MHz frequency antennae. Bulk ground electrical surveys showed 1 m probe separations were optimal, with datasets needed '*de-trending*' to reveal burial positions. Results were highly variable depending upon soil type; very coarse soils severely restricted successful detection of unmarked burials by resistivity. GPR therefore proved optimal, though resistivity data proved equally as useful as GPR in more clay-rich soils. Results, combined with subsequent archaeological investigations, showed targets were significantly different

from clandestine burials which are commonly used as analogues in forensic geophysics research.

This thesis finally presented multi-technique geophysical surveys to detect simulated unmarked illegal weapons, explosive devices and arms caches that were shallowly buried within a semi-urban environment test site. The site was then covered with a concrete patio before re-surveying in order to represent a common domestic household garden environment. Results showed that the easily-utilised magnetic susceptibility probe was, surprisingly, optimal for target detection in both semi-urban and patio environments in comparison to all other techniques trialled and, interestingly, compared to other magnetic equipment. Basic metal detector surveys had similar target detection rates though the handgun was not detected. High-frequency (900 MHz) GPR antennae was optimal for target detection in the semi-urban environment whilst 450 and 900 MHz frequencies had similar detection rates in the patio scenario. Resistivity surveys at 0.25 m probe- and sample-spacings were good for target detection in the semi-urban environment. 2D profiles were sufficient for target detection but resistivity datasets required site '*de-trending*' to resolve targets in map view.

Forensic geophysical techniques are shown here to be rapidly evolving to assist search investigators in the detection of hitherto difficult-to-locate buried forensic targets and, as such, further research in this field is suggested.

Contents	Page
Abstract	i
Acknowledgements	xxi
Chapter 1 - Thesis Introduction	1
1.1 Search	1
1.2 Forensic Geoscience	3
1.3 Forensic Geophysics	4
1.4 Thesis aims	5
Chapter 2 - Review of detection of forensic objects using geophysics	7
2.1 Introduction	7
2.2 Electromagnetic (EM) Techniques	8
2.2.1 <i>Ground Penetrating Radar (GPR)</i>	9
2.2.2 <i>Other EM techniques</i>	28
2.3 Electrical resistivity	31
2.4 Seismic methods	40
2.5 Magnetic methods	41
2.6 Geophysics as a forensic and archaeological search tool	44
2.7 Conclusions	46

Chapter 3 - Geophysical monitoring of simulated clandestine graves of murder victims using Ground Penetrating Radar: 0-3 years after burial	49
3.1 Introduction	49
3.2 Methodology	52
<i>3.2.1 Study site</i>	52
<i>3.2.2 Simulated clandestine graves</i>	53
<i>3.2.3 GPR data acquisition</i>	56
<i>3.2.4 GPR data processing</i>	59
3.3 Results	59
3.4 Discussion	71
3.5 Conclusions and further work	77
 Chapter 4 – GPR and bulk ground resistivity surveys in UK graveyards: Locating unmarked burials and geophysical best practice in contrasting soil types	 79
4.1 Introduction	79
4.2 Case study 1: St. James’ Church, Newchapel, Staffordshire, UK	84
<i>4.2.1 Case study 1: Background</i>	84
<i>4.2.2 Case study 1: Geophysical data collection and processing</i>	86
<i>4.2.3 Case study 1: Geophysical results</i>	90
<i>4.2.4 Case study 1: Archaeology excavation</i>	93
4.3 Case study 2: St. Luke’s, Endon, Staffordshire, UK	97
<i>4.3.1 Case study 2: Background</i>	97
<i>4.3.2 Case study 2: Geophysical data collection and processing</i>	98
<i>4.3.3 Case study 2: Geophysical results</i>	101

4.3.4 Case study 2: Archaeology excavations	104
4.4 Case study 3: St. John of Jerusalem, Hackney, North London, UK	107
4.4.1 Case study 3: Background	107
4.4.2 Case study 3: Geophysical data collection and processing	110
4.4.3 Case study 3: Geophysical results	111
4.4.4 Case study 3: Geophysical validation	113
4.5 Discussion	117
4.5.1 Identify the locations of any unmarked graves and/or burial plots/vaults within the respective survey areas. Identified remains could then be exhumed and re-interred elsewhere by archaeological teams (if necessary).	117
4.5.2 Compare GPR and resistivity geophysical equipment configurations and data acquisition strategies and processing methods to determine best practise.	118
4.5.3 Determine the effect of soil type	119
4.5.4 Quantify the variety of U.K. burial styles	120
4.6 Conclusion	122
 Chapter 5 - Comparison of magnetic, electrical and GPR to detect buried forensic objects in semi-urban and domestic patio environments	 124
5.1 Introduction	124
5.2 Methodology	127
5.2.1 Test site	127
5.2.2 Metal detector surveys	133
5.2.3 Magnetic susceptibility surveys	135
5.2.4 Fluxgate gradiometry surveys	137
5.2.5 Magnetic (potassium-vapour) gradiometry surveys	138

5.2.6 <i>Fixed-offset resistivity surveys</i>	139
5.2.7 <i>GPR surveys</i>	140
5.3 Results	142
5.3.1 <i>Success detection scheme</i>	142
5.3.2 <i>Metal detector</i>	144
5.3.3 <i>Magnetic susceptibility</i>	144
5.3.4 <i>Fluxgate gradiometry</i>	149
5.3.5 <i>Magnetic (potassium vapour) gradiometry</i>	152
5.3.6 <i>Electrical Resistivity</i>	157
5.3.7 <i>Ground penetrating radar</i>	161
5.4 Discussion	169
5.4.1 <i>Evaluate and find optimum magnetic detection technique(s) of the target buried material</i>	172
5.4.2 <i>Compare magnetic methods with electrical and GPR detection methods</i>	173
5.4.3 <i>Determine optimum GPR detection frequencies</i>	174
5.4.4 <i>Determine optimum respective equipment configuration(s) / survey specifications / optimum processing steps</i>	174
5.4.5 <i>Determine which technique(s) could determine target depth below ground level</i>	175
5.4.6 <i>Determine if different metal types could be distinguished</i>	176
5.5 Study limitations	177
5.5.1 <i>False measurement of the buried target positions</i>	177
5.5.2 <i>Data collection errors</i>	177
5.5.3 <i>Equipment limitations</i>	178
5.5.4 <i>Data processing effects</i>	178

5.6 Conclusions	179
 Chapter 6 - Discussion	 180
6.1 GPR	181
<i>6.1.1 2D GPR Profiles</i>	181
<i>6.1.2 GPR Timeslices</i>	185
6.2 Electrical resistivity	189
6.3 Other trialled geophysical methods	191
6.4 Study limitations	193
6.5 Integrated geophysical data	196
 Chapter 7 - Conclusions	 198
7.1 Key Outcomes	198
7.2 Recommendations for search teams	201
<i>7.2.1 Clandestine grave monitoring</i>	201
<i>7.2.2 Graveyards</i>	202
<i>7.2.3 Metals</i>	202
<i>7.2.4 All surveys</i>	203
 References	 204
 Appendices	 230

List of Figures	Page
Figure 1.1 Potential variety of search methods used for a target (in this case a grave), from Harrison & Donnelly (2009).	2
Figure 1.2. Schematic diagram showing suggested sequential search investigation best practice, for a clandestine grave in this case (from Harrison & Donnelly, 2009).	3
Figure 2.1. Schematic showing how GPR antennae passing over a buried object at positions 1, 2 and 3 produce a detectable response and hyperbola in a 2D profile. From Dupras <i>et al.</i> , (2006).	10
Figure 2.2. From Cassidy (2008) showing conductivity and relative permittivity for a range of subsurface materials.	14
Figure 2.3. From Cassidy (2008) showing the signal attenuation of an EM wave in a range of subsurface materials.	15
Figure 2.4. From Milsom and Eriksen (2011, p.197). The polar radiation patterns for transmitted GPR waves in both the H- and E-planes in (a) free space and (b) the ground with a permittivity of 4.	20
Figure 2.5. GPR 2D profile taken over a vault (marked). From Reynolds (2011).	25
Figure 2.6. GPR 2D profile across two pig graves in sandy soil, clearly discernable as the two noted anomalies (after Schultz <i>et al.</i> , 2006).	27
Figure 2.7. Schematic showing basic instrument operation EM (From Dupras <i>et al.</i> , 2006).	29
Figure 2.8. Example of an EM conductivity survey for a clandestine grave (marked) in a wooded environment. From Nobes (2000).	29

Figure 2.9. From Kvamme (2000). Map-view (a) plan of known graves and (b) 39
electrical resistivity contoured surface of the site, (c) courtesy of University of
Arkansas archaeological imaging lab.

Figure 2.10. ERI inversion 2D profile collected 78 days post-burial over a 40
simulated clandestine grave in a semi-urban environment. Modified from
Pringle *et al.*, (2008).

Figure 2.11. Bulk resistivity plot showing low-resistivity anomalies at the head 41
and foot of a pig grave (rectangle) interred six weeks previously (after Jervis *et*
al.,, 2009).

Figure 2.12. Magnetic susceptibility results (in SI dimensionless units, here 43
red indicates high values) over an Anglo-Saxon archaeological grave in East
Anglia (From Linfood, 2004.)

Figure 2.13. Detection strength of metallic firearms. From Dionne *et al.*, 45
(2011).

Figure 3.1. Four likely sequential decompositional stages of a clandestine 50
burial. (A) Recent burial, surface expression is most obvious. (B) Early
decomposition with search dogs and/or methane probes being optimal. (C) Late-
stage decomposition with conductive ‘leachate’ plume that should be resolved
by geophysical methods. (D) Final decomposition state that is the most difficult
to detect, GPR should locate. Modified from Pringle *et al.*, (2012b).

Figure. 3.2. (A) Map of survey area (dashed rectangle) with graves, lysimeter 54
positions and UK location map (inset). (B) Study site, (C) ‘naked pig grave’
and (D) ‘wrapped pig grave’ respectively. Modified from Pringle *et al.*,
(2012b).

Figure 3.3. Summary of monthly study site statistics of total rainfall (bars) and 55

average temperature (red line) data at 0.3 m bgl (below ground level), measured over the three-year study period. Modified from Pringle *et al.*, (2012b).

Figure 3.4. Site photographs showing (A) 110 MHz dominant frequency GPR antennae (with control PE 1000 equipment, laptop and 12 v leisure battery power source inset) and (B) 225 MHz dominant frequency antennae. 58

Figure 3.5. Key sequential processed 110, 225, 450 and 900 MHz dominant frequency GPR profiles that bisect the naked and wrapped pig ‘graves’ respectively (Fig. 3.2 for location) that include control profiles and data collected from 0 to 9 months after burial. Modified from Pringle *et al.*, (2012b). 63

Figure 3.6. Key sequential processed 110, 225, 450 and 900 MHz dominant frequency GPR profiles that bisect the naked and wrapped pig ‘graves’ respectively (Fig. 3.2 for location) that include data collected from 12 to 18 months after burial. Modified from Pringle *et al.*, (2012b). 64

Figure 3.7. Key sequential processed 110, 225, 450 and 900 MHz dominant frequency GPR profiles that bisect the naked and wrapped pig ‘graves’ respectively (Fig. 3.2 for location) that include data collected from 21 to 27 months after burial. Modified from Pringle *et al.*, (2012b). 65

Figure 3.8. Key sequential processed 110, 225, 450 and 900 MHz dominant frequency GPR profiles that bisect the naked and wrapped pig ‘graves’ respectively (Fig. 3.2 for location) that include data collected from 30 to 36 months after burial. Modified from Pringle *et al.*, (2012b). 66

Figure 3.9. 110 MHz frequency, quarterly GPR processed ‘time-slice’ datasets. Common amplitude scale shown in control dataset. Dotted squares indicate ‘graves’ (Fig. 3.2 for location). Modified from Pringle *et al.*, (2012b). 68

Figure 3.10. 225 MHz frequency, quarterly GPR processed ‘time-slice’ 69

datasets. Common amplitude scale shown in control dataset. Dotted squares indicate ‘graves’ (Fig. 3.2 for location). Modified from Pringle *et al.*, (2012b).

Figure 3.11. 450 MHz frequency, quarterly GPR processed ‘time-slice’ datasets. Common amplitude scale shown in control dataset. Dotted squares indicate ‘graves’ (Fig. 3.2 for location). Modified from Pringle *et al.*, (2012b).

Figure 3.12. Graphical timeline of targets detected by GPR over simulated graves (key shows relative anomaly strength). GPR results from Schultz and Martin (2012) and fixed-offset electrical resistivity results from Pringle *et al.*, (2012b) also shown for comparison. All graves in these studies were buried at 0.5 m bgl.

Figure 4.1. Generalised schematics of (A) typical clandestine grave with temporal changes (modified from Pringle *et al.*, 2012a). (B) An isolated grave burial in a cemetery or graveyard, with (1) post-burial soil, (2) shaft, (3) coffin and (4) contents identified geophysical targets named by Conyers (2006).

Figure 4.2. Mapview of case study 1 with location map (inset). Proposed building foot-print, geophysical survey grid, trial GPR profile and grave positions shown (see key).

Figure 4.3. Photographs of case study 1 site, also showing (A) 225 MHz dominant frequency GPR and (B) bulk ground resistivity (0.5 m fixed-offset) data being collected. Note trial 2D GPR L1043 profile position over burial vault (Fig. 4.3) marked in (B).

Figure 4.4. Processed 2D GPR profile L1043 (Fig. 4.5 for location). Modified from Hansen and Pringle (2011).

Figure 4.5. Mapview of GPR absolute amplitude 0-80 ns time-depth slice with background map. White areas indicate where 2D profiles could not be

acquired. Modified from Hansen et al. (2014).

Figure 4.6. Map view of processed bulk ground resistivity data with background map. Modified from Hansen and Pringle (2011). **92**

Figure 4.7. Case study 1 summary of known and unknown grave/vault positions. Modified from Hansen et al. (2014). **93**

Figure 4.8. Case Study 1 archaeology excavation photographs of (A) single brick-lined grave H and (B) double brick lined family vault C with 0.5 m scale bars. See Table 4.4 for details. Modified from Cramp *et al.*, (2010). **96**

Figure 4.9. Map view of St. Luke's Church, Endon, Staffordshire study site with location map (inset). Proposed building footprint (red rectangle) position shown (see key). Modified from Hansen *et al.* (2014). **98**

Figure 4.10. Photographs of case study 2 site, also (A) 225 MHz dominant frequency GPR and (B) bulk ground resistivity 0.5 m (E1) and 1 m (E2) fixed-offset data being collected. Modified from Hansen *et al.* (2014). **100**

Figure 4.11. (A) Processed 2D GPR profile L45 (Fig. 4.12 for location) with suggested burial locations marked (arrows). Modified from Hansen et al. (2014). **101**

Figure 4.12. Mapview of GPR absolute amplitude 20-40 ns time-depth slice with background map. Modified from Hansen *et al.* (2014). **102**

Figure 4.13. Map view of the processed bulk ground resistivity (0.5 m fixed-offset) probe spacing dataset with background map. Modified from Hansen *et al.* (2014). **103**

Figure 4.14. Case study 2 summary of known and unknown grave/vault positions. Modified from Hansen *et al.* (2014). **104**

Figure 4.15. Case Study 2 archaeological excavation; (A) map, (B) G02 and; **106**

(C) G5/08 photographs of earth-cut graves with 0.5 m scale bars (modified from Sutherland 2012). See Table 4.5 for details. Modified from Hansen *et al.* (2014).

Figure 4.16. Mapview of case study 3 with location map (inset). Proposed building foot-print, geophysical survey grids, trial GPR profile and grave positions shown (see key). Modified from Hansen *et al.* (2014). 108

Figure 4.17. Photographs of case study 3 site of (A) Area 1 and (B) Area 2 with remnant headstone (inset). GPR and bulk ground resistivity 0.5/1 m fixed-offset data collection also shown. Modified from Hansen *et al.* (2014). 109

Figure 4.18. (A) Processed 2D GPR profile L11 from Area A and L23 from Area B (Fig. 4.19) with burial locations marked (arrows). Modified from Hansen and Pringle (2011). 111

Figure 4.19. Mapview of GPR absolute amplitude 9-35 ns time-depth slices with background map. Modified from Hansen *et al.* (2014). 112

Figure 4.20. Map view of the processed bulk ground resistivity (0.5 m fixed-offset) probe spacing dataset with background map. See respective area keys. Modified from Hansen and Pringle (2011). 114

Figure 4.21. Map view of the processed bulk ground resistivity (1 m fixed-offset) probe spacing dataset with background map. See respective area keys. Modified from Hansen and Pringle (2011). 115

Figure 4.22. Case study 3 summary of known and unknown grave/vault positions. Modified from Hansen *et al.* (2014). 116

Figure 4.23. Generalised schematic of burial styles encountered in the three case studies discussed. Modified from Hansen and Pringle (2011) 121

Figure 5.1. Photographs of the 5 m x 5 m forensic test site on campus showing 128

(a) semi-urban environment and (b) simulated domestic concrete patio scenario on same area with location map (inset). Survey tapes on survey lines are shown. 0,0 position for all surveys is SW corner.

Figure 5.2. Photographs of forensic buried test objects. (A) Domestic brick and; (B) metallic bolt/screw and plate control objects. (C) Three domestic stainless steel kitchen bread knives; (D) 1943 allied wooden-handled entrenchment tool (E) (left) WW2 allied hand grenade and (right) WW1 allied Mk.1 No.5 decommissioned hand grenade; (F) Colt Government Cup Replica .45 calibre automatic handgun with solid brass ammunition; (G) UK mortar ammunition box (containing 2 shell casings shown in H). (H) 1943 75 mm M18 shell and two WW2 smaller diameter spent shells; Table 5.2 for details. Modified from Hansen *et al.* (2013). **130**

Figure 5.3. Sitemap showing location of buried forensic objects (see key for details) for both semi-urban environment and patio scenarios (Fig. 5.2 for selected object photographs). Modified from Hansen *et al.* (2013). **132**

Figure 5.4. Photographs of geophysical equipment used in this study. (A) Bloodhound Tracker™ IV metal detector; (B) Bartington™ magnetic susceptibility probe MS.1 with 0.3 m diameter probe; (C) Geoscan™ FM-15 fluxgate gradiometer; (D) GSMP-40™ potassium vapour magnetic gradiometer with sensors 1 m vertically separated; (E) Geoscan™ RM15-D mobile probe resistivity meter and; (F) pulseEKKO™ 1000 GPR equipment (450 MHz dominant frequency, bistatic fixed-offset antennae). Modified from Hansen *et al.* (2013). **134**

Figure 5.5. Classification of target detection used in this study. **143**

Figure 5.6. Magnetic susceptibility selected 2D profiles for control, semi-urban **147**

and patio surveys with respective target positions marked. (a) Profile 9 (X $\frac{1}{4}$ 2 m) over target (6), single knife; (b) profile 12 (X $\frac{1}{4}$ 2.75 m) over target (8), First World War hand grenade; (c) profile 15 (X $\frac{1}{4}$ 3.5 m) over target (9), handgun; and (d) profile 18 (X $\frac{1}{4}$ 4.25 m) over target (10), ammunition box (all marked). Table 5.2 for details. Modified from Hansen *et al.* (2013).

Figure 5.7. Magnetic susceptibility processed, gridded and contoured map view **148**
data plots of (A) pre-burial control with interpreted isolated anomalies, with respect to background values, marked (see text); (B) post-burial semi-urban environment and; (C) post-burial patio garden environment respectively. Scale for (A) and (B) are the same. Table 5.2 for target descriptions. Modified from Hansen *et al.* (2013).

Figure 5.8. Fluxgate gradiometry selected 2D surveys profiles. (A) Profile 9 **150**
(X=2 m) over target (6) single knife; (B) profile 12 (X=2.75 m) over target (8) WW1 hand grenade; (C) profile 15 (X=3.5 m) over target (9) handgun and; (D) profile 18 (X=4.25 m) over target (10) ammunition box (all marked). See key for survey type and Table 5.2 for details. Modified from Hansen *et al.* (2013).

Figure 5.9. Fluxgate gradiometry processed, gridded and contoured map view **151**
data plots of (A) pre-burial control with interpreted isolated anomalies, with respect to background values, marked (see text); (B) post-burial semi-urban environment and; (C) post-burial patio garden environment respectively. Scale for (A) and (B) are the same. Table 5.2 for target descriptions. Modified from Hansen *et al.* (2013).

Figure 5.10. Potassium vapour gradiometry selected 2D survey profiles. (A/B) **154**
Profile 9 (X=2 m) over target (6) single knife; (C/D) profile 12 (X=2.75 m) over target (8) WW1 hand grenade; (E/F) profile 15 (X=3.5 m) over target (9)

handgun and; (G/H) profile 18 (X=4.25 m) over target (10) box (all marked).

See key for and Table 5.2 for details. Modified from Hansen *et al.* (2013).

Figure 5.11. K+ vapour gradiometry (in 1000 nT) processed, gridded and 155
contoured map-view plots using upper sensor, lower sensor and gradient for pre-
burial, post-burial semi-urban and patio environments (A-I, respectively).
Modified from Hansen *et al.* (2013).

Fig. 5.12. K+ vapour gradiometry (in 1000 nT) processed, detrended, gridded 156
and contoured map view plots using upper sensor, lower sensor and gradient for
pre-burial, post-burial semi-urban and pre-burial patio environments (A-I,
respectively). Modified from Hansen *et al.* (2013).

Figure 5.13. Post-burial, semi-urban, bulk ground-resistivity contour plots using 159
raw and detrended datasets with 0.25 (A and B respectively) m and 0.5 m (C
and D respectively) probe spacings. Note the relatively high anomalies
corresponding to the knife (6), handgun (9) and mortar shell (11). Modified
from Hansen *et al.* (2013).

Figure 5.14. Bulk-ground resistivity 2D profiles for selected targets using 0.25 160
m and 0.5 m probe separations. Note generally high resistivity anomalies
associated with targets with exception of 0.5 m probe survey over the
ammunition box (H). Modified from Hansen *et al.* (2013).

Figure 5.15. 450 MHz GPR normalised time-slices over the test site of (A) 163 -
control, (B) semi-urban and (C) patio environments respectively. Some 164
relatively high and relatively low amplitude anomalies correspond to target
positions. See Table 5.2 for target details. Modified from Hansen *et al.* (2013).

Figure 5.16. 900 MHz GPR time-slices over the test site of (A) control, (B) 165 -
semi-urban and (C) patio environments respectively. Some relatively high and 166

relatively low amplitude anomalies correspond to target positions. See Table 5.2 for target details. Modified from Hansen *et al.* (2013).

Figure 5.17. 450 MHz GPR processed selected 2D profiles. (A-C) Profile 9 (X=2 m) over target (6) single knife; (D-F) profile 12 (X=2.75 m) over target (8) WW1 hand grenade; (G-I) profile 15 (X=3.5 m) over target (9) handgun and; (J-L) profile 18 (X=4.25 m) over target (10) ammunition box for control, semi-urban and patio environment scenarios respectively (all marked). Table 1 for details. Modified from Hansen *et al.* (2013). **167**

Figure 5.18. 900 MHz GPR processed selected 2D profiles. (A-C) Profile 9 (X=2 m) over target (6) single knife; (D-F) profile 12 (X=2.75 m) over target (8) WW1 hand grenade; (G-I) profile 15 (X=3.5 m) over target (9) handgun and; (J-L) profile 18 (X=4.25 m) over target (10) ammunition box for control, semi-urban and patio environment scenarios respectively (all marked). Table 1 for details. Modified from Hansen *et al.* (2013). **168**

Fig. 5.19. Summary bar graph showing percentage total of target detection success rates for the different geophysical techniques trialled in semi-urban, patio and rural environments (see key). Note rural environment results are from Rezos *et al.*, (2010) and Dionne *et al.*, (2011) for metal detector and conductivity surveys respectively. Modified from Hansen *et al.* (2013). **169**

Fig. 6.1. Generalised schematic of burial styles encountered in the three case studies discussed. Modified from Hansen and Pringle (2011). **184**

Table 2.14. Generalised table to indicate potential of search techniques(s) success for buried target(s) assuming optimal equipment configurations. Note this does not differentiate between target size, burial depth and other important specific factors. Key: Good; Medium; Poor chances of success. The dominant sand/clay soil end-types are detailed where appropriate for simplicity. Modified from Pringle <i>et al.</i> , (2012a).	48
Table 3.1. Summary of GPR data collected during this study. ⁺ Burial date was 7 th December 2007. *ADD date based on average daily site temperatures at 0.3 m bgl (see text). [#] First GPR surveys were controls. Modified from Pringle <i>et al.</i> , (2012b).	57
Table 3.2. Survey parameters using each antenna frequency. ¹ A smaller grid, focused directly over the naked pig was initially surveyed using 900 MHz antennae up to 18 months after burial; then a single profile (L1) was acquired until the end of the survey period.	58
Table 3.3. Sequential GPR data processing steps used in this study.	60
Table 4.1. Summary of case study 1 expected burials (locations shown in Fig. 4.2).	85
Table 4.2. Sequential GPR data processing steps used in these studies. Note 2D profiles were interpreted for target anomalies after step 5.	87
Table 4.3. Sequential electrical resistivity data processing steps used in these studies.	90
Table 4.4. Relevant archaeological characteristics of the case study 1 excavated burials (after Cramp <i>et al.</i> , 2010a). Condition categories for human	95

remains: Good = bones complete, Fair = bones mostly complete, Poor = Bones incomplete and/or damage/erosion. Burial letter locations marked in Fig. 4.4.

*Note depths were on excavation after removal of 1.4 m topsoil. Modified from Hansen *et al.* (2014).

Table 4.5. Relevant archaeological characteristics of the case study 2 105
excavated burials. Individual conditions: Good = bones complete, Fair = bones mostly complete, Poor = bones incomplete and/or damage/erosion. Modified from Sutherland (2012).

Table 5.1. Summary statistics of geophysical data collected during the study. 129
Survey types are: (C) Control, (S) Semi-urban and (P) Patio environments respectively. Bgl = below ground level. Survey line spacings were 0.25 m unless otherwise stated.

Table 5.2. Description of buried forensic objects used in this study and their 131
known properties (photographs in Fig. 5.2). Object numbers refer to those in Fig. 5.3 and geophysical datasets.

Table 5.3. Summary of parameters used for each geophysical survey in this 135
study.

Table 5.4. Summary of data processing steps conducted in GMT. 137

Table 5.5. Stages of GPR processing according to the best practise methods 141
(see text).

Table 5.6. Classification of geophysical responses of targets (see text). 142

Table 5.7. Max. and/or min. mag. susc. values at targets for burial scenarios 146
using raw, detrended and normalised data. SU = semi-urban.

Table 5.8. Max. and/or min. (0.25/0.5m probe-spacing) resistance values using 158
raw, detrended and normalised data. SU = semi-urban.

Table 5.9. Max. and/or min. reflection amplitudes using each of non- 162
detrended, detrended and normalised 900 MHz GPR data.

Table 5.10. Max. and/or min. reflection amplitudes using each of non- 163
detrended, detrended and normalised 450MHz GPR data.

Table 5.11. Summary of technique success in semi-urban environment 170
scenario. ●=very good, ●=good, ●=weak and ○=no detection.

Table 5.12. Summary of technique success in the patio environment scenario. 171
●=very good, ●=good, ●=weak and ○=no detection.

Acknowledgements

First of all, I would like to thank my lead supervisor Dr Jamie Pringle for all of his support, advice and patience over the past few years. For the countless hours of reading and editing drafts of chapters and papers, for keeping me on course no matter how often I wanted to follow a tangent, and for all the times he has told me I *can* do this, I feel there is not enough time in the world to thank him. I could not have asked for a better mentor and friend throughout this difficult process, and I am forever indebted to him.

I would also like to thank the other members of staff who have been involved in making this research possible: my other supervisors, Jon Cassella and Ian Stimpson, for providing other essential advice and another perspective on my work throughout the process; Dr Nigel Cassidy for always taking the time to answer my many questions about geophysical theory and providing me with support; Prof. Graham Williams for helping to secure my funding after my initial source of funding was unforeseeably withdrawn; Ian Wilshaw and Richard Burgess for all their technical assistance; Ann Billington and the Office staff in Earth Sciences for all of their help with administration and the other behind-the-scenes work which helped to keep things running smoothly; Keele University for awarding me the Acorn research grant; and all of my colleagues in the research department for all constant advice and support.

In particular, I would like to thank my predecessor Dr John Jervis for taking the time to show me the ropes and teach me how to use all of the necessary hardware and software. Despite being under the constant pressure of writing up his own thesis, he has been a fountain of

knowledge and advice. I am, however, not so thankful for him setting the standard for PhD students in forensic geophysics so ridiculously high.

Following the Code of Practice recommendations, it is clearly stated in Chapter 3, section 3.1, that ‘this study developed from a project initiated by Jervis (2010), in which simulated clandestine graves using wrapped and unwrapped pigs were surveyed over a 2-year post-burial period by resistivity and GPR. Jervis (2010) focused on bulk-ground resistivity and, although GPR data were collected, it was not processed nor analysed. It was decided that the project should be continued up to three years in order to compare the GPR responses of the graves since burial, and to process and interpret the first two years of collected data which I have undertaken. John Jervis, Tim Millington, Malcolm Wright and Jamie Pringle are also acknowledged for creating the Keele test site detailed in Chapter 3.

Numerous Keele University undergraduate and postgraduate students have assisted in collecting geophysical data throughout this study. Laura Ore, Sarah Reid, Leanne Patrick and Emily Postlethwaite are thanked for field assistance for the Chapter 4 study. Jon Goodwin, Richard Cramp and Zoe Sutherland of Stoke-on-Trent Archaeology Service are thanked for providing archaeological expertise and data for the Chapter 5 studies. Kristopher Wisniewski, David Kitley, Oliver Good, Sam Evans and Claire Holland are thanked for Chapter 5 field assistance.

To name all of the people who have helped or influenced me in some way, I’m sure, would be a hefty tome in itself, but I am thankful to all of them. However, for his constant encouragement and wasted weekends spent proof-reading chapters, I cannot thank Lewis Mullholland enough. Finally, since day one of this PhD, I have shared the highs and lows

with my fellow students Steven Rogers, Helen Doherty and Rosie Smithells. Between looming deadlines and late-night rewrites, we have managed to get each other through, and even find time to enjoy the experience. For that, I'm sure they know I am grateful, and I know that in them I have found friends for life.

Chapter 1 – Introduction

1.1 Search

Search has been defined as ‘*the application & management of systematic procedures & appropriate detection equipment to locate specified targets*’ (Harrison & Donnelly, 2009).

Traditional law enforcement search methods involve large-scale searches with personnel ‘finger-tip/line searches’, often conducting trial-and error excavations of suspect areas (Pringle *et al.*, 2009). These methods are still used and can prove very effective; however, law enforcement planning searches now have many more methods to assist their work.

Currently in the U.K., a search strategist is involved at an early stage during a case investigation for target detection. They will decide upon ‘*the most cost effective way to achieve the minimum standard (resolution) required for a high probability of search success*’ (Harrison & Donnelly, 2009). In other countries a search may not be as methodical, investigations may not be standardised and a variety of techniques, experts and scientific rigour are undertaken, depending upon local experience (Larson *et al.*, 2011). Usually forensic search investigators will use a host of proven methods for detecting targets, which can include *scenario-based*, *feature focused*, *intelligence-led* and lastly *systematic Standard Operating Procedures (SOPs)*. *Scenario-based* will use available case intelligence and psychological profiling. *Feature focused* will identify physical landmarks that may have been used by the offender to relocate a burial site. *Intelligence-led* will be based on available case information (including covert surveillance) and lastly *SOPs* will provide a proven search strategy (Pringle *et al.*, 2012).

The Pringle *et al.* (2012) review paper details the variety of methods used to detect near-surface buried objects, once a search area has been delimited, these include remote sensing, geomorphology, geology and soil mapping, search dogs and metal detector teams. Harrison & Donnelly (2009) also illustrates this graphically (Fig. 1.1). After a site reconnaissance has been conducted and a conceptual model of the target(s) has been created (Harrison & Donnelly 2009), phased site investigations are undertaken. A schematic diagram of the search process is shown in Figure 1.2.

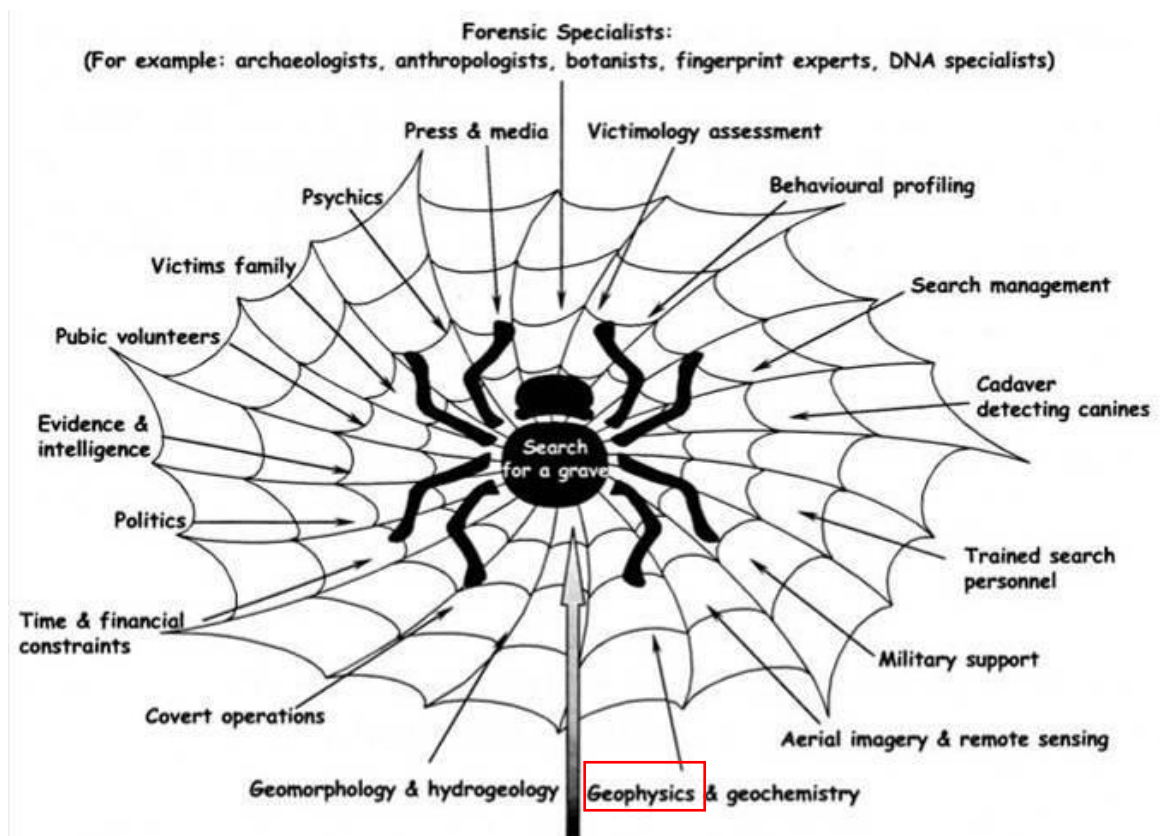


Figure 1.1. Potential variety of search methods used for a target (in this case a grave), from Harrison & Donnelly (2009).

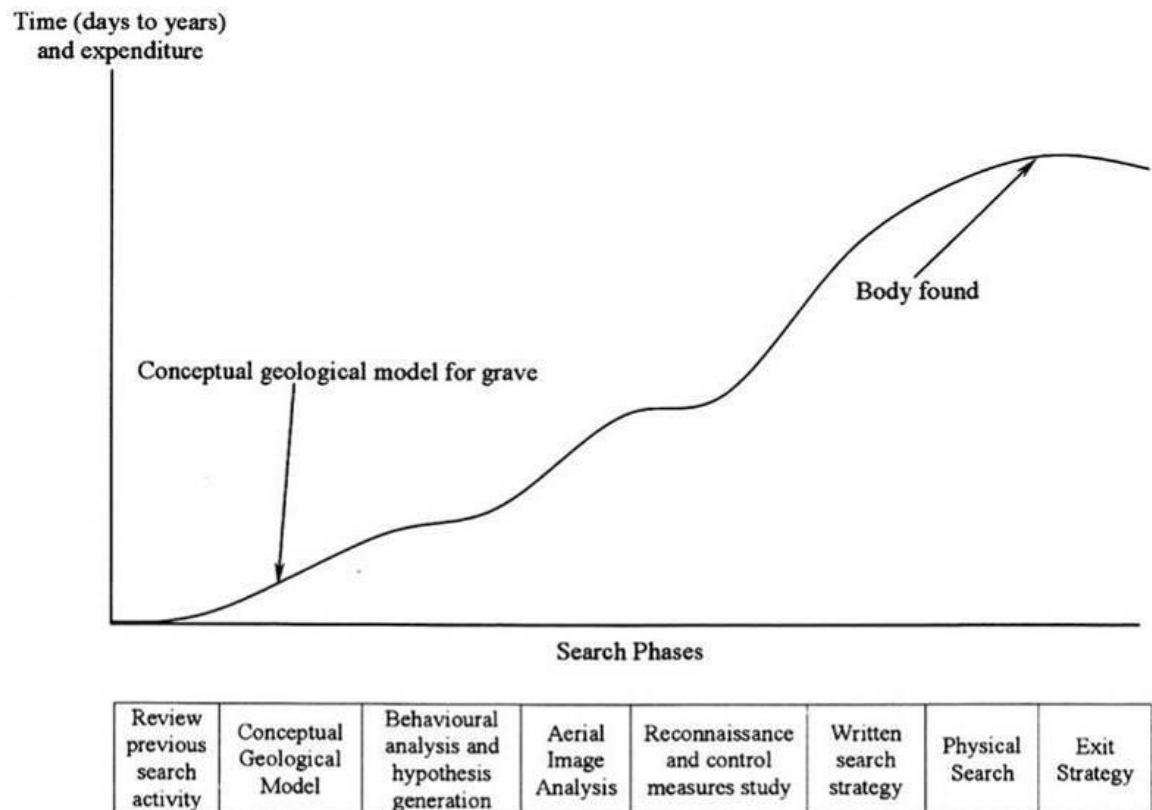


Figure 1.2. Schematic diagram showing suggested sequential search investigation best practice, for a clandestine grave in this case (from Harrison & Donnelly, 2009).

1.2 Forensic geoscience

Pye & Croft (2004) define forensic geoscience as “*the application of geoscience and wider environmental science techniques to investigations that could potentially be brought before a court of law*”. As such, it encompasses a number of sub-disciplines, such as forensic geology, forensic geophysics, forensic soil science, environmental forensics, forensic mapping, geomatics and remote sensing (Pringle *et al.*, 2012). There is also an overlap with related disciplines, such as forensic archaeology and forensic botany (Ruffell & McKinley, 2008), which has driven recent discussions on defining these varied scientific terms for clarification purposes (Ruffell, 2010).

Forensic geoscience is currently considered “*not only to be an emerging discipline that can bring significant benefits to policing, but an application of geoscience methods that can provide important results in environmental, humanitarian, military and engineering investigations*” (Pringle *et al.*, 2012). Geoscientific methods are being increasingly utilised and reported upon by forensic search teams for the detection and location of clandestinely buried material. In these situations, burials are usually shallow (less than 3 m below ground level or bgl). The forensic objects being searched for vary from illegally buried weapons and explosives, landmines and improvised explosive devices (IEDs), drugs and weapons caches to clandestine graves of murder victims and mass genocide graves (Pringle *et al.*, 2012).

1.3 Forensic Geophysics

Forensic geophysics has been defined as “*the application of geophysical methods related to legal investigations*” (Fenning & Donnelly, 2003) and “*the study of locating hidden objects or features that are underground or underwater*” (Dupras, 2006). It is being increasingly used a search tool for a variety of purposes, chiefly in criminal, civil, environment and humanitarian contexts. Typical targets include the search for clandestine graves, unmarked burials in graveyards and cemeteries, buried weapons or other items, illegally dumped waste and even disturbed ground (Pringle *et al.*, 2012). Many articles have been published regarding the search for near-surface targets (Pringle *et al.*, 2012). Advantages include that, typically, it is non-invasive, relatively rapid, and pinpoints likely areas for follow-up investigations.

1.4 Thesis aims

In the search for such near-surface objects, successful detection rates have varied. With GPR predominating as the tool of choice for forensic geophysicists, it is timely that scientific research is undertaken to improve current forensic detection rates by investigating common forensic near-surface targets. These have been chosen here to be; (1) the search for clandestine graves of murder victims (Chapter 3); (2) unmarked burials in graveyards and cemeteries (Chapter 4) and; (3) forensic metallic (typically weapons but also IEDs) targets (Chapter 5). The context of the following chapters is thus:

- Chapter 2 is a brief literature review of forensic search and of forensic geophysical methods in particular. Additional relevant literature is also reviewed at the beginning of each subsequent chapter.
- Chapter 3 details published results into a three year scientific monitoring study using ground penetrating radar (GPR) over simulated clandestine graves of murder victims. Temporal geophysical changes were documented with optimal antennae frequencies and data processing steps determined.
- Chapter 4 details results of GPR and electrical resistivity surveys of three U.K. church graveyards with contrasting soil types. Results showed optimal GPR antennae frequencies and resistivity probe separations as well as data processing steps with soil type deemed important. Two studies have subsequently been archaeologically excavated with results showing a variety of burial styles encountered.
- Chapter 5 shows published results into the use of forensic geophysical methods to detect small, near-surface buried objects in both a semi-urban and patio

environment. Optimal techniques, respective data processing and comparison to other studies were given.

- Chapter 6 is a discussion, in which the combined results of Chapters 3-5 are considered holistically.
- In Chapter 7, the thesis is concluded. The main results are summarised, and possible implications for search teams and some recommendations for future research are made.

Chapter 2 – A review of the detection of forensic objects using geophysics

This chapter briefly details the forensic geophysical methods commonly utilised in the detection of near-surface buried objects. More relevant references to the studies presented in subsequent chapters can be found in their respective chapter introductions.

2.1 Introduction

Forensic geophysics is a branch of forensic geology or *geoforensics* defined as ‘*the application of geophysical methods related to legal investigations*’ (Fenning & Donnelly, 2004). Though having gained popularity in this field over the past few decades, forensic geophysics is not limited to that of legal investigations. Geophysics has become a tool of engineering, archaeological and environmental investigation driving the development of many of the near-surface geophysical techniques used today (Pringle *et al.*, 2012a).

As early as the late 1800s there is anecdotal evidence for what can be considered forensic geoscience in China and India with the tracking of an accused criminal by footprints (Ruffell & McKinley, 2004). However, it wasn’t until the 20th century that geoscience came to be included in standard forensic practise; where in 1904 Georg Popp became the first scientist to present in court the evidence associated with soil found on the accused matching soil where his murdered victim was found (Murray & Tedrow, 1975). Since then, many criminal investigation establishments such as the Federal Bureau of Investigation (United States of America) and the now-closed U.K. Forensic Science Service had developed specialist laboratories capable of geological-type forensic science (Ruffell & McKinley, 2004).

Near-surface geophysics, that is to depths of around a maximum of ~30 m but in some cases as much as 300 m below ground level (Butler, 2006), has become a popular tool in archaeology whereby the subsurface can be visualised without the need for expensive and labour-intensive excavation (Conyers & Goodman, 1997). Near-surface geophysical techniques have also become a useful tool in engineering (Costello, 2007), environmental science (Ruffell & Kulesa, 2009 and Miller, 1996) and in humanitarian (Lopera & Milisavljevic, 2007 and Theera-Umpon, 2004) and military applications (Miller, 1996).

Some geophysical techniques have gained popularity in the field of geoforensics due to their success in the field of archaeology. These can be broadly divided into active and passive techniques. Active techniques are those in which a wave (electromagnetic or acoustic) is transmitted and the effects of the propagation material on the received signal are measured, whereas passive methods measure the inherent physical properties of the ground (Milsom & Eriksen, 2011). Here follows a brief introduction to the workings of these techniques, although a more comprehensive introduction into the physical phenomena can be found in references such as Cassidy (2008) and Reynolds (2011). Submerged (aquatic) searches are not considered here, though Parker *et al.* (2010) can be referred to for a useful review. More relevant literature to the case studies in this thesis is given in the respective introductions of Chapters 3 to 5.

2.2 Electromagnetic (EM) Techniques

Arguably, the most popular method of geophysical investigation for forensic and archaeological investigation has been in the form of electromagnetic (EM) surveys. The general principal of EM methods involves the transmission of an EM wave, which is

directed through a medium, usually rock or soil, and the remnant primary transmitted wave and any secondary waves produced from conductive objects are then measured (see Fig. 2.7 and Reynolds, 2011 for more detail). By examining the magnitude of any changes in the EM wave, and the spatial extent of these changes, interpretations can be drawn about the nature of the surveyed material.

2.2.1 Ground Penetrating Radar (GPR)

Ground penetrating radar (or GPR) is a form of EM geophysical technique, which is commonly-utilised in the search for clandestine graves, unmarked burials and for other buried objects (Pringle *et al.*, 2012a). EM waves are transmitted from an antenna and typically range from ~10 MHz to ~2 GHz (Cassidy, 2008 and Harrison & Donnelly, 2009), which propagate through the ground to a depth range of up to ~ 10 m bgl depending on local soil conditions (Fiedler *et al.*, 2009), and partially reflect where there are changes in bulk electrical properties, such as at soil horizons, rock-head or foreign objects. This is discussed in further detail later within this chapter.

A receiving antenna detects the returning, reflected waves and records their relative amplitude against arrival time since transmission. The pulse is transmitted and received at each sample point along a survey line and repeated at user specified rates to increase the signal to noise ratio. A 2D profile is subsequently created of distance along the survey line against two-way travel time (TWTT) which can then be converted to depth, either by obtaining an average propagation velocity through the ground or by analysing diffraction hyperbola in the data (see Milsom & Eriksen, 2011 and Reynolds 2011 for theoretical background and detail). Any near-surface variations in physical properties are typically

identifiable in 2D GPR profiles as $\frac{1}{2}$ hyperbolic reflections. This is due to the time taken for the EM wave to return to the antennae being minimal when transmitted from directly over the object, and taking progressively longer arrival times when further away from the object (Fig. 2.1).

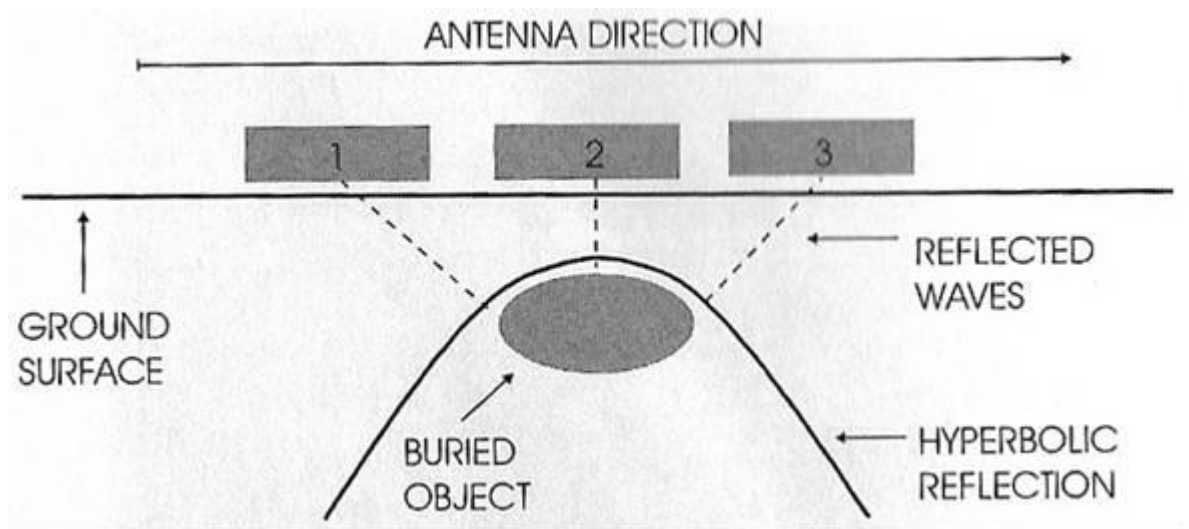


Figure 2.1. Schematic showing how GPR antennae passing over a buried object at positions 1, 2 and 3 produce a detectable response and hyperbola in a 2D profile. From Dupras *et al.* (2006).

In order to better understand how the properties of a material affect a propagating EM wave, one needs to first consider our current understanding of electrical and magnetic fields and their relationship. EM waves obey Maxwell's equations for EM fields, which quantitatively describe the interdependence between electric and magnetic fields, and which are valid for all frequencies of the EM spectrum as well as the energy storage and dissipation for all materials (Cassidy, 2008; Milsom and Eriksen, 2011). Maxwell's equations, as presented in their typical, time-domain, differential form are as follows:

Faraday's Law of Induction

$$\nabla \times E = -\frac{\partial B}{\partial t}$$

Maxwell's modified circuit Law

$$\nabla \times H = \frac{\partial D}{\partial t} + J$$

Gauss' theorem in electrostatics

$$\nabla \cdot D = \rho$$

Gauss' theorem in magnetostatics

$$\nabla \cdot B = 0$$

Where standard geophysical symbology are used to denote:

E = electric field strength (Volts per metre)

B = magnetic flux density (Tesla)

H = magnetic field strength (Amperes per metre)

D = electric flux density vector (Coulombs per metre squared)

J = current density (Amperes per metre squared)

ρ = charge density (Coulombs per metre cubed)

From these relationships, it is possible to derive the parameters for a material's EM properties:

electrical permittivity (ϵ - in Farads per metre);

$$D = \epsilon E$$

electrical conductivity (σ – Siemens per metre);

$$J = \sigma E$$

and magnetic permeability (μ - in Henrys per metre).

$$B = \mu H$$

Permittivity and conductivity are loosely termed as *dielectric* properties, that is, referring to a class of non-conducting materials that can allow an alternating EM field to propagate through them (Cassidy, 2008). In order to possess *dielectric* properties, and therefore be considered a true *dielectric*, a material must contain bound electric charges, for example those bound in a crystalline structure. A material which contains free electric charges (e.g. a fluid) will attenuate a propagating EM wave as these charges flow, resulting in a loss of energy. A material which possesses a high degree of free charges effectively acts as a conductor, where the majority of EM energy is lost as heat. EM methods are therefore ineffective in high-conductive environments such as saltwater environments or high-clay content soils (Cassidy, 2008), which are common in the UK.

Electric Permittivity (ϵ)

Electric Permittivity (ϵ) describes the ability of a material to store and release electric charge, and is commonly expressed as a *relative permittivity*:

$$\epsilon_r = \frac{\epsilon}{\epsilon_0}$$

Where:

ϵ_r = relative permittivity (dimensionless) in Faradays per metre (F/m)

ϵ = permittivity of a material

ϵ_0 = permittivity of a vacuum

Permittivity therefore also refers to the ability of a material to restrict the flow of free charges (Cassidy, 2008). An EM wave which propagates through a material causes previously unpolarised charges to become physically offset due to concentration of electrons on an atomic level. This induces a *dipole moment* in the material which is proportional to the strength of the applied electric field (E), with the constant of

proportionality being the permittivity (ϵ) (Cassidy, 2008). The leading and trailing edges of a propagating EM pulse supply energy to the separating charges in the form of acceleration which generates a small *displacement current* that produces radiating EM energy. As this localised energy is slightly out of phase with the incident pulse, the result is that the body of the wave is ‘slowed down’. Therefore, the permittivity is directly linked to the propagation velocity of the EM wave (Cassidy, 2008).

If separating charges are free to move (e.g. in free water), the displacement and polarisation process causes loss of EM energy in the conversion to heat. As such, the permittivity of a material can vary dramatically with the content and properties of fluids within them (Cassidy, 2008).

Electric Conductivity (σ)

Conductivity (σ) is the ability of a material to pass free electric charges under the influence of an applied field. In metals this refers to free electrons, whilst in fluids this refers to dissolved ions. As charge propagates via these electrons/ions, they collide, resulting in energy loss from the applied field as heat.

Magnetic Permeability (μ)

The magnetic effect of materials generally has little effect on the propagating GPR wave (Olhoeft, 1998) and their magnetic permeability is often simplified to the free-space value of 1.26×10^{-6} H/m (Cassidy, 2008). Generally, the amount of ferromagnetic material (typically <2%), which can have a considerable effect on GPR wave velocity and signal attenuation, is considered unimportant (Cassidy, 2008).

Material	Static conductivity, σ_s (mS/m)	Relative permittivity, ϵ_{ave}
Air	0	1
Clay – dry	1–100	2–20
Clay – wet	100–1000	15–40
Concrete – dry	1–10	4–10
Concrete – wet	10–100	10–20
Freshwater	0.1–10	78 (25 °C)–88
Freshwater ice	1–0.000001	3
Seawater	4000	81–88
Seawater ice	10–100	4–8
Permafrost	0.1–10	2–8
Granite – dry	0.001–0.00001	5–8
Granite – fractured and wet	1–10	5–15
Limestone – dry	0.001–0.0000001	4–8
Limestone – wet	10–100	6–15
Sandstone – dry	0.001–0.0000001	4–7
Sandstone – wet	0.01–0.001	5–15
Shale – saturated	10–100	6–9
Sand – dry	0.0001–1	3–6
Sand – wet	0.1–10	10–30
Sand – coastal, dry	0.01–1	5–10
Soil – sandy, dry	0.1–100	4–6
Soil – sandy, wet	10–100	15–30
Soil – loamy, dry	0.1–1	4–6
Soil – loamy, wet	10–100	10–20
Soil – clayey, dry	0.1–100	4–6
Soil – clayey, wet	100–1000	10–15
Soil – average	5	16

Figure 2.2. From Cassidy (2008) showing conductivity and relative permittivity for a range of subsurface materials.

EM wave propagation

The wave-front of an EM wave or “pulse” propagating through a conductive, dielectric medium can be represented by a series of propagating harmonic plane waves with $e^{i\omega t}$ dependence. Its propagation, velocity and impedance to propagation can be derived from the EM wave equations as follows (Cassidy, 2008):

Complex propagation constant (γ):

$$\gamma = \sqrt{(\sigma + j\omega\epsilon)j\omega\mu}$$

Velocity (v) in m/s:

$$v = \frac{c}{\left(\frac{\mu\epsilon}{2} \left[\sqrt{1 + \left(\frac{\sigma}{\omega}\right)^2} + 1 \right] \right)^{\frac{1}{2}}}$$

which can be simplified, based on the assumption that energy loss is negligible for low-conductivity materials, to:

$$v = \frac{c}{\sqrt{\epsilon\mu}}$$

Impedance of the medium (η in ohms):

$$\eta = \sqrt{\frac{j\omega\bar{\mu}}{\sigma + j\omega\bar{\epsilon}}}$$

Where:

c = the velocity of an electromagnetic wave in a vacuum

ω = angular frequency (Hz) = $2\pi f$

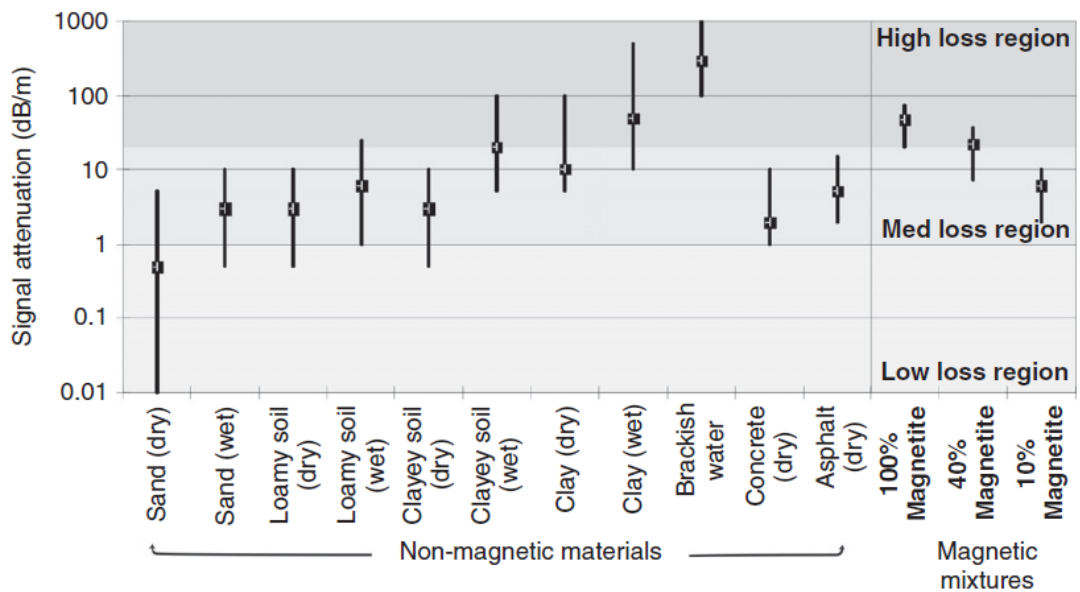


Figure 2.3. From Cassidy (2008) showing the signal attenuation of an EM wave in a range of subsurface materials.

Variations in physical properties of the subsurface therefore result in variations in electric conductivity (σ), electric permittivity (ϵ) and magnetic permeability (μ). However, as the effect of magnetic permeability is considered negligible, it is assumed that the propagation, attenuation and reflection of a wave are due to the effects of electrical conductivity and permittivity. Where a boundary occurs between two materials possessing differing electric conductivity and permittivity, a proportion (dependent upon the relative contrast in properties) of the wave energy is reflected, which can be detected by the receiving antenna, which forms the basis of GPR measurements. The greater the proportion of energy which is reflected from a surface, the greater the chance of the reflection being identifiable in the data. Additionally, the size, angle and nature of the reflective surface can influence the proportion of reflected wave energy (Milsom & Eriksen, 2011). Broad, smooth surfaces at right angles to the incident wave where reflection is mainly specular and directed back to the source produce the most likely chance of detection.

The maximum propagation depth into a medium is affected by *attenuation* (α in Np/m). This describes the loss of energy from the propagating wave-front due to factors including permittivity and conductivity and the frequency of the transmitted signal (Reynolds, 1997):

$$\alpha = \omega \sqrt{\mu \epsilon} \left(\frac{1}{2} \left[\sqrt{1 + \left(\frac{\sigma}{\omega \epsilon} \right)^2} - 1 \right] \right)^{\frac{1}{2}}$$

Attenuation increases with conductivity, which tends to have a greater contribution to attenuation than permittivity as it tends to vary over a greater range (Kearey, *et al.*, 2002). Conductive material, such as saturated, ion-rich soils tend to be more conductive, reducing the penetration depth of GPR (Reynolds, 2011). As such, the use of GPR may not be

entirely appropriate in soil environments such as saturated soil, saltwater environments and clay-rich soils.

Another important factor in GPR surveys is the ability to resolve subsurface features. One factor affecting the resolution of GPR data is the propagation velocity of the EM wave. With increasing velocity, the time spacing between reflections decreases, thereby reducing the vertical resolution (Davis & Annan, 1989). As previously discussed, the propagation velocity of the EM wave is affected by factors such as conductivity and permittivity, which depend strongly upon the saturation of the propagation material. As such, the soil type should be an important consideration when deciding upon the appropriateness of GPR for geophysical investigations.

The frequency of the transmitted wave is the most important factor in the resolving power of a survey (Milsom & Eriksen, 2011) as the bandwidth of a system increases with its frequency. For higher frequencies, reflected signals are shorter, allowing greater resolution of small features (Reynolds, 2011). A range of dominant antenna frequencies are available for use in geophysical investigations, though the majority of studies have concluded that a range of 100 MHz to 900 MHz are most common (France *et al.*, 1992; Koppenjan *et al.*, 2003; Fenning & Donnelly, 2004; Ruffell, 2005; Schultz *et al.*, 2006; Schultz *et al.*, 2008; Pringle *et al.*, 2012a). Generally, the rule of thumb is: *the larger the target, the lower the frequency*, and a range of 200 MHz to 500 MHz has proven most popular for resolving features associated with human burials (France *et al.*, 1992; Koppenjan *et al.*, 2003; Fenning & Donnelly, 2004; Ruffell, 2005; Schultz *et al.*, 2006; Schultz *et al.*, 2008). Ultimately, the choice of frequency should be based upon considerations for the subsurface conditions and the properties of the target (size and depth), as attenuation EM

energy is proportional to the frequency. Some studies suggest that different frequency antennae could be used within the same investigation to compliment data interpretation (Ruffell, 2005). The received wave must also be sampled at sufficiently small time intervals in order to gain an accurate representation of the waveform; if fewer than two samples are taken for each full period, then the data will suffer from *aliasing* (Milsom & Eriksen, 2011 and Booth & Pringle, 2016).

Lateral resolution of the data is dependent upon the parameters of the survey: namely the antenna separation, the distance between adjacent survey lines and the distance between sample points along a survey line. In order to resolve two laterally separated objects, the distance between sample points needs to be less than one quarter of the wavelength (λ in m) of the wave in the ground, given by (Cassidy, 2008 and Milsom & Eriksen, 2011):

$$\lambda = \frac{v}{f}$$

The majority of surveys maintain a fixed distance between the transmitting (T_x) and receiving antennae (R_x). This is known as *common-offset* profiling, and allows the user to assume that the reflected wave is received back at the source point, thereby avoiding any geometrical complications (Milsom & Eriksen, 2011). However, it is also possible to use a *common mid-point* profile, which involves separating the T_x and R_x by increasing distances about a mid-point and is mainly useful for gaining an estimation of the velocity of the wave in the subsurface material, which can be used in processing.

A common misconception held by non-specialists in geophysics is that GPR is a means of ‘*seeing*’ beneath the ground surface, and there is an expectation that the data will present an image of the physical features of the subsurface. In reality, the data represents a record

of the amplitude and time of EM waves detected by a receiving antenna over time, which can be plotted in such a way that it *approximately* represents the EM properties of the subsurface vertically beneath an acquisition point. The EM wave does not, of course, only propagate vertically beneath the source, but has a footprint which expands with depth. The signal also has a particular geometrical profile in both the H- and E-planes. Figure (2.4) shows these expressions in free space and in the ground, and indicates regions where there is zero energy. Where a feature is angled so that it is concordant with one of these null-regions, little or no energy will be reflected (Milsom & Eriksen, 2011), therefore the orientation of the antenna is an additional consideration for small or thin targets such as pipes or reinforcement bars (rebars) in concrete, and also whether the orientation is constant throughout a survey (Cassidy *et al.*, 2011).

Processing of data aims to manipulate the information in order to better represent physical features of the subsurface in terms of their relative position, dimensions and physical contrast to the surrounding material. Which processes to use, and how and when to use them, are often the cause of controversy and debate amongst GPR users. However, it is generally argued that no amount of processing can extract meaningful or useful information from poor quality data, therefore if something is not visible in raw data, it should be asked whether or not a feature is *really there*, or whether it is actually an artefact of the processing (Cassidy, 2008). The aim of processing should be to enhance the quality of raw data for interpretation, and to stop when nothing more can be gained from further manipulation (Cassidy, 2008).

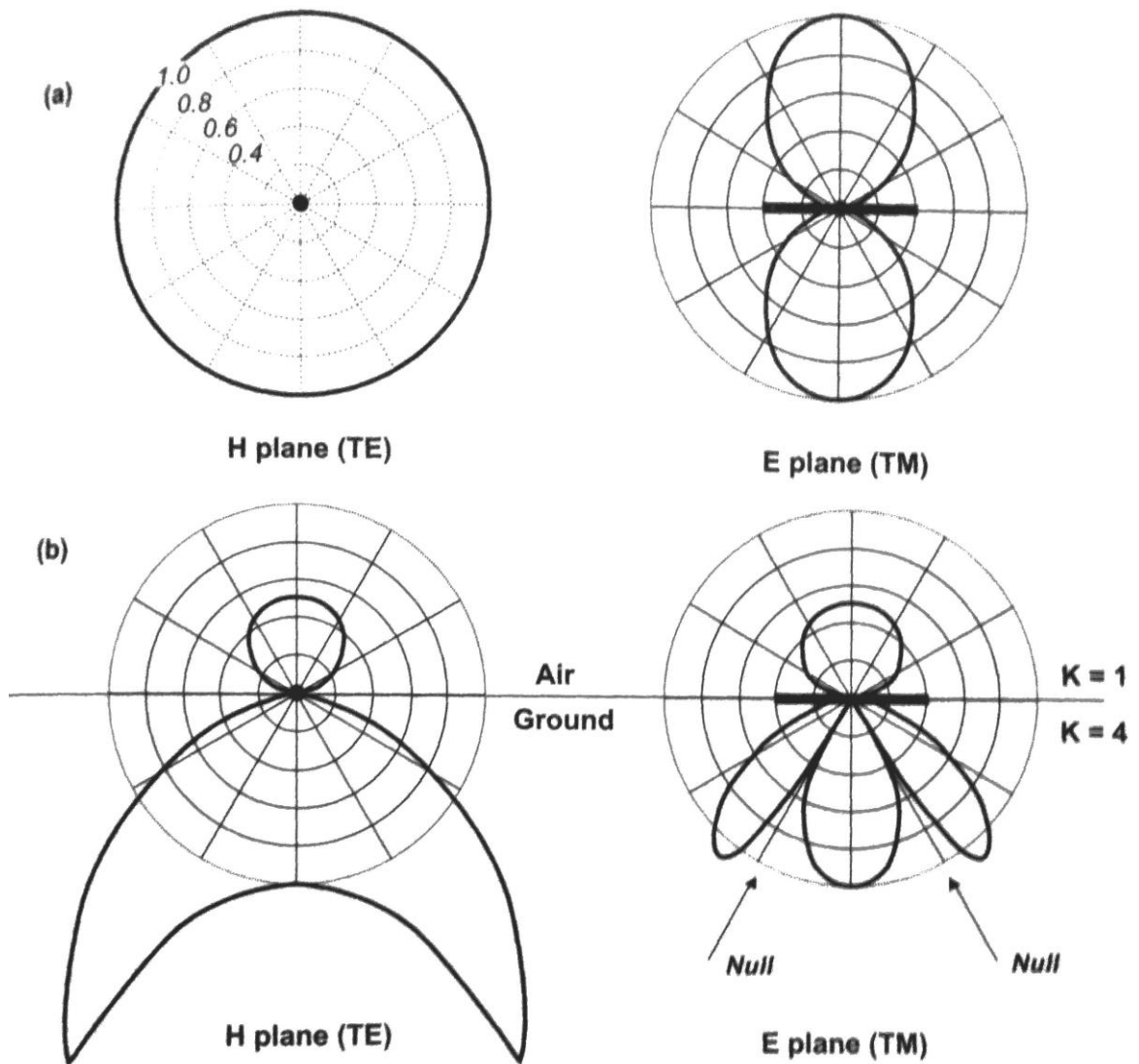


Figure 2.4. From Milsom & Eriksen (2011, p.197). The polar radiation patterns for transmitted GPR waves in both the H- and E-planes in (a) free space and (b) the ground with a permittivity of 4 F/m.

Enhancement of raw data, in practice, involves increasing the signal-to-noise ratio of the data. This should, ideally, strengthen coherent responses, producing an ‘image’ which seems a realistic and likely representation of the EM properties of the subsurface which can be used to interpret physical features (Cassidy, 2008). In doing so, however, data loses a lot of its value for quantitative analysis, and becomes more about qualitative

interpretation. Data is often filtered to remove horizontal features and make subtle, grave-related features more visible (Schultz *et al.*, 2006 and Schultz, 2008). Gain functions are often automatically applied to boost the amplitude on the trace with increasing time and thereby correct for the effect of signal attenuation with depth (Cassidy, 2008). Averaging of amplitudes on traces with those which are laterally adjacent produces a smoother lateral continuation of features. The processing steps used in the investigations of Chapters 3 to 5 of this thesis are discussed in further detail in their respective sections.

Ground Penetrating Radar (GPR) in forensic and archaeological investigations

Numerous investigations and studies have shown that forensic and archaeological targets provide a complex interaction of materials and structures which can produce detectable responses in EM investigations. In 1986, a USA serial murder investigation resulted in Project PIG (Pigs In Ground), whereby professionals from industry, academia and law enforcement worked together to compare multiple methods for the detection of buried pigs as a proxy for human remains (France *et al.*, 1992). France *et al.* (1992) stated that, of these techniques: “*GPR surveys offer the investigator the most useful tool to delineate possible graves*” though it was later recognised that this depended on favourable soil conditions (France *et al.*, 1997).

A surge of publications involving forensic GPR began in the late 1990s, possibly due to a combination of popularity and technical advancement. The technique allowed successful location of the buried victims of serial killers Frederick and Rosemary West in the UK in 1994 (Daniels, 2004). Media coverage led to GPR receiving major publicity and may have resulted in the greater use of GPR in criminal investigations which followed, sometimes where it was not appropriate (Watters & Hunter, 2004). Developments in GPR technology

resulted in the availability of small, more durable computer equipment, a greater range of antennae frequencies, shielded antennae and, arguably the most important development; the ability to record data digitally. This solved many of the problems faced by operators of the technique and allowed greater use of GPR (Ruffell *et al.*, 2009). An additional advantage of GPR over other geophysical surveying techniques is that the equipment is generally versatile, and can be applied to a number of different environments and surface conditions – e.g. under concrete (Ruffell *et al.*, 2014), beneath ice or snow (Davis *et al.*, 2000 and Instanes *et al.*, 2004) or even in freshwater environments such as lakes or ponds (Parker *et al.*, 2010).

In the 21st century, research had moved towards developing the understanding of how GPR is capable of detecting human remains and its limitations in such investigations. Hammon *et al.* (2000) computationally modelled the expected GPR response from human remains in different soil types, soil moisture contents, burial depths and using different antenna separations and radar frequencies. The results indicated differences in electric permittivity of organic tissue and surrounding soil were significant enough for the soil-tissue interface to create a detectable reflection in GPR profiles (Hammon *et al.*, 2000). The results also suggested that increasing soil clay content, soil moisture and burial depth will reduce the ability to detect this reflected wave due to increased signal attenuation. Additionally, results indicated that the high electrical conductivity of a cadaver would also result in rapid attenuation of the GPR signal, resulting in a loss of data from beneath it (Hammon *et al.*, 2000). In fact, if no response is detectable from the cadaver, as observed in at least one study (Calkin *et al.*, 1995), the signal attenuation could be responsible for a complete loss of reflection data. The data certainly indicates that there is no uniform GPR response from a burial, nor a guarantee that the target will be detected at all. For example, investigations

over unmarked graves (Bevan, 2001), known graves in cemeteries (Fenning & Donnelly, 2004) and historical burial plots (Vaughan, 1986 and King *et al.*, 1993) have shown that some graves may not produce any detectable response.

Generally, however, a burial is associated with strong hyperbolic reflectors in 2D GPR profiles (Fig. 2.5). Controlled studies and data from investigations has supported the models produced by Hammon *et al.* (2000), as strong hyperbolic reflectors were observed in data over a pig grave compared to weaker features in a control grave containing no body (Schultz *et al.*, 2006; Schultz *et al.*, 2008 and Pringle *et al.*, 2012b).

Miller *et al.* (2002) used GPR to investigate the effects of buried, decomposing, human targets over time and showed that changes in the geophysical response related to stages in body decomposition. Decomposition has a potential two-fold effect on the detectability of buried human or animal remains. Firstly, the bloating of the chest cavity due to the build-up of decompositional gases and eventual collapse will change the volume of a potentially detectable “void” in the subsurface; a large, bloated chest cavity provides a large volume of low conductivity and low permittivity gas, which provides a large contrast in EM properties with the surrounding soil medium which could be resolved even with relatively low frequency GPR (e.g. 110 MHz). Secondly, the release of ion-rich, conductive fluids due to decomposition of the cadaver can alter the EM properties of the surrounding soil.

In fact, other research and investigations suggest that GPR may be more successful in indirectly locating bodies due to the detectable change in the soil overlying the cadaver (Unterberger, 1992; Conyers, 2006; Schultz *et al.*, 2008 and Harrison and Donnelly, 2009). Generally, *undisturbed* soil is formed in laterally-continuous stratigraphic layers which

may have differing EM properties due to variations in physical properties such as porosity, moisture content, grain size and material. Where the contrast in dielectric conductivity and permittivity are significant, and the resolution of the GPR data is smaller than that of the strata thickness, a reflection can be detected in 2D profiles. *Disturbed* soil of the grave shaft has been cited as identifiable in vertical 2D GPR profiles (Hammon *et al.*, 2000 and Hilderbrand *et al.*, 2002) due to a number of features: “fill scattering” (Bevan, 2001); the presence of several, small hyperbolae in the position of the grave shaft is thought to be a consequence of disturbed soil. The previously compacted soil has been dug out and used to refill the grave, resulting in a less structured unit of material, where soil types are inter-mixed and the porosity character has been altered (Doolittle & Bellantoni, 2010). A different porosity affects the ability of the soil to retain conductive moisture, which provides a different conductivity and permittivity character for the grave soil compared to the surrounding *undisturbed* soil. Additionally, the grave shaft may be visible as a unit of soil which does not display the typical continuous reflectors of the surrounding, undisturbed soil (Conyers, 2006; Schultz *et al.*, 2006; Doolittle and Bellantoni, 2010). “Pull-up” features occur where there is a noticeable difference in the travel-time of some traces to a continuous reflector than is observed in the adjacent traces. This has been attributed to the increased propagation velocity of the wave-front through more porous, disturbed soil, resulting in a decreased two-way travel time of the wave (Unterberger, 1992). Eventual subsidence of the soil in the grave can result in concave features in above the cadaver (Doolittle and Bellantoni, 2010).

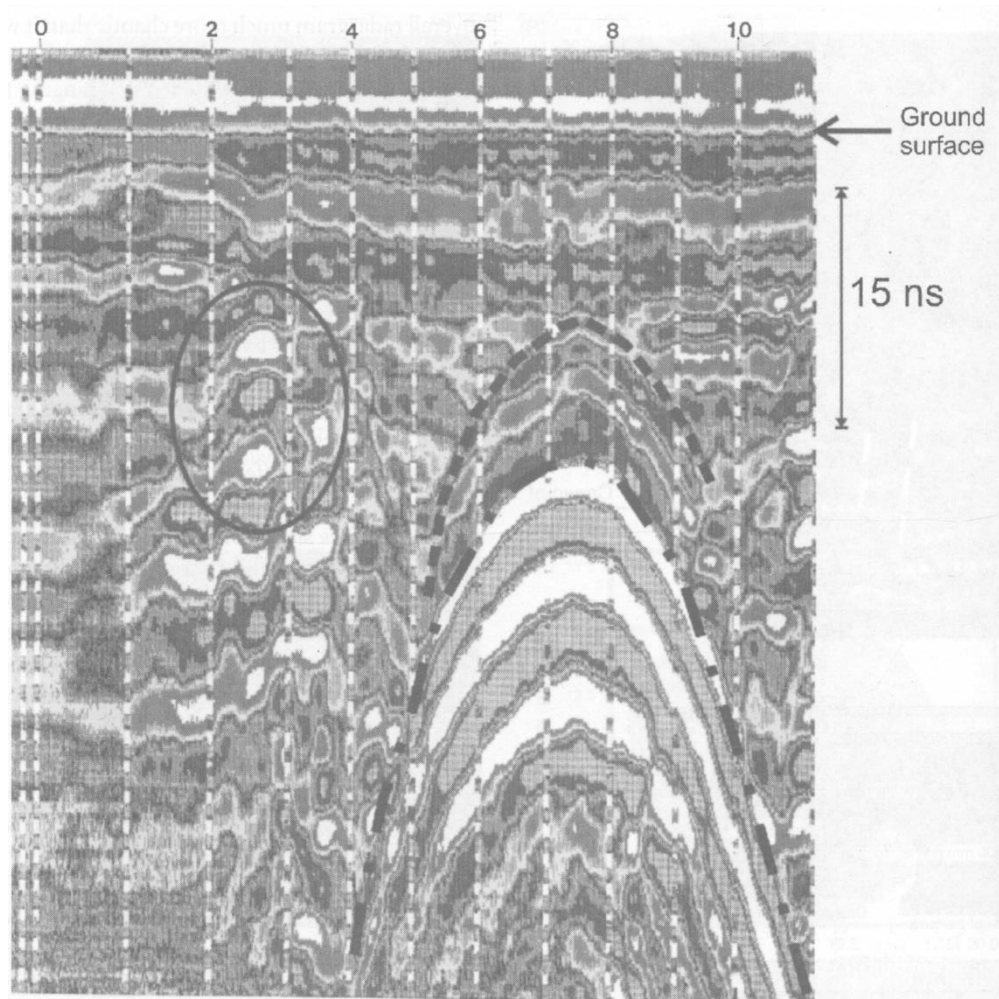


Figure 2.5. GPR 2D profile taken over a vault (marked). From Reynolds (2011).

One major issue for forensic geophysics in ‘real-world’ investigations is that the kind of homogeneous burial media studied in simulations is rarely encountered, therefore some investigators began experimenting with different soil types. Koppenjan *et al.* (2003) conducted monthly time-lapse GPR using 24 pig carcasses in two different soil environments: sandy soil and clay-rich soil overlain by ~1m of sandy soil (common soil in Florida, USA). The investigation was further varied by using two different pig sizes (~25 kg and ~65 kg) and at two different depths (~1.0 m or ~0.5 m). The difference in carcass size was found to have little effect on the appearance of anomalies in GPR profiles; however soil type was a major factor (Koppenjan *et al.*, 2003). Targets in sandy soil were

detectable for the duration of the 21-month study; however those buried in clay were much more difficult to distinguish, with the deepest buried (1.0 m) becoming undetectable after 9 months. Medium frequency antennae (500 MHz) were found to be preferential over high frequency (900 MHz). Schultz *et al.* (2006) also surveyed 12 pig burials (Fig. 2.6) over a period of either up to ~13 or ~21 months. The burials were also varied by depth and soil type (all within sandy soil topped by clay-rich soil, so that the shallowly buried pigs were in contact with the clay horizon). Some pigs were excavated to correlate the decompositions stage with the GPR response and it was discovered that pigs at all decomposition stages over the time period, even when completely skeletonised, were easily detectable. Pigs buried within the clay, however, were far more difficult to detect even when the carcasses retained extensive soft tissue.

There are, however, few control studies which assess the ability to detect remains for a significant time post-burial. Relatively long-term control studies and comparisons of responses from graveyards for burials of different ages do suggest, however, that the maximum strength of a GPR response for a burial will decrease over time, making target detection more difficult (Bevan, 1991; Koppenjan *et al.*, 2003; Ruffell *et al.*, 2009; Schultz *et al.*, 2011; Schultz *et al.*, 2012).

Despite these comparisons of soil types, all control investigations have included sandy soil as the major, if not only component of the burial medium. In the United Kingdom, however, soils are dominated by glacial deposits, which are characterised by a high clay content and inhomogeneity; two of the key properties which have been identified as limiting factors on the success of GPR investigations. Several studies suggested the

contrast between burials and surrounding clay soils may not be sufficient to detect burials (Hammon *et al.*, 2000).

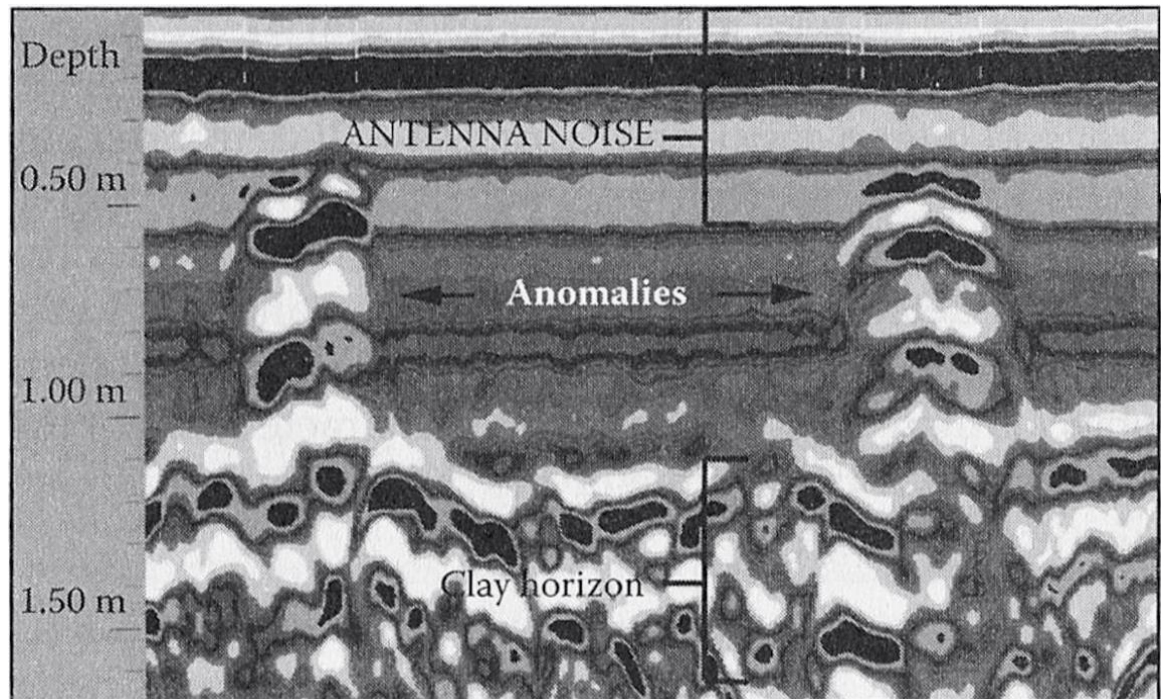


Figure 2.6. GPR 2D profile across two pig graves in sandy soil, clearly discernable as the two noted anomalies (after Schultz *et al.*, 2006).

Koppenjan *et al.*, 2003; Fenning & Donnelly, 2004) and that the “cluttered” nature of heterogeneous soils causes issues for target detection (Nobes, 2000). Through investigations on historical cemeteries in New Zealand, Nobes (2007) argues that graves can be difficult to distinguish from the sedimentary structures in sandy soils which dominate the GPR profiles. However, clay- or silt-rich soils are generally deposited in layers or massive units, allowing any disturbances due to burial to be easily distinguished. Therefore, GPR may still be suited to such investigations in the UK.

2.2.2 Other EM Techniques

There has been limited use of other Electromagnetic (EM) methods for forensic investigations (Bigman, 2012), which may seem surprising considering their relatively rapid survey rate (Pringle *et al.*, 2012a). The most commonly-utilised methods, however, have been measurements of conductivity. Frohlich & Lancaster (1986) undertook an electrical conductivity survey in Jordan to locate and characterise unmarked burials and tombs. Nobes (2000) documented the successful search for buried 12 year old human remains in a wood, initially by an electrical conductivity survey to identify anomalous areas, with follow-up investigations over suspect areas (Fig. 2.8). France *et al.* (1992) also found EM surveys could locate simulated clandestine burials of pig cadavers in the Western US. Witten *et al.* (2001) used an initial EMI survey to look for mass graves in Tulsa, USA, before follow-up magnetic and GPR investigations were undertaken. Pringle *et al.* (2008) conducted a controlled experiment in a UK urban garden environment and found conductivity surveys did not resolve the target pig grave. This was attributed to the local urban environment and ‘made ground’ nature of the site. Nobes (1999) also found drawbacks using EM methods to locate unmarked graves in a New Zealand cemetery, due to the difficulty in differentiating target-related anomalies from significant background effects caused by fence boundaries and local topography.

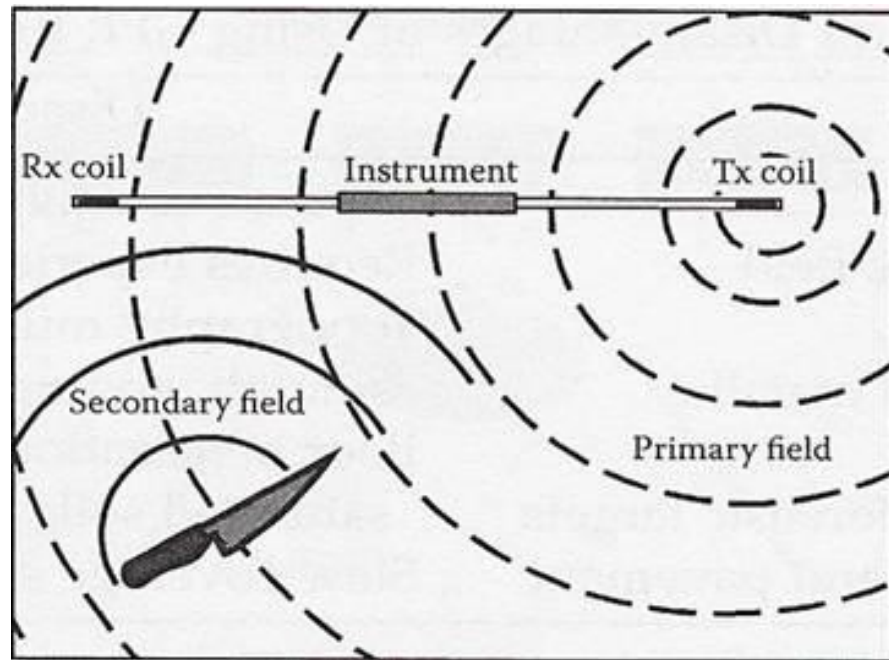


Figure 2.7. Schematic showing basic instrument operation EM (From Dupras *et al.*, 2006).

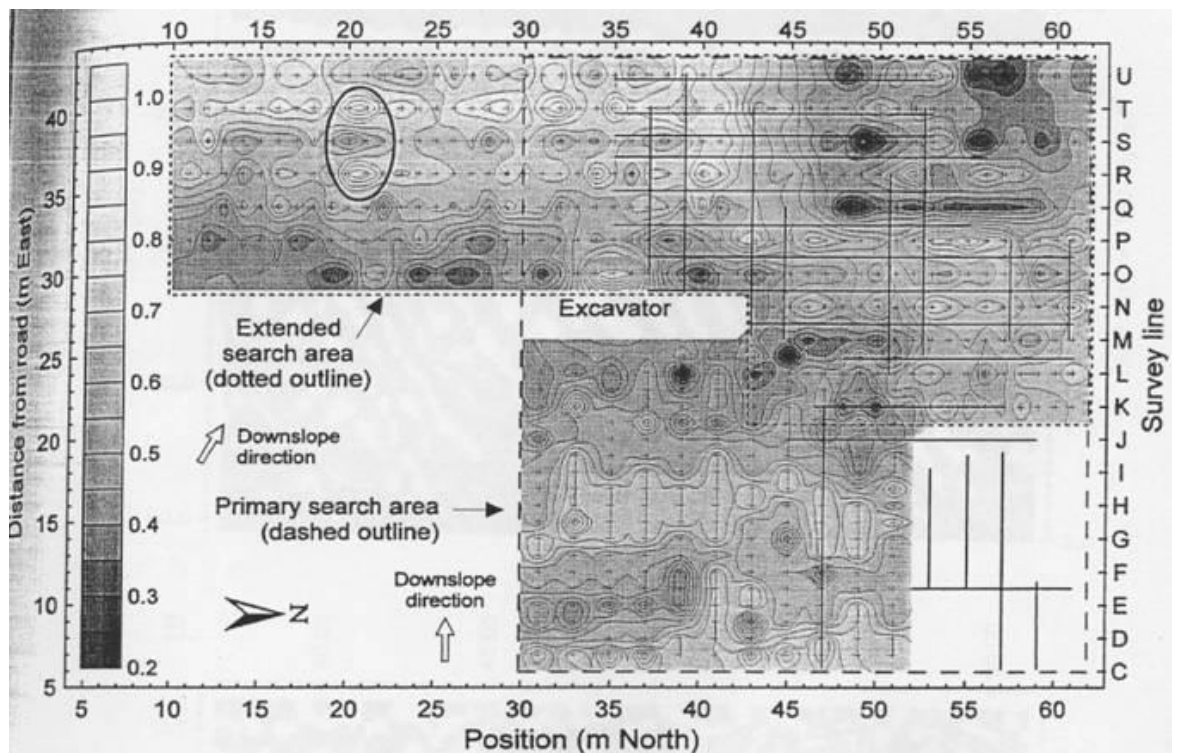


Figure 2.8. Example of an EM conductivity survey for a clandestine grave (marked) in a wooded environment. From Nobes (2000).

Saey *et al.* (2011) have shown that a combined EM induction sensor approach can be used to detect UXOs (Un-Exploded Ordnance devices) in former WWI battlefields in Belgium and high resolution time-domain EM surveys have also shown promise for UXO detection (Pasion *et al.*, 2007). Researchers have also used EM methods to detect landmines (Combrinck, 2001) and buried weapons in a controlled environment (Dionne *et al.*, 2011), although equipment resolution and background variations in soil type can make the detection of small targets problematic. EM survey equipment needs to not only be carefully calibrated to account for the bgl site conditions, but can also be significantly affected by above-ground conductive objects such as metal fences, electricity pylons, cars, etc. Such complications may preclude the use of EM equipment in certain search areas and environments, particularly urban areas (Milsom & Eriksen, 2011; Reynolds, 2011). EM surveys can be used for environmental forensic geophysical surveys (Reynolds, 2011), as the target is usually more conductive than background site materials. Bavusi *et al.* (2006) detail a case study in which an EM survey was used to characterise a waste dump in Southern Italy. Vaudelet *et al.* (2011) shows an urban contaminant case study characterising different source sites. As conductivity surveys using conventional instruments (such as the Geonics™ EM31 or EM38 [Geonics Ltd., Mississauga, Canada]) are orientation-dependent, they can focus on either the top 5–8 m bgl (using the horizontal model component or HMD) or up to 15 m bgl (using the vertical mode component data or VMD), depending upon the estimated depth of burial bgl and the local site ground conditions.

2.3 Electrical resistivity (ρ)

Ohm's law describes the proportional relationship between the current and voltage across a conductor when an electric field is applied:

$$R = \frac{V}{I}$$

Where:

R = Resistance (Ohms (Ω))

V = Voltage (Volts (V))

I = Current (amps (A))

The constant here is resistance (R), which describes the opposing force to the flow of current through a medium. Resistance is affected by the size of the conductor – a larger conductor will have a greater resistance. This means that the resistance of two materials cannot be directly compared unless they are the exact same size. Resistivity (ρ) in Ohm-metres (Ωm), however, takes the size of the conductor into account. It is, in essence, the resistance of a cubic metre of material to a current flowing between opposite faces (Milsom & Eriksen, 2011). Therefore the material's resistivity is an intrinsic property which can be directly compared with the resistivity of another material, which makes it particularly useful in geophysical surveying. Resistivity measurements in electrical applications generally involve measuring the current and voltage across a conductor (usually a wire) of known volume, and using the relationship:

$$\rho = \frac{RA}{l}$$

Where:

A = cross sectional area of conductor (m^2)

l = length of conductor (m)

In geophysical investigations, resistivity surveys are usually conducted by injecting an electrical current into the measured medium (e.g. soil) through probes or electrodes and subsequently measuring differences in the resulting potential field (Reynolds, 2011). This is known as a direct current (DC) injection, though the current is rarely unidirectional. Periodically reversing of the flow direction and taking an average value allows the effects of naturally-occurring, unidirectional currents to be eliminated (Milson & Eriksen, 2011).

The current can travel through a medium in two main ways: electronic conduction, the current carried by free electrons; and electrolytic conduction, the current carried by dissolved ions (Reynolds, 2011, p.420; Telford *et al.*, 1990, p.286). Current can also be carried by dielectric conduction; a result of polarisation of atoms in an alternating electric field, though these are typically small in comparison to electronic and electrolytic currents (Grant and Phillips, 1990, p.353).

For most subsurface materials, electric current is mainly carried by dissolved ions in the contained fluids as electrolytic conduction. The amount and arrangement of pore spaces, saturation and pore-fluid composition are therefore the most important properties in determining the electrical conductivity of soils and rocks (Friedman, 2005; Telford *et al.*, 1990, p.286).

Indeed, for many porous media, the empirical relationship between conductivity (σ , the inverse of resistivity), and its fractional porosity (f), saturation (S) and conductivity of the pore fluid (σ_w) can be represented by Archie's Law (Archie, 1942):

$$\sigma_a = f^m S^n \sigma_w$$

Where:

σ_a = apparent conductivity

f = fractional porosity (the fraction of the soil's volume which is pore space)

m = an empirical constant: ~ 1.3 for unconsolidated sand and $\sim 1.8 - 2.0$ for sandstone

S = saturation (the fraction of the pore space filled with fluid)

n = an empirical constant, approximately 2 for sand and sandstone

σ_w = conductivity of the pore fluid

Archie's Law therefore provides a useful means of estimating the conductivity and, therefore, resistivity, of a range of porous media. However, the presence of fine-grained, conductive material can result in a conductivity greater than would be calculated using the equation. Clay minerals, in particular, absorb ions on their surface, providing a pathway for conductance as well as through the pore fluid. Archie's Law can be modified to account for the presence of conductive pore material using an additional term; surface conductivity (σ_s) as follows (Sen, *et al.*, 1988):

$$\sigma_s = \frac{AQ_v f^m}{1 + CQ_v/\sigma_w}$$

Where:

Q_v = clay charge contribution per unit volume

A = an empirical constant

C = an empirical constant

This surface effect therefore contributes less to the overall conductivity when the conductivity of the pore fluid is high.

In geophysics, we consider the measured medium to be a conducting *half-space*, for which the electric potential (U) for a point source of current (I) at the surface is given by (Telford *et al.*, 1990):

$$U = \frac{\rho I}{2\pi d}$$

Where:

d = distance from the source (m)

The geometrical factor $2\pi d$ indicates that, in an electromagnetically-homogeneous half-space, equipotential lines form concentric circles radiating from the point source. However, the subsurface is rarely homogeneous, and an additional property of porous media which affects the resistivity, is *isotropy*. An *isotropic* material is one whose resistivity is constant in all directions (i.e. between any two opposite faces of the cube) as opposed to an *anisotropic* material (Milsom & Eriksen, 2011). Anisotropy can result from a combination of the shape and alignment of particles and/or pores in the medium, and

affects the empirical value m of Archie's Law (Friedman, 2005). A number of formulae have been derived which factor for such effects, for example:

$$\sigma_a = F_G(\theta)\sigma_w + \sigma_s$$

Where:

θ = fractional volumetric moisture content of the soil

$F_G(\theta)$ = geometry factor of the pore geometry

Generally, $F_G(\theta)$ is increases with connectivity of pores, and thus overall conductivity of the soil increases (Grant & West, 1965). In reality this represents the freedom of fluid flow, and thereby the contribution of electrolytic conduction. Estimation of $F_G(\theta)$, however, can be very difficult due to the complicated micro- and macro-structure of soils as, even in knowing the size distribution of particles of a medium, the physical distribution of these different particle sizes can vary greatly between media and even within one medium (Mualem & Friedman, 1991).

For an anisotropic homogeneous half-space, we can introduce a term λ , to the equation for U (Telford *et al.*, 1990):

$$U = \frac{\rho_x \lambda I}{2\pi d}$$

Where:

ρ_x = resistivity in a given dimension (x)

λ = coefficient for anisotropy, given as:

$$\lambda = \left(\frac{\rho_z}{\rho_x} \right)^{\frac{1}{2}}$$

Anisotropy cannot be detected from measurements made at the surface of the half-space. Therefore, any estimations about the degree of anisotropy of a measured medium will need to be factored into calculations based on other evidence.

Measurement of Electrical Resistivity

As previously explained, measurement of electrical resistivity of the subsurface requires the injection of a current into the ground using two electrodes. The frequency of this current is kept sufficiently low so that the effects of attenuation and induction can be ignored. Voltage is measured using an additional two electrodes inserted into the ground (Telford *et al.*, 1990). Simple resistance measurements (e.g. of wires) in theory only require two contacts with the measured medium. In practice, however, the measured resistance using two electrodes is dependent upon the contact resistance, which can vary hugely in soils due to their heterogeneous nature and surface features. When four probes are used, measuring separate current and potential electrode pairs, the measured resistance will be independent of contact resistance (Clark, 1996).

In fact, the measured resistivity is not an entirely true representation of the EM properties of the subsurface. Soil environments are rarely homogeneous in physical structure, though the measured resistance and, therefore, calculated resistivity, will be a single value. Therefore, this resistivity is known as *apparent resistivity* (Milsom & Eriken, 2011) as it assumes a homogeneously resistive half-space which, as has been discussed in the previous section, is in reality a combination of several factors which contribute to the overall resistivity. As such, apparent resistivity can even produce negative values due to the effect of regions of low resistivity which cause the potential gradient to decrease.

It is possible to represent apparent resistivity of the subsurface in two main ways: horizontal profiles or vertical profiles. In order to obtain these two different datasets, four electrodes are arranged in a number of different configurations known as *arrays*.

In horizontal profiling, the electrode separation is kept constant, but the whole array is moved between acquisition points on a line or grid to build up a *map* of the horizontal resistivity variations for a fixed depth range (Fig. 2.9; Milson & Eriksen, 2011). There are, however, a number of possible fixed-separation arrays, each of which has its own advantages and disadvantages in terms of penetration depth and data resolution (in particular directions), which should be considered in combination with the intended purpose of an electrical resistivity survey. Three of the most common electrode configurations are Wenner, pole-pole and dipole-dipole arrays. Wenner arrays involve all four electrodes arranged in line at equal separations (a) on a frame, with the outermost electrodes being the current electrodes.

The Wenner array offers high vertical resolution, but can produce complex patterns in data where even simple lateral variations in resistivity occur. This is due to the geometrical expression of equipotential lines in the sampled subsurface, which allows high sensitivity with close proximity to the electrodes, but flat regions of sensitivity between the electrodes (Barker, 1989). This means that the region between the electrodes is more sensitive to vertical variations in resistivity.

Pole-pole and dipole-dipole arrays consist of two electrodes at fixed spacing (a) on a frame, which are moved with each reading. The other two electrodes remain in a fixed position in the ground at a considerable distance from the survey area (Milsom & Eriksen,

2011). In dipole-dipole arrays, the current electrodes are adjacent to one another, with their paired potential electrodes at a distance from the current electrodes which is several times larger than a . This results in a geometrical profile of equipotential lines which has a lower vertical resolution, but a greater horizontal resolution compared to the Wenner array (Barker, 1989), and is typically considered the best array for mapping horizontal variations in resistivity (Reynolds, 2011).

The distance (L) between the current electrodes determines the sample depth of the resistivity measurement, with around half of the current flowing to a depth of $L/2$ (Telford *et al.*, 1990). The measured region of the subsurface, in practice, is usually between L and $2L$, but is dependent on the electrical properties of the sample medium, therefore the greater the distance between the current or potential probes, the deeper the penetration (Barker, 1989).

It is this relationship between electrode separation and penetration depth which is employed in order to conduct vertical profiling of electrical resistivity. Equally-separated electrodes are inserted into the ground in a line or geometrical grid and connected to a control unit. Computer software in connection with the control unit can control the current passage between a particular set of four electrodes at a time in a Wenner array. By starting with closely spaced sets and then using electrodes of greater separation, the configuration builds up a 2D cross-section of the subsurface according to variations in its electrical resistance (Fig. 2.10). Bespoke software can convert apparent resistivity into true resistivity profiles (Loke & Barker, 1996).

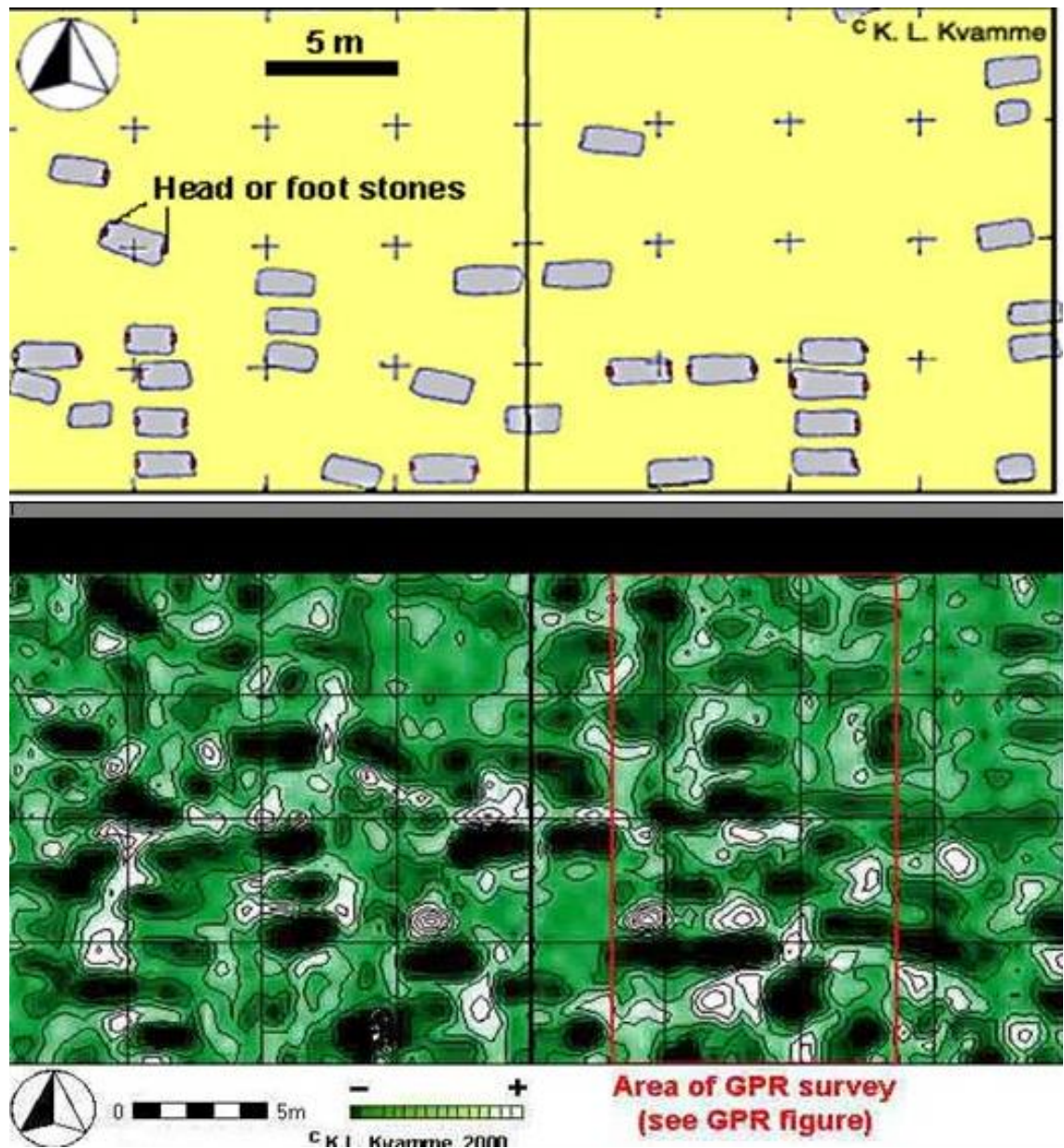


Figure 2.9. From Kvamme (2000). Map-view (a) plan of known graves and (b) electrical resistivity contoured surface of the site, (c) courtesy of University of Arkansas archaeological imaging lab.

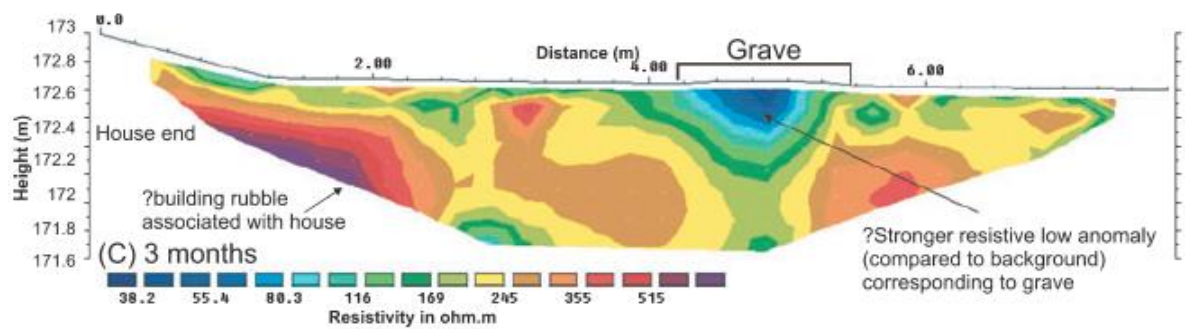


Figure 2.10. ERI inversion 2D profile collected 78 days post-burial over a simulated clandestine grave in a semi-urban environment. Modified from Pringle *et al.* (2008).

Electrical resistivity in forensic and archaeological geophysics

Recent control studies using pig cadavers have begun to further our understanding of how resistivity can be used to detect buried human remains (Cheetham, 2005; Pringle *et al.*, 2008; Molina *et al.*, 2016). Graves commonly appear as areas of relatively low resistivity (Cheetham, 2005) or, as equivalent in other electromagnetic surveys, areas of relatively high conductivity (see Fig. 2.8; France *et al.* 1992; Nobes, 2000). Possible causes of this have been attributed to increased porosity of backfill soil (France *et al.*, 1992; Scott & Hunter, 2004), moisture trapped within the grave (Nobes 2000; Jervis & Pringle, 2014) or ion-rich fluids released by decomposition (Vass *et al.*, 1992; Jervis *et al.*, 2009). However, no previous resistivity study of this kind has been supported by porosity, moisture or fluid conductivity measurements (Jervis *et al.*, 2009).

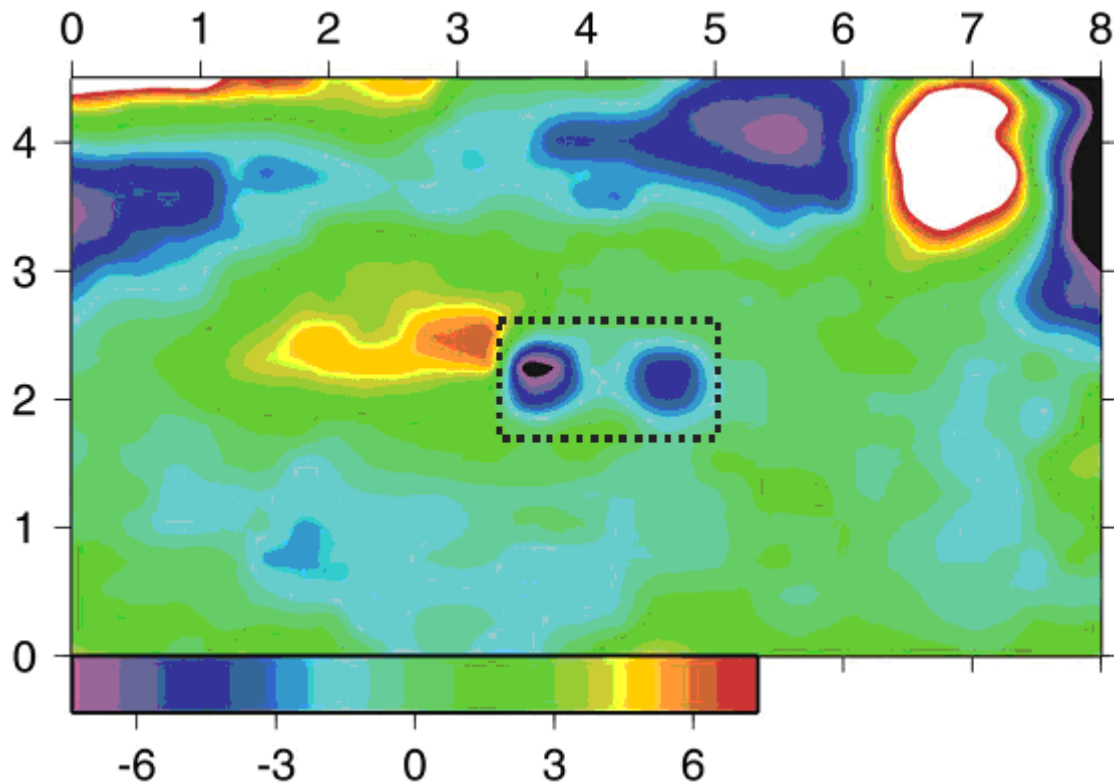


Figure 2.11. Bulk resistivity plot showing low-resistivity anomalies at the head and foot of a pig grave (rectangle) interred six weeks previously (after Jervis *et al.*, 2009).

2.4 Seismic methods

Seismology has been used in the investigation of international incidents involving explosions and impacts, as the energy released can be detected by seismic networks (Pringle *et al.*, 2012a). Examples of forensic seismology include the Kursk submarine disaster (Koper *et al.*, 2001), the Lockerbie (Scotland) aeroplane crash (Redmayne & Turbitt, 1990), the Oklahoma City (US) bombing (Holzer *et al.*, 1996) and the Nairobi US Embassy bombing (Koper *et al.*, 2001; Koper, 2003). A major advantage of this technique is that it works well for non-magnetic material, e.g. for detection of plastic mines, and can discriminate mines from smaller, metallic non-target material (Pringle *et al.*, 2012a).

Hildebrand *et al.* (2002) showed seismic reflection surveys could be effective in locating a dead pig in a wooden coffin at 2 m bgl in an unmarked grave, if closely-spaced geophones were utilised. However, they also showed that GPR surveys were as effective in detecting the graves and could be completed much faster and Nobes (2007) stated that seismic methods lack the resolution necessary for the detection of graves.

2.5 Magnetic methods

Magnetic techniques have proven more popular in archaeological investigations than forensic investigations since they are more appropriate for the detection of ferrous and metallic objects associated with burials such as metal parts of coffins, clothing and other adornments (Jones, 2008; Bevan, 1991) that are mostly absent from clandestine burials (Juerges *et al.*, 2010). However, in suitable soil conditions, soil disturbance can produce detectable variations in magnetic susceptibilities (Fig. 2.12).

Highly sensitive magnetometers have been used with varying success in forensic applications (Pringle *et al.*, 2012). Ancient archaeological graves have been shown to produce high magnetic susceptibility readings, potentially due to long term mineral changes caused by bacterial action (Linford, 2004). However, magnetic data over simulated recent clandestine burials in a variety of depositional environments have not proven to be particularly useful (Juerges *et al.*, 2010). Ellwood (1990) and Witten *et al.* (2001) encountered difficulties in locating 19th century graves in cemeteries and a mass grave from 1921, respectively, using magnetic methods, although Stanger & Roe (2007) showed the fluxgate gradiometry method was successful for 20th century graves in an Australian cemetery. Magnetic susceptibility analysis undertaken on illegally dumped soil

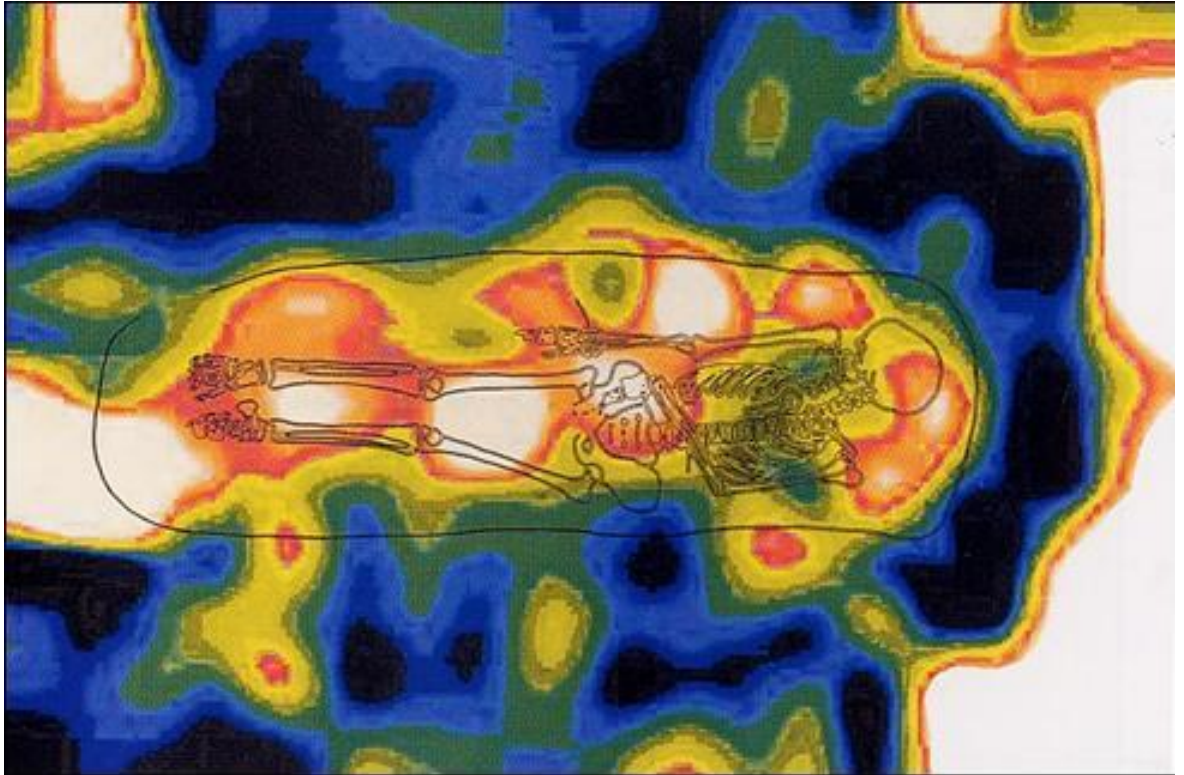


Figure 2.12. Magnetic susceptibility results (in SI dimensionless units, here red indicates high values) over an Anglo-Saxon archaeological grave in East Anglia (From Linford, 2004.)

on a motorway in China which caused multiple fatalities led to successful identification of its origin (Manrong *et al.*, 2009). Hannam & Dearing (2008) used magnetics in Bosnia and Herzegovina for landmine clearance operations. Pringle *et al.* (2008) pointed out that magnetic susceptibility datasets can also be used for quality control checking of magnetic gradiometry datasets: e.g. for assisting with the removal of anomalous spikes from magnetic data. Recent field trials by the authors have shown magnetic susceptibility methods are optimal in detecting buried metallic targets beneath domestic patios versus total field and gradient methods (see Reynolds, 2011 for background). Magnetic surveys collected by helicopters flying at a low altitude have also proven useful in identifying UXOs; Billings & Wright (2010) provide a good example from a former army range in Canada. For land-based UXO detection surveys, case studies using specialised

magnetometers have been published on multi-sensor 3-axis magnetometers (Munschy *et al.*, 2007), quad-sensor arrays (Billings & Youmans, 2007) and borehole magnetometry (Zhang *et al.*, 2007). However, Butler (2003) details the importance of understanding the environmental background magnetic susceptibility for identifying and locating UXOs and uses case examples from Indiana and Hawaii, USA. In environmental forensic applications, Marchetti *et al.* (2002) describe how magnetic methods were used to locate over 160 illegally buried solid metal drums, with a recent paper showing how test sites can aid magnetic data interpretation (Marchetti & Settini, 2011).

2.6 Geophysics as a forensic and archaeological search tool

Despite the range of geophysical techniques available, GPR has, in many cases rightly, claimed the status of the optimal tool in forensic investigation. Very few publications exist which compare techniques for the location of buried forensic targets, especially human or animal remains, whether in test sites or actual criminal investigation. Despite Lynam's (1970) early success in delineating shallow pig graves using resistivity equipment, the potential of this technique (even considering advances in the technology) has been largely under-realised. Even cases which find some success with resistivity generally conclude that the method is excessively time-consuming (Buck, 2003). Cheetham (2005) attributes this to differences in practice between North America and Europe. North American practice largely involves the use of the time-consuming Wenner array whereas European archaeology has been making use of the more rapid pole-pole array technique for some time. Scott and Hunter (2004) also recognise this, stating the use of wide-separation Wenner in searches for relatively small targets as graves is "*highly inappropriate.*"

Although previous studies have favoured the use of GPR and generally considered electrical resistivity as an inappropriate method for detection of buried human remains, it is important to remember that the results of these investigations are not directly applicable to all other similar scenarios (see Table 2.1). This is particularly important when considering that soil types in the USA and Australia; where the majority of research has been conducted, are considerably different from those commonly encountered in the UK. Another important observation in many of the investigations which conclude that resistivity is inappropriate (either due to lack of success or time consumption) often only consider one of the many available configurations and/or pre-date advancements in technology allowing acquisition and processing of digital data.

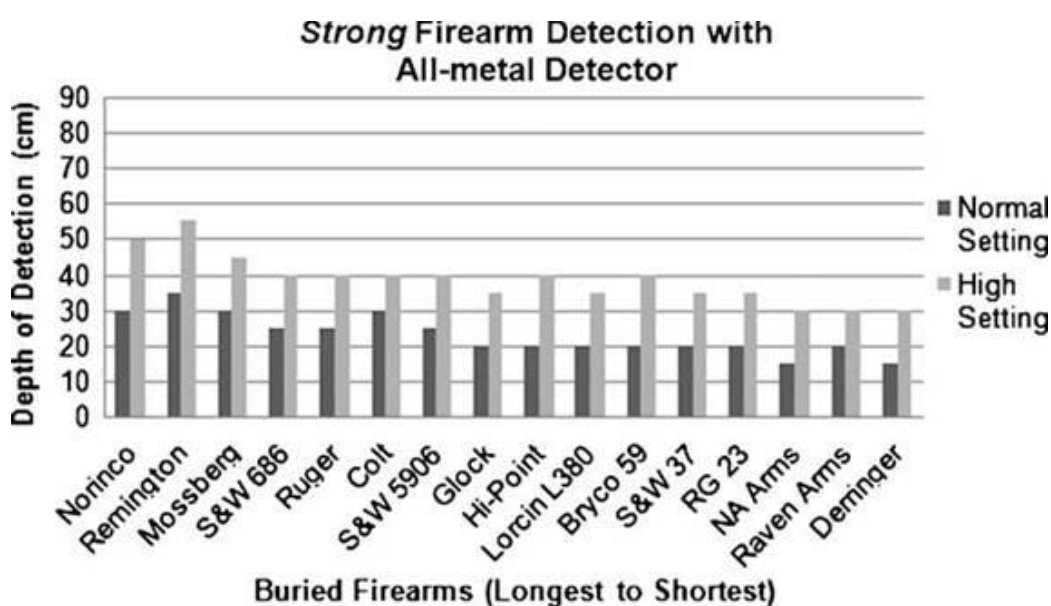


Figure 2.13. Detection strength of metallic firearms. From Dionne *et al.* (2011).

Much of the published forensic geophysics research favours the study of buried human or animal remains but there is very little relating to the search for other, non-organic buried evidence in criminal investigations. For example, the burial of firearms relating to gang neighbourhoods is well documented in both the UK and the USA (Murphy & Cheetham,

2008) but there are very few published studies relating to the search for clandestinely buried evidence. Dionne *et al.* (2011) use a basic all-metal detector to locate buried firearms and concludes that most are undetectable at depths of greater than 0.40 m (Fig. 2.13). Murphy & Cheetham (2008), and Rezos *et al.* (2010) found success in detecting buried firearms using magnetometry, GPR, conductivity and GPR respectively.

2.7 Conclusions

Much of the forensic and archaeological geophysical studies and casework in the past have focussed on the use and development of GPR technology, so that a good understanding of how human remains can be detected and the limitations of its application has been reached. A large number of studies leading to the popularity of GPR have been conducted in countries such as the U.S.A. where sandy soils are dominant. Homogeneous, sandy soils have been shown to be optimal for the detection of cadaver burials in multiple studies; however, such conditions are rarely encountered (e.g. in the U.K. where clay-rich, inhomogeneous, glacial soils are dominant). This has resulted in GPR being incorrectly applied under the impression that success in one study can be replicated in another, without proper consideration for target and soil variability. Arguably, this has led to a lack of confidence in, or complete disregard for the potential of geophysical methods to improve archaeological and forensic investigations. Other survey techniques, particularly resistivity, show great potential for application in these fields, particularly in soil environments where GPR is not considered optimal. Some time-lapse investigations have been conducted in order to determine the detectability of decomposing targets over time; however the longest running investigation (currently published) only covers a post-burial time of 24 months.

Forensic and archaeological geophysics could therefore benefit from a greater understanding of the limitations of other geophysical techniques in the search for buried targets with consideration for soil properties, target properties and burial time, as “...*there is no remote sensing method that will consistently find a body or piece of evidence*” (Davenport, 2001).







































































































































Target(s)	Remote sensing		Site work									
	Photo-graphs	Infra-Red	Geomorpho-logy / probing	Thermal imaging	Specialist search dogs	Seis-mology / Sidescan sonar	Conductivity	Resistivity	GPR	Magnetics	Metal detector	Element analysis
Soil type:  sand  clay												
Unmarked grave(s)												
Clandestine grave(s)												
UXOs/IEDs												
Weapons												
Drug / cash dumps												
Illegal waste												
Influence of search environment on chosen method(s) (above) effectiveness												
Woods												
Rural												
Urban												
Coastal												
Underwater												

Table 2.14. Generalised table to indicate potential of search techniques(s) success for buried target(s) assuming optimal equipment configurations. Note this does not differentiate between target size, burial depth and other important specific factors. Key: Good; Medium; Poor chances of success. The dominant sand|clay soil end-types are detailed where appropriate for simplicity. Modified from Pringle *et al.* (2012a).

Chapter 3 - Geophysical monitoring of simulated clandestine graves of murder victims using Ground Penetrating Radar: 0-3 years after burial

3.1 Introduction

Key and high-profile targets for forensic search teams to detect and locate are human remains of murder victims buried within clandestine graves (Davenport *et al.*, 1990; Harrison & Donnelly, 2009). Whilst more common forensic search team methods include, for example, the use of remote sensing (Brilis *et al.*, 2000a,b), trained search dogs (Lasseter *et al.*, 2003), metal detector teams (Ruffell & McKinley, 2008), probing (Owsley, 1995), geochemical surveys (Ruffell & McKinley, 2008) and physical excavations (Cheetham, 2005), forensic geophysical surveys are starting to be utilised, albeit sporadically, in criminal search investigations (Harrison *pers. comm.*; Pringle *et al.*, 2012a).

Geophysical surveys have been used to locate clandestine graves in a number of reported criminal search investigations (e.g. Mellet, 1992; Calkin *et al.*, 1995; Nobes, 2000; Davenport, 2001; Scott & Hunter, 2004; Cheetham, 2005; Ruffell, 2005; Pringle & Jervis, 2010; Novo *et al.*, 2010) and geophysical surveys collected over simulated clandestine burials have been undertaken to collect control data for comparison and best practice purposes (e.g. France *et al.*, 1992; Strongman, 1992; Freeland *et al.*, 2003). These studies have shown that the resulting geophysical responses could be reasonably well predicted, although responses do vary both temporally after burial and between different study sites. A few studies have also included time-lapse geophysical surveys (e.g. Cheetham, 2005; Schultz *et al.*, 2006; Schultz, 2008; Pringle *et al.*, 2008; Pringle *et al.*, 2012a), which

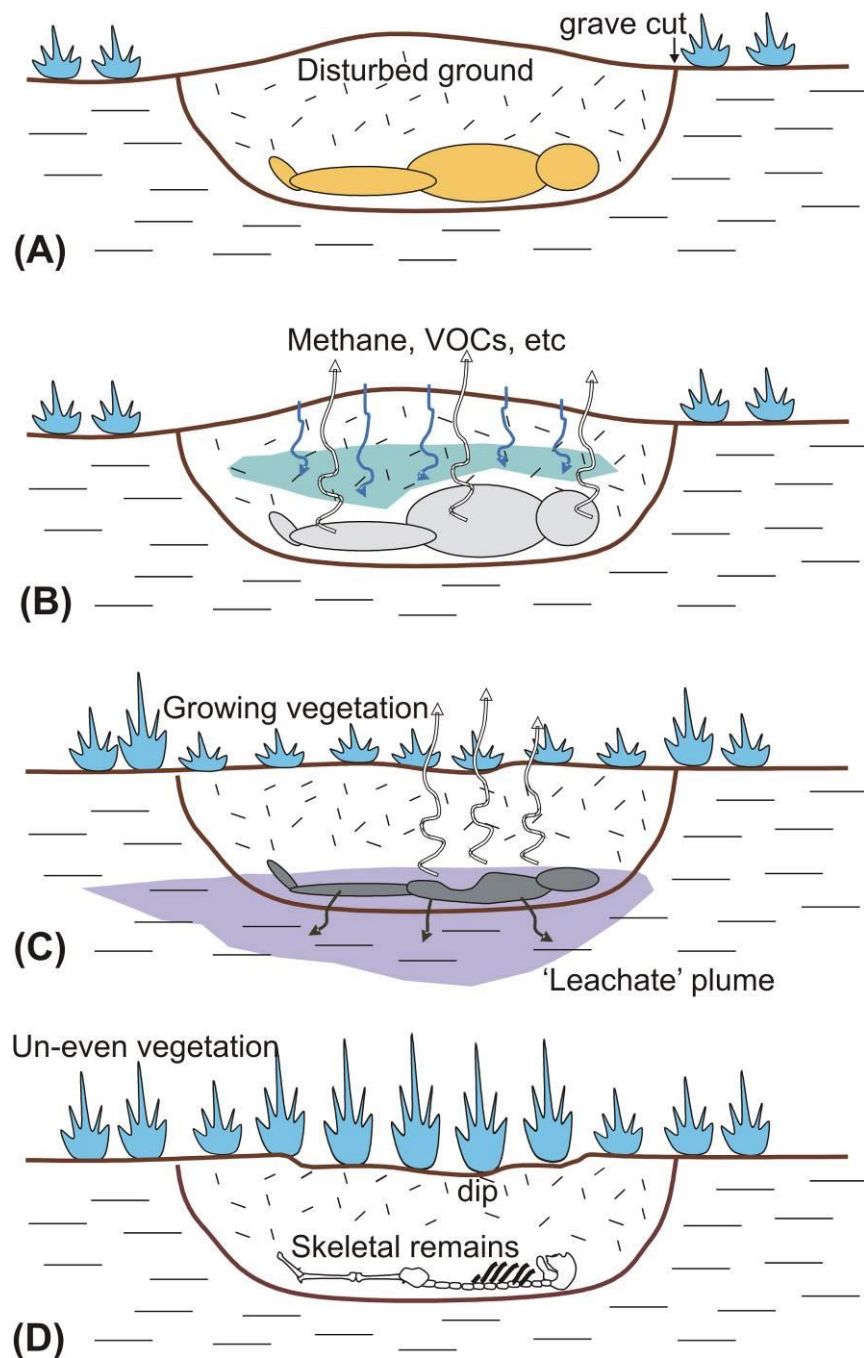


Figure 3.1. Four likely sequential decompositional stages of a clandestine burial. (A) Recent burial, surface expression most obvious. (B) Early decomposition with search dogs and/or methane probes being optimal. (C) Late-stage decomposition with conductive ‘leachate’ plume that should be resolved by geophysical methods. (D) Final decomposition that is most difficult to detect, GPR should locate. Modified from Pringle *et al.* (2012b).

document temporal changes over their study periods. Uncertainties still remain with regards to the nature and longevity of such temporal variations in geophysical data after burial, with sites requiring quantitative evaluation for comparison and transferability. Documenting temporal change is critical as geophysical survey data from recent clandestine burials are known to vary more than archaeological graves (e.g. Jervis *et al.*, 2009a). Potential reasons are changing grave soil characteristics, decomposition products, climatic variations and other factors (Fig. 3.1 and Jervis *et al.*, 2009a).

This study developed from a project initiated by Jervis (2010), in which simulated clandestine graves using wrapped and unwrapped pigs were surveyed over a 2-year post-burial period by resistivity and GPR. Jervis (2010) focused on bulk-ground resistivity and, although GPR data were collected, it was neither processed nor analysed. It was decided that the project should be continued up to three years in order to compare the GPR responses of the graves since burial.

The aims of this geophysical monitoring study were to answer some basic questions posed by forensic search teams. Appropriate site data were also simultaneously collected in order to allow comparisons with other research studies and criminal search investigations. Forensic search questions were:

- 1. Could GPR surveys successfully locate both simulated clandestine burials throughout the three year monitoring period? And if so, how long are they geophysically detectable for? And finally, which dominant frequency antennae are optimal?*
- 2. When is the optimal time (post-burial and seasonally) to undertake a forensic GPR geophysical search survey?*

3. *What effect does soil type have on a forensic geophysical survey's success in detecting a burial?*
4. *What is important when processing GPR survey datasets?*
5. *When should a forensic geophysical GPR survey be undertaken in a search scenario?*

3.2 Methodology

3.2.1 Study site

The chosen burial area is within a restricted area on Keele University campus, ~200 m above sea level, near the town of Newcastle-under-Lyme in Staffordshire, UK (Fig. 3.2). The local climate is temperate, which is typical for the UK (Peel *et al.*, 2007). The survey area is a grassed plot of land, 25 m by 25 m in total area, sloping ~3° from NW to SE. It is surrounded by small deciduous trees on the south, east and west sides, with a tall brick wall at the north, and is therefore considered to be representative of a semi-rural environment.

According to borehole data obtained from an engineering borehole located ~150 m from the study site, the subsurface consists of 'made-ground' layers due to the presence of now-demolished greenhouses, with Carboniferous (Westphalian) Butterson Sandstone bedrock geology present at ~2.6 m below ground level or bgl (Nicholls Colton, 2005). Initial soil sampling indicated a vertical site succession of a shallow (0.01 m) organic-rich, top soil (Munsell colour chart colour (Mccc): 5 YR/2/2.5), with underlying 'A' Horizon (Mccc: 5 YR/3/3) comprising predominantly of a natural sandy loam which contains ~5% of isolated brick and coal fragments (Pringle *et al.*, 2012b). The natural ground 'B' Horizon was encountered at ~0.45 m bgl, dominated by sandstone fragments from the underlying

bedrock, which suggests a shallower bedrock depth than at the borehole locality (Pringle *et al.*, 2012b). The weather conditions over the study period (taken from the nearby Keele University meteorological weather station) are presented in Figure 3.3.

3.2.2 Simulated clandestine graves

Preparation of the site required the removal of the turf before three ‘graves’, measuring ~ 1.5 m long, ~ 0.75 m wide and ~ 0.6 m deep, were dug by two people using shovels (Pringle *et al.*, 2012b). Since The Human Tissue Act (2004) prevents the use of human cadavers for research in the UK, two of the graves were used to bury pig cadavers of the species *Sus scrofa* as proxies for human cadavers. Pig cadavers are commonly used as they are not only easily obtainable, but their chemical compositions, size, skin and hair types, and tissue-body fat ratios quite closely resemble those of humans (Fig. 3.1 and Manhein 1996; Carter & Tibbett 2009; Pringle *et al.*, 2012b). Each of the pigs weighed approximately 80 kg and were collected from a local abattoir on the day of burial (7th December, 2007) after necessary permissions had been granted by the UK’s Department for Environment, Food and Rural Affairs (DEFRA). The pigs had been dead for less than 5 hours at the time of collection. One pig was buried naked (Fig. 3.2c) and the other wrapped (Fig. 3.2d), prior to burial, in a tarpaulin sheet (Duratool Corporation product number D00065, measuring 1.8 m by 2.7 m, and made of woven, 3 mm wide, polyethylene strands – see Jervis 2010). After interment of the pig cadavers, the graves were backfilled with soil (leaving a slight mound to account for later settlement) and the turf replaced. Leftover grave soil was disposed of off-site. A third grave was dug the day prior (6th of December, 2007) to the same depth using the same methods and completely backfilled with soil. This empty grave was to be used as a control during the surveys to differentiate any effects

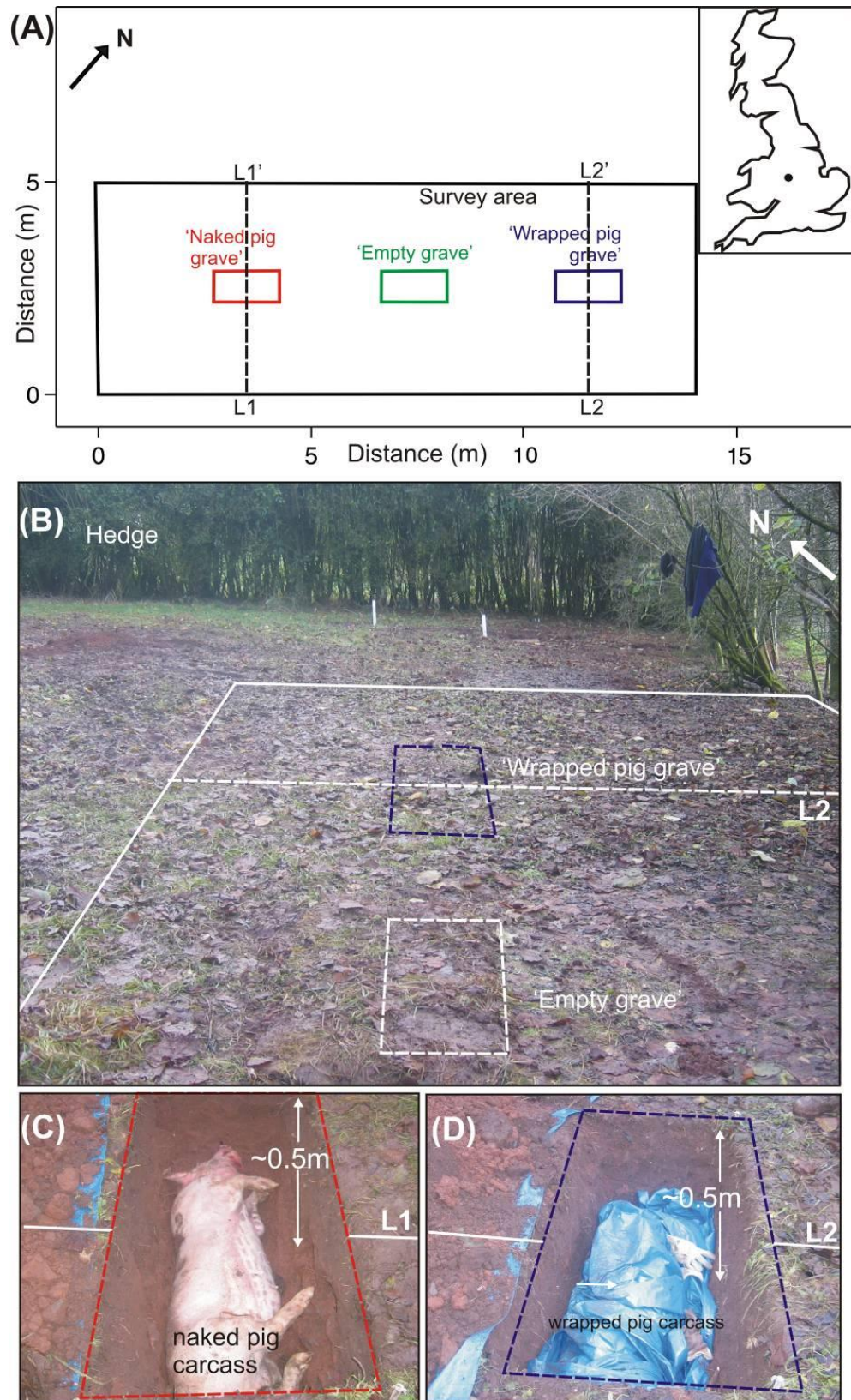


Figure. 3.2. (A) Map of survey area (dashed rectangle) with graves, lysimeter positions and UK location map (inset). (B) Study site, (C) 'naked pig grave' and (D) 'wrapped pig grave' respectively. Modified from Pringle *et al.* (2012b).

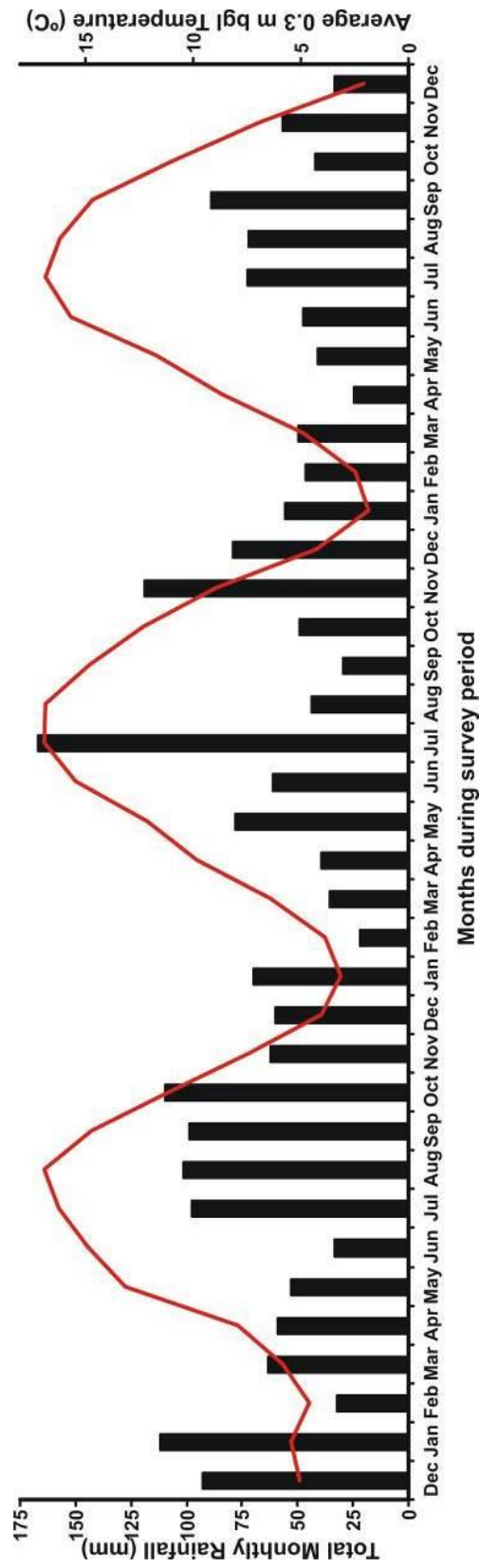


Figure 3.3. Summary of monthly study site statistics of total rainfall (bars) and average temperature (red line) data at 0.3 m bgl (below ground level), measured over the three-year study period. Modified from Pringle *et al.* (2012b).

produced by the grave itself as opposed to the pig buried within. All three graves were aligned to their long axes in an approximately north-west to south-east direction (Fig. 3.2).

3.2.3 Ground Penetrating Radar data acquisition

Repeat GPR survey datasets were collected within the survey area (Fig. 2) at approximately three-monthly intervals after burial (Table 3.1). Note that the Post-Burial Interval (PBI), in addition to Accumulated Degree Days (ADD) are detailed in Table 3.1. ADD is a robust method of recording time in forensic investigations to account for local temperature variation between study sites (Vass *et al.*, 1992) and is calculated by adding each day's average temperature to the previous day cumulatively.

There are numerous published studies of forensic GPR surveys for criminal (Mellett 1992; Calkin *et al.*, 1995; Ruffell 2005; Novo *et al.*, 2011) and simulated clandestine burials (Schultz *et al.*, 2006; Schultz *et al.*, 2008; Pringle *et al.*, 2008), in which most utilise medium frequency(200-500 MHz) antennae (e.g. (Nobes 2000; Novo *et al.*, 2011; Ruffell *et al.*, 2009).

In this study, PulseEKKO™ 1000 equipment in combination with the commonly used 225 MHz and 450 MHz, and less-used 100 MHz and 900 MHz dominant frequency antennae were utilised to collect four datasets for each repeat survey post burial. It was decided that 50 MHz and 1,200 MHz dominant frequency antennae would not be used as resulting datasets would be too low resolution (50 MHz) and take too long to acquire (1,200 MHz) respectively to be effectively used in forensic searches.

The 14 m x 5 m survey area (Fig. 2) was surveyed on 0.5 m spaced, 5 m long SE-NW orientated, parallel survey lines by 110 MHz, 225 MHz and 450 MHz dominant frequency GPR antennae (Figure 3.4). Using 0.5 m spaced survey lines for the 450 MHz frequency datasets was due to time constraints – ideally 0.25 m spaced survey lines should be used for this frequency as Schultz *and* Martin (2011) document. The transmitter antennae always led each profile for consistency. The 900 MHz dominant frequency antennae were used to acquire datasets on 0.25 m spaced lines over a small area, centred over the ‘naked pig’ (Fig. 3). Table 3.2 summarises the GPR data acquisition parameters.

Survey date(s)	Survey day after burial ⁺	Accumulated Degree Day (ADD)*
04 – 05.12.2007 [#]	-3 – -2	-14 – -7
04–06.03.2008	88 – 90	439 – 448
26–27.05.2008	171 – 172	1,176 – 1,187
26–27.08.2008	263 – 264	2,625 – 2,642
10–13.11.2008	339 – 342	3,573 – 3,595
02–05.03.2009	451 – 454	4,059 – 4,076
22–23.06.2009	563 – 564	5,243 – 5,258
13–14.08.2009	615 – 616	6,119 – 6,137
09–10.11.2009	703 – 704	7,337 – 7,345
03–04.03.2010	817 – 818	7,781 – 7,784
22–23.06.2010	928 – 929	8,870 – 8,888
28–29.09.2010	1,026–27	10,446 – 460
06–07.12.2010	1,092–93	11,033 – 035

Table 3.1. Summary of GPR data collected during this study. ⁺Burial date was 7th December 2007. *ADD date based on average daily site temperatures at 0.3 m bgl (see text). [#]First GPR surveys were controls. Modified from Pringle *et al.* (2012b).

Antenna Frequency / MHz	Line spacing /m	Sample interval /m	Nº of repeats (stacks) per trace	Approximate completion time /mins
110	0.5	0.2	32	60
225	0.5	0.2	32	150
450	0.5	0.1	32	240
900 ¹	0.25	0.05	32	120

Table 3.2. Survey parameters using each antenna frequency. ¹A smaller grid, focused directly over the naked pig was initially surveyed using 900 MHz antennae up to 18 months after burial; then a single profile (L1) was acquired until the end of the survey period.

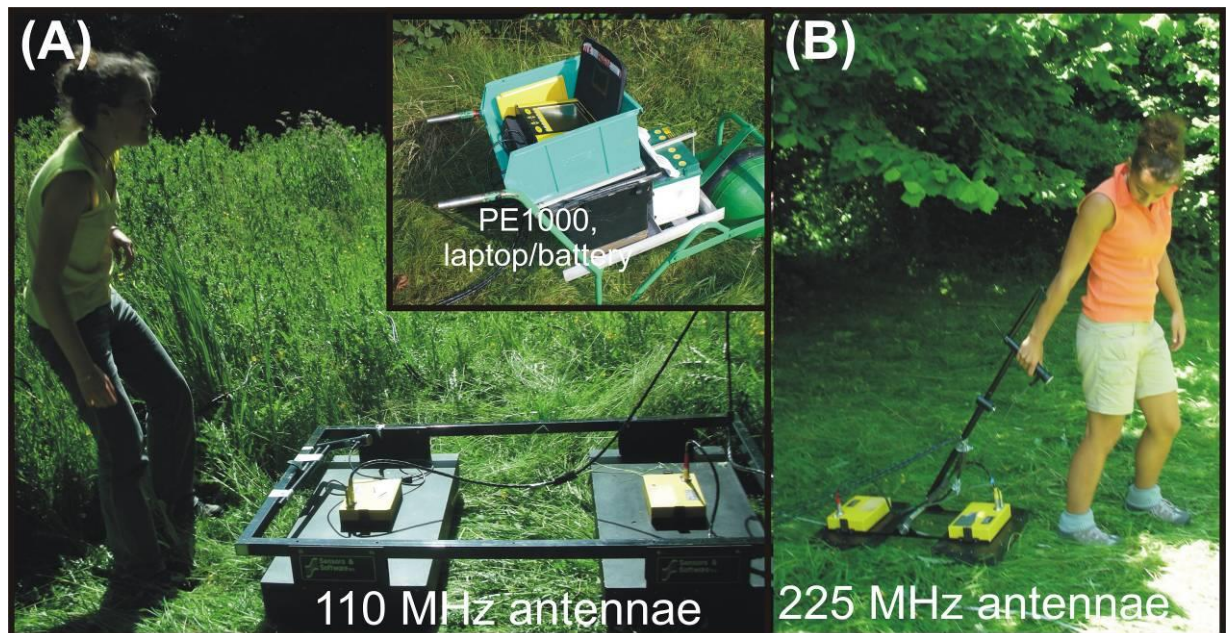


Figure 3.4. Site photographs showing (A) 110 MHz dominant frequency GPR antennae (with control PE 1000 equipment, laptop and 12 v leisure battery power source inset) and (B) 225 MHz dominant frequency antennae.

3.2.4 Ground Penetrating Radar data processing

Once the 2D GPR profiles for each dominant frequency antennae were acquired, they were downloaded and imported into REFLEX-Win™ v.3.0 processing software. For each 2D profile, the sequential data processing steps listed in Table 3.3 were used and horizontal time-slices of the four main dominant frequencies datasets for each survey were then generated using the processed 2D profiles. Absolute amplitude time-depth slices were generated for a 9 ns – 15 ns time window containing target hyperbolae. To eliminate the effects of background trends, time-depth slices were de-trended using Generic Mapping Tools (GMT) computer software (Wessel & Smith 1998; Wessel *et al.*, 2005).

3.3 Results

Key 2D GPR profiles acquired through the survey period are shown in Figures 3.5-3.8 (see Fig. 3.2 for respective profile locations). Pre-burial profiles (as controls) are also shown, with the exception of 900 MHz frequency data for which no control dataset was acquired.

The 110 MHz dominant frequency 2D profiles showed the ‘wrapped pig’ grave could be consistently and clearly identified by a strong hyperbola throughout the survey period, although there was a continual reduction in reflection amplitude. The ‘naked pig’ grave produced detectable hyperbola up to 18 months (~5,200 ADD) after burial, but this had significantly lower amplitudes when compared to ‘wrapped pig’ grave hyperbolae (*cf.* Figs. 3.5-3.8). After 18 months of burial it was difficult to detect a hyperbola over the ‘naked pig’ grave. There were no clear hyperbolae other than those associated with target graves within 2D profiles.

Step	Process	Description
1	Subtract mean ('de-wow')	Remove any positive or negative bias of the trace
2	Move start-time	Move traces to uniform time, based on common reflector: 0 ns here. This allowed all features of uniform depth below ground-level to appear uniform in GPR profiles.
3	1D Bandpass filter (Butterworth)	The upper/lower extents of frequency histogram removed.
4	2D filter Back-ground removal	Removes average from entire trace, thereby removing interfering 'ringing' created during the bandpass filter stage.
5	Migration (Stolt)	Collapse hyperbolae to discrete focus points
6	Horizontal time-slice generation	Collapse a specific time region across all profiles to create a 'map-view' of total amplitude over this time/depth domain
7	Exported as xyz data file	Amplitude data exported as Z data into 0.25 m (X) x 0.025 m (Y) spaced .xyz file for GMT processing
8	Gridding	Minimum curvature gridding algorithm interpolates data to a cell size of 0.0125 m by 0.0125 m to create smooth image
9	Detrending	Removal of long-wavelength trends from data by fitting a cubic surface to grid and then subtracting from surface data, allows small-wavelength features to be better distinguished
10	Normalisation	Dividing dataset by its SD Z value created grid with mean Z of ~0 and SD of ~1 allowing dataset comparison.

Table 3.3. Sequential GPR data processing steps used in this study.

The 225 MHz dominant frequency 2D profiles showed the ‘wrapped pig’ grave could also be clearly identified by an obvious hyperbola throughout the survey period, although there was a continual reduction in reflection amplitudes that was noticeable after two years of burial (*cf.* Figs. 3.5-3.8). There was also a second, slightly deeper reflector, which was first resolved after 15 months of burial (~4,000 ADD) within the ‘wrapped pig’ grave. The ‘naked pig’ grave was detectable as a hyperbola up to 15 months after burial, but this had significantly lower amplitude when compared to the ‘wrapped pig’ grave hyperbolae at the same frequency. Following 18 months after burial, identification of an anomaly over the ‘naked pig’ grave becomes difficult. Other, smaller hyperbolae were present in the ‘naked pig’ profiles which are not associated with the target positions but are typical of a semi-urban soil environment. These non-target hyperbolae would have made it difficult to identify the target grave after 18 months of burial to the end of the survey period.

The 450 MHz dominant frequency 2D profiles showed the ‘wrapped pig’ grave could also be identified by a hyperbola throughout the survey period with a continual reduction in reflection amplitudes after 27 months of burial (*cf.* Figs. 3.5-3.8). A second, slightly deeper hyperbola was also first resolved after 3 months of burial. The ‘naked pig’ grave was detectable as a hyperbola up to 12 months post-burial (~3,800 ADD), but this had significantly lower amplitude when compared to ‘wrapped pig’ grave hyperbolae and was difficult to detect after 15 months post-burial. Again, numerous other, smaller hyperbolae were present in both profiles but were not associated with the target graves.

The 900 MHz dominant frequency 2D profiles could only identify the ‘naked pig’ grave from 9 to 12 months after burial (~3,800 ADD); apart from these times after burial, the

grave location could not be identified (*cf.* Figs. 3.5-3.8). There were numerous other, smaller hyperbolae present which would have made it difficult to locate the target grave.

The 110 MHz dominant frequency repeat survey time-slices generally showed good results (Fig. 3.9). The control dataset did not show any anomalies at the target 'grave' positions, but did show two high amplitude anomalies at the NW border of the survey area which were mostly present in subsequent 110 MHz dominant frequency datasets. High amplitude isolated radar anomalies, generally significantly larger than the 'graves' in plan-view, were generally present within the 'naked pig' and 'wrapped pig' target grave positions throughout the three year study period, except for the 'naked pig' position in the year 2 and 3 winter datasets. Generally, the data for the wrapped pig cadaver displays a larger and higher amplitude anomaly than the naked pig cadaver (Fig. 3.9). Radar anomalies were also present in the 'empty grave' position in most datasets. There were a number of radar anomalies also present within the datasets that were not associated with the target 'grave' positions, notably in the year 0 winter, year 1 spring and summer, year 2 and year 3 summer respective survey datasets (see Fig. 3.9).

The 225 MHz dominant frequency repeat survey time-slices generally showed more variable results compared to the 110 MHz time-slices (Figs. 3.9 and 10). The control dataset did not present any anomalies at the target 'grave' positions, though one high amplitude anomaly was present in all subsequent 225 MHz dominant frequency datasets at the NW border of the survey area. High amplitude isolated radar anomalies, slightly larger than the 'graves' in plan-view, were generally present at the 'naked pig' and 'wrapped pig' target grave positions throughout the three year study period, except for the 'naked pig' position in the year 2 and 3 autumn datasets. 'Target' anomalies generally decreased

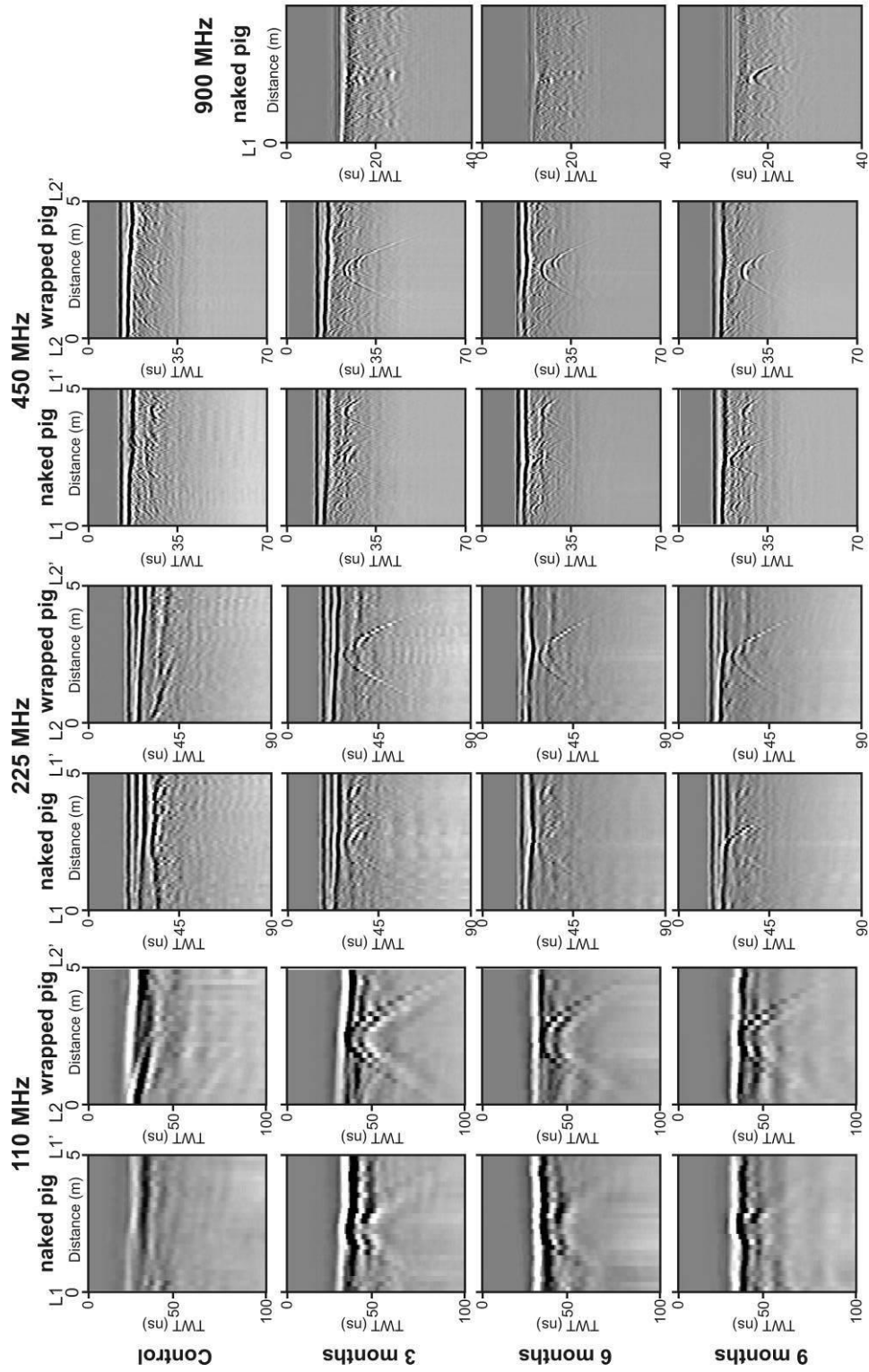


Figure 3.5. Key sequential processed 110, 225, 450 and 900 MHz dominant frequency GPR profiles that bisect the naked and wrapped pig ‘graves’ respectively (Fig. 3.2 for location) that include control profiles and data collected from 0 to 9 months after burial. Modified from Pringle *et al.* (2012b).

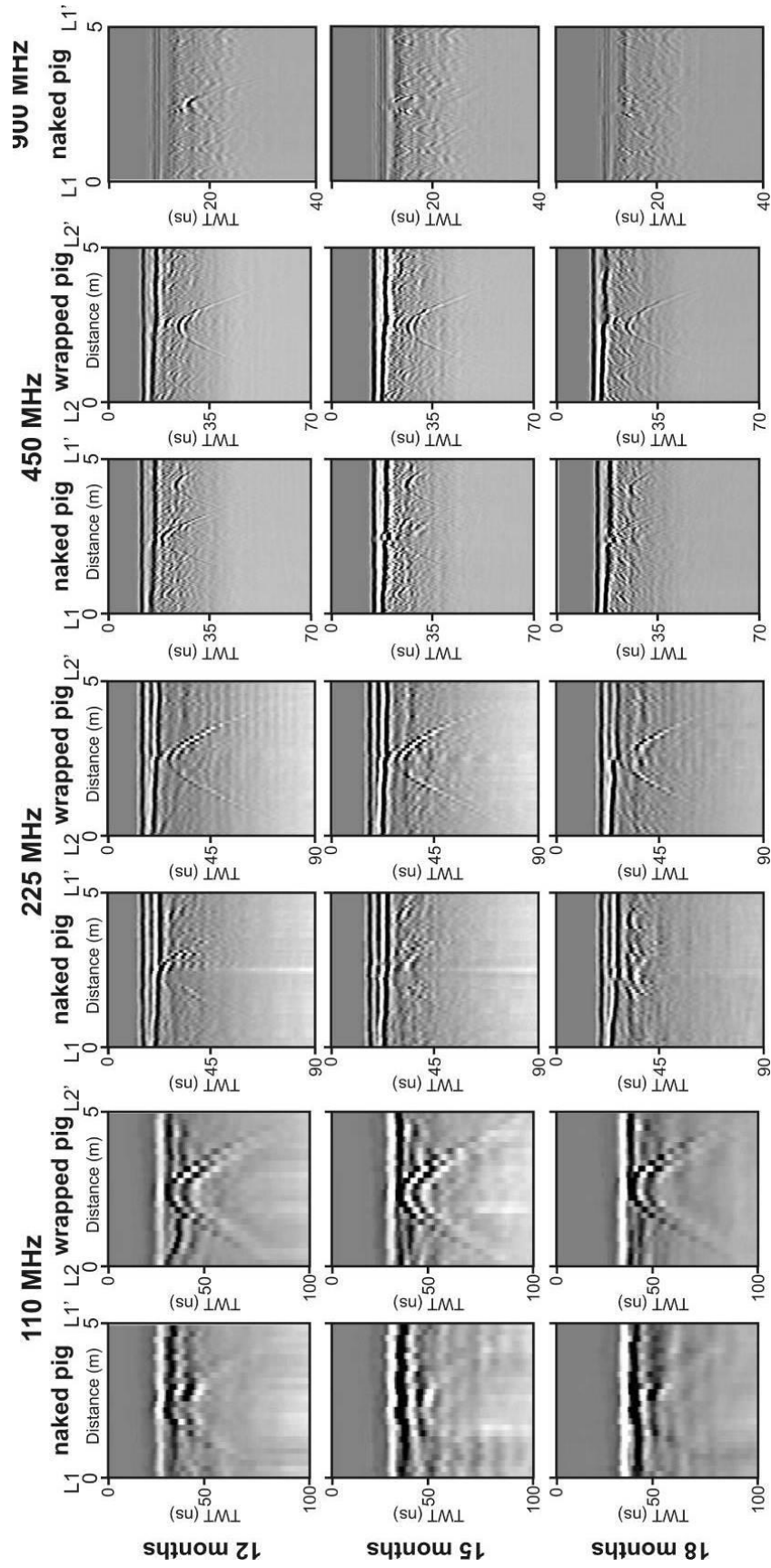


Figure 3.6. Key sequential processed 110, 225, 450 and 900 MHz dominant frequency GPR profiles that bisect the naked and wrapped pig ‘graves’ respectively (Fig. 3.2 for location) that include data collected from 12 to 18 months after burial. Modified from Pringle *et al.* (2012b).

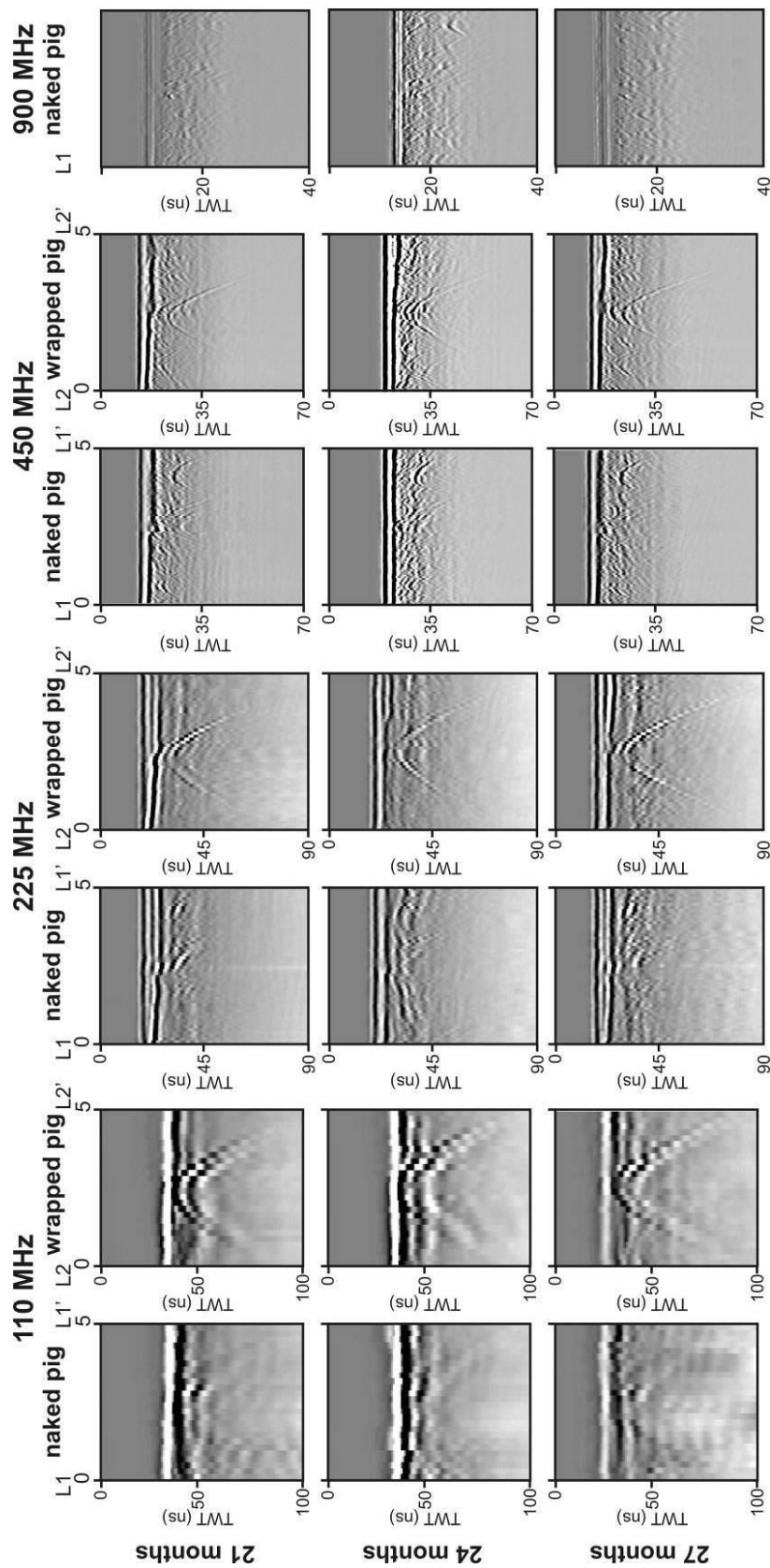


Figure 3.7. Key sequential processed 110, 225, 450 and 900 MHz dominant frequency GPR profiles that bisect the naked and wrapped pig ‘graves’ respectively (Fig. 3.2 for location) that include data collected from 21 to 27 months after burial. Modified from Pringle *et al.* (2012b).

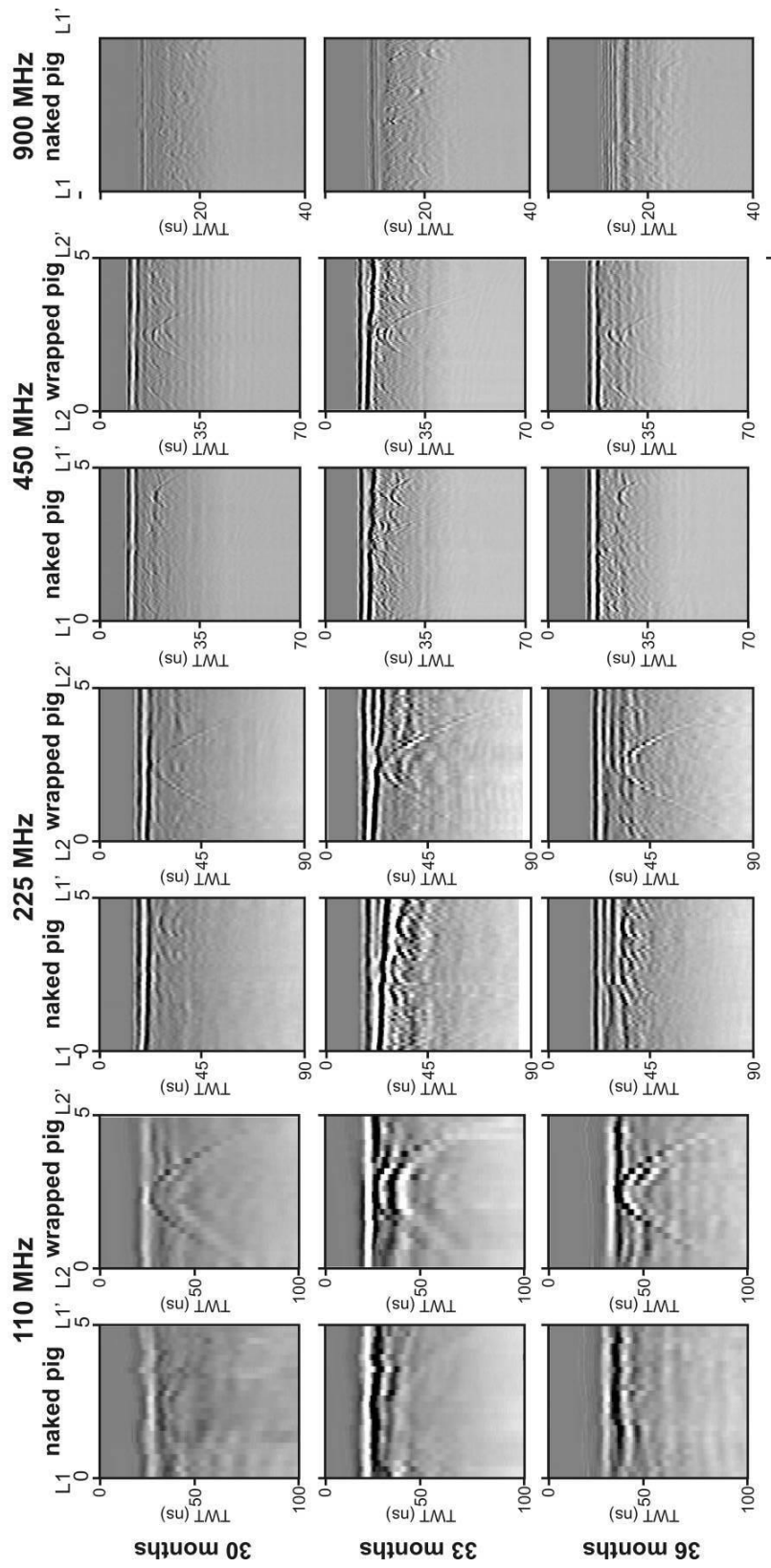


Figure 3.8. Key sequential processed 110, 225, 450 and 900 MHz dominant frequency GPR profiles that bisect the naked and wrapped pig 'graves' respectively (Fig. 3.2 for location) that include data collected from 30 to 36 months after burial. Modified from Pringle *et al.* (2012b).

in spatial extent and amplitude after year 1. At the wrapped pig cadaver position, an anomaly of larger horizontal extent and higher amplitude compared to the naked pig cadaver is observed (Fig. 3.10). Radar anomalies were not present in the 'empty grave' position, except for the year 2 winter dataset. There were a number of radar anomalies also present within the datasets that were not associated with the target 'grave positions, especially from year 2 spring survey datasets onwards (Fig. 3.10) which would make locating the 'target graves' in these datasets problematic.

The 450 MHz dominant frequency repeat survey time-slices also showed variable results (Fig. 3.11). No anomalies are visible at the target 'grave' positions in the control data, though one high amplitude anomaly at the SW border of the survey area was mostly present in subsequent 225 MHz dominant frequency datasets. High amplitude, isolated radar anomalies, smaller than the 'graves' in plan-view, were present within the 'naked pig' and 'wrapped pig' target grave positions throughout the three year study period. 'Target' anomalies were generally consistent in spatial extent and amplitude strength throughout the survey period. Generally the wrapped pig cadaver also showed as a larger and higher amplitude anomaly than the naked pig cadaver (Fig. 3.11). Radar anomalies were not present in the 'empty grave' position. There were a number of radar anomalies also present within the datasets that were not associated with the target 'grave positions, present in the year 0 winter survey and especially from year 2 autumn survey datasets onwards (Fig. 3.11) which would make locating the 'target graves' in these datasets problematic.

900 MHz dominant frequency survey time-slices were not generated due to the small survey size over the naked pig grave position and the incomplete record.

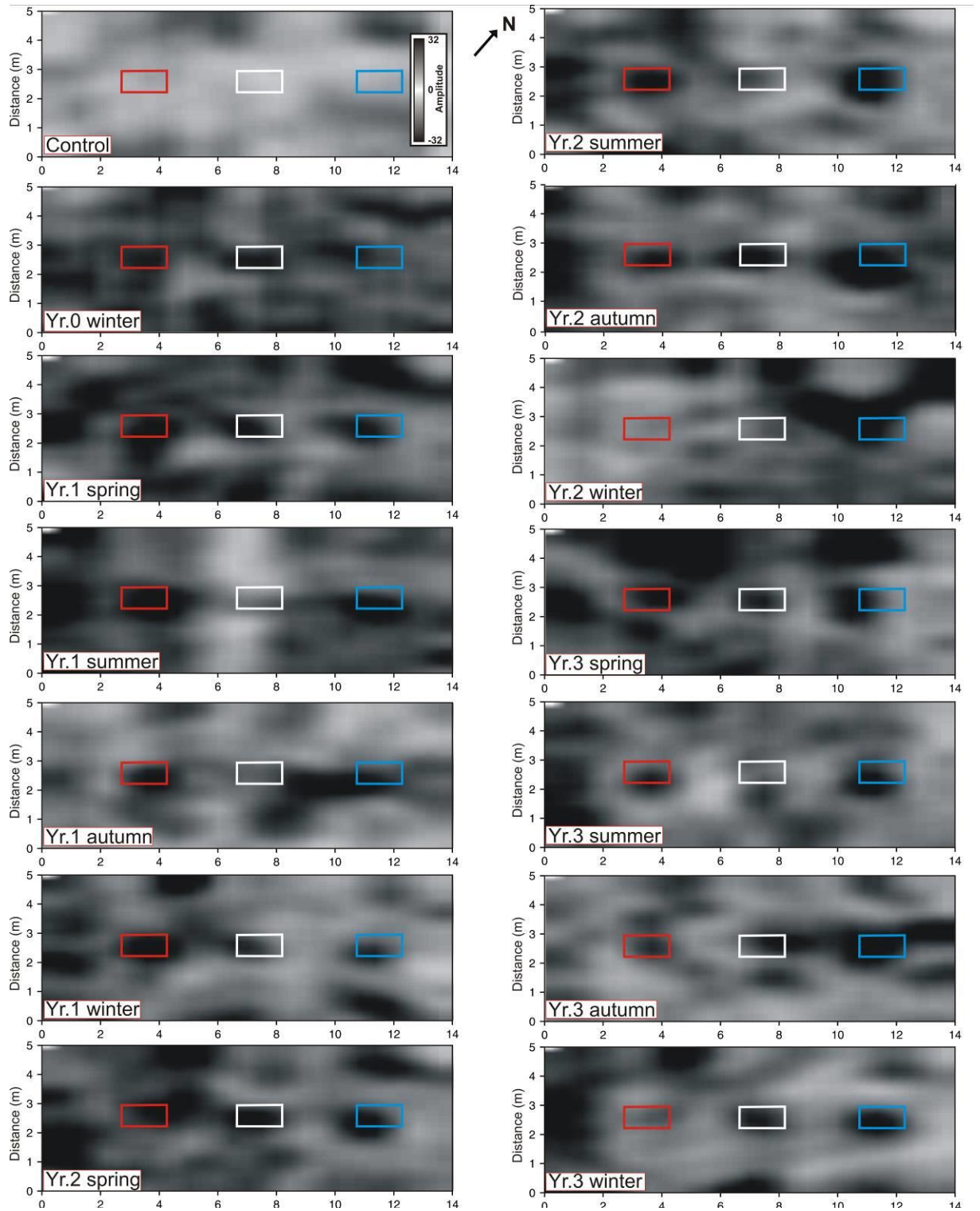


Figure 3.9. 110 MHz frequency, quarterly GPR processed ‘time-slice’ datasets. Common amplitude scale shown in control dataset. Dotted squares indicate ‘graves’ (Fig. 3.2 for location). Modified from Pringle *et al.* (2012b).

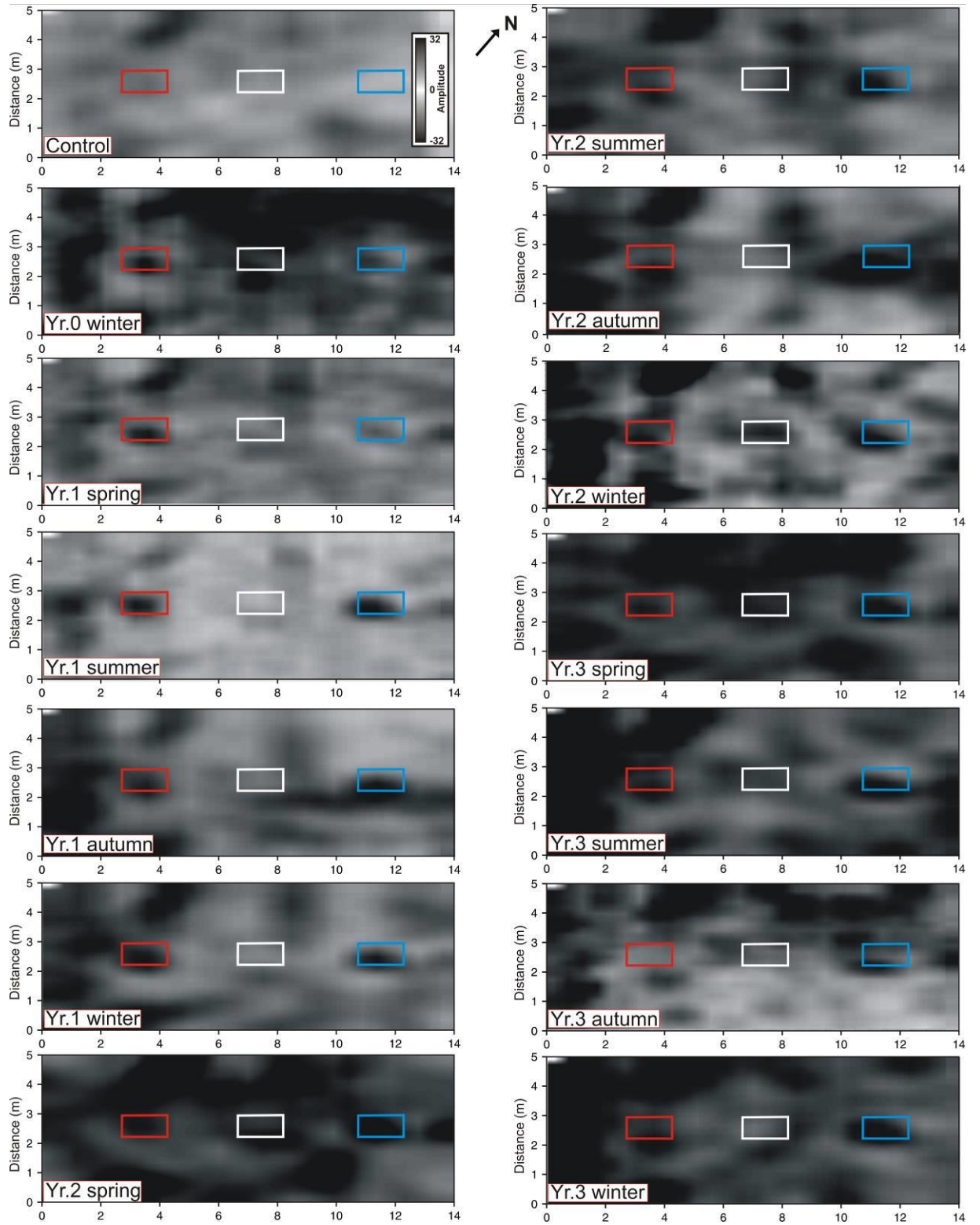


Figure 3.10. 225 MHz frequency, quarterly GPR processed ‘time-slice’ datasets. Common amplitude scale shown in control dataset. Dotted squares indicate ‘graves’ (Fig. 3.2 for location). Modified from Pringle *et al.* (2012b).

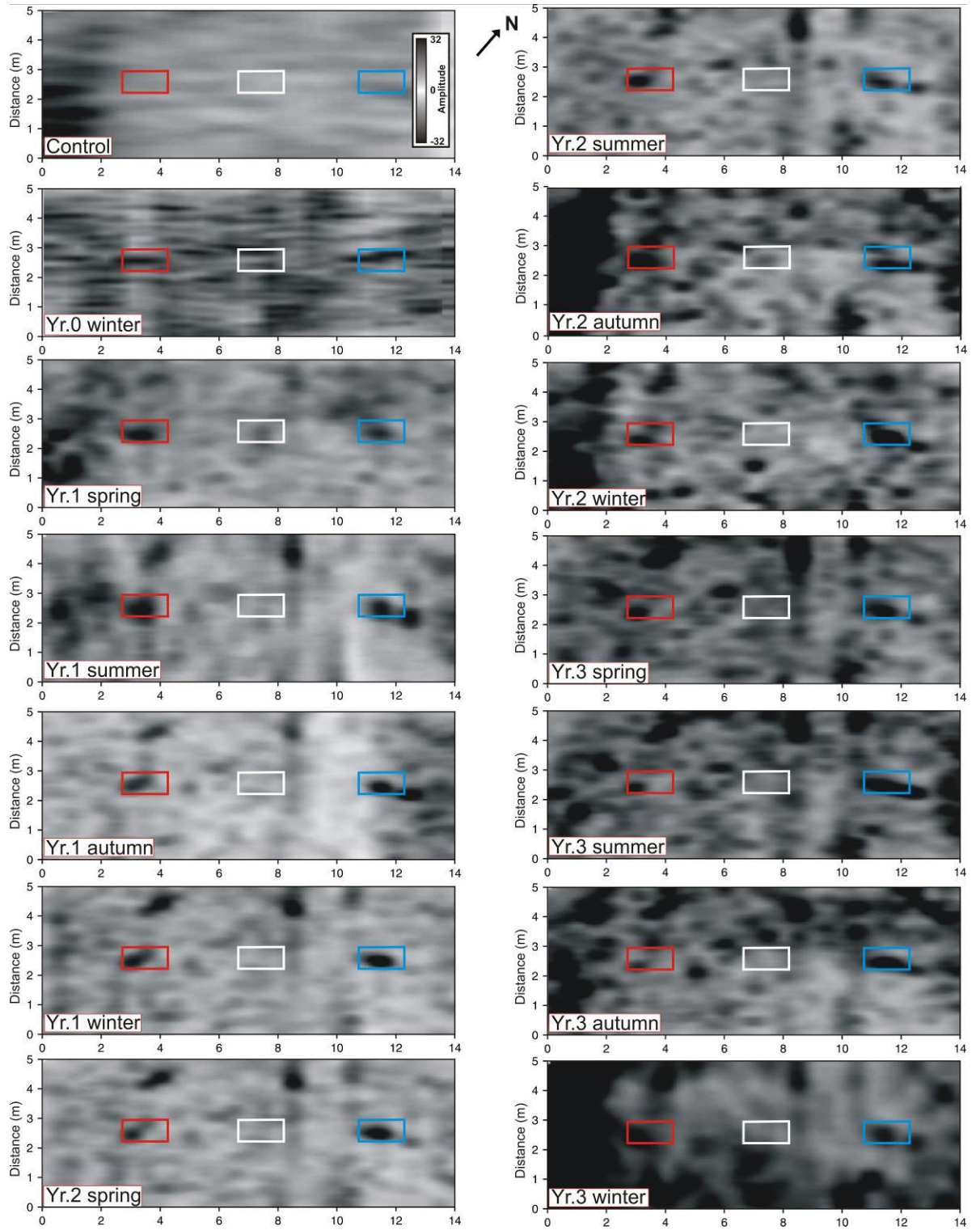


Figure 3.11. 450 MHz frequency, quarterly GPR processed ‘time-slice’ datasets. Common amplitude scale shown in control dataset. Dotted squares indicate ‘graves’ (Fig. 3.2 for location). Modified from Pringle *et al.* (2012b).

3.4 Discussion

This long-term study has allowed some basic questions by forensic search teams listed in Section 3.1 to be answered. These were:

1. Could GPR surveys successfully locate both simulated clandestine burials throughout the three year monitoring period? And if so, how long are they geophysically detectable for? And finally, which dominant frequency antennae are optimal?

From the results of this study, it was possible to initially locate both the ‘naked’ and ‘wrapped’ cadavers on GPR 2D profiles using the frequencies trialled, namely the 110, 225, 450 and 900 MHz dominant frequency antennae (note the 900 MHz antennae only collected data over the ‘naked’ cadaver). However after 18 months post-burial, only the ‘wrapped’ cadaver was relatively easy to locate in the 2D profiles, interestingly being the opposite outcome of the resistivity survey results which found the ‘wrapped’ cadaver to be harder to locate (Jervis 2010; Pringle *et al.*, 2012b). This was presumably due to the wrapping surface providing a better-defined physical contrast with the soil and thereby producing higher amplitude GPR reflections, whereas the decomposing ‘naked’ cadaver presumably attenuated a greater proportion of the GPR signal. This radar absorption would be exacerbated by the pig-chest cavity collapse during later decomposition stages (Fig. 3.1c), which is a probable explanation for the two GPR hyperbolae present in 225 and 450 MHz dominant frequency data over the target location later on during the survey period (Figs. 3.6 and 3.7). The potential size of the target(s) may also be a factor; Schultz (2008) found small pig cadavers were difficult to locate after 23 months of burial. The lower GPR frequencies trialled (110 and 225 MHz frequencies)

were shown in this study to be preferable to the higher frequencies (450 and 900 MHz frequencies) in the 2D profiles as there were less non-target hyperbolae present in the data. Additionally, these low-frequency surveys took less time in the field to acquire, which could be an important factor for a forensic search team to consider if the proposed area is significant in size or if manpower and/or budget are limited. Note Schultz & Martin (2011) suggested that 2D GPR profiles should be collected in both orientations over a survey site if possible to have the best chance of detection. The GPR results have also been graphically summarised in Figure 3.12.

The horizontal time-slices for the frequencies trialled showed generally good results throughout, with the radar responses from the wrapped cadaver again being larger in horizontal extent and of higher amplitude when compared to the ‘naked’ cadaver, presumably due to the better reflective surface of the former as previously noted. However, the 225 and 450 MHz dominant frequency time-slices contained a number of non-target anomalies that would make it difficult for search teams to confidently identify the grave locations from this data alone (Figs. 3.10 and 3.11). Results from this study, and in comparison with the resistivity monitoring study detailed in Jervis *et al.* (2010) and Pringle *et al.* (2013), therefore suggest that both GPR and fixed-offset resistivity surveys should be undertaken in forensic search surveys if the style of burial (i.e. wrapping) is unknown.

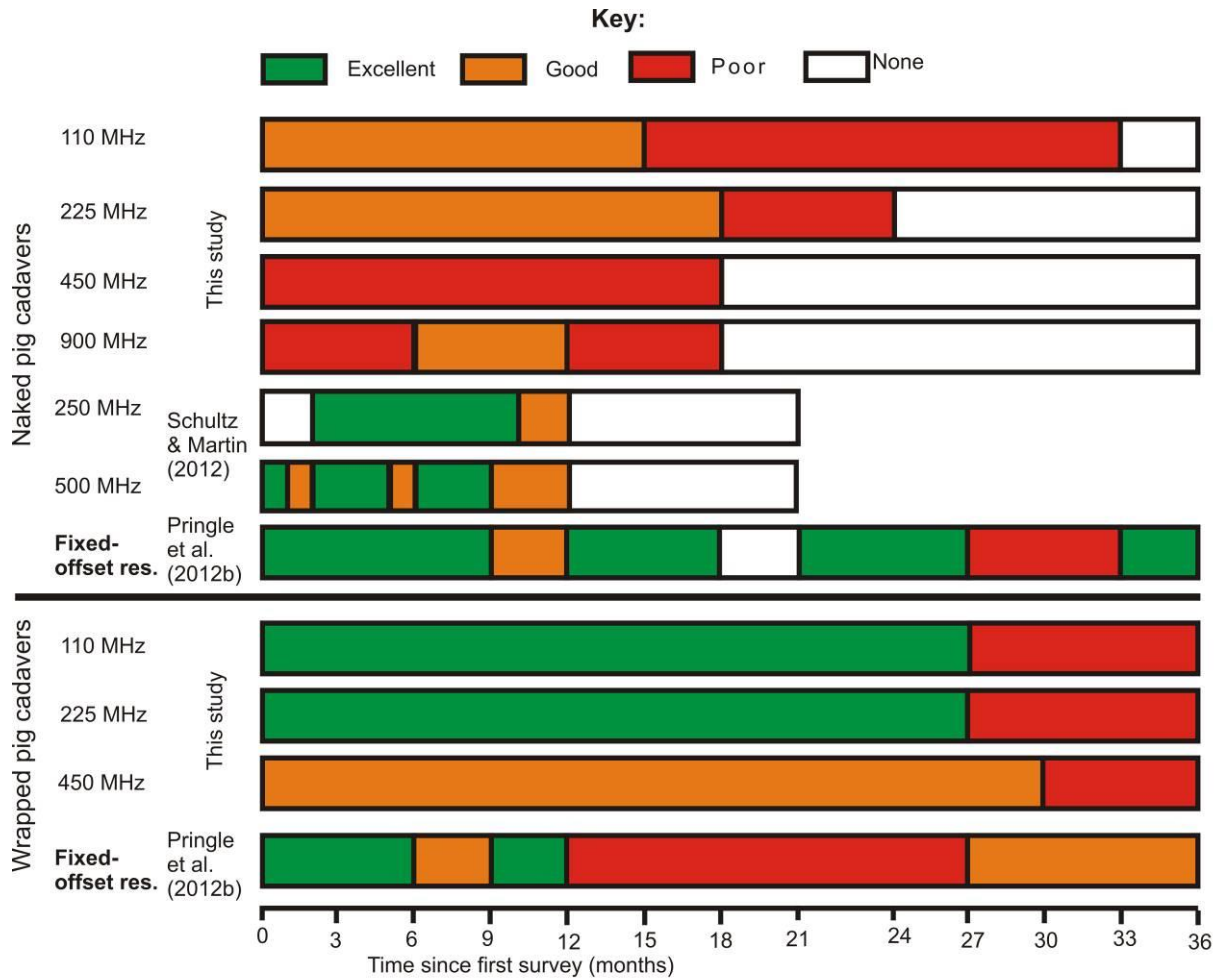


Figure 3.12. Graphical timeline of targets detected by GPR over simulated graves (key shows relative anomaly strength). GPR results from Schultz & Martin (2012) and fixed-offset electrical resistivity results from Pringle *et al.* (2012b) also shown for comparison. All graves in these studies were buried at 0.5 m bgl.

2. When is the optimal time (post-burial and seasonally) to undertake a forensic GPR geophysical search survey?

Based on the results of this study, a GPR survey should be undertaken ideally within the first 18 months of burial, if the burial style is unknown, as a ‘naked’ cadaver may be more difficult to locate after this time of burial (Figs. 3.5-3.8 and 3.12). Note, however, that other studies have shown favourable GPR survey results over much older burials in different ground conditions (e.g. (Davenport 2001; Strongman 1992; Bevan 1991). In this study, however, the time of year in which a GPR survey was undertaken did not seem to affect interpretation of 2D profiles, although the horizontal time-slice data showed ‘target’ anomalies to have lower amplitudes in winter surveys, possibly due to higher soil moisture contents (Jervis, 2010, for detailed analysis of site soil moisture for the first year of burial). This was in contrast to the resistivity surveys collected at this site (Jervis 2010; Pringle *et al.*, 2012b), in which data collected during winter to mid-spring months proved the best aid to detect a clandestine burial (Fig. 3.12). This has also been reported by Clark (1996) who undertook time-lapse resistivity surveys over UK Roman fortification defence ditches.

3. What effect does soil type have on a forensic geophysical survey’s success in detecting a burial?

This was more of a difficult question to answer. This study was undertaken on a study site with a sandy loam soil with an underlying shallow (>3 m bgl) sandy bedrock geology. Pringle *et al.*’s (2008) simulated clandestine burial in sandy soil did not find GPR to be particularly useful for detecting a grave, presumably due to the variety of non-target objects present in

typical urban environments. Pringle *et al.* (2012b) also concluded that finer-textured (i.e. clay-rich) soils, which better retain grave ‘fluids’, may provide better results than similar surveys undertaken in more sand-rich soils. The Schultz *et al.* (2006) GPR simulated burial study also concludes that pig cadavers were easier to locate in sandy rather than clay-rich soil types. Therefore it is suggested that resistivity surveys would be more favourable than GPR surveys in clay-rich soil study sites. However, the environment of deposition would also be a factor, for example, Eberhardt (2008) found decomposition rates varied significantly from cadavers in a coastal environment versus a rural field environment. Saline soil water, such as some soil types found in coastal foreshore environments, would also significantly attenuate radar signals and thus result in poor penetration depths of GPR signals in this environment as Pringle *et al.* (2012c) documents. An urban garden environment would also likely contain significant heterogeneity of subsurface materials, such as those observed in the Jervis *et al.* (2009b) study, which would make identifying potential target areas in GPR surveys in this environment problematic.

4. What is important when processing GPR survey datasets?

Reviewing this study results, clear hyperbola anomalies were present in the raw data 2D profiles acquired over the target ‘graves’ and thus only limited processing was necessary in order to identify their locations (*cf.* Figs. 3.5-3.8). This was similar to that found in the Schultz *et al.* (2006), Schultz (2008) and Schultz & Martin (2011) simulated studies. Horizontal time-slices were also generated from the 110, 225 and 450 MHz dominant antennae frequency datasets, where the simulated burial locations were mostly identifiable from isolated, high amplitude hyperbolae. However, there was also a significant number of isolated, high

amplitude hyperbolae present in the respective datasets which were not associated with the targets, which would make locating the targets difficult using time-slice data alone. This was also found in the Novo *et al.* (2011) forensic search in a mountainous environment and the Pringle *et al.* (2008) simulated study in an urban garden environment. Generating time-slices also takes significantly more processing time and may be difficult to undertake during a forensic active search, though could be undertaken later if time permitted. However, if the survey site ground conditions were moderately to highly heterogeneous then 2D profiles would be sufficient.

5. When should a forensic geophysical GPR survey be undertaken in a search scenario?

Comparing the results of this study to those of Nobes (2000), Ellwood *et al.* (1994), Powell (2004), Ruffell (2005), Ruffell *et al.* (2009), Pringle & Jervis (2010), Jervis (2010) and Pringle *et al.* (2012b), it is recommended that, depending upon the search area, forensic geophysical surveys should be undertaken prior to other, more invasive search methods (e.g. metal detectors, soil/methane probes and cadaver dogs). Due to the time spent collecting GPR data, some intelligence would be required, informing search teams of potential burial positions to reduce the size of the survey area, and thus time spent onsite and the amount of datasets requiring to be processing and interpretation. Once areas of geophysical interest within the survey area are identified, these should be prioritised and subsequently subjected to further detailed scientific investigations, which include other geophysical surveys (e.g. bulk ground resistivity surveys, higher frequency 2D/3D GPR surveys), cadaver dogs, invasive probing, etc.

3.5 Conclusions and further work

Geophysical survey results over the simulated clandestine burials in this study should be used as a reference for comparison with data collected by forensic investigation teams during searches for clandestine burials of murder victims.

A *buried 'naked' victim* within a clandestine burial, if shallowly buried, can potentially be located using GPR surveys if less than 18 months (~5,200 ADD) post-burial. GPR surveys are optimal in sandy soil environments whereas resistivity is optimal in clay-rich soils, due to the likelihood of highly conductive 'leachate' being retained in the surrounding soil and GPR experiencing poor penetration depths in these soil types (Jervis 2010; Pringle *et al.*, 2012b). GPR surveys would not be recommended if an advanced state of decomposition is anticipated (e.g. after significant post-burial time), although skeletal material could still be detected for shallow burial depths and preferably soil conditions. A buried 'wrapped' or clothed victim, if shallowly buried, is best located using medium (110-450 MHz) dominant frequency GPR antennae rather than resistivity methods, due to the 'wrapping' material producing a good reflective surface for the EM wave. Seasonality does not seem to affect the quality of GPR data, in contrast to electrical resistivity surveys (Jervis 2010; Pringle *et al.*, 2012b).

For forensic geophysical data processing, GPR data should present clear target hyperbola(e) in raw 2D data profiles in ideal ground conditions. However, in more heterogeneous ground, or where the time since burial is significant (after 18 months post-burial), then horizontal 'time-slices' could be generated to locate more subtle features that otherwise may be missed using 2D profile data interpretation alone. However, a variety of non-target anomalies may also be

present in time-slices, particularly in semi-urban or urban depositional environments, which may make locating forensic targets more problematic.

This study will be continued to discover *at what time* period after burial geophysical surveys will no longer be useful to determine the location of a clandestine burial. Further analysis of the geophysical data could also be undertaken; both to determine if there are diagnostic GPR signal spectra for clandestine burials versus background signals and to determine whether both GPR and resistivity datasets can be simultaneously inverted to identify not only location(s), but other physical features of the target(s).

This experimental methodology should be repeated in other, contrasting soil types, in order to determine whether soil type is a major factor in the ability of forensic geophysical surveys to successfully locate a clandestine burial. On a longer time scale, it is recommended that the experiment be repeated using human cadavers rather than pig analogues, as this may introduce other important, unforeseen variables.

Chapter 4 – GPR and bulk ground resistivity surveys in UK graveyards: locating unmarked burials and geophysical best practice in contrasting soil types

4.1 Introduction

U.K. graveyards and cemeteries are currently suffering from a chronic lack of burial space (London Planning Advisory Committee, 1997), with the need to accommodate ~140,000 burials every year (Environment Agency, 2004). A 2006 U.K. Government report listed less than one quarter of current burial grounds have room to accept new burials, with only 20% having designated land as yet unused, the latter expected to be filled within 25-30 years (Ministry of Justice, 2006). In some graveyards, reports suggest comparatively shallow graves are being utilised (Ministry of Justice, 2006). There has also been the rapid expansion of so-called ‘green’ burial sites, over 200 created in the UK since 2004 (Jim *et al.*, 2008) and with a variety of burial styles (Rumble, 2010). Re-use of existing graveyards and cemeteries is one solution, with U.K. burial regulation relaxations already in force in London boroughs (Ministry of Justice, 2006). However, burial records, if present, rarely indicate burial positions, and even gravestones are not always reliable indicators as Fiedler (2009) documents. In order to determine the positions of unmarked burials, probing methods (see Owsley, 1995) would not be deemed considerate of religious and social sensitivities, and thus the use of non-invasive detection techniques should be considered.

Other authors used remote sensing methods, including aerial photography and satellite imagery, to identify unmarked burials (see, e.g. Brilis *et al.*, 2000a,b). Ruffell *et al.*, (2009)

identified historic (150-160 years old) unmarked graves using aerial photographs and confirmed positions by subsequent geophysical surveying. Grave-site vegetation growth may also have different characteristics to background areas, e.g. different species and/or with more or stunted growth (Killam, 2004; Dupras *et al.*, 2006), which Larson *et al.*, (2011) attributes to localised pH changes and differing ground characteristics.

It is important to note that graves are quite different from clandestine burials (see Chapter 3; Pringle *et al.*, 2012a); burials in graveyards and cemeteries are commonly much deeper, have coffins and varying contents (Ruffell & McKinley, 2008), which Conyers (2006) cites as potential burial targets (Fig. 4.1). Average burial depths of clandestine graves are ~0.5 m bgl (Pringle *et al.*, 2012a) whereas typically isolated grave burials (Fig. 4.1) are ~1.8 m bgl (Cox & Hunter, 2005). Vaughan (1986) also points out that burials are difficult to detect due to their typically old-age, deep burial and limited, skeletal contents. The schematic Figure 4.1 is a generalisation, as there will be site specific variables, including soil type and local depositional environment (Harrison & Donnelly, 2009; Pringle *et al.*, 2012b), specific age of burials, burial style and decomposition rates, which have even been documented within the same burial site (Nobes, 1999).

One potential ground-based, non-invasive detection method is near-surface geophysics. Magnetic surveys are commonly used to detect near-surface geotechnical targets (Reynolds, 2011). Forensic magnetic surveys have had varied grave detection success: detection using magnetics for ancient archaeological graves have been successful (e.g. Linford, 2004), though Ellwood (1990) and Witten *et al.*, (2001) encountered difficulties in locating 19th century graves in cemeteries and a mass grave from 1921. Above-ground sources of magnetic interference seem to cause significant issues with this technique as

Pringle *et al.*, (2012b) note. Stanger & Roe (2007) concluded that fluxgate gradiometry was successful in detecting 20th century Australian cemetery graves.

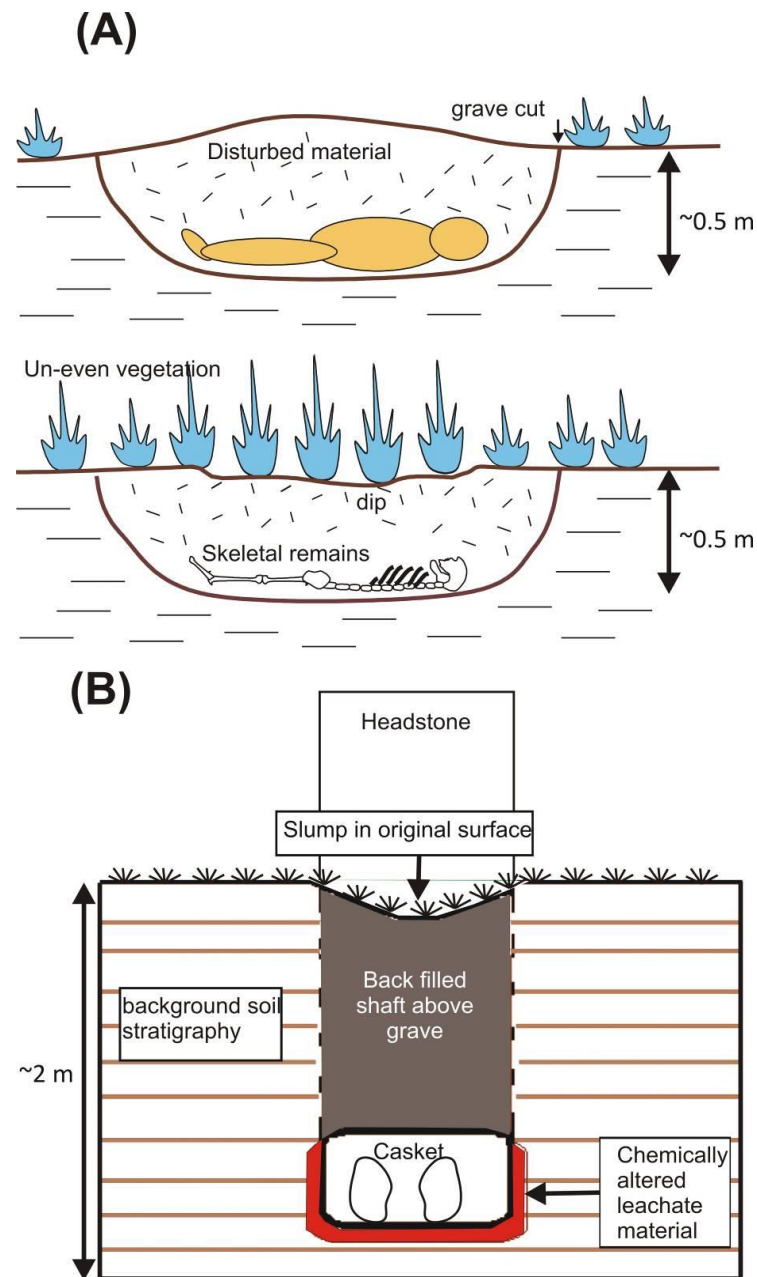


Figure 4.1. Generalised schematics of (A) typical clandestine grave with temporal changes (modified from Pringle *et al.*, 2012a). (B) An isolated grave burial in a cemetery or graveyard, with (1) post-burial soil, (2) shaft, (3) coffin and (4) contents identified geophysical targets named by Conyers (2006).

Electromagnetic (EM) surveys have shown to have variable detection success; Nobes (1999) attempted to locate unmarked graves in a New Zealand cemetery, but was largely unsuccessful due to the difficulty in differentiating target-related anomalies from background effects such as fence boundaries and local topography. Bigman (2012) undertook an EM survey over historic Native North American burial grounds and identified over 60 anomalies where previous excavations had found burials >2m bgl, and there were no above-ground structures present. Interestingly, Nobes (1999) found that the 'head' ends of unmarked graves were easier to identify than the 'foot' ends for reasons that were unclear.

Bulk-ground electrical resistivity surveys should be less affected by above-ground interference as probes/electrodes are physically inserted into the ground (see Chapter 2 and Milsom & Eriksen, 2011). There is also now evidence that the presence of decomposition fluids may be the dominant factor for clandestine grave detection (Jervis *et al.*, 2009; Pringle *et al.*, 2012a) which may be retained in grave soil for considerable periods post-burial (Juerges *et al.*, 2010). Resistivity surveys have been successfully used to locate unmarked burials in cemeteries (e.g. Buck, 2003; Powell, 2004 and Matias *et al.*, 2006), although local variations in soil moisture content, particularly in dry conditions in heterogeneous ground, affected many surveys by masking target locations (Ellwood *et al.*, 1990; 1994) and resulted in numerous non-target anomalies being imaged (see Chapter 3; Pringle *et al.*, 2012a). Milsom & Eriksen (2011) show that data acquisition from areas surrounding graves can be problematic due to the inability of probes to penetrate concrete, tarmac or other hard surfaces.

There are numerous published papers in which Ground Penetrating Radar (GPR) is employed to locate unmarked grave burials with varying degrees of success (Kenyon, 1977; Ellwood, 1990; Bevan, 1991; King *et al.*, 1993; Nobes, 1999; Powell, 2004; Watters & Hunter, 2004; Stanger & Roe, 2007; Fiedler *et al.*, 2009; Doolittle & Bellantoni, 2010). Ruffell *et al.*, (2009) and Davis *et al.*, (2000) both document searches for rapidly-dug grave burials for mass fatalities (Irish Potato famine and Spanish Flu victims, respectively) which were significantly shallower than 1.8 m bgl. GPR has become the geophysical tool of choice for unmarked graves due to detection success, lower susceptibility to above-ground interference (especially using shielded antennae) and, importantly, ability to determine the depth to target(s). However, this has resulted in GPR being applied without proper consideration for its limitations or optimal antennae frequencies, and where other methods may be more suitable. One potential issue arises where sites contain particular soil types; e.g. in clay-rich soils radar waves become rapidly attenuated resulting in poor penetration (see Chapter 2; Reynolds, 2011). This poses problems in the UK, where soil types are dominantly clay-rich (Chapman, 2005). GPR data processing also requires a good understanding of radar theory, and therefore either specialist operators or training of non-specialists; either of which is costly.

In 2009-10 an opportunity arose to assist in the detection of unmarked burials in three U.K. graveyards with clergy and archaeology teams. The overall aims of this forensic archaeology geophysical study were:

1. to identify the locations of any unmarked graves and/or burial plots/vaults within the respective survey areas. Identified remains could then be exhumed and re-interred elsewhere by archaeological teams (if necessary);

2. to compare GPR and resistivity geophysical equipment configurations, data acquisition strategies and processing methods to determine best practise;
3. to determine the effect of soil type;
4. to quantify the variety of U.K. burial styles.

4.2 Case Study 1: St. James' Church, Newchapel, Staffordshire, UK

4.2.1 Case study 1: Background

St. James' Church in Newchapel village (SJ 8623 5450) lies ~220 m above sea level on a hill in the north-east of Stoke-on-Trent, UK (Fig. 4.2). A clay-rich soil overlies the Carboniferous Coal Measures Formation sandstone bedrock. However, three boreholes drilled for site investigation (Fig. 4.2 for location) showed that the top 2 m bgl is comprised predominantly of 'made ground', gravelly-clay, occasional brick and coal fragments, with an average moisture content of 16% (Fairclough, 2008). A stone chapel, previously onsite before 1573 was rebuilt in brick in 1766 and 1777, and again in 1878-1915 due to mining subsidence (Cramp *et al.*, 2010). Burial within the churchyard was underway by 1722, although earlier interments may have taken place. The burial ground was periodically extended between the late 18th and early 20th century. In 2004 planning permission was granted for a community hall over part of the graveyard (Fig. 4.2). An existing plan identified 18 separate grave plots, within the proposed development area, each marked by memorial stone (Fig. 4.2 and Table 4.1). It was estimated that these plots represented the burial of up to 68 individuals, interred between 1821 and 1966.

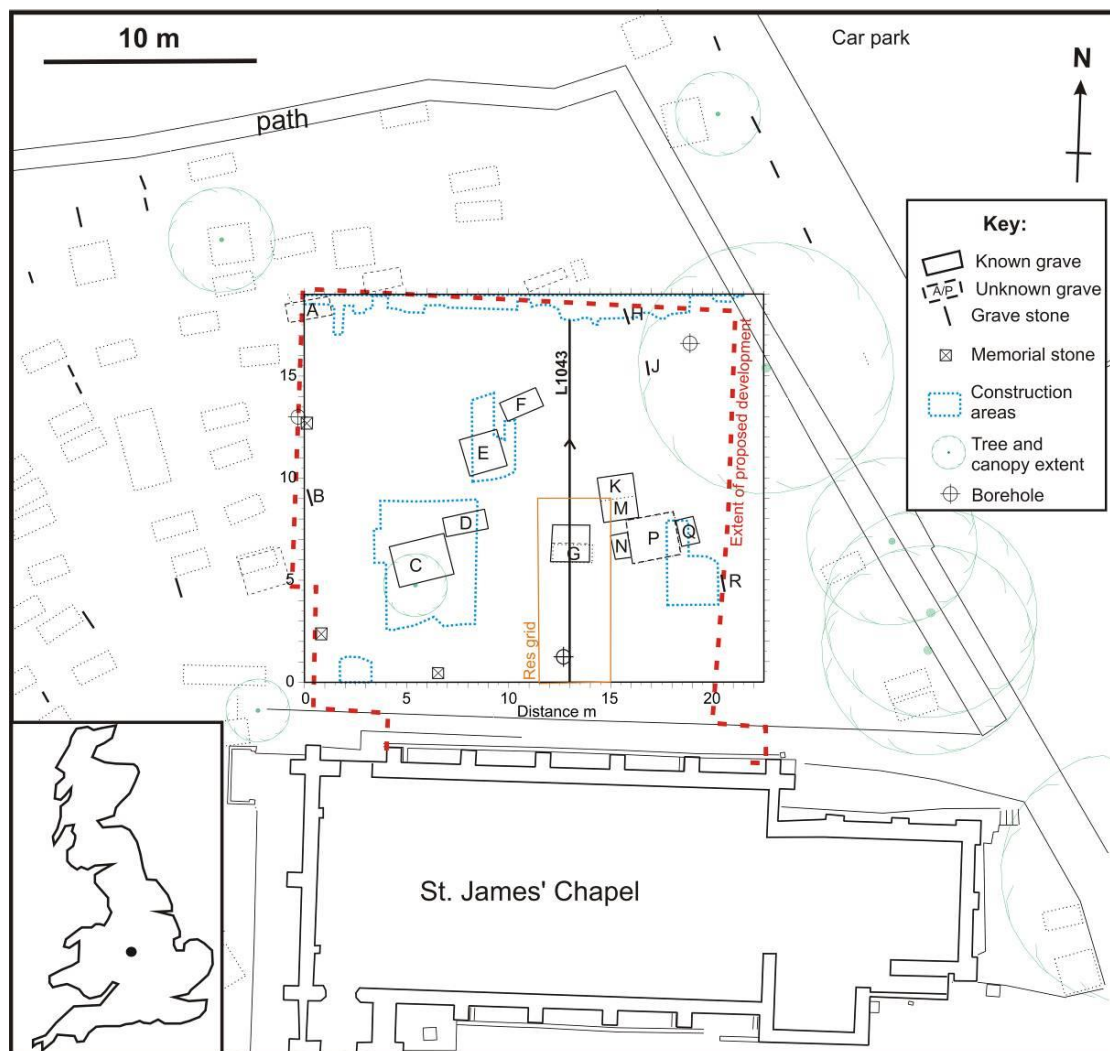


Figure 4.2. Map-view of case study 1 with location map (inset). Proposed building footprint, geophysical survey grid, trial GPR profile and grave positions shown (see key).

Grave	Nº of individuals	Burial Dates
A	Unknown	Unknown – not marked
B	6	1822, 1832, 1834, 1845, 1847, 1874.
C	8	1821, 1831, 1851, 1877, 1880, 1885, 1895, 1931.
D	4	1919, 1943, 1962, 1966.
E	13	1824, 1830, 1832, 1842, 1849, 1860, 1864, 1871, 1873, 1875, 1887, 1900, 1908.
F	2	1827, 1833.
G	5	1842, 1846, 1853, 1867, 1876.
H	3	1834, 1834, 1837.
J	1	1874
K	3	1881, 1882, 1895.
L	3	1846, 1868, 1874.
N	8	1817, 1824, 1854, 1867, 186(-9?), 1870, 1878, 1879.
P	Unknown	Unknown – not marked
R	4	1869, 1876, 1916.

Table 4.1. Summary of case study 1 expected burials (locations shown in Fig. 4.2).

After memorials had been cleared, an archaeological team were on site during the mechanical removal of ~1.4 m of soil within the development area. This operation not only revealed the presence of several known burials (Fig. 4.2), but also two unmarked graves (marked A and P in Fig. 4.2). Geophysicists at Keele University were subsequently contacted to help identify any additional unmarked burials within the area.

4.2.2 Case study 1: Geophysical data collection & processing

Upon arrival at the site on 23rd September 2009, three of the burials exposed within the survey area were already being excavated by the archaeologists (Fig. 3). A North-South orientated survey grid was established with 0.5 m spaced lines, avoiding both areas of archaeological excavations and ongoing construction work (Fig. 2). Trial GPR 2D profiles were collected over an exposed burial vault (Figs. 4.2 and 4.3b) using PulseEKKO™ 1000 225 MHz and 450 MHz dominant frequency antennae. After viewing the raw data on the data viewer, it was determined that 225 MHz frequency fixed-offset antennae were optimal on this site, due to good penetration depths and known graves being resolved, in addition to the relatively rapid speed of data collection and best practice recommendations (Ruffell *et al.*, 2009). The area was surveyed (Fig. 4.3a) using a 150 ns time window, 0.1 m trace interval and 32 constant signal stacks. This took ~8 hours to acquire and any potential graves identified in the raw data were marked for intrusive archaeological investigation. A Common-Mid Point (CMP) survey obtained onsite indicated a 0.07 m/ns average site velocity which was used to convert 2D GPR profiles from two-way time to depth following standard methodologies (Milsom & Eriksen, 2011).

Once the 2D GPR profiles were acquired, they were downloaded and imported into REFLEX-Win™ v.3.0 processing software. For each 2D profile, the sequential data

processing steps listed in Table 4.2 were applied. Absolute amplitude time-depth slices were generated at the likely burial depth, from which potential burials were identified based upon their size, orientation and dimensions. Finally the time-slices were imported into Generic Mapping Tools (GMT) software for visualisation purposes.

Step	Process	Description
1	Subtract mean (‘de-wow’)	Remove any positive or negative bias of the trace
2	Move start-time	Move traces to uniform time, based on common reflector: 0 ns here. This allowed all features of uniform depth below ground-level to appear uniform in GPR profiles.
3	1D Bandpass filter (Butterworth)	The upper/lower extents of frequency histogram removed.
4	2D filter Back-ground removal	Removes average from entire trace, removing interfering ‘ringing’ created during the bandpass filter stage
5	Gain function	Energy decay (SEC) function applied to enhance late arrival wave amplitudes.
6	Migration (Stolt)	Collapse hyperbolae to discrete focus points
7	Horizontal time-slice generation	Collapse specific time region across all profiles to create a ‘map-view’ of total amplitude over time/depth domains
8	Exported as xyz data file	Amplitude data exported as Z data into 0.25 m (X) x 0.025 m (Y) spaced .xyz file for graphical presentation

Table 4.2. Sequential GPR data processing steps used in these studies. Note 2D profiles were interpreted for target anomalies after step 5.



Figure 4.3. Photographs of case study 1 site, also showing (A) 225 MHz dominant frequency GPR and (B) bulk ground resistivity (0.5 m fixed-offset) data being collected. Note trial 2D GPR L1043 profile position over burial vault (Fig. 4.3) marked in (B).

A small, twin-probe (0.5 m fixed-offset) bulk-ground resistivity survey was also collected over a small area (Fig. 4.2) for comparison with the GPR data, using a Geoscan[™] RM15-D resistivity meter and PA20 probe-array (Fig. 4.3b). The mobile 0.10 m long stainless steel electrode probes were separated by 0.50 m, whilst the remote probes were placed 1.00 m apart at a distance of at 10.00 m from the survey position following best practice procedures (Milsom & Eriksen, 2011). For each 0.25 m spaced resistivity measurement on 0.50 m spaced profile lines, the mobile probes were inserted ~0.05 m into the ground. The data logger automatically collected and recorded resistivity measurements at each sample position. The whole RM15 survey took ~1 hour to acquire.

The resistivity data were downloaded from the resistivity meter, converted into XYZ format data and X,Y raw positions moved, where appropriate, before being processed in Generic Mapping Tools (GMT) software (Wessel & Smith, 1998) using the data processing steps listed in Table 4.3. To aid visual interpretation of the data, a minimum curvature gridding algorithm was used to interpolate each dataset to a cell size of 0.125 m by 0.125 m. Long-wavelength, trends were then removed from the data to allow smaller, grave-sized features to be more easily identified. Trend removal was achieved by fitting a cubic surface to the gridded data and then subtracting this surface from the data.

All processed map-view datasets were then combined with site satellite images, and archaeological and engineering information within CorelDRAW[™] v.12 graphical software.

Step	Process	Description
1	Conversion	Spatially-corrected data to XYZ in GMT (where applicable)
2	Gridding	Minimum curvature gridding algorithm interpolates data to a cell size of 0.0125 m by 0.0125 m to create smooth image
3	Detrending	Removal of long-wavelength trends from data by fitting a cubic surface to grid and then subtracting from surface data, allows small-wavelength features to be better distinguished
4	Normalisation	Dividing dataset by its SD Z value created grid with mean Z of ~0 and SD of ~1 allowing dataset comparison.

Table 4.3. Sequential electrical resistivity data processing steps used in these studies.

4.2.3 Case study 1: Geophysical results

Numerous discrete hyperbolic reflectors were observed on 2D GPR profiles at 10 – 40 ns ~0.4 – 1.2 m depth bgl (e.g. see Fig. 4.4). A number of different burial styles were interpreted from the data within the graveyard based on the character and depth of high amplitude hyperbolae (Fig. 4.4). Identified hyperbolae spatial positions and time-depths were graphically marked on the study map before potential unmarked burials and vault positions were interpreted. The positions of high amplitude regions in the horizontal time-slices were also compared to 2D profiles and grave marker positions (Fig. 4.5). Time-slices were then used to confirm the approximate depths of burials based on the presence (or lack thereof) of associated features, namely those representing east-west orientated rectangular anomalies. These features were ~1-2 m long, correlating with the approximate dimensions of isolated adult human burials (Fig. 4.5).

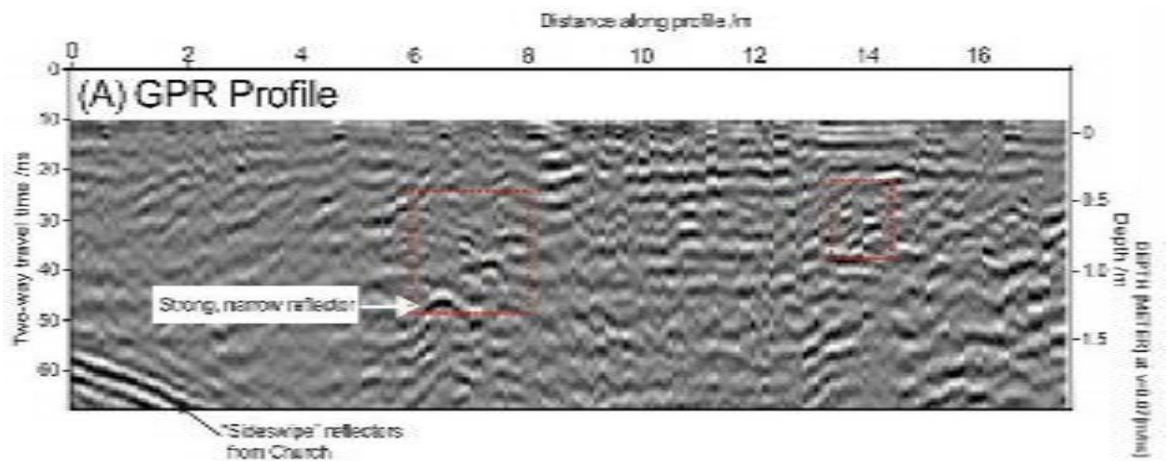


Figure 4.4. Processed 2D GPR profile L1043 (Fig. 4.5 for location). Modified from Hansen & Pringle, (2011).

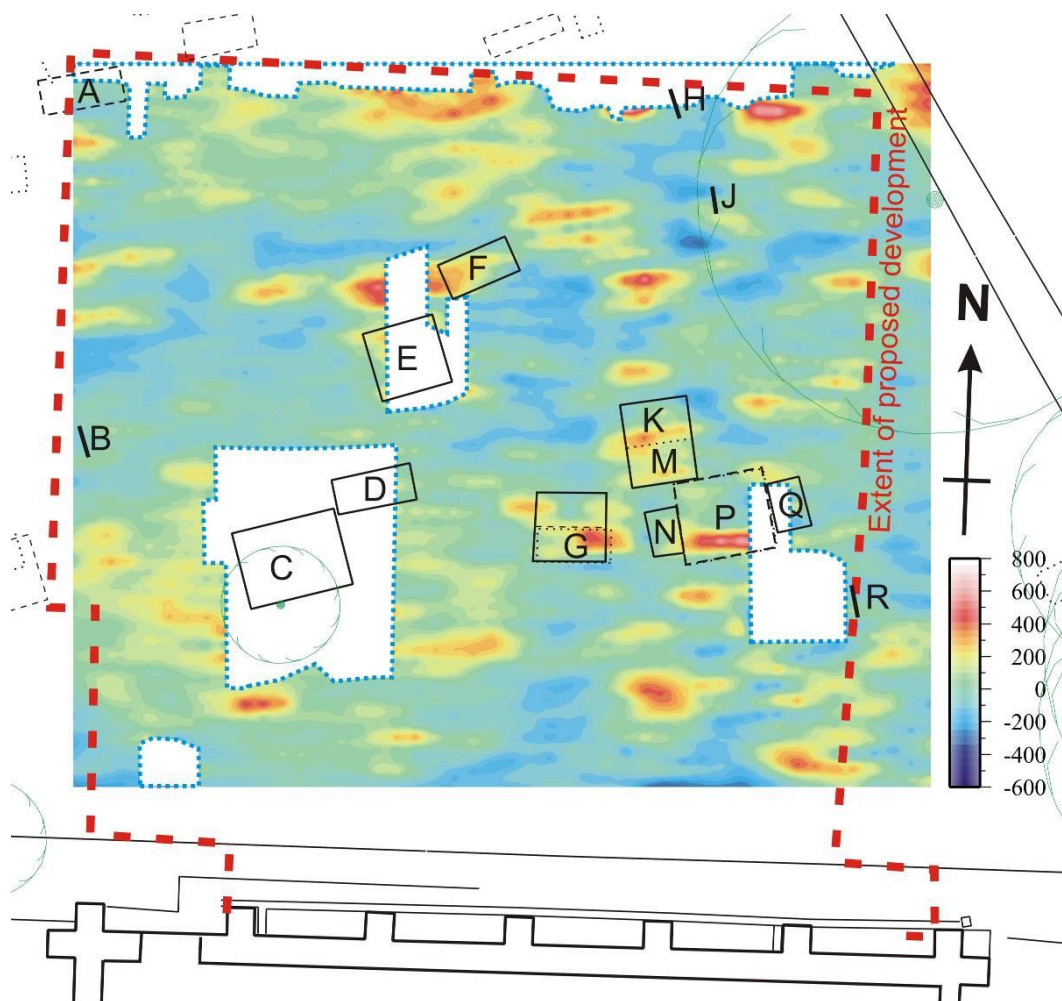


Figure 4.5. Map-view of GPR absolute amplitude 0-80 ns time-depth slice with background map. White areas indicate where 2D profiles could not be acquired. Modified from Hansen *et al.* (2014).

The raw resistivity dataset had 73/88/204.7 $\Omega\cdot\text{m}$ (minimum/average/maximum) values recorded with a 14.4 SD. A relatively high resistivity 2 m by 2 m anomaly, with respect to lower background values, was correlated to the double burial vault (G, Fig. 4.6). The highest relative resistivity values were at vault edges, suggesting low porosity construction material (e.g. brick, which was observed).



Figure 4.6. Map-view of processed bulk ground resistivity data with background map. Modified from Hansen and Pringle (2011).

After considering all of the geophysical data, it was suggested that there were an extra ten unmarked burials that were not previously identified (Fig. 4.7). Two main burial

orientations were observed in the known burials, some being concordant with the present church footprint but the majority at $\sim 20^\circ$ clockwise angle different from these (Fig. 4.7).

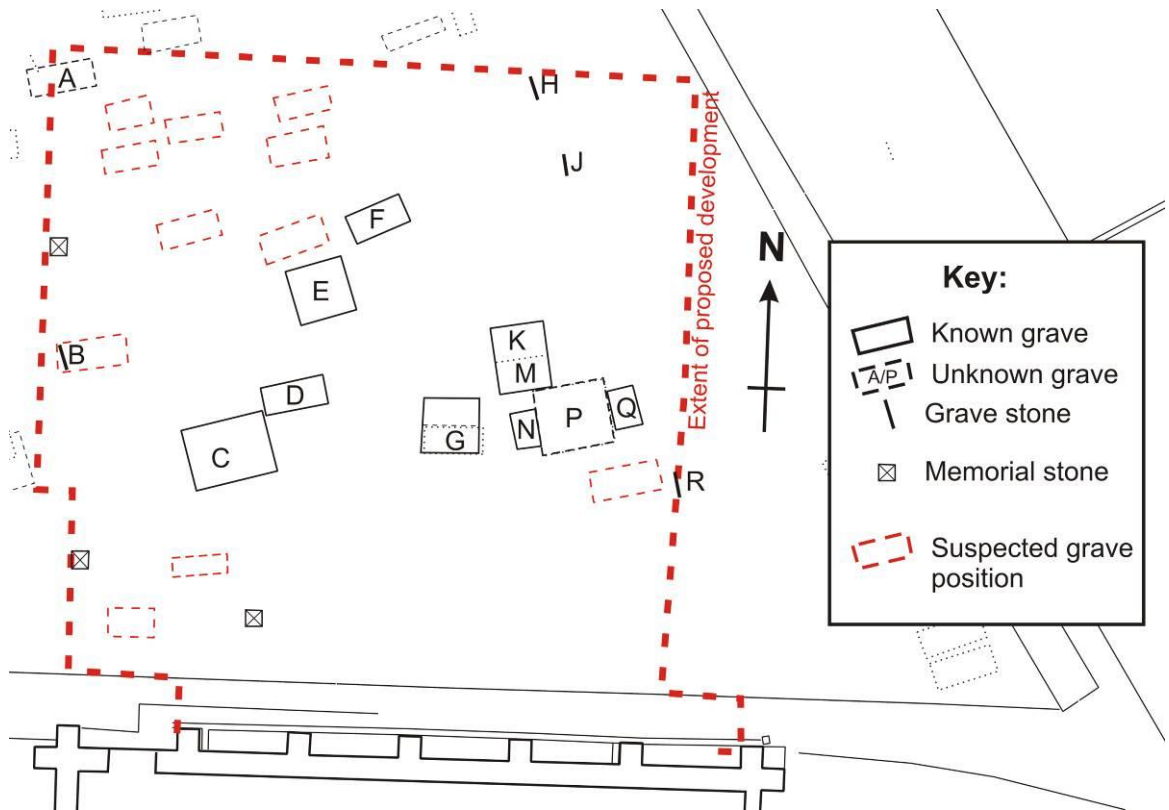


Figure 4.7. Case study 1 summary of known and unknown grave/vault positions. Modified from Hansen *et al.* (2014).

4.2.4 Case Study 1: Archaeology excavations

Archaeological excavation subsequently confirmed many of the interpretations from the geophysical data (Fig. 4.7 and Table 4.4). Seven confined burials were exhumed from three different burial environments within the graveyard: three from a single vault, three from brick-lined graves and one (A) from an unmarked earth-cut grave (Table 4.4). Vaults are brick-built, sub-ground chambers accessed via a discrete surface entrance which is sealed between interments (Stock, 1998). They are typically of sufficient area to accommodate

two burials positioned side by side and usually in layers (Litten, 1992; Buteux & Cherrington, 2006). In contrast, brick-lined (and indeed earth-cut) graves are wide enough in plan to take only a single coffin (and are often coffin-shaped), although they can be cut deep enough to take a stack of several interments, each separated by a stone slab.

The coffins, although in varying states of decay, all featured copper-alloy fittings, principally *deposita* (breastplates), but also grips (handles), grip plates, escutheons and carrying rings (Cramp *et al.*, 2010). Coffin ornamentation with such mass-produced items was a common practice during the 19th and early 20th centuries (Litten, 1992).

The excavated earth-cut grave (A) featured a single coffin placed directly into the ground. The brick-lined graves accommodated either one or two burials; the base of the single-interment (Eb) comprised un-mortared flagstones, whereas two stacked burials (Ea) used a suspended sandstone floor to separate the coffins (Fig. 4.8). An unusual glass viewing face panel was recovered from one coffin remains (CF200). The brick burial vault (C) contained four interments laid in pairs on two levels, separated by sandstone slab floor. The occupants belonged to one family and recorded on the monument that marked the burial site. The monument also commemorates an additional three individuals who were not present within the vault, suggesting that limited space was managed through intermittent removal of remains.

Grave / Vault & №	Dimensions*	Contents & burial date	Detailed description
Earth-cut grave A	2.2 m × 0.75 m × 0.85 m	1 adult, unknown	Wood coffin rotted but skeletal remains in good condition
Vault C	2.10 m × 1.35 m x 0.9 m deep	3 adults and 1 juvenile, 1880 - 1913	Crudely lime-mortar jointed, double-skinned red brick walls. Slate roof with 3 stone capping slabs ~0.15 m thick. Wood coffins completely rotted, skeletal remains varied from 2 complete and 2 poor.
Brick-lined grave E _a	2.5 m × 0.25 m × 1.25 m deep	2 adults, 1873 and 1887.	Curvilinear in shape (following coffin), 1 red brick thick wall, horizontal flagstone in between. Wood coffins rotted but skeletal remains in fair condition.
Brick-lined grave E _b	2.5 m × 0.25 m × 1.25 m deep	1 adult, 1908	Curvilinear, one red brick thick lined. Wood coffin rotted but skeletal remains in good condition
Brick-lined grave H	2.6 m × 0.25 m × 0.75 m deep	1 adult, 1887	Curvilinear, one red brick thick lined, with sandstone slab atop. Wood coffin rotted but skeletal remains in fair condition.

Table 4.4. Relevant archaeological characteristics of the case study 1 excavated burials (after Cramp *et al.*, 2010a). Condition categories for human remains: *Good* = bones complete, *Fair* = bones mostly complete, *Poor* = Bones incomplete and/or damage/erosion. Burial letter locations marked in Fig. 4.4. *Note depths are based on excavation after removal of 1.4 m topsoil. Modified from Hansen *et al.* (2014).

(A)



(B)



Figure 4.8. Case Study 1 archaeology excavation photographs of (A) single brick-lined grave H and (B) double brick lined family vault C with 0.5 m scale bars. See Table 4.4 for details. Modified from Cramp *et al.*, (2010).

4.3 Case Study 2: St. Luke's, Endon, Staffordshire, UK.

4.3.1 Case study 2: Background

St. Luke's Church in Endon village (SJ 9281 5380) lies ~190 m above sea level on a hill 10 km north-east of Stoke-on-Trent, U.K. (Fig. 9). A coarse sandy soil containing, predominantly, sandstone pebbles overlies the Triassic Hawkesmoor Formation sandstones and conglomerate bedrock geology. The Audley family established a chapel in the 13th century (Tringham, 1996), although the exact location and date it fell into disuse is unknown (Speake, 1974). The present church was constructed between 1719 and 1721 (Speake 1974), with periodic alterations in 1830, 1870, 1970 and 1981.

The first recorded burial in the grounds was in March 1731 and by 1830 part of the churchyard had been turned into a garden with landscaping at the western reach shortly thereafter (Speake 1874). The graveyard was extended in 1898 and it is likely that some burial relocation and memorial clearance took place (Kelly, 1921). Additional monuments were removed in the mid-1970s (Sutherland, 2012). Planning permission for single-storey extensions to the west and north was granted in 2007. The construction of both buildings would impact upon adjacent burials, some of which had headstones and Grade II Listed chest tombs (Fig. 4.9). The northern side church extension was geophysically surveyed on the 20th and 21st October 2010. The west extension area was not surveyed due to the presence of steps and hard paths which would limit the use of much of the equipment (Fig. 4.9).

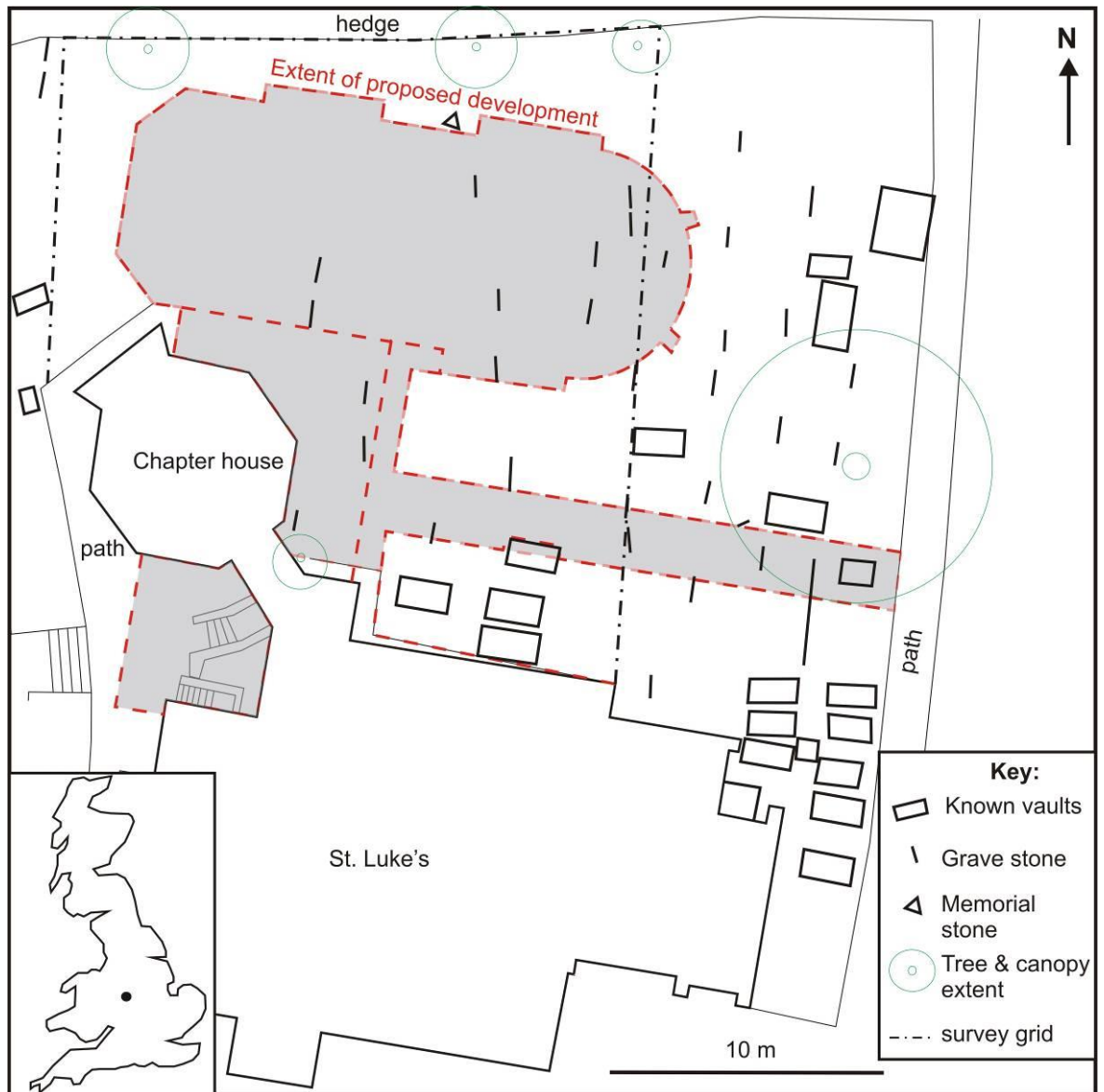


Figure 4.9. Map view of St. Luke's Church, Endon, Staffordshire, study site with location map (inset). Proposed building footprint (red rectangle) position shown (see key). Modified from Hansen *et al.* (2014).

4.3.2 Case study 2: Geophysical data collection and processing

Observed grave stones were all E-W oriented as is common for UK burials (Litten, 1992), A N-S orientated survey grid was therefore established with 0.5 m spaced lines (Fig. 4.9). Trial GPR 2D profiles were collected over a known burial position using available

PulseEKKO™ 1000 dominant frequency antennae, from which it was determined that 225 MHz frequency fixed-offset antennae were optimal on this site as per Case Study 1 recommendations. The full survey grid was then surveyed (Fig. 4.10) using a 80 ns time window, 0.1 m trace intervals and 32 constant signal stacks. A CMP survey was also obtained onsite to gain a 0.12 m/ns average site velocity to convert 2D GPR profiles from two-way time to depth. The GPR survey took ~12 hours to acquire. As resistivity surveys had shown great potential to detect burials in Case Study 1, a full survey dataset was acquired using the Geoscan™ RM15-D resistivity meter and PA20 probe-array. Sample positions were acquired using a twin-probe at both 0.5 m and 1.0 m fixed-offset probe spacings (Fig. 4.10b), using the same methodology as Case Study 1. Contact resistances were very high and needed remote probe separations to be >1.5 m, though a number of sample points were still over the recordable range. The RM15 survey took ~8 h to acquire.

Both GPR and resistivity dataset processing was the same as for Case Study 1 (see section 4.1.2). All processed map-view datasets were combined with site satellite images, archaeological and other information within CorelDRAW™ v.12 graphical software.

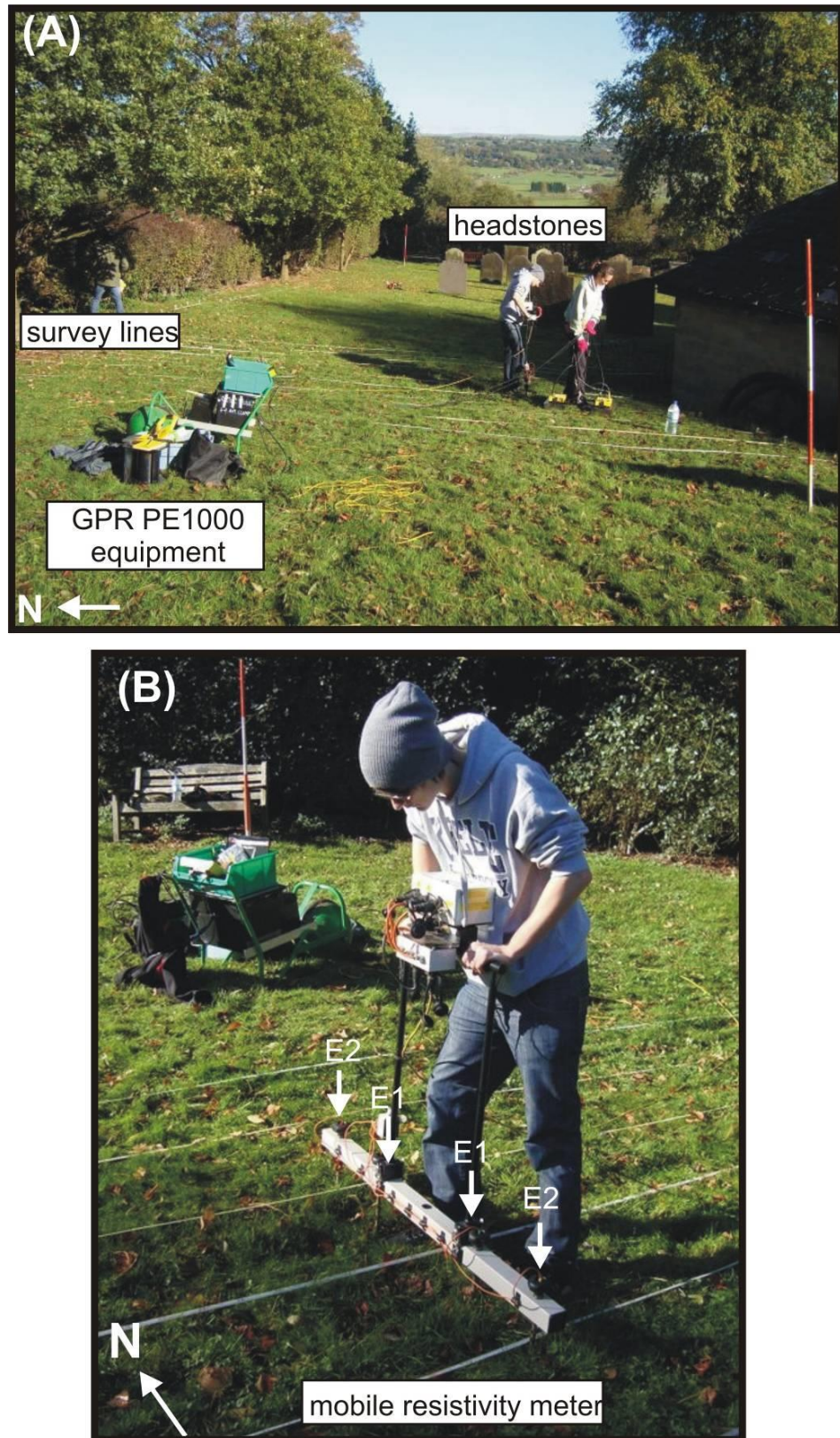


Figure 4.10. Photographs of case study 2 site, also (A) 225 MHz dominant frequency GPR and (B) bulk ground resistivity 0.5 m (E1) and 1 m (E2) fixed-offset data being collected. Modified from Hansen *et al.* (2014).

4.3.3 Case study 2: Geophysical results

Multiple discrete hyperbolic reflectors were observed on 2D GPR profiles at 8 – 20 ns corresponding to ~0.6 – 1.8 m depth bgl (for example, see Fig. 4.11). Most potential burials seemed to be earth-cut graves, based on the narrow shape and depths of high-amplitude waveforms (*cf.* Figs. 4.4 and 4.11). Spatial positions and depths of identified hyperbolae were marked on the map of the study area. The positions of high-amplitude regions observed in horizontal time-slices were also compared to 2D profiles and grave marker positions (Fig. 4.12). Time-slices were used to confirm the approximate depths of burials based on the presence (or lack thereof) of associated features also observed in time-depth slices. High priority features were elongate regions of high amplitude in east-west orientation. These features were ~1–2 m long, correlating with approximate dimensions of isolated adult burials (Fig. 4.12).

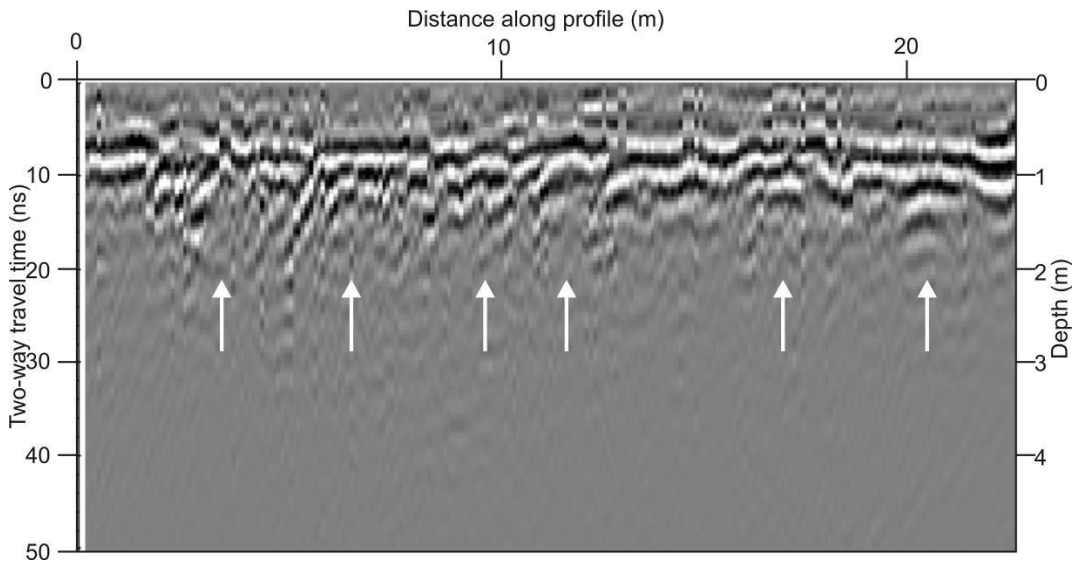


Figure 4.11. (A) Processed 2D GPR profile L45 (Fig. 4.12 for location) with suggested burial locations marked (arrows). Modified from Hansen *et al.* (2014).

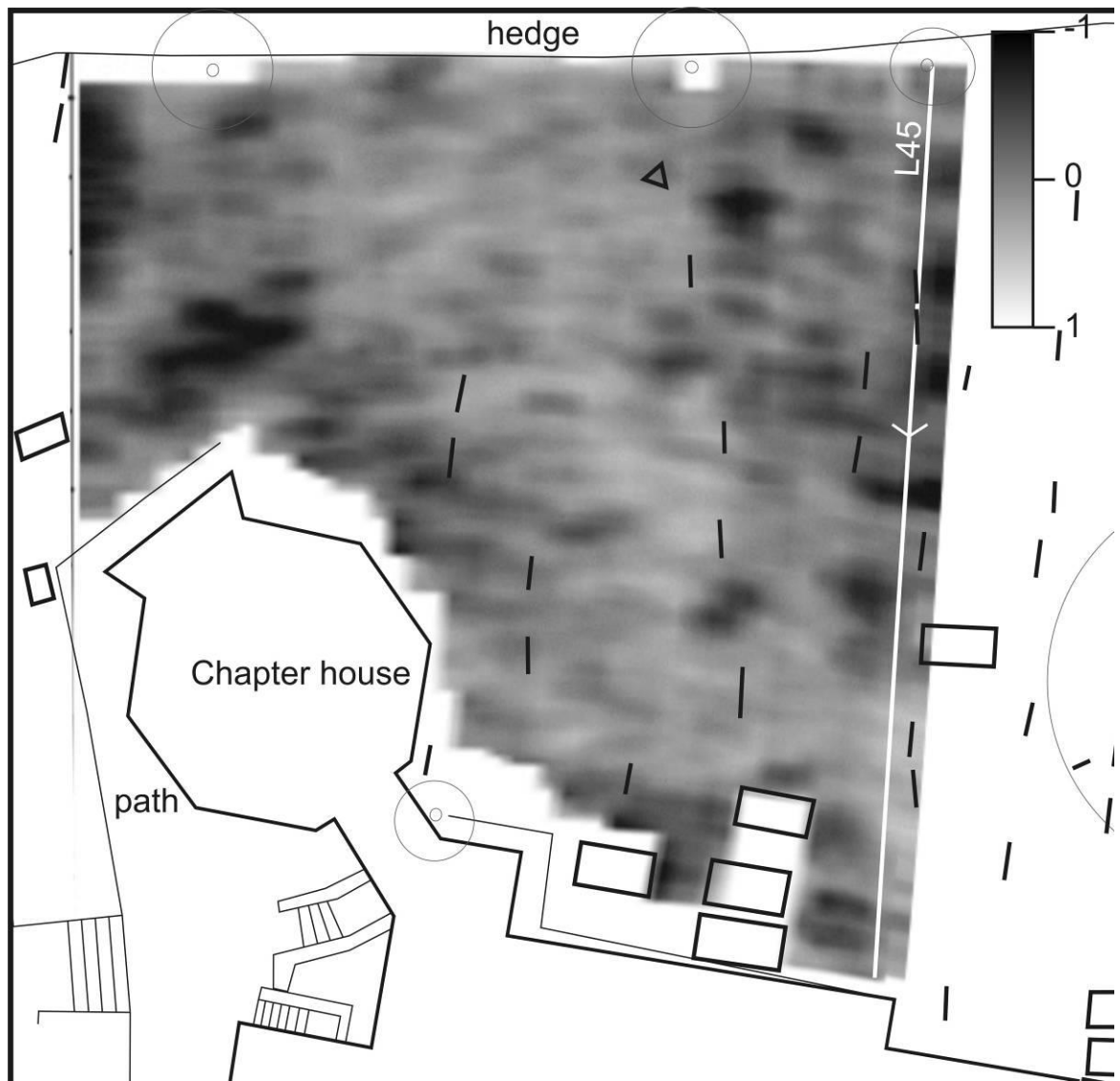


Figure 4.12. Mapview of GPR absolute amplitude 20-40 ns time-depth slice with background map. Modified from Hansen *et al.* (2014).

The raw 0.5 m fixed-offset probe spacing resistivity dataset had 26/89.9/204.7 $\Omega.m$ (minimum/average/maximum) values recorded with a 37.9 Standard Deviation (SD). The raw 1.0 m fixed-offset probe spacing resistivity dataset had -91.7/71.8/204.5 $\Omega.m$ (min./av./max.) values recorded with a 56.6 SD. It was not possible to acquire data for ~43% of the survey area using the 1 m separated (fixed-offset) mobile probes, therefore the remaining data have been omitted. The processed 0.5 m spaced resistivity dataset is shown in Figure 4.13. There were no clear burial-sized anomalies present in this dataset,

though a relatively high resistivity region correlates with tree positions and a cluster of gravestones at the east of the survey area (Fig. 4.13).

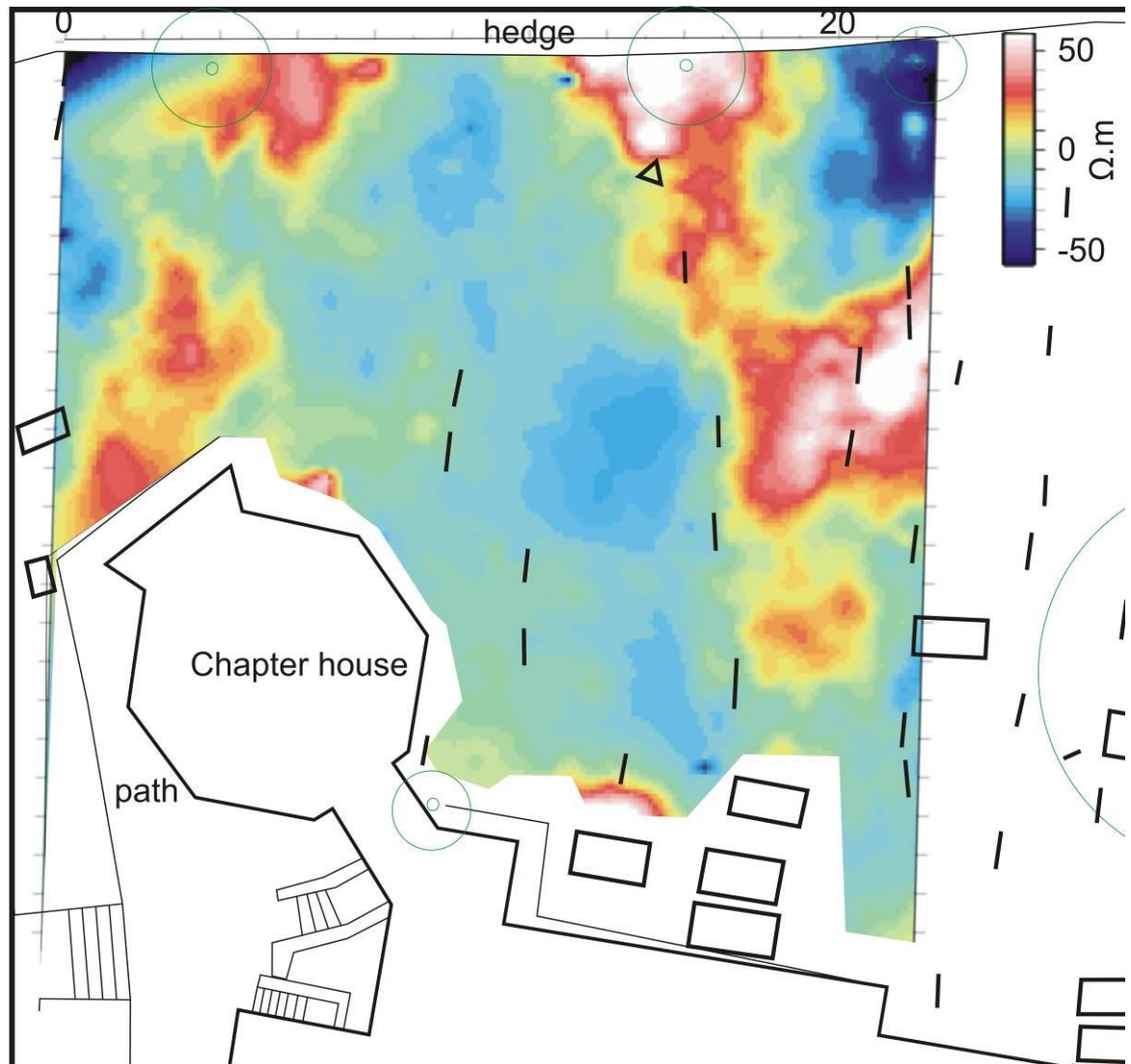


Figure 4.13. Map view of the processed bulk ground resistivity (0.5 m fixed-offset) probe spacing dataset with background map. Modified from Hansen *et al.* (2014).

Combining the geophysical results with the surviving surveyed headstone data, it was suggested that there were an extra nineteen unmarked burials that were not previously identified (Fig. 4.14).



Figure 4.14. Case Study 2 summary of known and unknown grave/vault positions. Modified from Hansen *et al.* (2014).

4.3.4 Case study 2: Archaeology excavations

An archaeological evaluation was undertaken within the western extension area (Fig. 4.9). This showed fifteen earth-cut graves, two of which (G03 and G10) were intercut with one another. Four (G01/G02 and G05/G08) were stacked in pairs, perhaps indicating family plots (Fig. 4.15 and Table 4.5). Average burial depth was 1 m bgl (minimum burial depth was 0.80m bgl, the maximum 1.25m bgl) although this was ~1 m below present ground level. All burials contained coffins, although both caskets and skeletal remains were typically in poor condition; five showed evidence of post-burial disturbance. Copper-alloy and iron coffin furniture were present in many cases, but were generally poorly preserved.

Conversely, three graves (G03, G05 and G14) included well-preserved items of clothing and footwear.

Grave №	Dimensions	Contents & burial date	Coffin & individual description
G01/2 Fig.4.15	2.0 m x 0.5 m x 0.8 m bgl	2 adults (unknown)	Wood coffins completely rotted, skeletal remains fair and disturbed
G03	2.0 m x 0.25 m x 0.8 m bgl	1 adult d. 1963	Wood coffin, skeletal remains fair
G04	1.5 m x 0.25 m x 0.8 m bgl	1 adult, d. 1894?	Wood coffin stain only, incomplete set skeletal remains poor.
G05/8 Fig.4.15	2.00 m x 0.5 m x 0.9 and 1.2 m bgl	2 adults	Wood coffin rotten, adipocere present, skeletal remains fair
G06	1.5 m x 0.25 m x 1.2 m bgl	1 adult	Wood coffin fragments, incomplete skeletal remains poor and disturbed
G07	0.6 m x 0.3 m x 0.8 m bgl	1 adult, d. 1875?	Coffin stain only, no surviving human remains
G09	2.0 m x 0.5 m x 1.0 m bgl	1 adult, below G02	Wood coffin rotten, skeletal remains poor
G10	2.0 m x 0.5 m x 1.15 m bgl	1 adult, below G03	Coffin stain only, skeletal remains poor and disturbed
G11	0.5 m x 0.25 m x 0.8 m bgl	1 adult, d. 1926?	Coffin stain only, no surviving human remains
G12/13	0.5 m x 0.25 m x 1.0 m bgl	2 juveniles	Wood coffin fragments, incomplete skeletal remains poor
G14	2.0 m x 0.75 m x 1.25 m bgl	1 adult	Wood coffin fragments, incomplete skeletal remains poor and disturbed
G15	1.0 m x 0.25 m x 1.1 m bgl	1 adult	Wood coffin fragments, incomplete skeletal remains good

Table 4.5. Relevant archaeological characteristics of the case study 2 excavated burials.

Individual conditions: *Good* = bones complete, *Fair* = bones mostly complete, *Poor* = bones incomplete and/or damage/erosion. Modified from Sutherland (2012).

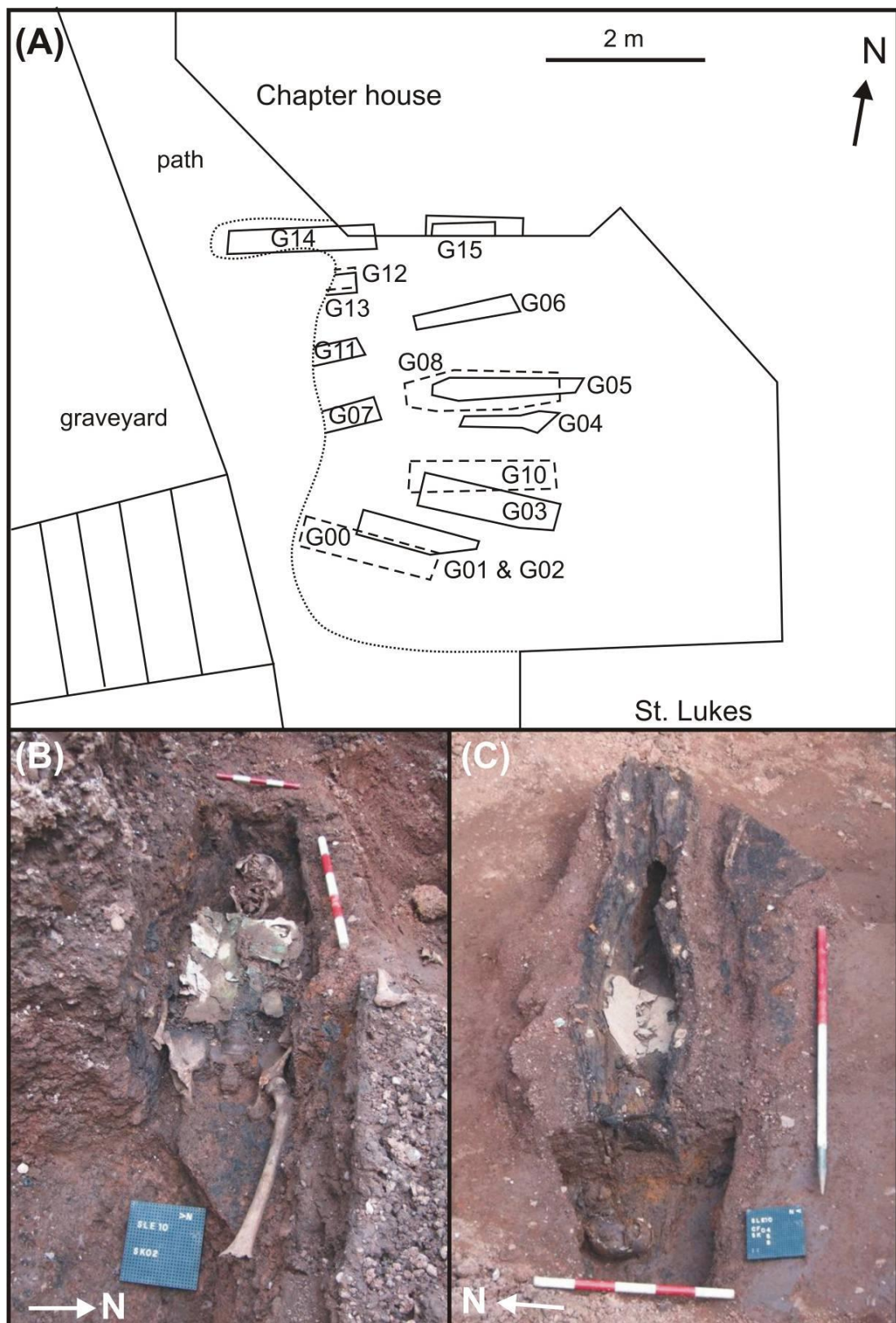


Figure 4.15. Case Study 2 archaeological excavation; (A) map, (B) G02 and (C) G5/08 photographs of earth-cut graves with 0.5 m scale bars (modified from Sutherland, 2012). See Table 4.5 for details. Modified from Hansen *et al.* (2014).

4.4 Case Study 3: St. John of Jerusalem, Hackney, London, UK.

4.4.1 Case study 3: Background

St. John of Jerusalem church in South Hackney (TQ 3555 8455) lies ~15 m above sea level around 10 km north-east of the centre of London, UK (Fig. 4.16). The Hackney Gravel Member alluvium soils overlies the Eocene London Clay Formation bedrock geology. The present stone church was completed in 1848 and the graveyard was filled by 1868. The stone spire replaced by copper after bomb damage during WW2 (Taylor, 2002). Grave stones from significant areas of the graveyard were removed at some period during the 1960s (Rev. A. Wilson, *pers. comm.*), leaving large areas of the graveyard unmarked. However, elongate depressions were observed in the graveyard, together with some exposed, broken head stone bases and remaining stone tombs which may or may not be *in situ* (Fig. 4.17). The church vicar was planning for an extension on the west of the church over part of the graveyard (Area A) and also wished to know the location of unmarked burials in another area of the graveyard (Area B) (see Fig. 4.16). The site was topographically and geophysically surveyed on the 9th – 10 September 2010.

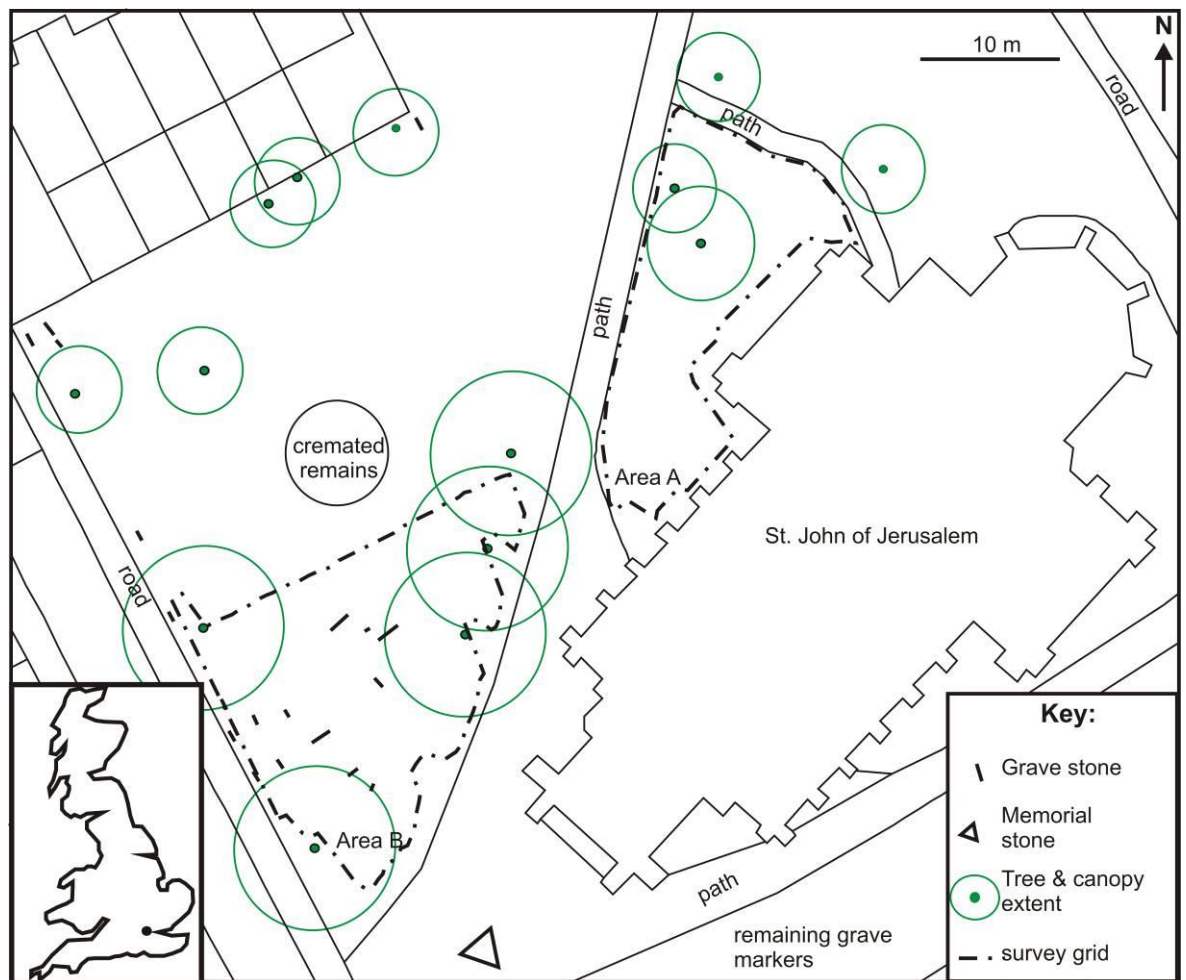


Figure 4.16. Plan-view of Case Study 3 with location map (inset). Proposed building footprint, geophysical survey grids, trial GPR profile and grave positions shown (see key). Modified from Hansen *et al.* (2014).



Figure 4.17. Photographs of case study 3 site of (A) Area 1 and (B) Area 2 with remnant headstone (inset). GPR and bulk ground resistivity 0.5/1 m fixed-offset data collection also shown. Modified from Hansen *et al.* (2014).

4.4.2 Case study 3: Geophysical data collection & processing

Remaining grave stones and visible snapped head stone bases (Fig. 4.17b) were topographically surveyed within both survey areas. A N-S orientated survey grid was constructed over both survey areas with 0.5 m – spaced lines (Fig. 4.17), avoiding trees and densely vegetated borders (Fig. 4.16). Trial GPR 2D profiles were collected over suspected burial depressions in both areas, from which it was determined that 450 MHz dominant frequency antennae were optimal in Site A and 225 MHz in Site B as per Case Study 1 recommendations. Area A was surveyed (Fig. 4.17a) using the 450 MHz antennae with a 80 ns time window, 0.05 m trace intervals and 32 constant signal stacks. Area B was surveyed (Fig. 4.17b) with the 225 MHz antennae using a 100 ns time window, 0.1 m trace intervals and 32 constant signal stacks. A CMP survey was also obtained onsite to gain a 0.1 m/ns average site velocity which was used to convert 2D GPR profiles from two-way time to depth. The GPR survey took ~14 h to acquire. Both survey grids were also surveyed using the Geoscan™ RM15-D resistivity meter and PA20 probe-array. Data were again acquired using a twin-probe array at both 0.5 m and 1 m fixed-offset spacings simultaneously (Fig. 4.17b), using the same methodology as Case Study 2. The RM15 survey took ~10 h to acquire. In the west part of Area B, a number of animal burrows were present (including one ~0.5 m by 0.25 m) into which an urban fox was observed entering.

Both GPR and resistivity dataset processing followed the same routine as for Case Study 1 (see section 4.1.2). All processed plan-view datasets were combined with site satellite images, archaeological and other available information within CorelDRAW™ v.12 graphical software.

4.4.3 Case study 3: Geophysical results

In Area A, multiple discrete hyperbolic reflectors were observed in 2D profiles at 5 – 20 ns (~0.2 – 1.0 m depth bgl) (e.g. Fig. 4.18a). In Area B, multiple discrete hyperbolic reflectors were also observed in 2D profiles at 10 – 40 ns (~0.5 – 1.5 m depth bgl) (e.g. Fig. 4.18b). Most burial positions indicated isolated earth-cut graves, based on the narrow, shallow high-amplitude hyperbolae, which were similar to those observed at the locations of confirmed graves in Case Study 1 (*cf.* Figs. 4.4 and 4.18). Identified hyperbolae spatial positions and time-depths were graphically marked on the plan of the survey area.

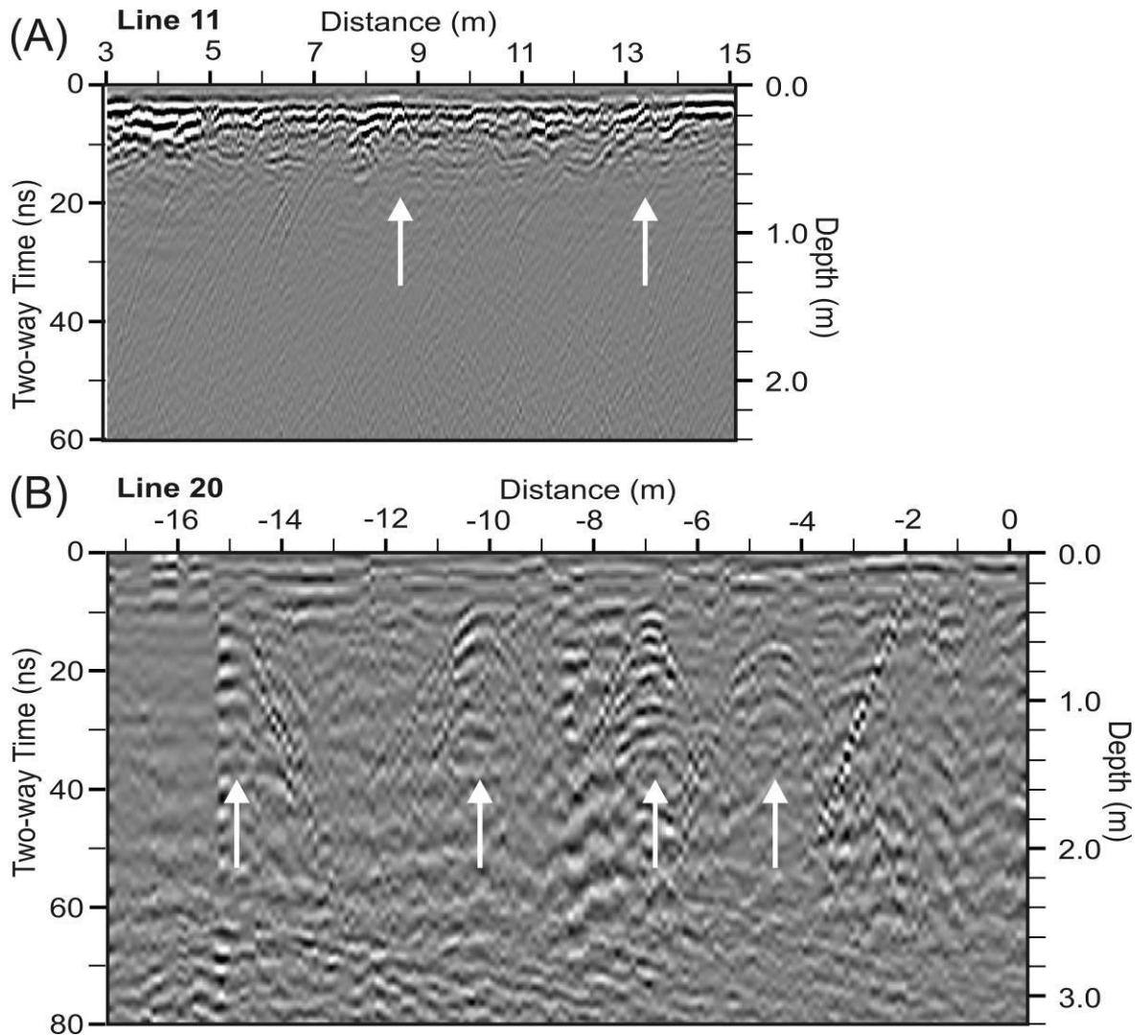


Figure 4.18. (A) Processed 2D GPR profile L11 from Area A and L23 from Area B (Fig. 4.19) with burial locations marked (arrows). Modified from Hansen & Pringle (2011).

High-amplitude GPR anomaly positions in horizontal time-slices were also compared to 2D profiles and grave marker positions (Fig. 4.19). Time-slices were used to confirm the approximate depths of burials based on presence (or lack thereof) of associated features at time-depth slices, with anomalies occurring as northeast-southwest orientated elongate regions. These features were ~1-2 m long, correlating with approximate dimensions of isolated adult burials (Fig. 4.19).

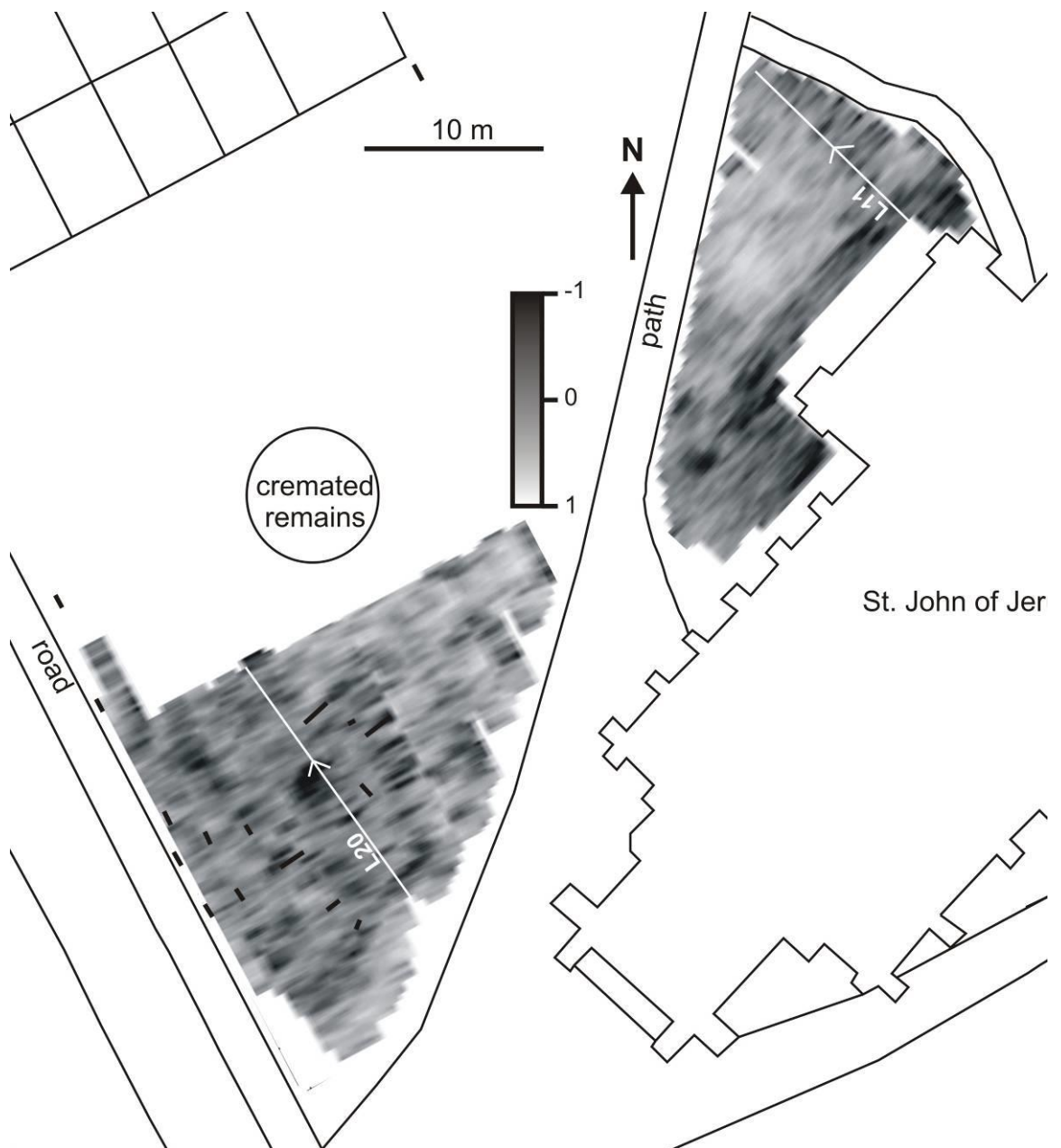


Figure 4.19. Mapview of GPR absolute amplitude 9-35 ns time-depth slices with background map. Modified from Hansen *et al.* (2014).

For Area A, the raw 0.5 m fixed-offset probe spacing resistivity dataset had 74/101/178 $\Omega\cdot\text{m}$ (minimum/average/maximum) values recorded with a 11.8 Standard Deviation (SD). The raw 1.0 m fixed-offset probe spacing resistivity dataset had 55.6/73.1/200 $\Omega\cdot\text{m}$ (min./av./max.) values recorded with a 7.2 SD. For Area B, the raw 0.5 m fixed-offset probe spacing resistivity dataset had 49/114.7/204.7 $\Omega\cdot\text{m}$ (minimum/average/maximum) values recorded with a 29.8 Standard Deviation (SD). The raw 1.0 m fixed-offset probe spacing resistivity dataset had -1.4/68.6/204.5 $\Omega\cdot\text{m}$ (min./av./max.) values recorded with a 11.5 SD. The processed 0.5 m and 1 m probe-spaced resistivity datasets are shown in Figures 4.20 and 4.21 respectively. There were numerous burial-sized anomalies present in these datasets; note the large relatively high resistivity anomaly area in the south-west of Area B could be correlated with the observed fox den burrow.

In Area A the geophysical results suggested there were thirteen unmarked burials (Fig. 4.22). In Area B four potential burials were located by partially-buried, damaged headstone bases, and the geophysical data here additionally suggested that there were an extra forty-six unmarked burials which were not previously identified (Fig. 4.22).

4.4.4 Case study 3: Geophysical validation

Unfortunately there was no subsequent archaeological excavation to confirm the geophysical survey results. However, part of the graveyard to the south of the church (~200 m²) contained 21 intact grave markers, orientated NE-SW, predominantly isolated (presumably) earth-cut graves with two family vaults containing four individuals. The geophysical survey results, which has interpreted predominantly earth-cut grave, would seem to confirm a similar style to the observed intact grave markers.

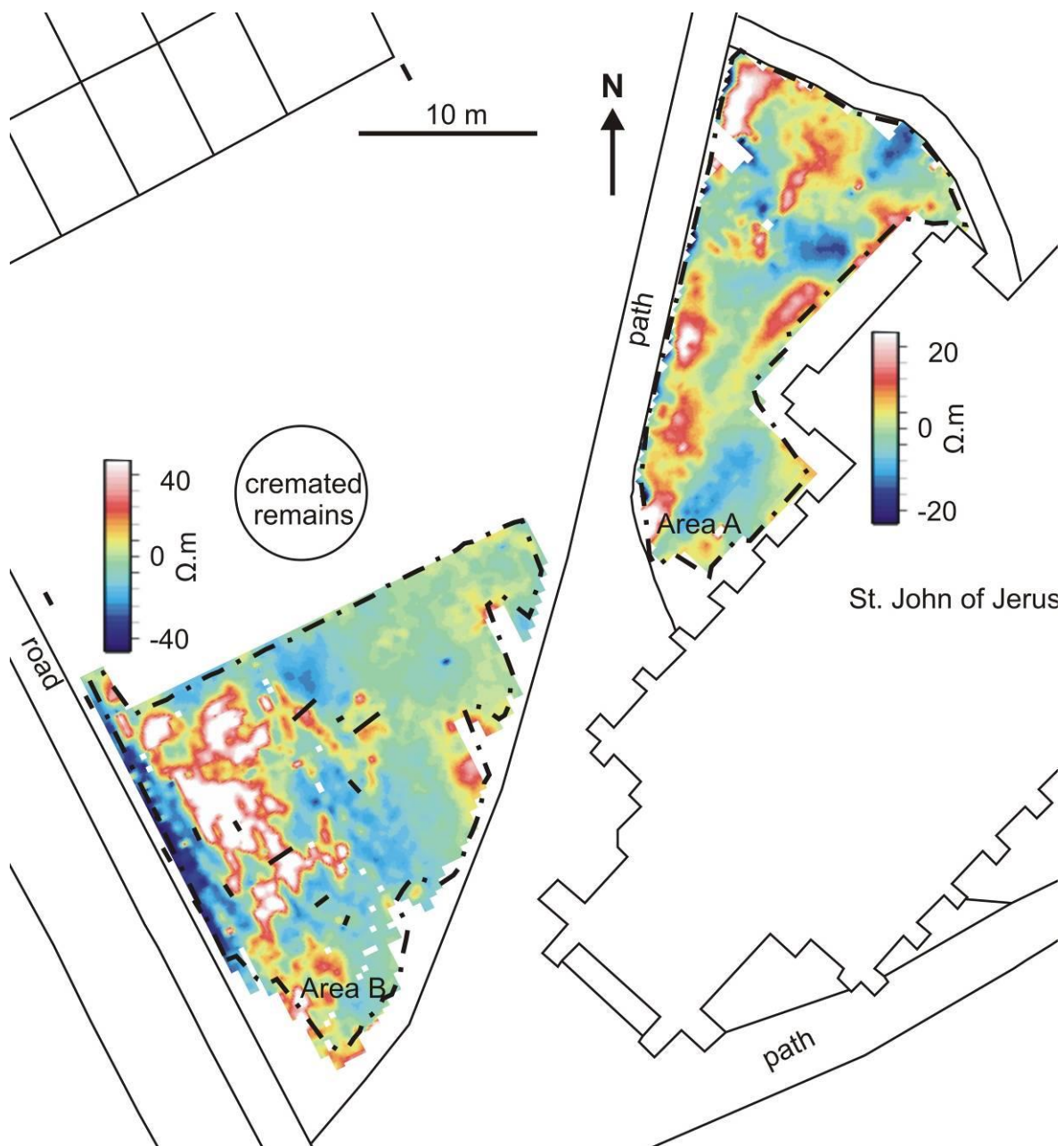


Figure 4.20. Map view of the processed bulk ground resistivity (0.5 m fixed-offset) probe spacing dataset with background map. See respective area keys. Modified from Hansen & Pringle (2011).

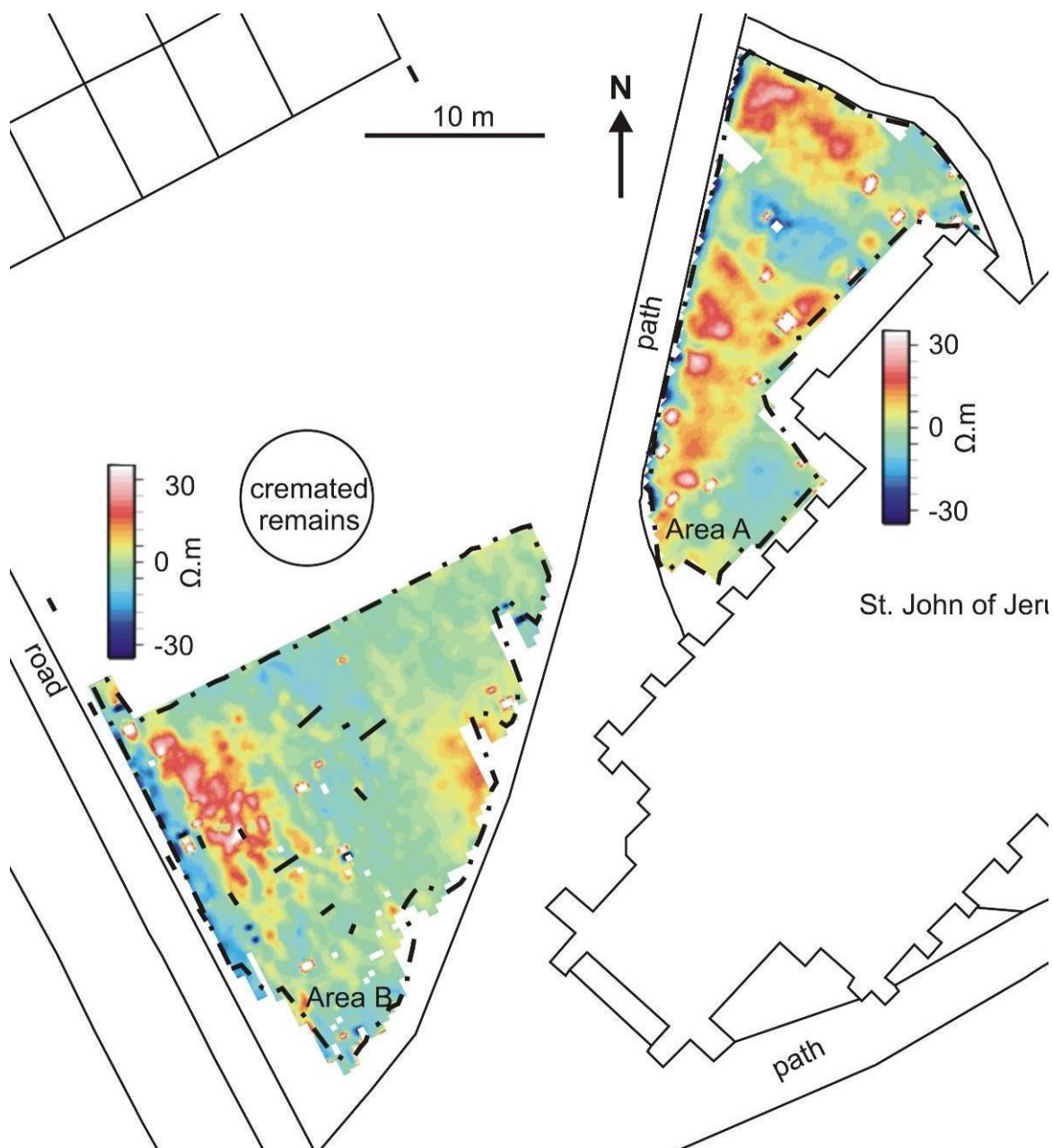


Figure 4.21. Map view of the processed bulk ground resistivity (1 m fixed-offset) probe spacing dataset with background map. See respective area keys. Modified from Hansen & Pringle (2011).

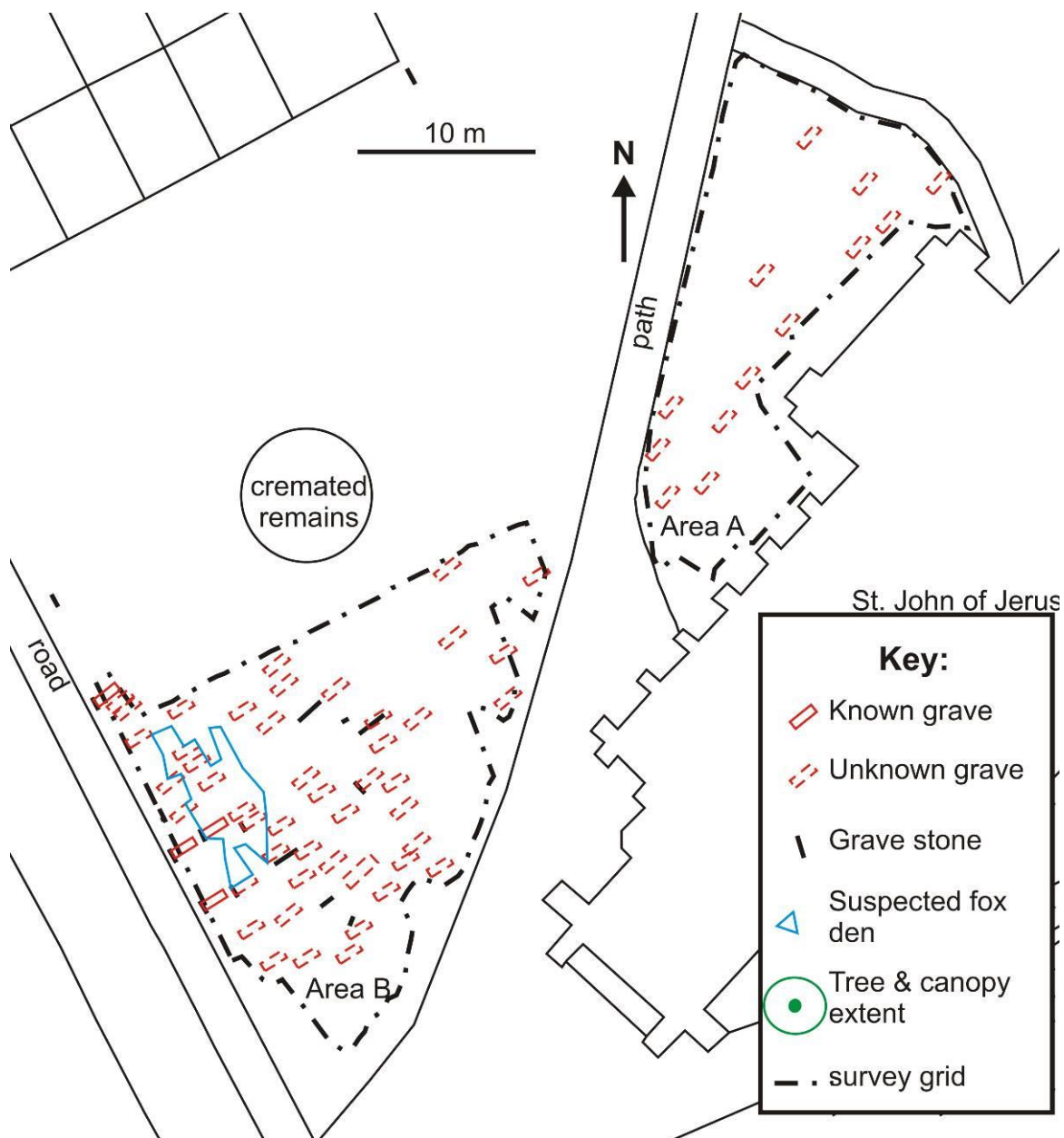


Figure 4.22. Case study 3 summary of known and unknown grave/vault positions.

Modified from Hansen *et al.* (2014).

4.5 Discussion

This section is organised to answer and discuss the study objectives in sequential order.

4.5.1 Identify the locations of any unmarked graves and/or burial plots/vaults within the respective survey areas. Identified remains could then be exhumed and re-interred elsewhere by archaeological teams (if necessary).

All three case studies evidenced that near-surface geophysical methods could detect the locations of both unmarked graves and vaults, with some confirmed by subsequent archaeological excavations in Case Studies 1 and 2. Distribution of graves within the graveyards were either highly non-uniform or there were many undetectable burials. For example, Area A in Case Study 3 appeared to contain surprisingly few graves (Fig. 4.22), despite its relatively close proximity to the church, whereas the area archaeologically excavated in Case Study 2 had a relatively dense clustering of graves at various depths bgl, some even cross-cutting each other (e.g. Fig. 4.15). Geophysical anomalies (in map view) also allowed relative orientations of burials to be established. For example, in Case Study 1 it could be argued that the grave ages could be approximately dated by alignment to one of the different orientations of the two churches that were built onsite during different periods (Fig. 4.7). However, in Case Study 1, two known burial positions were not identified in the geophysical data, therefore suggesting that these methods may not find *all* unmarked burials.

Grave markers were not necessarily accurate in marking burial positions, as other authors have evidenced (Fiedler *et al.*, 2009). All case studies found more unmarked burials than

could be discerned by grave markers and respective parish records alone. Subsequent archaeological excavations found named individuals where expected, extra unnamed individuals and missing individuals which highlights the unreliability of burial records.

In addition to the clear GPR hyperbolic reflectors from the tops of coffins and disturbed soil, relatively strong reflectors were also observed from coffin bases and brick-lined burial walls (where present), which were particularly prevalent in Case Study 1. An unforeseen outcome using electrical resistivity surveys was that a number of unmarked burials were located accidentally by using the instrument probes themselves, encountering overgrown horizontal stone slabs laid on top of the graves; particularly in Case Studies 2 and 3.

Deciduous trees were present in all three case studies, and are indeed common in UK graveyards (Litten 1992). Apart from the trunk being an obstacle to data acquisition, tree roots can interfere with successful identification of buried anomalies, either directly by producing GPR reflection events or by producing relative high resistance anomalies in the surrounding soil (see Fig. 4.20) which other authors (e.g. Jones *et al.*, 2010) have attributed to reduced soil moisture content.

4.5.2 Compare GPR and resistivity geophysical equipment configurations and data acquisition strategies and processing methods to determine best practise.

It was determined that GPR 225 MHz dominant frequency antennae were optimal in all three case studies (although note that the top 1 m of soil was removed before surveying in Case Study 1). This was in contrast to other authors, e.g. Fiedler *et al.*, (2009), who

concluded that 500 MHz frequency antennae were optimal for grave detection. GPR anomaly identification on 2D profiles was deemed sufficient to locate most burials, though the horizontal time-slices were also found to be useful to correlate targets with resistivity datasets as Doolittle & Bellantoni (2010) observed. Electrical resistivity fixed-offset probe separations of both 0.5 m (common in geophysical surveys) and 1 m were trialled in Case Studies 2 and 3; and in Case Study 3 it could be argued that the 1 m probe separation data was better at locating graves (*cf.* Figs. 4.20 and 4.21). However, the 1 m probe separation dataset from Case Study 2 was unusable due to most of the data being over-range. As penetration depths are typically 1-2 times the probe separation (see Milsom & Eriksen, 2011) the 1 m dataset would penetrate further bgl and would be less affected by heterogeneous material in the very top surface. Animal burrows were a considerable issue in Area B in Case Study 3, therefore in this case GPR was deemed optimal over resistivity methods.

GPR data processing showed careful utilisation of bandpass filtering, coupled with background removal (Nobes 2000) and gain significantly improved the image quality of 2D profiles. Usable horizontal time-slices also require significant data processing time. Resistivity data processing requires data de-spiking as a minimum, with site de-trending in 3D to remove long wavelength trends and reveal anomalous regions deemed important as authors (e.g. Pringle *et al.*, 2012a; Pringle & Jervis, 2010) have shown.

4.5.3 Determine the effect of soil type.

Soil type had a major effect on the electrical resistivity surveys in these case studies, for example, in Case Study 2 the relatively coarse site soil with pebbles resulted in resistivity

survey data being largely useless for delineating grave positions (Fig. 4.13). However, where soils were either sandy loams and/or typical black earths (e.g. Case Study 3), then both GPR and resistivity surveys showed clear geophysical grave-sized anomalies.

Subsequent archaeological excavations in Case Studies 1 and 2 indicated that graveyard soils were surprisingly heterogeneous, showing significant re-use. The predominance of brick-lined, earth-cut graves in Case Study 1 may have been due to the grave-diggers encountering difficult ground. Wooden coffin preservation (and indeed individuals contained within) was highly varied (from good to poor preservation) on the same site and even for similarly-aged burials (Tables 4.4 and 4.5) for reasons presently unclear.

4.5.4 Quantify the variety of U.K. burial styles

All three case studies indicated wooden coffins in earth-cut graves (Fig. 4.1) were present (typical of UK graveyards during the 19th – early 20th century (Litten, 1992)); however subsequent archaeological excavations found a variety of other burial styles, for example, brick-lined graves predominant in Case Study 1 (Table 4.4), which also featured brick-built family vaults containing individuals interred side-by-side in at least two layers. Figure 4.23 summarises the variety of burial styles encountered in these case studies.

Subsequent archaeological excavations revealed some named individuals where expected, but also that additional unnamed individuals were present, and some recorded individuals missing altogether. Most coffins also had numerous copper-alloy fittings which may or may not be magnetic and/or conductive.

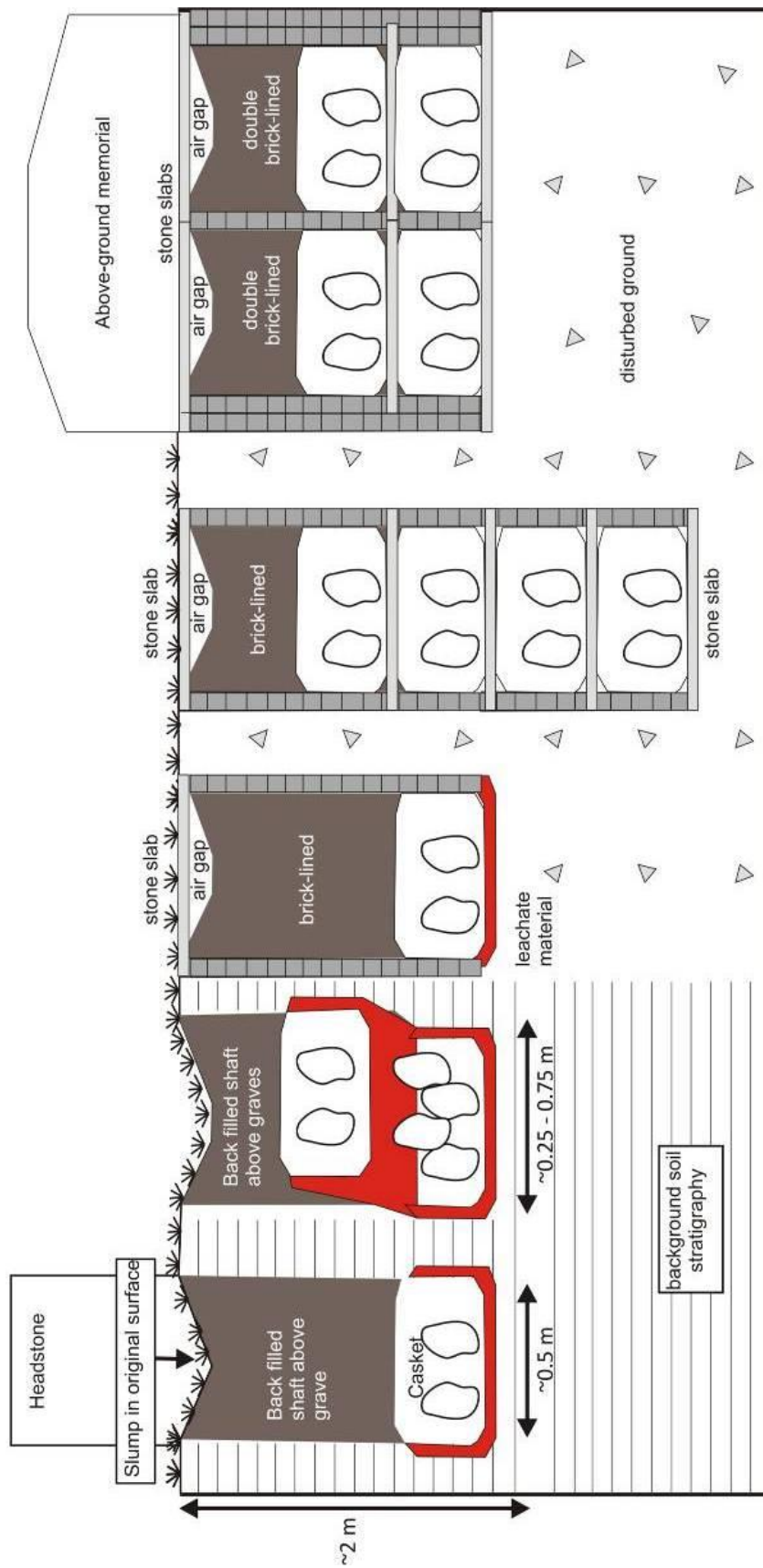


Figure 4.23. Generalised schematic of burial styles encountered in the three case studies discussed. Modified from Hansen & Pringle (2011).

4.6 Conclusions

Combined GPR and electrical resistivity geophysical methods were used to successfully identify and locate both known and unknown graves and burial vault positions in three UK case studies. Subsequent archaeological excavations in two case studies evidenced these successes as well as documenting a surprising variety of burial styles, from earth-cut and brick-lined graves, to cross-cut graves, multiple occupancy and horizontally stacked family vaults. Coffin contents also varied, including missing or extra individuals when compared to burial records and various items of coffin furniture. Grave and vault markers also did not always indicate the presence, location or character of burials. Parish records should therefore be used with caution.

225 MHz dominant frequency GPR antennae were deemed optimal in these surveys due to successful detection of burial positions, penetration depths bgl and acquisition rates. 1 m (fixed offset) probe separations were recommended for electrical resistivity surveys, but resistivity surveys should be used with caution on sites with very coarse grained soils, as soil type was a major factor in successful data acquisition. Careful data processing is essential, and resistivity data should be de-trended to resolve geophysical anomalies. Areas with extensive tree root networks can also be problematic.

Further studies from other graveyards, with contrasting soil types and burial ages, would provide a greater understanding of how geophysical surveys can be used to detect such forensic targets. It is recommended that geophysical surveying be undertaken before site development work is initiated, particularly as in Case Study 1 where some parts of the

graveyard could not be surveyed. Forensic geophysical surveys for such targets will likely become increasingly common due to the current lack of burial space in the U.K.

Chapter 5 - Comparison of magnetic, electrical and GPR surveys to detect buried forensic objects in semi-urban and domestic patio environments

5.1 Introduction

Keele University's Geophysics department was approached in 2011 by a representative from Staffordshire Police force with a request for information regarding the detection of buried weapons caches in urban and semi-urban environments, such as brownfield sites or domestic gardens. A particular concern for the investigation teams was found to be the detection of criminal evidence beneath patio coverings; a common feature of domestic garden environments. The police teams were keen to gather information or recommendations for non-invasive means of detecting and locating targets beneath such patio coverings, which could potentially save man-power, investigation time and money.

Geotechnical investigations routinely use near-surface geophysical methods to identify buried locations of, for example, cleared building foundations and underground services (Reynolds, 2011), as well as environmental forensic objects such as illegally buried waste (Bavusi *et al.*, 2006; Ruffell & Kulessa, 2009). Magnetic detection methods are commonly used in geotechnical (e.g. Marchetti *et al.*, 2002; Reynolds, 2004; Reynolds, 2011) and forensic archaeological investigations (Linford, 2004; Hunter & Cox, 2005).

However, little control research has been published which provides information about the use of geophysical methods in the detection of forensic objects, other than to confirm metal detector results (e.g. Davenport 2001; Rezos *et al.*, 2010), and for human remains (e.g. Miller,

1996; Davenport, 2001; Schultz *et al.*, 2006, Schultz, 2008; Pringle *et al.*, 2008; Pringle *et al.*, 2012b). Dionne *et al.*, (2011) conducted a control study involving buried weapons and found that electro-magnetic (EM) equipment could detect metallic objects buried in a grid in a rural environment but this study did not make use of a Geonics™ EM38 instrument. Murphy & Cheetham (2008) found difficulty in differentiating between background materials and target buried weapons in a control study using magnetic methods, even after surface metallic items were cleared from the survey site prior to data acquisition. Murphy & Cheetham (2008) also found that GPR methods could be used to locate buried forensic targets, but that it was difficult to locate these objects in certain orientations.

In a law enforcement context, burials occur at a maximum of 10 m below ground level (bgl), but are usually much shallower (Fenning & Donnelly, 2004; Harrison & Donnelly, 2009). Forensic objects vary from illegally buried weapons and explosives, landmines and improvised explosive devices (IEDs), weapons and drug caches to clandestine graves of murder victims and mass genocide graves (Pringle *et al.*, 2012a). Acheroy (2007) provides a useful review of field detection of anti-personnel mines using Ground Penetrating Radar (GPR). In the U.S.A, neighbourhood criminal gangs often hide used illegal weapons for later recovery (Dionne *et al.*, 2011). Buried firearms have also been searched for and recovered in South Africa; from historic abandonment of British colonial military bases to Nelson Mandela's pre-1963 arrest firearm (Smith, 2011).

Recovery of buried forensic material often results in successful criminal convictions and it is therefore often critical that they be located (Harrison & Donnelly 2009). Due to limited manpower and resources, law enforcement agencies often need prioritise locations for physical

excavation especially if the search areas are large. Specialist trained search dogs have been widely used to locate a variety buried objects, commonly IEDs (Curran *et al.*, 2010), drugs and human remains, the latter teams referred to as cadaver dogs (Rebmann *et al.*, 2000), but are less successful with buried inorganic objects. Metal detector search teams are used when deemed appropriate, especially when there is a strong physical contrast between the target and local background environment (Nobes, 2000).

This relative lack of necessary information led to the development of a control study which would utilise a variety of commercially-available, near-surface geophysical techniques to both detect and locate small-scale metallic objects buried in a semi-urban environment, using survey procedures which are commonly used in geotechnical and archaeological investigations.

Study objectives for both semi-urban and patio environments were to:

- 1) evaluate and find optimum magnetic detection technique(s) for the target buried forensic material,
- 2) compare magnetic methods with electrical and GPR,
- 3) determine optimum GPR detection frequencies,
- 4) determine optimum respective equipment configuration(s), survey specifications and optimal processing steps,
- 5) determine which technique(s) could determine target depth below ground, and
- 6) determine if different buried metal types could be distinguished.

It would also be useful to consider how easily the detection techniques could be utilised by forensic investigators to acquire, process and interpret forensic geophysical datasets.

5.2 Methodology

5.2.1 Test site

The forensic test site situated on Keele University campus was chosen as a representative of semi-urban U.K. environments, as the site history indicated the presence of domestic greenhouses with remnant cleared foundations still present (Fig. 5.1). Previous site studies confirmed this and indicated that the local mixed sand and clay soil was predominantly ‘*made ground*’ with Triassic Butterson Sandstone Formation bedrock present at a shallow level, only ~2.6 m bgl (Jervis *et al.*, 2009). The local climate is temperate, which is typical for the U.K.

A five metre by five metre survey area was selected as this was deemed small enough to keep data acquisition time for the multi-geophysical techniques reasonable, but sufficiently large to allow resolvable space between the objects in the data. Permanently marked by plastic tent pegs, survey lines were laid 0.25 m apart (Fig. 5.1a) and multi-technique geophysical datasets were then acquired to provide control data for later comparison (Table 5.1). A variety of (mostly) metallic objects (see Fig. 5.2 and Table 5.2 for details) were buried ~15 cm bgl in a non-uniform configuration within the survey area and their locations recorded (Fig. 5.3). Note that the ammunition box (Fig. 5.2g) had to be buried partly below this depth to ensure the depth to the top of the target was consistent with other target depths.

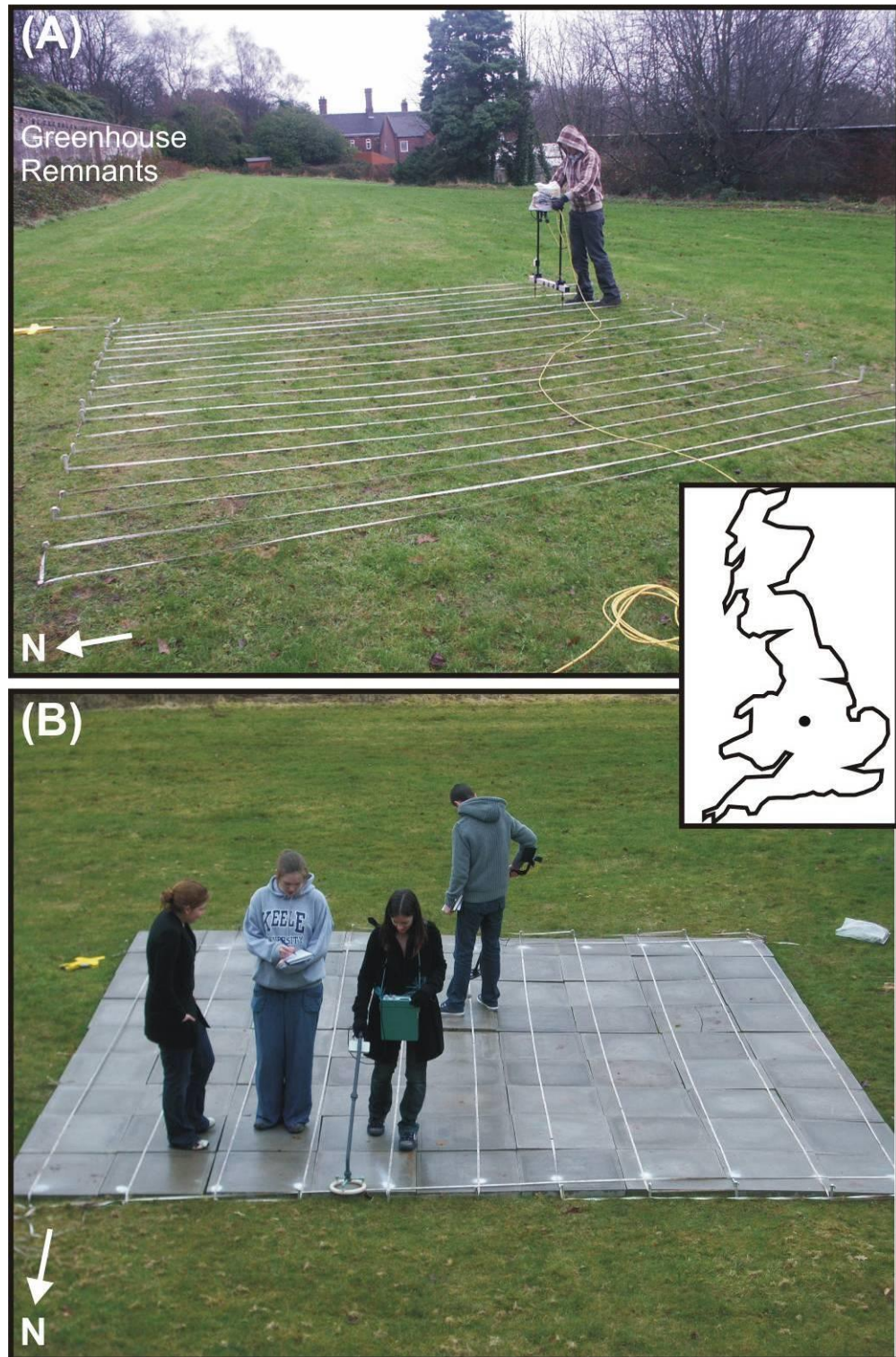


Figure 5.1. Photographs of the 5 m x 5 m forensic test site on campus showing (a) semi-urban environment and (b) simulated domestic concrete patio scenario on same area with location map (inset). Survey tapes on survey lines are shown. 0,0 position for all surveys is SW corner.

Geophysical technique	Survey date (type)	Setup time (mins)	Acquisition time (mins)	Station spacing (m)	Precision	Advantages / Disadvantages
Metal Detector (Bloodhound Tracker™ IV all-metal))	10-11-09 (C), 10-12-09 (S) & 25-02-10 (P)	1	30	N/A	Unknown	Easy to operate. Picks up all metals. Limited penetration depth
Magnetic Susceptibility (Bartington™ MS.1 with 0.3m diameter probe)	10-11-09 (C), 10-12-09 (S) & 25-02-10 (P)	1	90	0.25	~1 S.I.	Easy to operate. Limited to ~8cm bgl.
Fluxgate gradiometer (Geonics™ FM15)	10-11-09 (C), 10-12-09 (S) & 25-02-10 (P)	60	45	0.25	0.1 nT	Can detect subtle targets. Difficult to calibrate and needs careful acquisition.
Magnetic gradiometer (GSMP-40™ K+ vapour, 2 sensors 1 m vertical separation)	10-11-09 (C), 10-12-09 (S) & 22-03-10 (P)	60	30	~0.05 (collected at 0.05 s)	0.01 nT	Small sample spacing, collects both total field and gradient data. Expensive.
GPR (PulseEKKO™ 1000) 450 MHz antennae	02-11-09 (C), 10-12-09 (S) & 25-02-10 (P)	30	60	0.05	~0.1 m	Resolves fairly small objects and depth to target(s).
GPR (PulseEKKO™ 1000) 900 MHz antennae	02-11-09 (C), 10-12-09 (S) & 25-02-10 (P)	30	90	0.025	~0.05 m	Resolves small objects and depth to target(s). Slow.
Bulk ground resistivity (Geoscan™ RM15-D) using 0.5m spaced probes	29-10-09 (C) & 10-12-09 (S)	10	45	0.5	~0.25 m	Relatively quick. Will detect objects up to 1 m bgl. Not usable on patios.
Bulk ground resistivity (Geoscan™ RM15-D) using 0.5m spaced probes	29-10-09 (C) & 10-12-09 (S)	10	60	0.25	~0.125 m	Will detect objects up to 0.5 m bgl. Not usable on patios.

Table 5.1. Summary statistics of geophysical data collected during the study. Survey types are: (C) Control, (S) Semi-urban and (P) Patio environments respectively. Bgl = below ground level. Survey line spacings were 0.25 m unless otherwise stated.



Figure 5.2. Photographs of forensic buried test objects. (A) Domestic brick and; (B) metallic bolt/screw and plate control objects. (C) Three domestic stainless steel kitchen bread knives; (D) 1943 allied wooden-handled entrenchment tool (E) (left) WW2 allied hand grenade and (right) WW1 allied Mk.1 No.5 decommissioned hand grenade; (F) Colt Government Cup Replica .45 calibre automatic handgun with solid brass ammunition; (G) UK mortar ammunition box (containing 2 shell casings shown in H). (H) 1943 75 mm M18 shell and two WW2 smaller diameter spent shells; Table 5.2 for details. Modified from Hansen *et al.* (2013).

Number	Forensic Buried Object	Size (m)	Description
1	Brick (Fig. 5.2a)	0.17×0.11	Clay house-brick, orientated horizontally
2	Bolt and screw (Fig. 5.2b)	0.08×0.05	Unknown metal alloy
3	Steel plate (Fig. 5.2b)	$0.2 \times 0.2 \times 0.05$	Stainless steel, flat, square plate, orientated horizontally.
4	Breadknives (Fig. 5.2c)	0.3×0.05	Two domestic stainless steel kitchen bread knives wrapped in thin plastic bag. Orientated N-S.
5	Spade (Fig. 5.2d)	Handle: 0.4×0.07 . Head: 0.32	1943 allied wooden-handled entrenchment tool with metallic head, orientated NW-SE.
6	Knife (Fig. 5.2c)	0.3	One domestic stainless steel kitchen bread knife, orientated E-W.
7	WWII Grenade (Fig. 5.2e)	0.08 diameter	World War 2 allied decommissioned metallic hand grenade, orientated vertically.
8	WWI Grenade (Fig. 5.2e)	0.08 diameter	1915 No. 5 Mk 1 allied decommissioned metallic hand grenade, orientated vertically.
9	Handgun (Fig. 5.2f)	0.18×0.14	Colt Government Cup Replica .45 calibre automatic replica handgun with solid brass ammunition. Most likely zinc alloy with
10	Mortar shell (Fig. 2h)	0.37×0.17	Brass spent mortar shell: 1943, 75mm M18, orientated E-W.
11	Ammunition box (Fig. 5.2g)	$0.55 \times 0.4 \times 0.45$	UK mortar ammunition metallic box with 2 small WW2 spent mortar shells (Fig. 2h), orientated N-S.

Table 5.2. Description of buried forensic objects used in this study and their known properties (photographs in Fig. 5.2). Object

numbers refer to those in Fig. 5.3 and geophysical datasets.

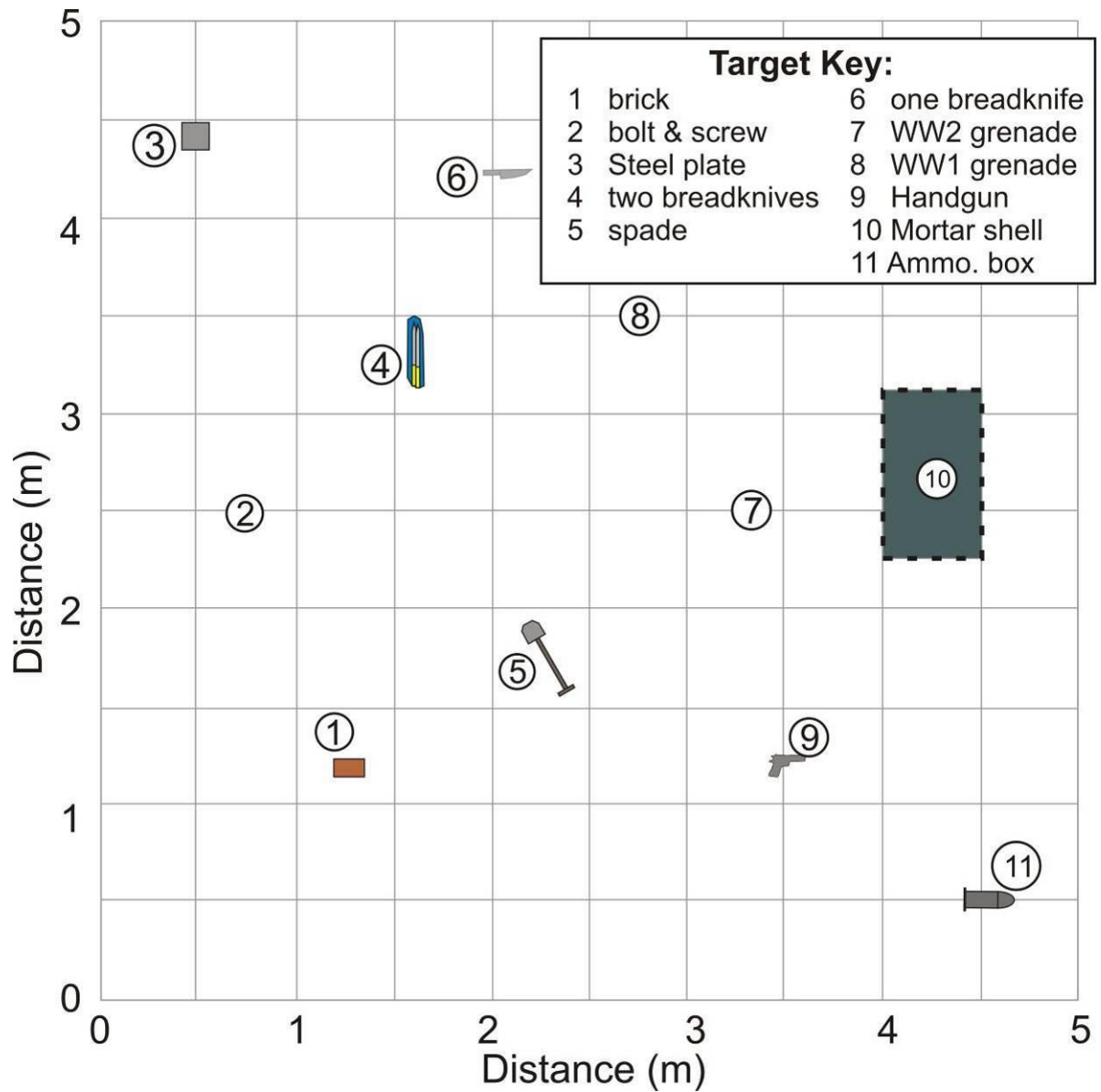


Figure 5.3. Sitemap showing location of buried forensic objects (key for details) for both semi-urban environment and patio scenarios (Fig. 5.2 for selected object photographs). Modified from Hansen *et al.* (2013).

Buried objects considered *non-forensic targets* included a domestic house brick, a steel plate and a metallic bolt for control and comparison purposes (Fig. 5.2 and Table 5.2). This approach therefore differed from the single-technique and uniformly-arranged target control studies undertaken by Rezos *et al.* (2010) and Dionne *et al.* (2011) and was considered more representative of true forensic search scenarios. The survey area was re-surveyed with the geophysical techniques approximately two weeks after burial in order to ensure some settlement of the replaced topsoil. Finally a 0.06 m thick layer of concrete paving slabs (~0.5 m by ~0.5 m) was laid over the grid (Fig. 5.1b) and the area was then re-surveyed using all techniques, with the exception of a bulk ground resistivity survey due to the inability to insert the resistivity probes into the concrete patio material.

5.2.2 Metal detector surveys

Standard metal detectors produce an audible but, generally, non-quantifiable response, if the transmitted EM signals induce a secondary field in near-surface conductive material (Milsom & Eriksen, 2011 and Dupras *et al.*, 2006). The Bloodhound Tracker™ IV all-metal detector results were acquired using a side-to-side sweeping method in parallel transects 0.5 m apart (Dupras, 2006 and Rezos *et al.*, 2010) at a constant height of ~5 cm (Table 5.3). Where the detector produced an audible signal, the positions on the grid were marked and recorded. This was repeated by three different operators to account for any variations in operator technique. The survey area was then re-surveyed after forensic objects were buried and again after the domestic patio was laid (Table 5.1) with audible response locations again noted.

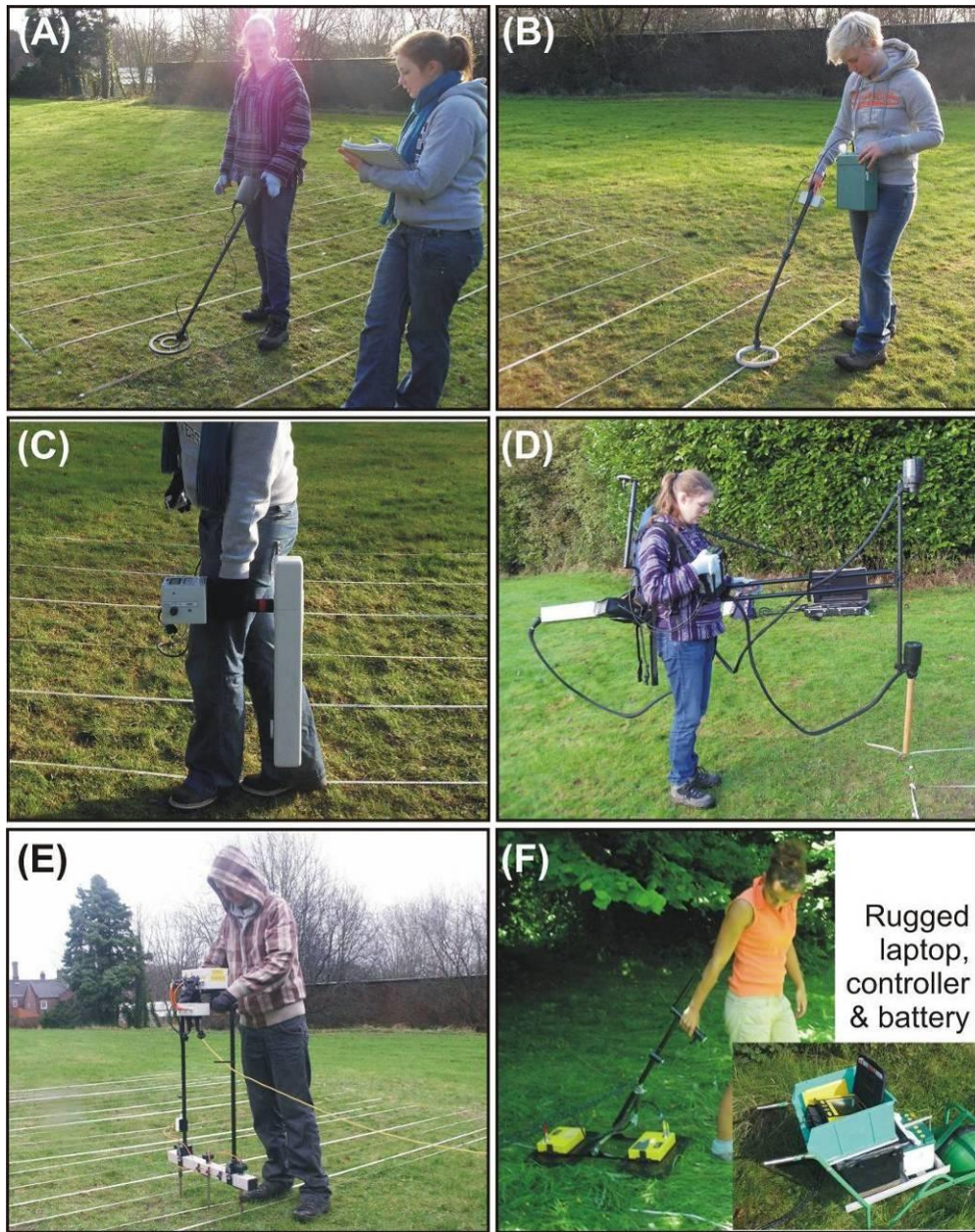


Figure 5.4. Photographs of geophysical equipment used in this study. (A) Bloodhound Tracker™ IV metal detector; (B) Bartington™ magnetic susceptibility probe MS.1 with 0.3 m diameter probe; (C) Geoscan™ FM-15 fluxgate gradiometer; (D) GSMP-40™ potassium vapour magnetic gradiometer with sensors 1 m vertically separated; (E) Geoscan™ RM15-D mobile probe resistivity meter and; (F) pulseEKKO™ 1000 GPR equipment (450 MHz dominant frequency, bistatic fixed-offset antennae). Modified from Hansen *et al.* (2013).

Technique	Transect spacing (m)	Sample interval (m)	Approximate time to complete 1 survey (mins.)
Metal detector	0.50 (nominal although covered all area)	Continuous	5
Magnetic susceptibility	0.25	0.25	60
Fluxgate gradiometry	0.25	0.25	30
Potassium-vapour magnetic gradiometry	0.25	~0.01	20
Resistivity (both probe spacings simultaneously)	0.25	0.25	30
450 MHz GPR	0.25	0.05	60
900 MHz GPR	0.25	0.025	180

Table 5.3. Summary of parameters used for each geophysical survey in this study.

5.2.3 Magnetic susceptibility surveys

Magnetic susceptibility meters generates a low intensity, AC magnetic field, and equipment records the resulting changes in positive or negative susceptibility in S.I. (dimensionless units) by the sampled medium. This bulk reading is usually due to a combination of highly magnetic minerals (e.g. magnetite), man-made ferro-magnetic material (if present), other materials and background magnetism (Milsom & Eriksen, 2011 and Reynolds, 2011). Magnetic

susceptibility data were collected using a Bartington™ MS.1 susceptibility instrument with a 0.3 m diameter probe placed on the ground surface at each sampling point (Fig. 5.4b). Data samples were collected on a 0.25 m grid over the survey area before forensic object burial to act as control, then resurveyed after burial and finally again after the patio was laid (Table 5.4). This was a smaller sample spacing than typically used for clandestine grave surveys (Pringle *et al.*, 2008). Initial data processing involved manual de-spiking to remove anomalously large isolated data points caused by operator/equipment error.

Magnetic survey data were processed using the Generic Mapping Tools (GMT) software (Wessel & Smith, 1998). To aid visual interpretation of the data, a minimum curvature gridding algorithm was used to interpolate each dataset to a cell size of 0.0125 m by 0.0125 m. In addition, '*de-trending*' of the data was conducted to remove long-wavelength site trends and allow smaller, target-sized features to be more easily identified. This was achieved by fitting a cubic surface to the gridded data and then subtracting this surface from the data, as the method was found to produce optimal results. Table 5.4 details the GMT processing steps undertaken.

Step	Process	Description / Justification
1	Conversion	Converting data to XYZ format usable in GMT (where applicable)
2	Gridding	Minimum curvature gridding algorithm used to interpolate data to a cell size of 0.0125 m by 0.0125 m to create a smoother image
3	De-trending	Removal of long-wavelength trends from the data by fitting a cubic surface to the grid and then subtracting this from surface data. This allows subtler small-wavelength features to be better distinguished
4	Normalisation	Dividing dataset by standard deviation Z value created new grid with mean Z of ~0 and standard deviation of ~1. Allowed comparison between datasets collected at different dates and in different burial scenarios.

Table 5.4. Summary of data processing steps conducted in GMT.

5.2.4 Fluxgate gradiometry surveys

Fluxgate gradiometry equipment records only the vertical (Z) component of the Earth's magnetic field, which is affected by proximal ferro-magnetic materials, their orientation, depth bgl, etc. (Milsom & Eriksen, 2011 and Reynolds, 2011). Due to the short data acquisition time (Table 5.4) it was deemed unnecessary to undertake diurnal correction (Milsom & Eriksen, 2011). Fluxgate gradiometry data were collected using a Geoscan™ FM18 gradiometer held at a constant height (Fig. 5.4c). For all three surveys (Table 5.1), following best practice, the meter was first carefully zeroed over a magnetically 'quiet' area outside of the survey grid in

order to eliminate any effects which can result from positional variation in instrument orientation relative to magnetic North when acquiring data (Milsom and Eriksen, 2011). Survey lines were also orientated to magnetic north to avoid any orientation issues (Fig. 5.1). Basic data processing was again undertaken which involved de-spiking and de-trending (Table 5.4) as previously described.

5.2.5 Magnetic (potassium-vapour) gradiometry surveys

Magnetic gradiometry data were collected using a GSMP-40 potassium vapour magnetic gradiometer using 1 m vertically separated total field sensors (Fig. 5.4d and Table 5.1). The advantages of this equipment were that it collects both upper/lower sensor total magnetic vertical (Z) field readings as well as gradient measurements between the two sensors, and is industry standard for geotechnical investigations (Reynolds, 2004 and Reynolds 2011). Due to the short data acquisition time (Table 5.1) it was again deemed unnecessary to undertake diurnal correction. Data were acquired over the 0.25 m spaced survey lines with readings recorded every 0.2 s, which roughly equated to a sample spacing of ~0.01 m. The equipment was maintained at a constant height above the ground surface for all surveys (to reduce any data variation) by attaching a non-magnetic (wooden) stick to the bottom sensor which was kept in contact with the ground surface (Fig. 5.4d). Minimal data processing was undertaken which involved data de-spiking and de-trending as previously described (Table 5.4).

5.2.6 Fixed-offset resistivity surveys

The inverse of conductivity, resistivity, is measured by applying a constant current through a sample (soil) of known size and measuring the drop in voltage (Milsom & Eriksen, 2011 and Reynolds, 2011). Bulk-ground resistivity data were collected using a Geoscan™ RM15-D resistance meter mounted on a custom-built frame which allowed the almost simultaneous acquisition of both 0.25 m and 0.5 m spaced, pole-pole electrode array measurements using 0.1 m long stainless steel electrodes (Fig. 5.4e). The pole-pole probe array was used as it is both rapid, popular and deemed sensitive to near-surface lateral variations (Milsom & Eriksen, 2011). Remote probes were fixed at a 1 m separation and at a distance of 15 m from the survey area to ensure probe configurations do not interfere in the resulting data (Milsom & Eriksen, 2011). For the control and semi-urban surveys (Table 5.1), resistivity measurements were conducted at 0.25 m intervals along survey lines 0.25 m apart (Table 5.1). This sample spacing was smaller than the typical 0.5 m spaced resistivity datasets (Pringle & Jervis 2010) but high resolution datasets were deemed important for comparison purposes to the magnetic surveys. A post-burial survey was not possible over the patio as the electrodes could not be inserted into the ground using the utilised equipment. Minimal data processing was undertaken which involved data de-spiking and de-trending as previously described (Table 5.4).

5.2.7 GPR surveys

Ground penetrating radar (or GPR) is a well-documented technique, whereby an EM pulse is transmitted into the ground, which then reflects at boundaries of contrasting di-electric permittivity. This reflected signal is recorded at a receiving antenna and subsequently used to generate a digital image of the subsurface (Milsom & Eriksen, 2011 and Reynolds, 2011). The signals stored in time formats can be converted to depth if the local site velocity is known. As discussed in Chapter 2, GPR signal penetration depth and resolution are a function of antennae set frequencies; high frequency (450+ MHz) gives high resolution but poor penetration whilst low frequency gives low resolution but good penetration (Jol, 2009). GPR datasets were collected using PulseEKKO™ 1000 equipment using both 450 MHz (Fig. 5.4f) and 900 MHz dominant frequency bi-static, fixed-offset (0.34 and 0.17 m respectively) antennae along 0.25 m spaced lines with trace sample intervals of 0.05 m and 0.025 m respectively (Table 5.1). The grid was surveyed three times; before target burial to provide a control dataset, then over the buried forensic objects before and after the addition of the patio.

The resulting GPR datasets were sequentially processed using Reflex-Win Version 3.0 (Sandmeier) software (Table 5.5) following best practice (Milsom & Eriksen, 2011).

Step label	Process	Description / Justification
1	Subtract mean ('de-wow')	Remove any positive or negative bias of traces
2	Move start-time	Move traces to uniform time based on common reflector here 0 ns. Allowed all features of uniform depth below ground-level to appear uniform in profiles.
3	1D Bandpass filter (Butterworth)	Upper and lower extents of frequency histogram removed.
4	2D filter – Background removal	Removes trace average, removing any destructively interfering 'ringing' created during bandpass filter stage (3).
5	Migration (Stolt)	Collapse hyperbolae to discrete focus points
6	Horizontal time-slice generation	Collapse a specific time region across all profiles to create a 'map-view' of total amplitude over this time/depth domain
7	Exported as xyz data file	Amplitude data exported as Z data into 0.25 m (X) x 0.025 m (Y) spaced .xyz file for GMT processing

Table 5.5. Stages of GPR processing according to the best practise methods (Milsom & Eriksen, 2011).

5.3 Results

5.3.1 Successful detection scheme

A target was considered to be detected or not by analysing the change between pre-burial control data and post-burial semi-urban and patio data using normalised, de-trended datasets. Any significant change in geophysical response at, or near to, a target location was considered to be an effect of the target's presence since, presumably, the values at all other sample locations would remain unchanged in terms of variation from mean. In this way, the effect of seasonal change in soil properties (namely moisture content) was negated. Anomalies were categorised according to their association with a target (Table 5.6). A discrete, strong contrast anomaly was considered related to a target if it (a) occurred at or/within close proximity of a target (accounting for offset of sample points between surveys) and (b) was not present within the control dataset. The normalised, de-trended datasets was used to better appreciate the relative intensity of target and non-target responses: standard deviations (σ) above or below the mean (interpreted as 'background'). In this way, it was possible to compare the relative intensity of target and non-target anomalies between different environments and techniques.

Classification	Geophysical response of the target
Good detection: ●	highly anomalous compared to background
Poor detection: ●	Significant change between pre-burial and post-burial datum/data
Undetected: ○	indistinguishable from background and no post-burial change

Table 5.6. Classification of geophysical responses of targets.

Considering that this research was being conducted with the aim of aiding forensic investigation, the post-burial datasets were the most important for consideration, as real investigations would not be supplied with control data. The purpose of comparing the post-burial data to control data was to evaluate whether the target has had a significant effect upon the geophysical response at the target location, regardless of whether or not there was a high-contrast anomaly within the post-burial datasets. A significant change was potentially more important considering that within a different soil environment a target anomaly may contrast considerably more with the background. The classification system applied is shown in Figure 5.5.

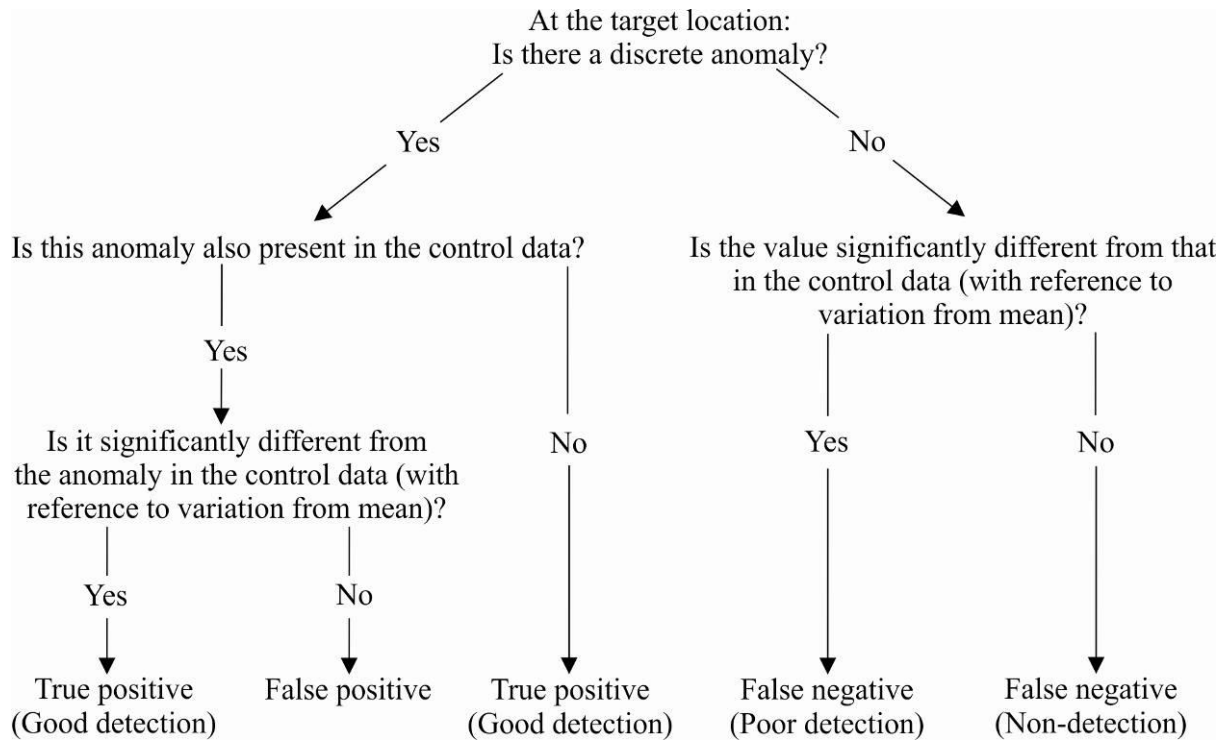


Figure 5.5. Classification of target detection used in this study.

5.3.2 Metal detector

For the post-burial semi-urban environment survey, only the two control buried objects were undetected using the metal detector; the (1) brick (as might be expected) and, (2) the metallic bolt (*cf.* Fig. 5.3 and Table 5.2). For the post-burial patio survey, in addition to the control buried targets again being undetected, the (5) entrenching tool and both the (7) WWII and (8) WW1 hand grenades were also undetected. For both surveys, six non-target anomalies were detected; therefore leading to a 57% (semi-urban) and 43% (patio) total target detection success rate for the respective metal detector surveys.

5.3.2 Magnetic susceptibility

Magnetic susceptibility datasets (441 data points for each survey) for the control, post-burial semi-urban and patio environment scenarios were highly variable between surveys, having average and 2σ values of 68.3 S.I. and 214.8 2σ (control), 128.4 S.I. and 412.2 2σ (semi-urban) and 50.5 S.I. and 110.8 2σ (patio) respectively. The 2σ (two standard deviations) given here and throughout represents a 95% confidence limit and provides the variance of each respective dataset. The control and semi-urban survey results indicated significant heterogeneous ground conditions as would be expected for a semi-urban environment. Target results are detailed in Table 5.6.

Magnetic susceptibility data for the post-burial semi-urban environment also showed significant site variations with the same magnitude of readings acquired as for the control dataset (Table 5.7). In addition to the control, isolated, high-magnitude anomalies again being

present, several other isolated high-magnitude anomalies were present which could be correlated with (2) the bolt, (3) the steel plate, (4) the two breadknives, (5) the entrenching tool, (6) the single breadknife, and (7) the WW2 hand grenade and locations. Low-magnitude isolated anomalies, with respect to background values, could also be correlated with (9) the handgun, (10) the ammunition box and (11) the spent mortar shell locations (*c.f.* Figs. 5.3, 5.6 and 5.7). Magnetic susceptibility data for the post-burial patio environment had significantly less site variations ranging from -242 to 496 S.I. units.

Selected 2D profiles are shown in Figure 5.6. In addition to isolated, high-magnitude anomalies being present in control data, several other isolated high-magnitude anomalies could be correlated with (2) the bolt, (3) the steel plate, (4) the two breadknives, (5) the entrenching tool and (7) the WW2 hand grenade locations (*c.f.* Figs. 5.3, 5.6 and 5.7). Low-magnitude isolated anomalies, with respect to background values, could also be correlated with (9) the handgun, (10) the ammunition box and (11) the spent mortar shell locations (*c.f.* Figs. 5.3, 5.6 and 5.7). This therefore gave an 82% (semi-urban) and 73% (patio) total target detection success rate respectively.

Target number	Description	Raw response (S.I.)			De-trended data response (S.I.)			Normalised, de-trended data response (SD from mean (σ))		
		Ctrl	SU	Patio	Ctrl	SU	Patio	Ctrl	SU	Patio
1	Brick	71	93	40	13.4	-21.03	-5.39	0.13	-0.1	-0.1
2	Bolt & screw	39	1105	294	-9.31	1012.78	251.015	-0.09	4.95	4.66
3	Steel plate	42	1619	465	-9.89	1492.15	415.93	-0.09	7.3	7.73
4	Breadknives	41	1413	171	-12.36	1294.74	124.08	-0.09	-0.16	2.31
5	Spade	73	686	189	14.43	198.45	143.54	0.14	0.96	2.67
6	Knife	59	802	41	2.61	680.34	-4.93	0.03	3.33	-0.09
7	WWII grenade	35	1232	168	-26.11	1120.06	121.65	-0.25	5.48	2.26
8	WWI grenade	38	321	400	-23.52	203.71	353.076	-0.22	1	6.56
9	Handgun	93	-102	-100	10.92	-204.85	-143.15	0.1	-1	-2.66
10	Ammunition box	31 & 89	-625 & 2161	-184 & 336	-26.26 & 27.02	-727.08 & 2060.47	-228.92 & 291.33	-0.25 & 0.22	-3.56 & 10.08	-4.25 & 5.41
11	Mortar shell	86	-571	-86	14.53	-652.55	-121.36	0.14	-3.19	-2.26
Average for whole dataset		68.28	128.49	48.9	9.57	23.45	4.95	0.09	0.11	0.09
SD for whole dataset		107.41	206.05	54.17	106.54	204.42	53.82	1	1	1
Range for whole dataset		1716	2786	740	1698.02	2787.55	738.6	15.94	13.64	13.73

Table 5.7. Maximum and/or min. magnetic susceptibility values at target-locations for burial scenarios using raw, de-trended & normalised data. Ctrl = Control datasets, SU = semi-urban.

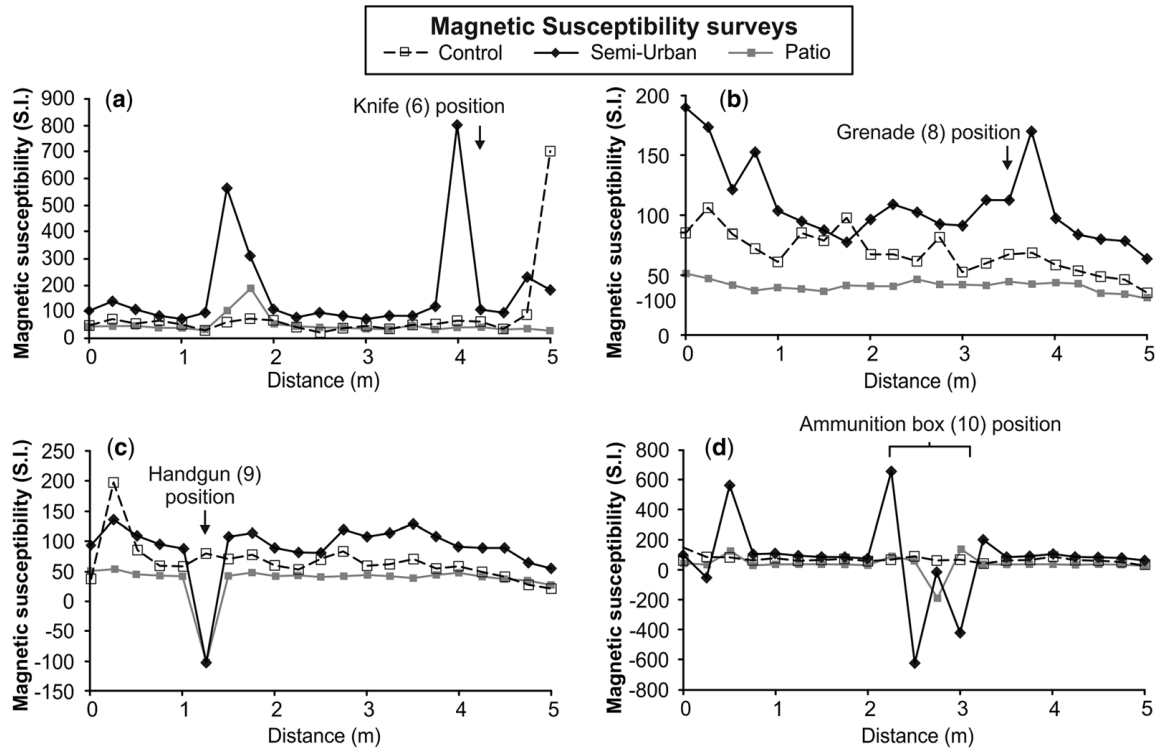


Figure 5.6. Magnetic susceptibility selected 2D profiles for control, semi-urban and patio surveys with respective target positions marked. (a) Profile 9 ($X = 2$ m) over target (6), single knife; (b) profile 12 ($X = 2.75$ m) over target (8), First World War hand grenade; (c) profile 15 ($X = 3.5$ m) over target (9), handgun; and (d) profile 18 ($X = 4.25$ m) over target (10), ammunition box (all marked). See key for survey type and Table 5.2 for details. Modified from Hansen *et al.* (2013).

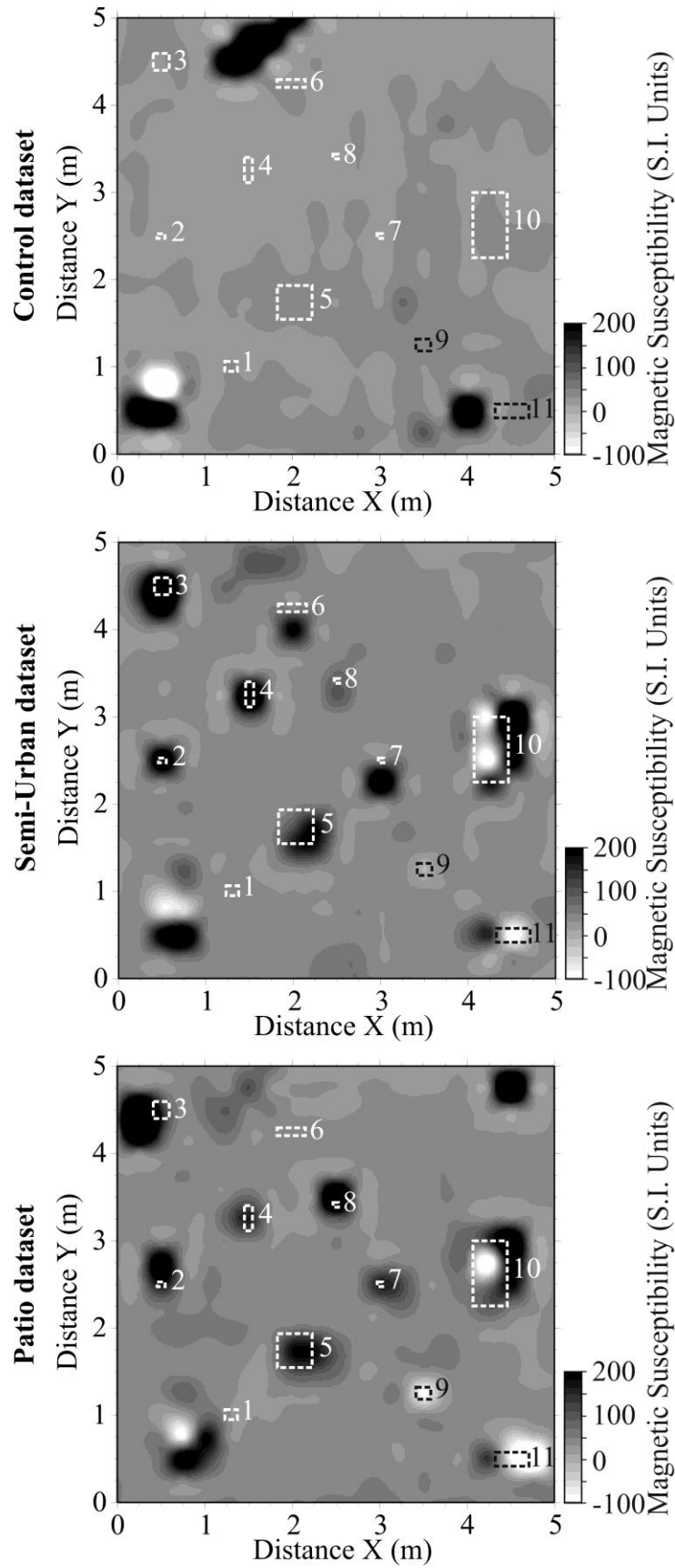


Figure 5.7. Magnetic susceptibility processed, gridded and contoured map view data plots of (A) pre-burial control with interpreted isolated anomalies, with respect to background values, marked (text); (B) post-burial semi-urban environment and; (C) post-burial patio garden environment respectively. Scale for (A) and (B) are the same. Table 5.2 for target descriptions. Modified from Hansen *et al.* (2013).

5.3.3 Fluxgate gradiometry

Fluxgate gradiometry datasets (441 data points in each survey) for the control, post-burial semi-urban and patio environment scenarios were very variable and geophysically ‘noisy’, having survey averages and 2σ values of -45.6 nT / 145 2σ (control), -0.21 nT / 157 2σ (semi-urban) and -44 nT / 144 2σ (patio) surveys respectively. This could be expected in such heterogeneous ground conditions, with a significant proportion of the datasets (32%, 31% and 30% respectively) not recording data at sampling positions due to over-range values. However these non-sample areas were consistent which suggested the instrument was not faulty nor incorrectly calibrated. 2D data profiles acquired over the forensic objects (Fig. 5.8) did allow some estimation of target detection to be undertaken. With such a high proportion of the survey area being over-range, the resulting gridded and contoured map view plots of the control, post-burial semi-urban and patio environment scenarios were largely unusable, containing significantly large proportions of very high and low magnetic gradiometry areas with respect to background values (Fig. 5.9).

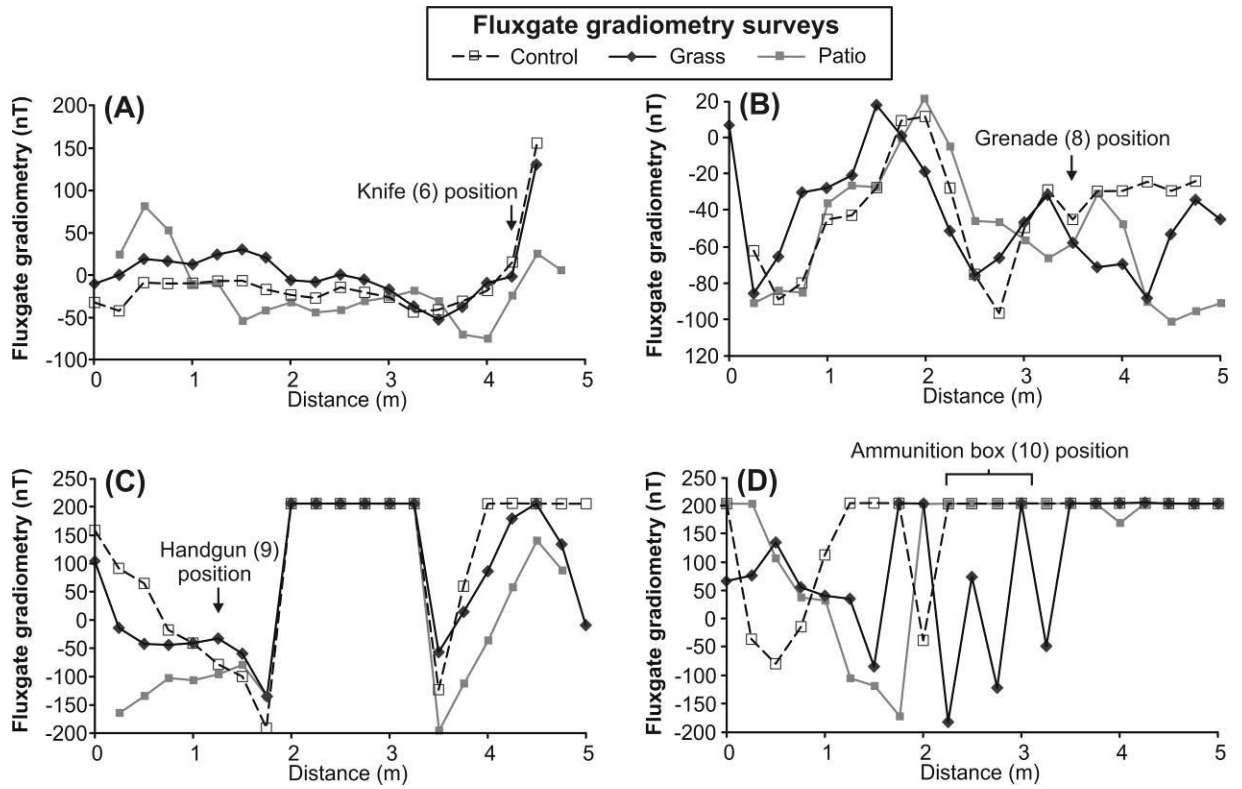


Figure 5.8. Fluxgate gradiometry selected 2D surveys profiles. (A) Profile 9 ($X=2$ m) over target (6) single knife; (B) profile 12 ($X=2.75$ m) over target (8) WW1 hand grenade; (C) profile 15 ($X=3.5$ m) over target (9) handgun and; (D) profile 18 ($X=4.25$ m) over target (10) ammunition box (all marked). See key for survey type and Table 5.2 for details. Modified from Hansen *et al.* (2013).

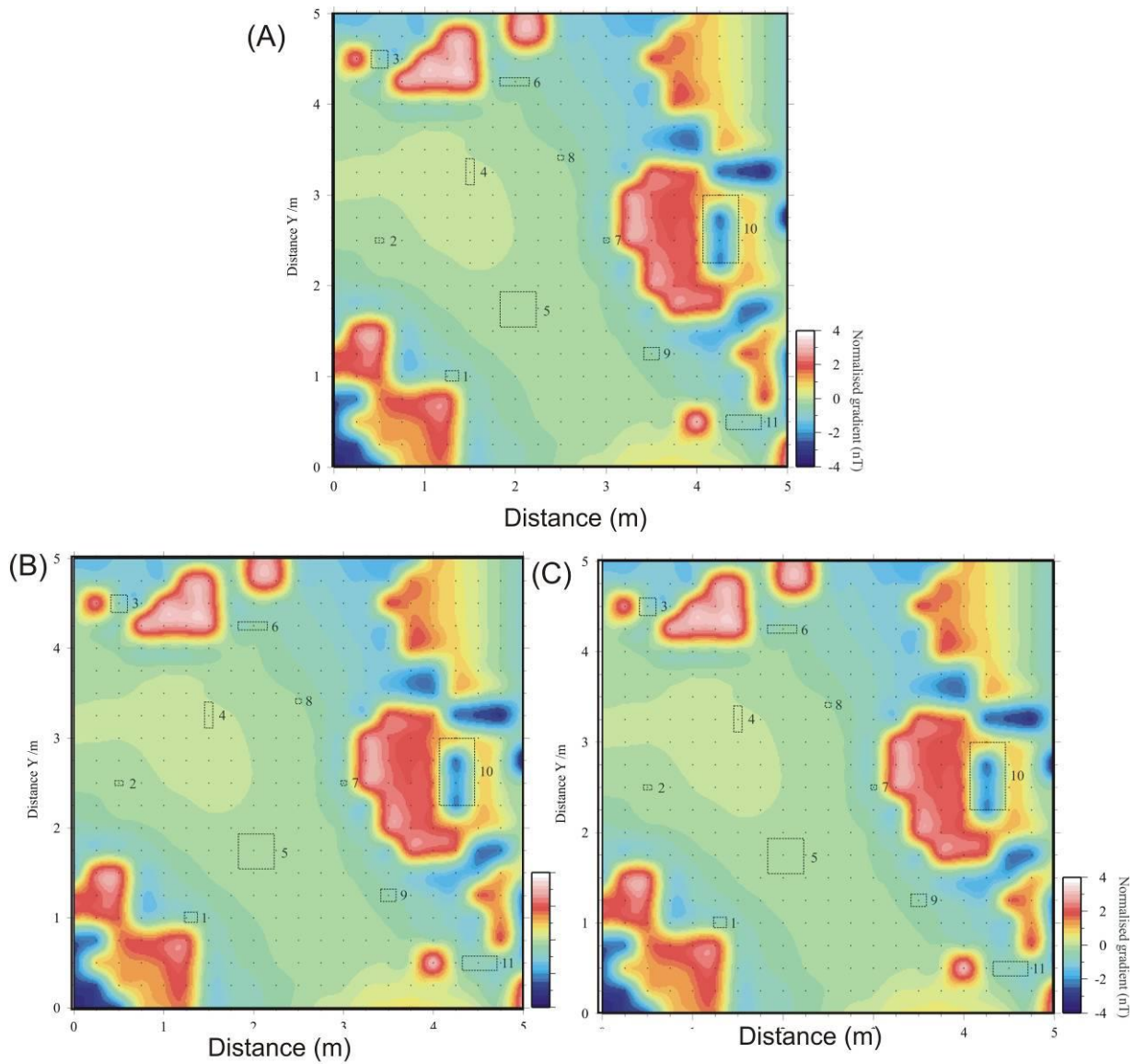


Figure 5.9. Fluxgate gradiometry processed, gridded and contoured map view data plots of (A) pre-burial control with interpreted isolated anomalies, with respect to background values, marked (text); (B) post-burial semi-urban environment and; (C) post-burial patio garden environment respectively. Scale for (A) and (B) are the same. Table 5.2 for target descriptions. Modified from Hansen *et al.* (2013).

Within the post-burial semi-urban environment, high magnetic anomalies, with respect to background values, could be correlated with (3) the steel plate, (4) two breadknives, (5) the entrenchment tool, (6) the single breadknife, (8) the WW1 hand grenade and (10) the ammunition box locations (*c.f.* Figs. 5.3, 5.8 and 5.9). Within the post-burial domestic patio environment, high magnetic anomalies, with respect to background values, could be correlated with (3) the steel plate, (4) two breadknives, (6) the single breadknife, (8) the WW1 hand grenade and (10) the ammunition box locations (*c.f.* Figs. 5.3, 5.8 and 5.9). Fluxgate gradiometry survey results therefore gave a 55% (semi-urban) and 45% (patio) total target detection success rate respectively.

5.3.4 Magnetic (potassium-vapour) gradiometry

Magnetic (potassium-vapour) gradiometry data for the three surveys (total data points of 5,437 (control), 3,729 (semi-urban) and 4,050 (patio), respectively) were also geophysically ‘noisy’. Survey averages and 2σ of lower sensor total field data were 49,245 nT / 450 2σ (control), 49,251 nT / 1,112 2σ (semi-urban) and 49,270 nT / 1106 2σ (patio) scenarios respectively. Survey averages and 2σ of gradiometry data were 13.6 nT / 860 2σ (control), -0.1 nT / 742 2σ (semi-urban) and 6.2 nT / 708 2σ (patio) scenarios respectively that gave a generally good survey repeatability.

The analysis of 2D profiles was found to be optimal for estimation of target detection (selected examples shown in Fig. 5.10). Magnetic gradiometry map view plots of the control, post-burial semi-urban and patio environment scenarios are shown in Figure 5.11 and de-trended versions shown in Figure 5.12. Within the post-burial semi-urban environment magnetic

dataset, high magnetic anomalies, with respect to background values, could be correlated with (3) the steel plate, (6) the single breadknife, (7) the WW2 hand grenade, (8) the WW1 hand grenade, (9) the handgun and (10) the ammunition box positions (*c.f.* Figs. 5.3, 5.10 and 5.11). Within the patio scenario magnetic dataset, high magnetic anomalies, with respect to background values, could be correlated with (2) the bolt, (3) the steel plate, (4) two breadknives, (6) the single breadknife, (7) the WW2 hand grenade, (8) the WW1 hand grenade, (9) the handgun and (10) the ammunition box locations (*c.f.* Figs. 5.3, 5.10 and 5.11). Potassium vapour gradiometry survey results therefore gave a 55% (semi-urban) and 72% (patio) total target detection success rate respectively.

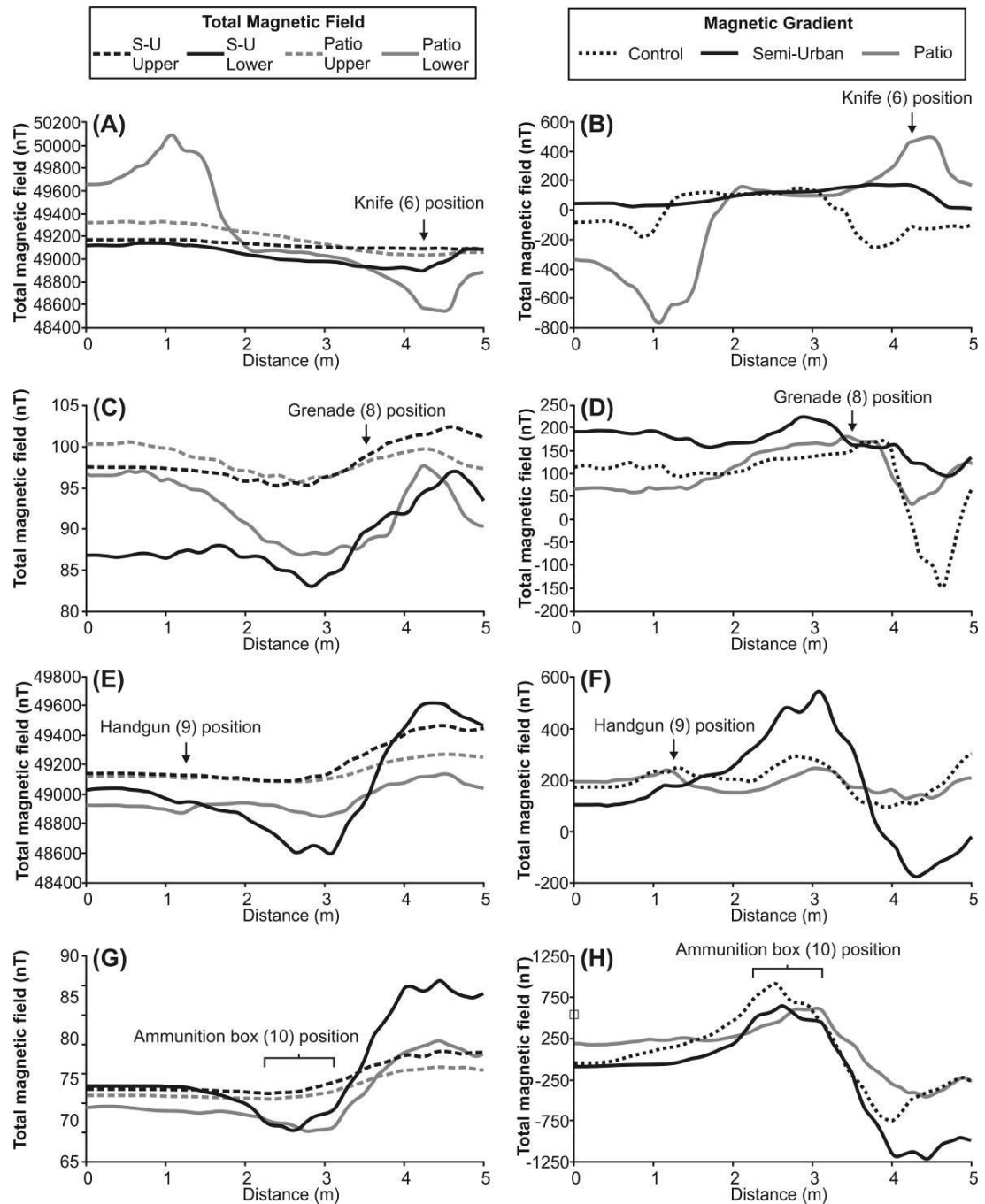


Figure 5.10. Potassium vapour gradiometry selected 2D survey profiles. (A/B) Profile 9 ($X=2$ m) over target (6) single knife; (C/D) profile 12 ($X=2.75$ m) over target (8) WW1 hand grenade; (E/F) profile 15 ($X=3.5$ m) over target (9) handgun and; (G/H) profile 18 ($X=4.25$ m) over target (10) ammunition box (all marked). See key for and Table 5.2 for details. Modified from Hansen *et al.* (2013).

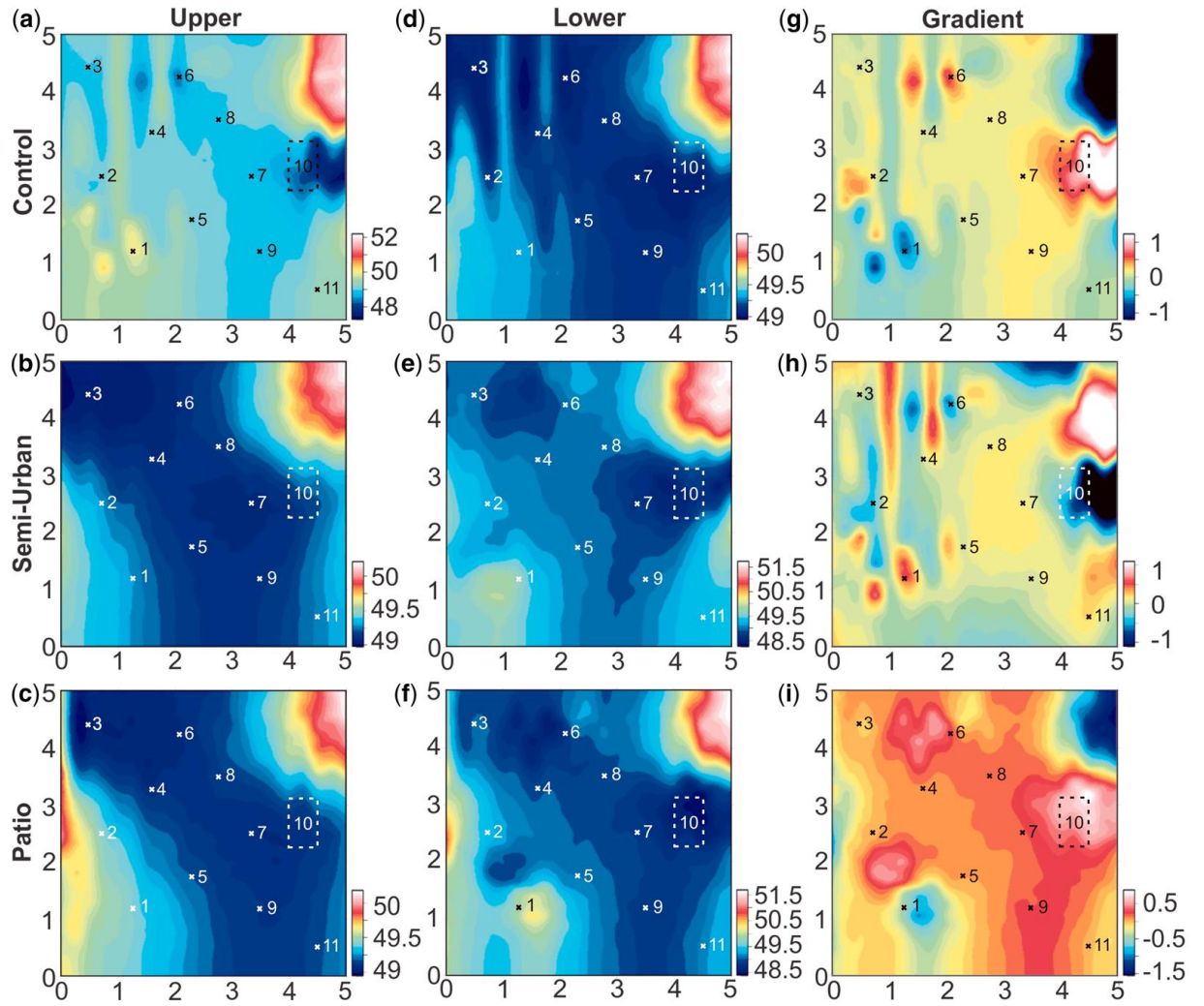


Figure 5.11. K⁺ vapour gradiometry (10³ nT) processed, gridded and contoured map-view plots using upper sensor, lower sensor and gradient for pre-burial, post-burial semi-urban and patio environments (A-I, respectively). Modified from Hansen *et al.* (2013).

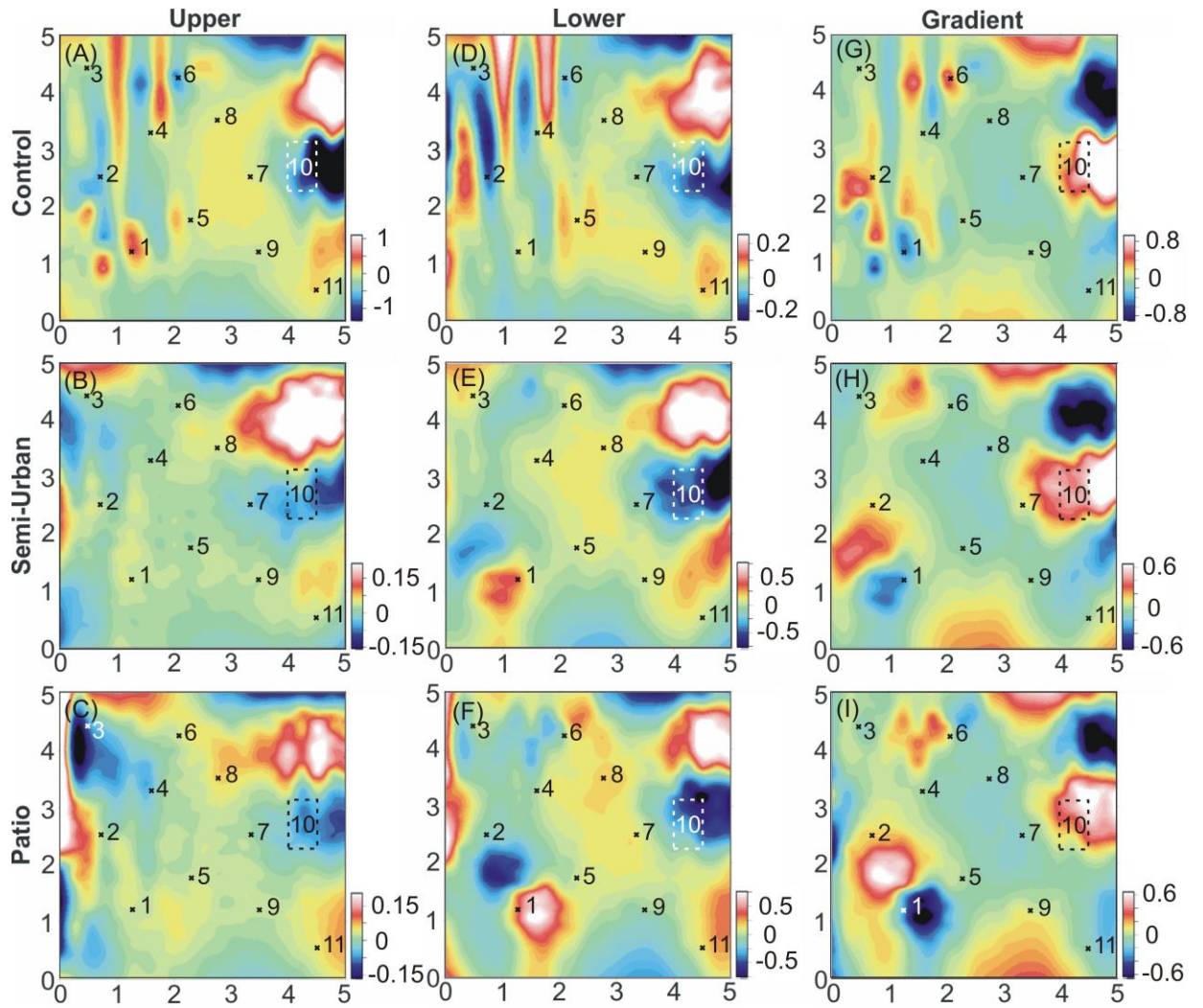


Fig. 5.12. K⁺ vapour gradiometry (10^3 nT) processed, de-trended, gridded and contoured map view plots using upper sensor, lower sensor and gradient for pre-burial, post-burial semi-urban and pre-burial patio environments (A-I, respectively). Modified from Hansen *et al.* (2013).

5.3.5 Electrical Resistivity

Fixed-offset (0.5 m) resistivity data for the control dataset (441 data points) had resistance maximum / minimum values of 111.7 Ω / 47.3 Ω with an average of 78.4 Ω and 25.4 2σ value. This confirmed that the site was relatively heterogeneous electrically. The post-burial (semi-urban) 0.25 m and 0.50 m fixed-offset repeat surveys had resistance maximum / minimum values of 194.5 Ω / 76.0 Ω (25 cm) and 129.5 Ω / 51.5 Ω (50 cm), with averages of 124.1 Ω (25 cm) / 83.0 Ω (50 cm) and 37.2 2σ (25 cm) / 27.2 2σ (50cm) values respectively (Table 5.8). Data repeatability for the 0.5 m fixed-offset surveys was therefore generally good.

Within the post-burial semi-urban environment, high resistance anomalies, with respect to background values, could be correlated with resistivity (0.25 m fixed-offset) survey, the (5) entrenching tool, (6) the single knife, (7) the WW2 hand grenade, (9) the handgun, (10) the ammunition box and (11) the spent shell locations (*c.f.* Figs. 5.3, 5.13 and 5.14). A low resistance anomaly, with respect to background value, could be correlated with (1) the brick and (3) the steel plate. Within the semi-urban environment resistivity (0.5 m fixed-offset) survey, only high resistance anomalies, with respect to background values, which could be correlated with buried targets were (10) the ammunition box and (11) the spent shell locations (*c.f.* Figs. 5.3, 5.13 and 5.14). Selected 2D profiles are shown in Figure 5.12. This therefore gave a 73 % (25 cm) and 18 % (50 cm) total target detection success rate respectively.

Target number	Description	Raw response (Ω)				De-trended data response (Ω)				Normalised, de-trended data response (SD from mean (σ))			
		0.5 m		0.25 m		0.5 m		0.25 m		0.5 m		0.25 m	
		Ctrl	SU	Ctrl	SU	Ctrl	SU	Ctrl	SU	Ctrl	SU	Ctrl	SU
1	Brick	97.9	105.6	129.8	129.8	2.01	3.91	8.99	8.99	0.43	0.83	0.94	0.94
2	Bolt and screw	87.55	91.95	153.3	153.3	3.1	2.89	6.74	6.74	0.66	0.62	0.7	0.7
3	Steel plate	62.2	72.55	87.2	87.2	-4.67	1.45	6.55	6.55	-0.99	0.31	0.68	0.68
4	Breadknives	78.2	81	139.5	139.5	-0.09	-1.77	2.65	2.65	-0.02	-0.38	0.28	0.28
5	Entrenching tool	88.35	96.4	97.25	97.25	2.77	5.82	12.3	12.3	0.59	1.24	1.28	1.28
6	Knife	68.15	78.1	121.55	121.55	-3.13	2.26	12.43	12.43	-0.66	0.48	1.3	1.3
7	WWII grenade	67.6	71.7	75.95	75.95	-7.59	-7.39	-2.4	-2.4	-1.6	-1.58	-0.25	-0.25
8	WWI grenade	71	76.95	134.45	134.45	-3.31	-1.44	-2.4	-2.4	-0.7	-0.31	-0.25	-0.25
9	Handgun	78.2	82.8	105.15	105.15	0.39	0.64	12.92	12.92	0.08	0.14	1.35	1.35
10	Ammunition box	71.7	72.7	125.25	125.25	4.34	2.3	29.13	29.13	0.92	0.49	3.04	3.04
11	Mortar shell	78.3	96.5	103.1	103.1	1.06	14.7	34.58	34.58	0.22	3.15	3.6	3.6
Average for whole dataset		82.9	78.4	123.77	123.77	0.01	0	-0.01	-0.01	0	0	0	0
SD for whole dataset		13.5	12.8	18.9	18.9	4.68	4.74	9.6	9.6	1	1	1	1
Range for whole dataset		68	64.4	120.9	120.9	31.1	31.9	73.4	73.4	6.74	6.64	7.65	7.65

Table 5.8. Max. and/or min. (0.25/0.5m probe-spacing) resistance values using raw, de-trended and normalised data. SU = semi-urban.

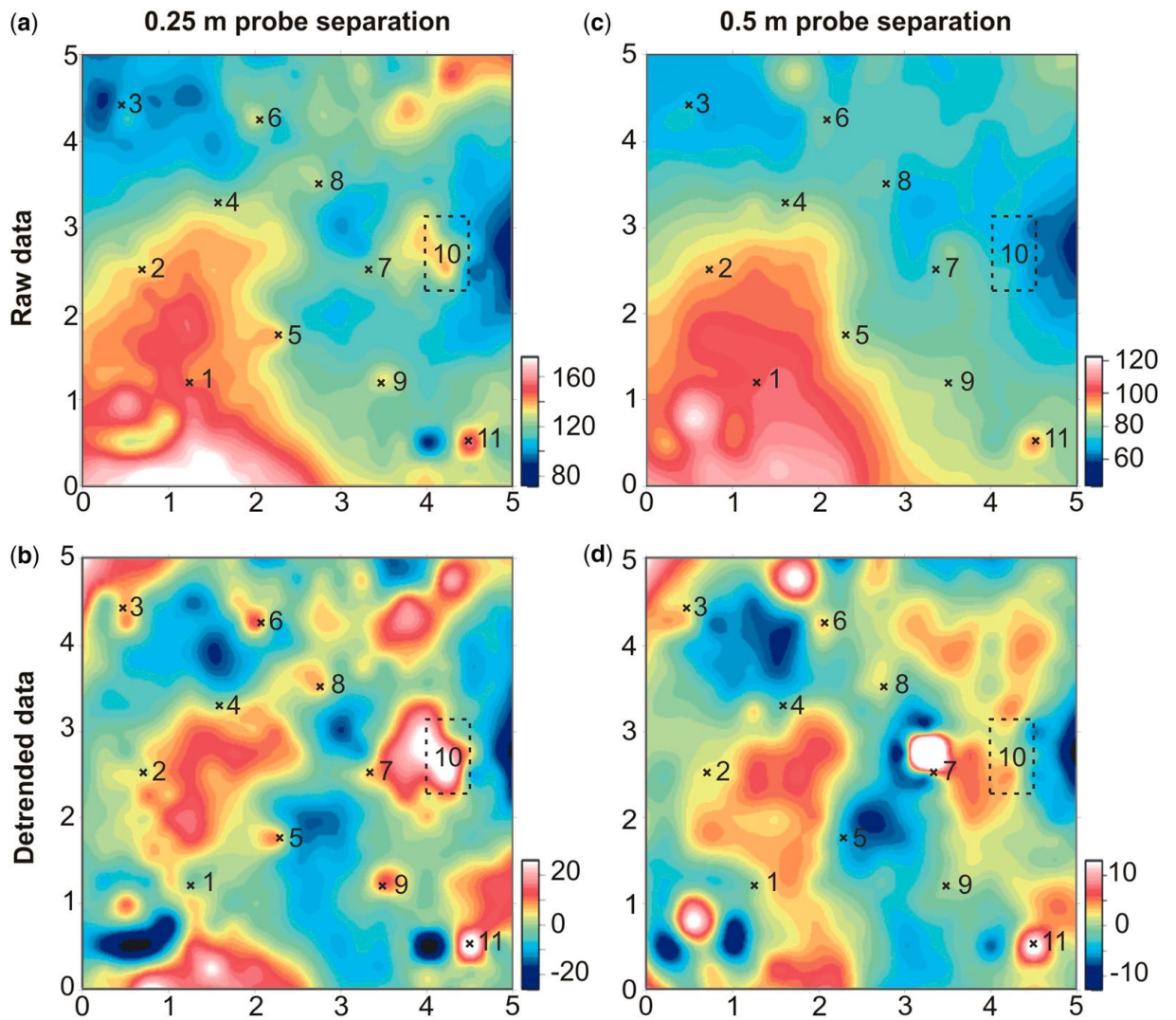


Figure 5.13. Post-burial, semi-urban, bulk ground-resistivity (Ωm) contour plots using raw and de-trended datasets with 0.25 (A and B respectively) m and 0.5 m (C and D respectively) probe spacings. Note the relatively high anomalies corresponding to the knife (6), handgun (9) and mortar shell (11). Modified from Hansen *et al.* (2013).

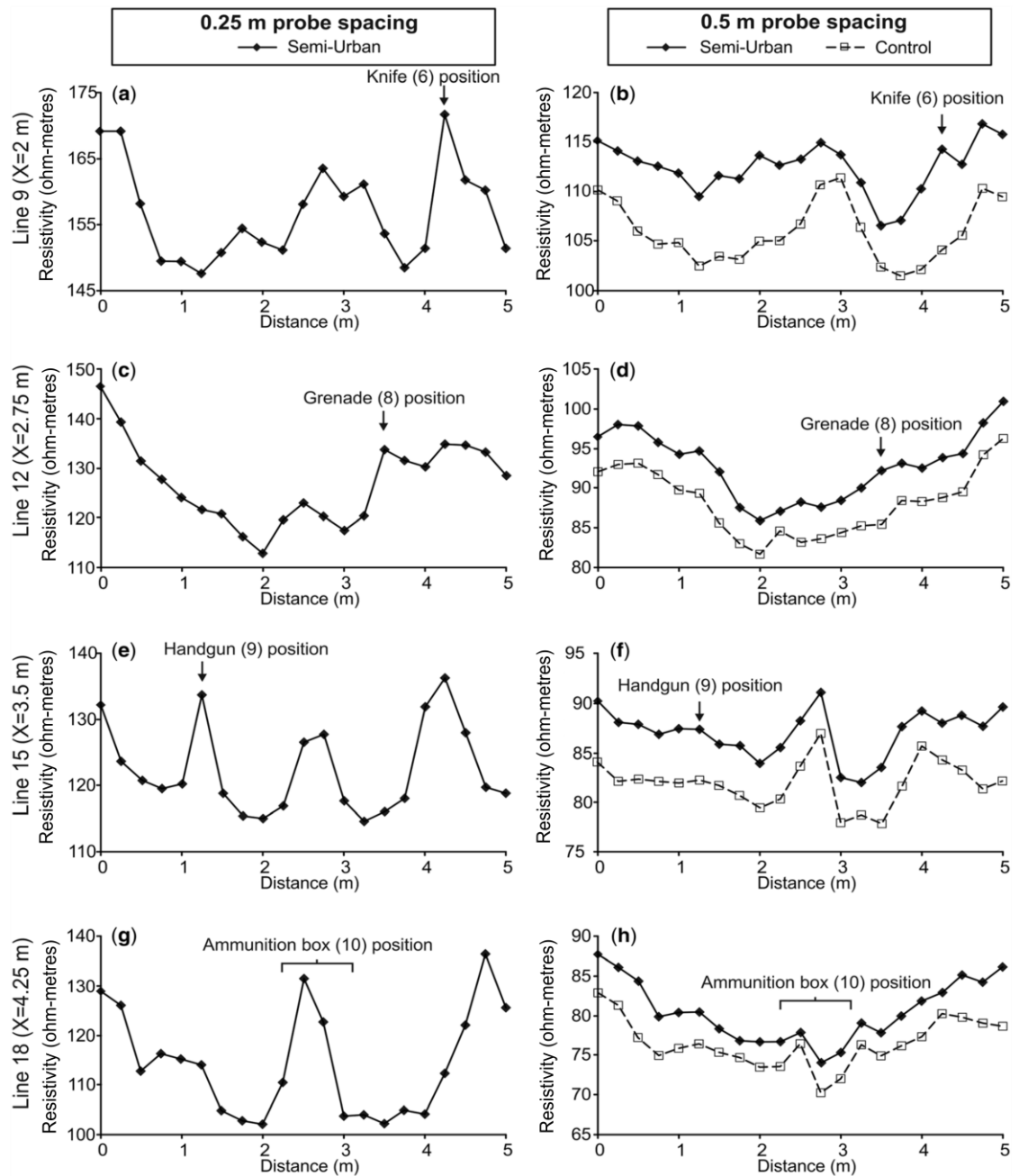


Figure 5.14. Bulk-ground resistivity 2D profiles for selected targets using 0.25 m and 0.5 m probe separations. Note generally high resistivity anomalies associated with targets with the exception of 0.5 m probe separation survey over the ammunition box (H). Modified from Hansen *et al.* (2013).

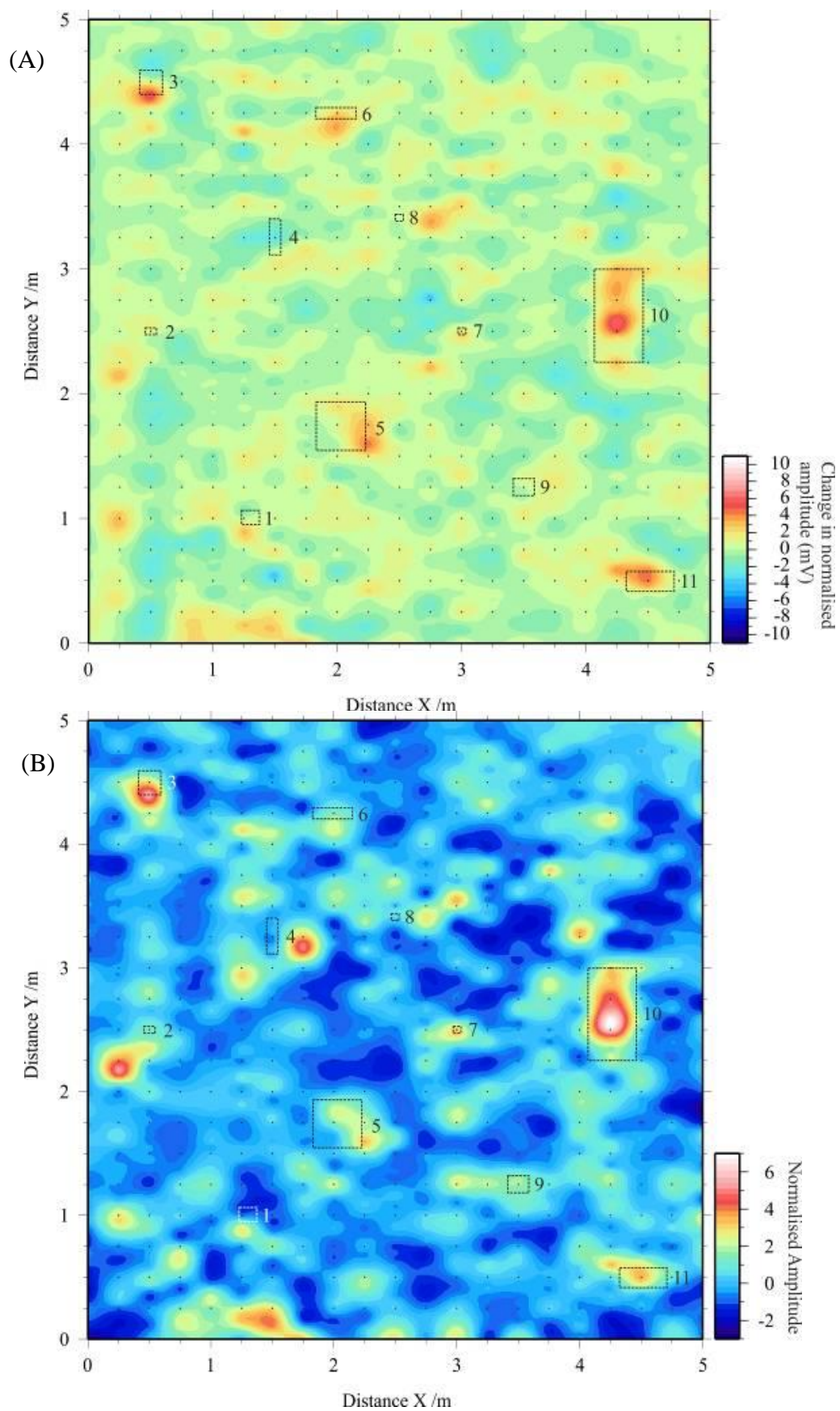
5.3.6 Ground penetrating radar

Both the 450 MHz and 900 MHz dominant frequency GPR control datasets showed a number of non-target objects were located within the survey area; this therefore provides confirmation that the study site is representative of a semi-urban, heterogeneous site. Within the post-burial semi-urban environment dataset, hyperbolae in the 450 MHz frequency dataset could be correlated with (3) the steel plate, (7) WW2 hand grenade, (9) the handgun, (10) the ammunition box and (11) the spent mortar shell locations (*c.f.* Figs. 5.3, 5.15 and 5.16). Within the 900 MHz frequency dataset, hyperbolae could be correlated with (3) the steel plate, (4) the two breadknives, (6) the single breadknife, (7) WW2 hand grenade, (9) the handgun, (10) the ammunition box and (11) the spent mortar shell locations (*c.f.* Figs. 5.3, 5.15 and 5.16). Selected 2D profiles shown in Figures 5.17 and 5.18. This gave a 45 % (450) and 64 % (900) total target detection success rate respectively. Tables 5.9 and 5.10 summarises the respective relative amplitudes for each target.

Within the post-burial patio environment dataset, hyperbolae in the 450 MHz frequency dataset could be correlated with (3) the steel plate, (6) the single breadknife, (8) the WW1 hand grenade, (9) the handgun, (10) the ammunition box and (11) the spent mortar shell locations (*c.f.* Figs. 5.3, 5.15 and 5.16). Within the 900 MHz frequency dataset, hyperbolae could be correlated with (3) the steel plate, (4) the breadknives, (5) the entrenching tool, (6) the single breadknife, (10) the ammunition box and (11) the spent mortar shell locations (*c.f.* Figs. 5.3, 5.15 and 5.17). Selected 2D profiles are shown in Figures 5.16 and 5.17. This gave a 54 % (450) and 54 % (900) total target detection success rate respectively.

Target number	Description	Non-de-trended response (mV)			De-trended data response (mV)			Normalised, de-trended data response (SD from mean (σ))		
		Ctrl	SU	Patio	Ctrl	SU	Patio	Ctrl	SU	Patio
1	Brick	803.00	2543.00	646.00	-333.41	1365.85	-811.22	0.83	3.00	-1.17
2	Bolt and screw	663.00	978.00	1124.00	-450.59	-163.59	-110.16	0.03	-0.42	-0.21
3	Steel plate	1065.00	3838.00	4639.00	-139.84	2544.66	3256.58	-1.03	5.64	4.42
4	Breadknives	2011.00	1384.00	1043.00	908.66	177.97	-326.00	-1.39	0.34	-0.51
5	Entrenching tool	724.00	2363.00	1939.00	-271.92	1240.58	625.21	1.50	2.72	0.80
6	Knife	698.00	1282.00	1859.00	-457.48	-16.60	216.58	0.52	-0.09	0.24
7	WWII grenade	1439.00	2293.00	1520.00	316.85	1015.89	180.83	1.05	2.22	0.19
8	WWI grenade	637.00	974.00	1491.00	-535.55	-358.12	20.74	0.69	-0.86	-0.03
9	Handgun	1806.00	3451.00	1423.00	774.27	2317.73	126.98	-0.86	5.43	0.12
10	Ammunition box	2190.00	3726.00	8756.00	954.89	2527.18	7315.03	2.41	5.60	10.01
11	Mortar shell	977.00	2203.00	1205.00	-45.41	1339.97	-202.26	-0.01	2.94	-0.34
Average for whole dataset		1164.42	1202.75	1506.46	17.60	25.53	41.41	0.00	0.00	0.00
SD for whole dataset		430.07	480.99	753.01	409.67	446.79	726.74	1.00	1.00	1.00
Range for whole dataset		4471.00	4847.00	8756.00	4650.60	4646.30	9387.03	11.35	10.40	12.92

Table 5.9. Max. and/or min. reflection amplitudes using each of non-de-trended, de-trended and normalised 900 MHz GPR data.



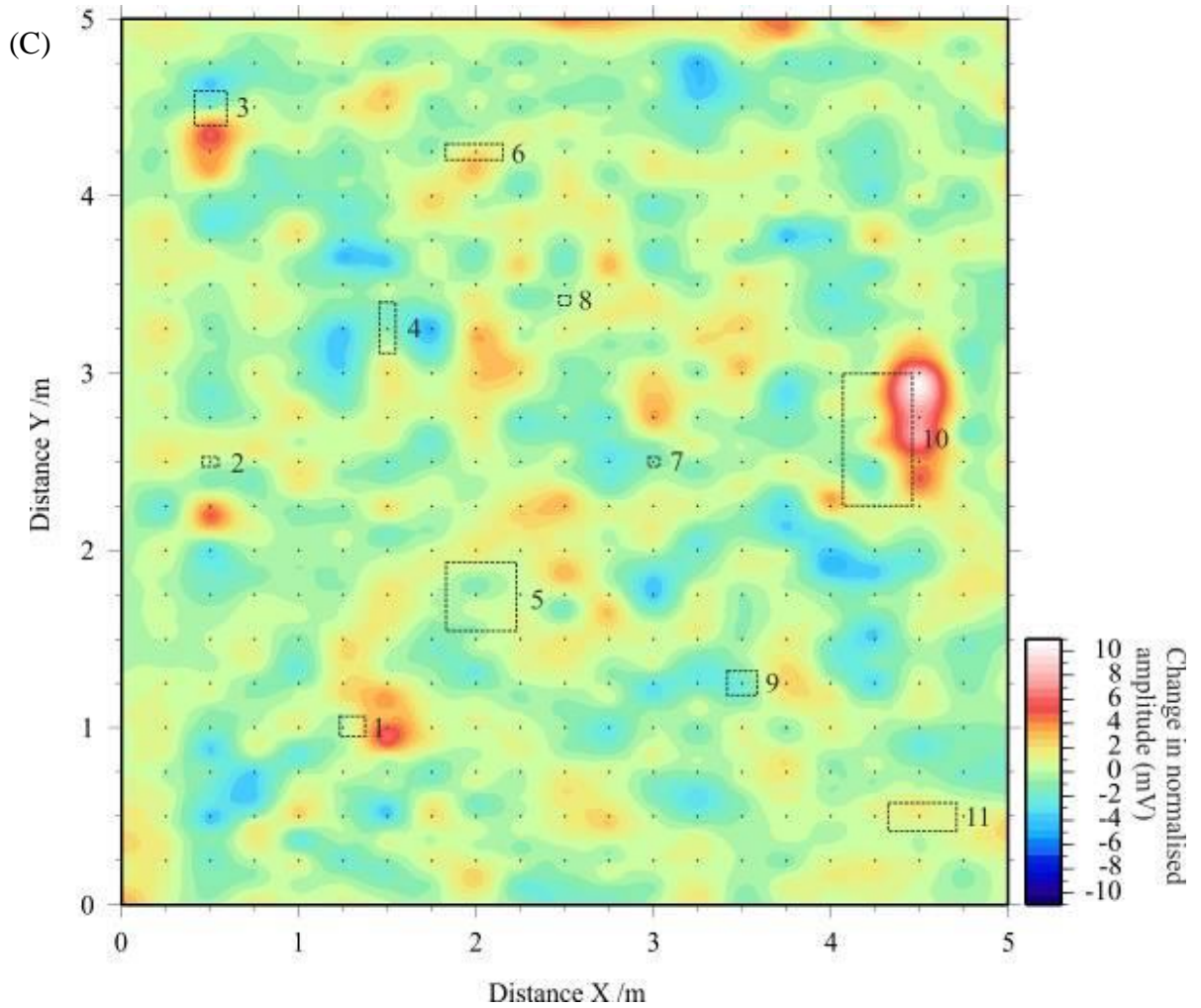
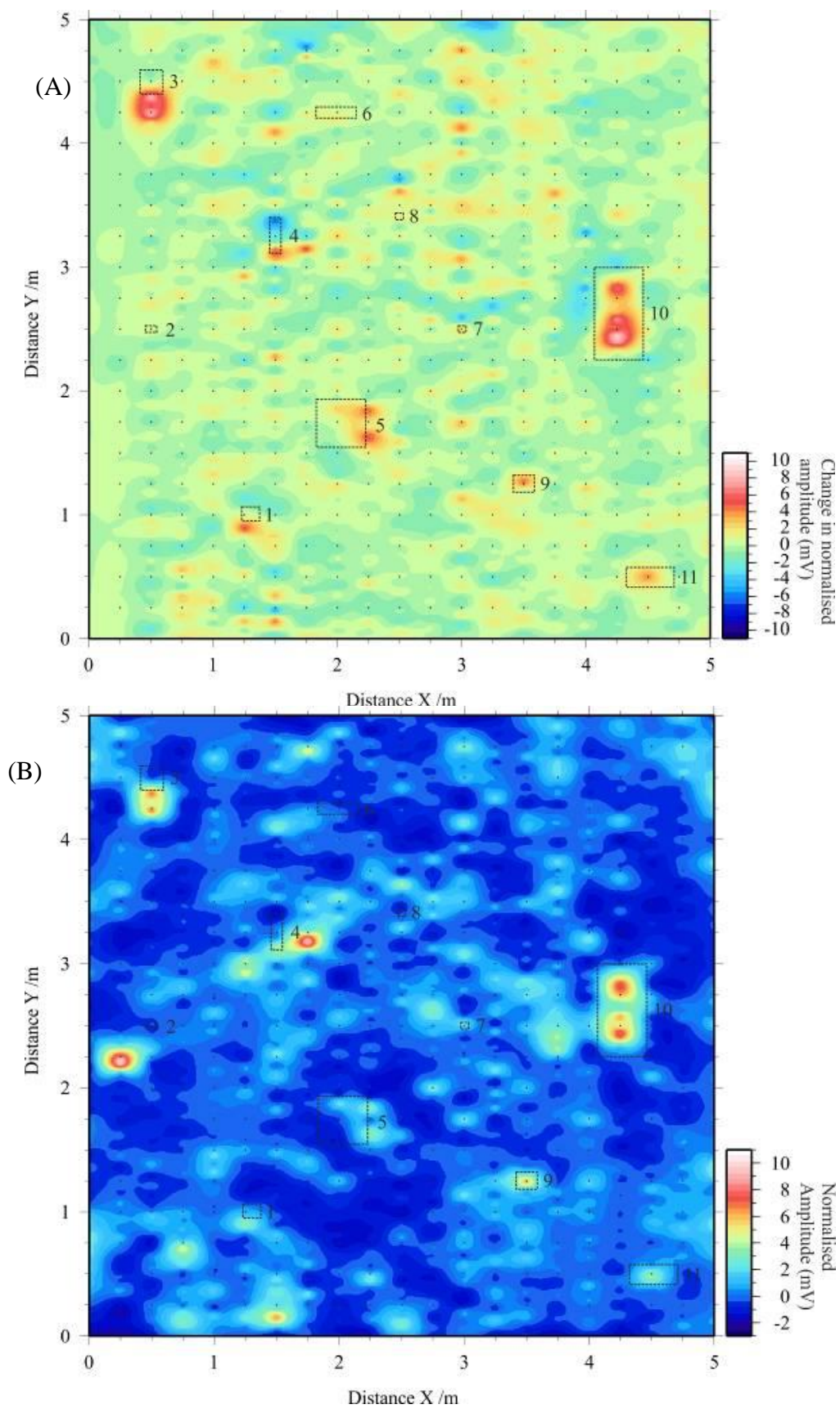


Figure 5.15. 450 MHz GPR normalised time-slices over the test site of (A) control, (B) semi-urban and (C) patio environments respectively. Some relatively high and relatively low amplitude anomalies correspond to target positions. See Table 5.2 for target details. Modified from Hansen *et al.* (2013).



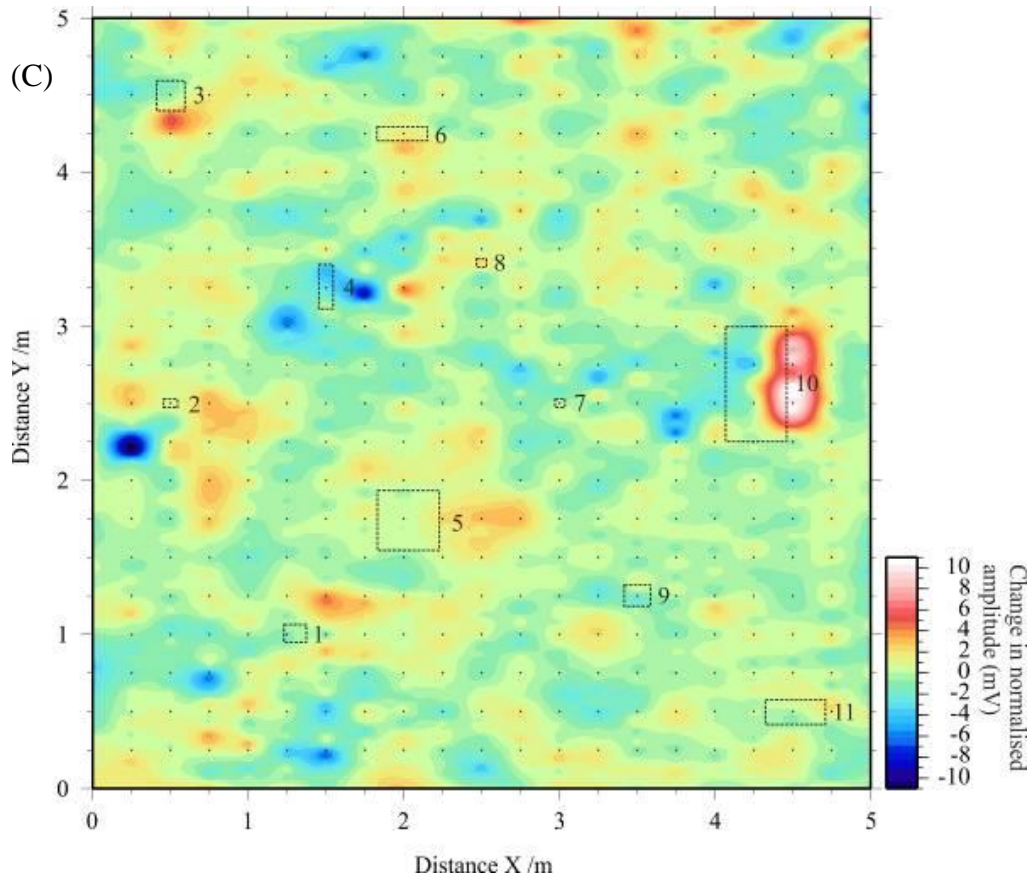


Figure 5.16. 900 MHz GPR time-slices over the test site of (A) control, (B) semi-urban and (C) patio environments respectively. Some relatively high and relatively low amplitude anomalies correspond to target positions. See Table 5.2 for target details. Modified from Hansen *et al.* (2013).

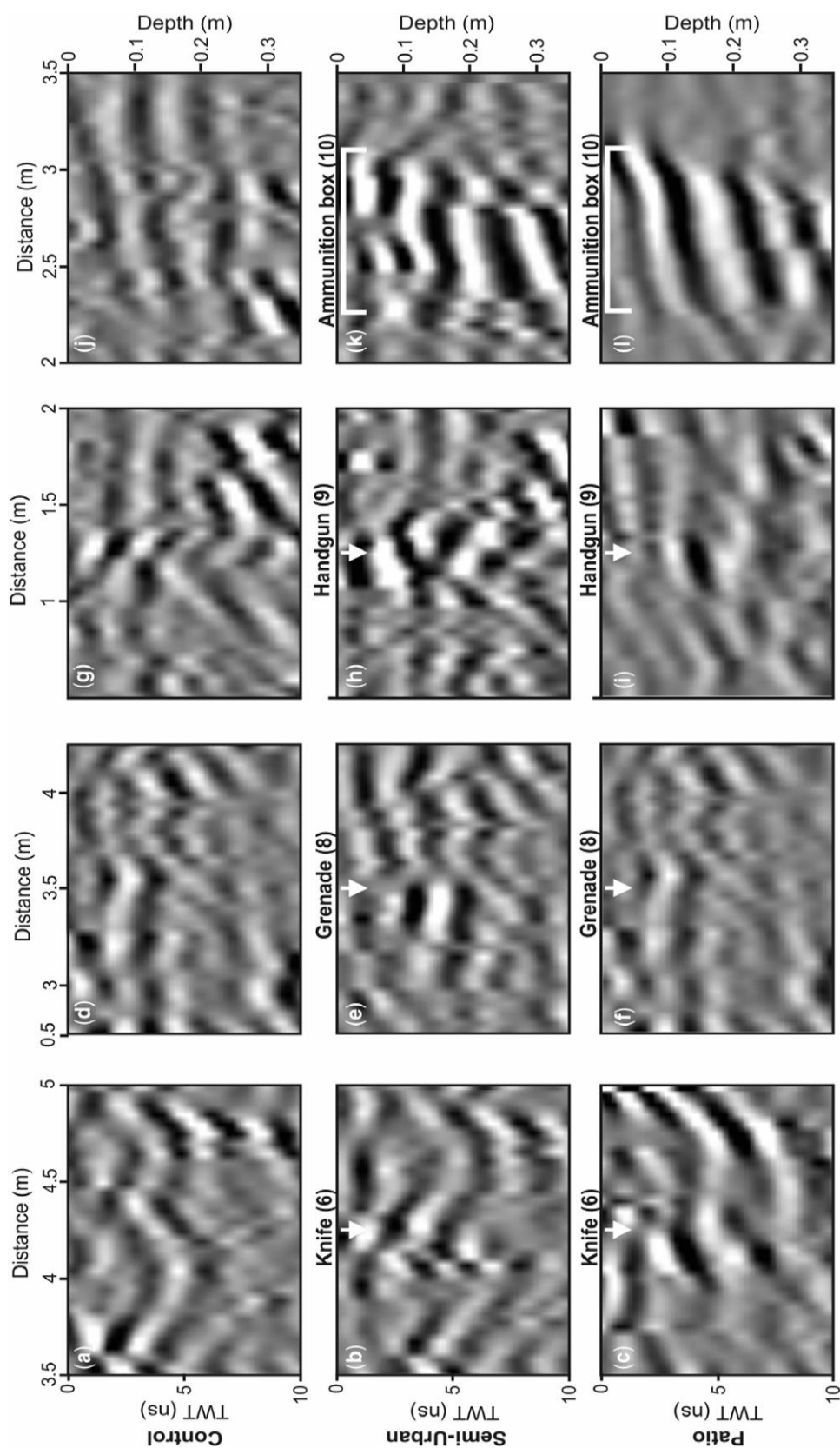


Figure 5.17. 450 MHz GPR processed selected 2D profiles. (A-C) Profile 9 ($X=2$ m) over target (6) single knife; (D-F) profile 12 ($X=2.75$ m) over target (8) WW1 hand grenade; (G-I) profile 15 ($X=3.5$ m) over target (9) handgun and; (J-L) profile 18 ($X=4.25$ m) over target

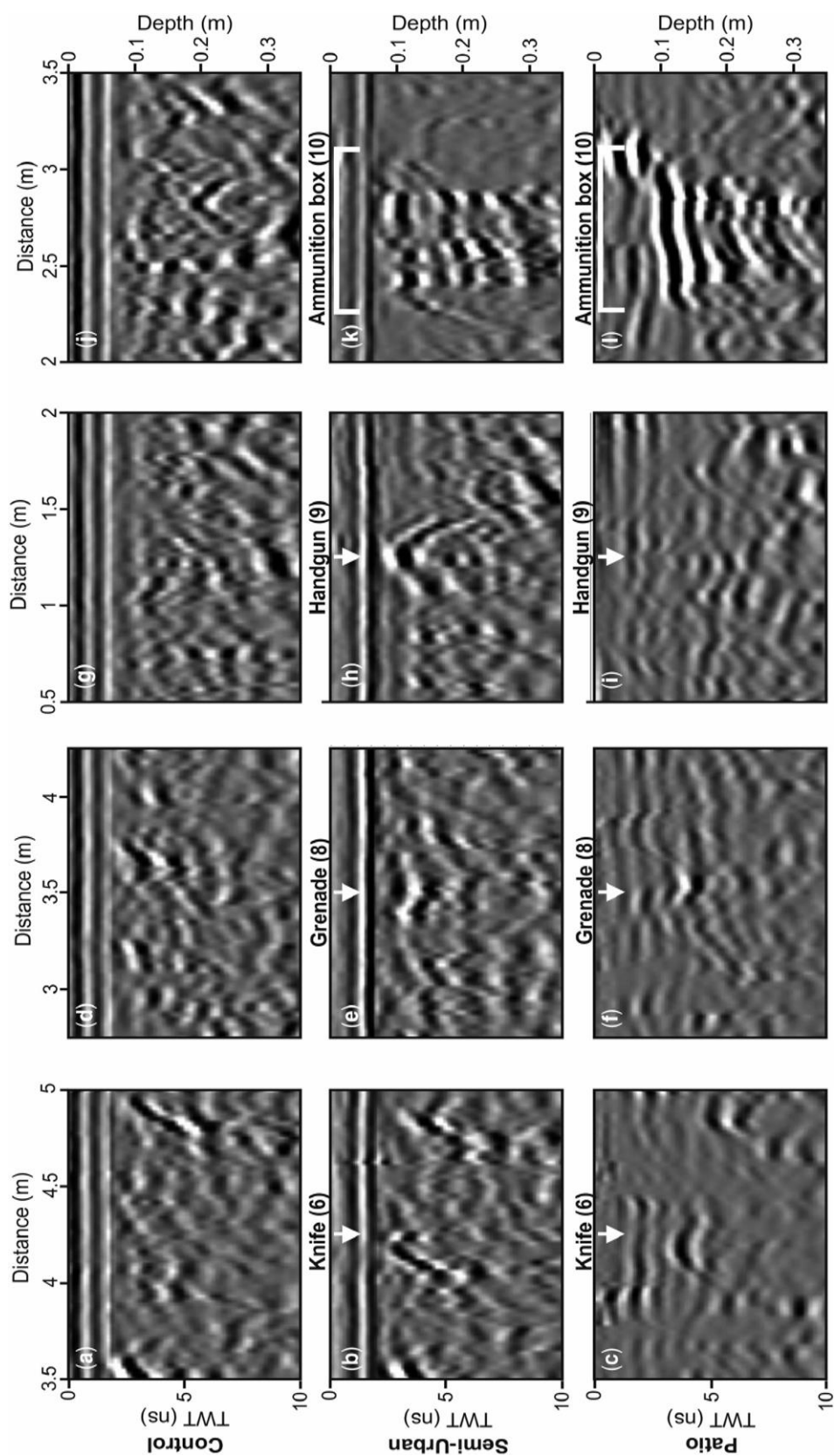


Figure 5.18. 900 MHz GPR processed selected 2D profiles. (A-C) Profile 9 ($X=2$ m) over target (6) single knife; (D-F) profile 12 ($X=2.75$ m) over target (8) WW1 hand grenade; (G-I) profile 15 ($X=3.5$ m) over target (9) handgun and; (J-L) profile 18 ($X=4.25$ m) over target (10) ammunition box for control, semi-urban and patio environment scenarios respectively (all marked). See Table 1

5.4 Discussion

This section has been organised so as to answer and discuss the study objectives in sequential order. Using the success detection scheme discussed in section 5.3.1, tabulated graphical summaries of the study results for both the semi-urban environment and patio environment scenarios have been generated (Table 5.11 and 5.12 respectively). The success rates of the different techniques have also been presented as bar graphs and compared to other studies for comparison (Fig. 5.19).

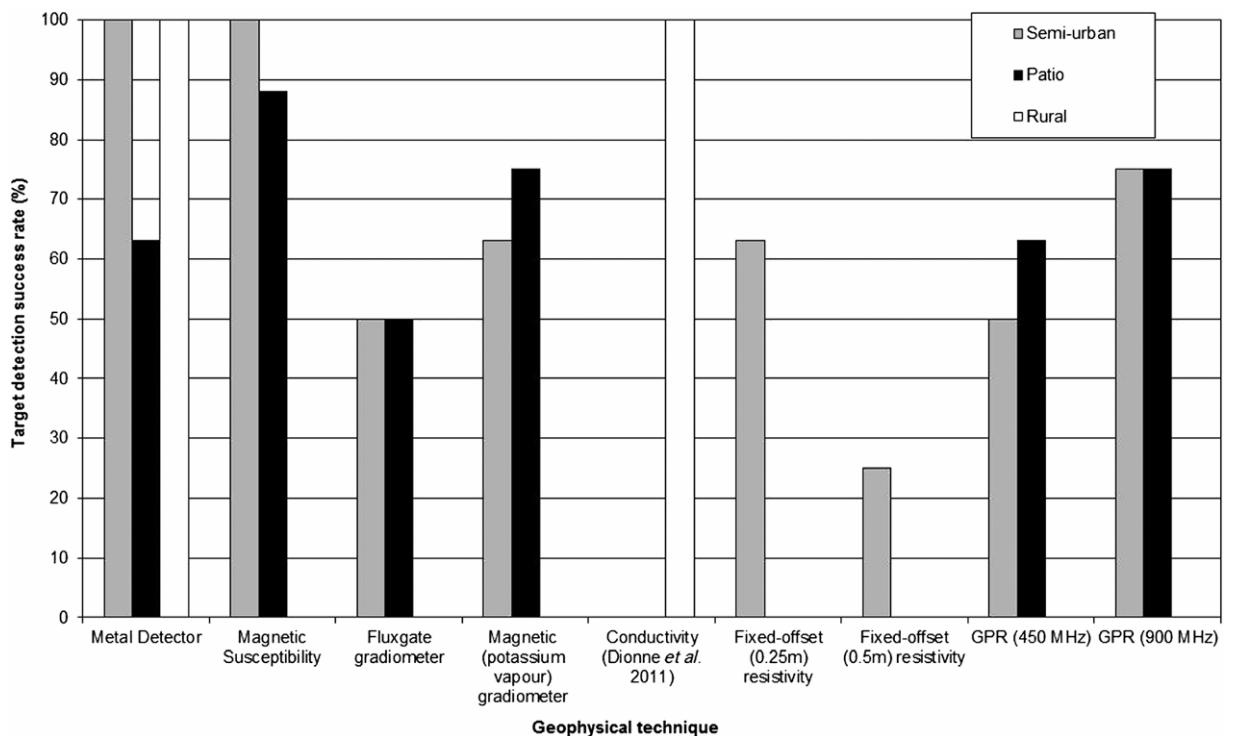


Fig. 5.19. Summary bar graph showing percentage total of target detection success rates for the different geophysical techniques trialled in semi-urban, patio and rural environments (key inset). Note rural environment results are from Rezos *et al.* (2010) and Dionne *et al.* (2011) for metal detector and conductivity surveys respectively. Modified from Hansen *et al.* (2013).

Target number	Description	Metal detector	Magnetic susceptibility	Fluxgate gradiometry	K ⁺ vapour gradiometry	Resistivity ¹			GPR		
						0.50 m	0.25 m	450 MHz	900 MHz	450 MHz	900 MHz
1	Brick	○	○	○	●	○	○	●	●	●	●
2	Bolt and screw	○	●	○	●	○	○	○	○	○	○
3	Steel plate	●	●	●	○	●	●	●	●	●	●
4	Breadknives	○	●	○	○	○	○	●	●	●	●
5	Entrenching tool	●	●	○	○	○	●	●	●	●	●
6	Knife	●	●	●	●	●	●	●	●	●	●
7	WWII grenade	●	●	○	○	○	○	●	○	○	○
8	WWI grenade	●	●	○	○	○	○	●	○	○	○
9	Handgun	●	●	○	○	○	●	○	○	○	○
10	Ammunition box	●	●	●	●	●	●	●	●	●	●
11	Mortar shell	●	●	●	●	●	●	●	●	●	●

Table 5.11. Summary of technique success in semi-urban environment scenario. ●=very good, ●=good, ●=weak and ○=no detection.

Target number	Description	Metal detector	Magnetic susceptibility	Fluxgate gradiometry	K ⁺ vapour gradiometry	Resistivity ¹			GPR	
						0.50 m	0.25 m	450 MHz	900 MHz	
1	Brick	○	○	○	●	N/A	N/A	●	●	●
2	Bolt and screw	○	●	○	○	N/A	N/A	●	○	○
3	Steel plate	●	●	●	○	N/A	N/A	●	●	●
4	Breadknives	●	●	○	●	N/A	N/A	●	○	○
5	Entrenching tool	○	●	○	○	N/A	N/A	●	●	●
6	Knife	●	○	○	●	N/A	N/A	●	●	●
7	WWII grenade	○	●	○	○	N/A	N/A	●	○	○
8	WWI grenade	○	●	○	●	N/A	N/A	●	○	○
9	Handgun	●	●	○	○	N/A	N/A	●	●	●
10	Ammunition box	●	●	●	●	N/A	N/A	●	●	●
11	Mortar shell	●	●	●	●	N/A	N/A	●	●	●

Table 5.11. Summary of technique success in patio environment scenario. ●=very good, ●=good, ●=weak and

○=no detection.

5.4.1 Evaluate and find optimum magnetic detection technique(s) of the target buried material

Interestingly, the metal detector was not particularly successful, with target detection success rates of only 57% (semi-urban) and 43% (patio) (see Tables 5.11 and 5.12 respectively). The lower success rate over the patio was presumably due to the reduced penetration depth of the electro-magnetic waves through the low-conductivity concrete paving slabs. If a metal detector was the sole detection method in a forensic search within a semi-urban or patio environment, as this study simulated, the results suggest that key targets may go undetected. These results also contrasted with Rezos *et al.* (2010) results within a rural environment which gained a 100% target detection success rate using a metal detector (Fig. 5.19).

The magnetic susceptibility survey results proved target detection was very good, with success rates of 82% (semi-urban) and 73% (patio) (Fig. 5.19) (see Tables 5.11 and 5.12, respectively). In fact, all the forensic buried target objects were detectable in the semi-urban environment scenario; only the two control buried objects, (1) the brick and (2) the bolt and screw, went undetected. The larger buried forensic objects were successfully located but the handgun was not detected in either of the post-burial surveys.

Fluxgate gradiometry was not particularly successful, with target detection success rates of 55% (semi-urban) and 45% (patio) (Fig. 5.19). Both the single and grouped breadknives were successfully detected, as was the ammunition box and one hand grenade although, again, the handgun went undetected. The use of this technique may also be problematic in urban environments, as recording of data was not possible over a high proportion of area (averaging 31% over the three surveys), as other authors discuss (Reynolds, 2011).

The potassium vapour gradiometry survey results were relatively good, with target detection success rates of 55% (semi-urban) and 72% (patio) (Fig. 5.19). Again, the target detection success rates increased over the patio versus the semi-urban environment – perhaps due to a dampening effect of the patio which could geophysical ‘noise’ (see Tables 5.11 and 5.12, respectively). A very small sampling increment resulted in good data resolution, though target detection success rates were lower than the magnetic susceptibility surveys which had a much wider sampling point separation. Data repeatability was reasonable, with similar 2σ values for both post-burial surveys. Using this instrument, however, it was often difficult to gain a digital ‘lock’ between sensors and gain usable data, which may prove problematic in forensic surveys where there may be limited survey time. Therefore, a suggestion would be to mount the equipment on a wheeled-frame in order to improve data quality (Reynolds, 2004).

5.4.2 Compare magnetic methods with electrical and GPR detection methods

The variability in the control resistivity dataset confirmed the presumed heterogeneous ground conditions of the survey site. The target detection success rates for the 0.25 m and 0.50 m fixed-offset probe spacings were very different; 73% and 18% respectively (Fig. 5.19 and Table 5.11). The 0.25 m spaced probe survey data therefore compared favourably to the magnetic survey techniques as both the handgun and single knife were detected. However this technique could not be utilised over the patio due to the inability to insert the steel probes into the concrete. However, other manufacturers do produce equipment which can record data over hard ground by using a flat-ended probe; an alternative which may be worth exploring in future research.

The GPR survey results were mixed, with only 45% and 54% of targets detected using 450 MHz dominant frequency antennae over the urban and patio environments respectively. This contrasted with 64% and 54% of targets detected using 900 MHz dominant frequency antennae over the urban and patio environments respectively. Importantly the handgun was detected in both environments using 450 MHz antennae, but only in the semi-urban environment using 900 MHz frequency antennae. Results therefore suggested GPR was relatively successful in detecting targets but could miss some potentially important targets in true investigations (Tables 5.11 and 5.12).

5.4.3 Determine optimum GPR detection frequencies

900 MHz was the optimal GPR frequency. Murphy and Cheetham (2008) also proposed that higher frequency (800 MHz rather than 400 MHz) GPR antennae were optimal for buried handgun detection in rural environments.

5.4.4 Determine optimum respective equipment configuration(s) / survey specifications / optimum processing steps

Magnetic susceptibility data suggests 0.25 m spaced, gridded sampling points were adequate for resolving even the smallest objects, with little data processing required. For the majority of techniques, creating simple 2D graphical plots along survey lines was sufficient to detect targets with a relatively high success rate (see Figs 5.10 and 5.14). Fluxgate gradiometry datasets were geophysically ‘noisy’ and required significant removal of erroneous data points and de-trending to gain usable data for interpretation. Magnetic (potassium-vapour)

gradiometry equipment proved useful at 1 m vertical sensor separations in order to obtain gradient data. There were, however, significant amounts of data which needed processing and de-trending before being usable. Equipment operators also needed to be careful that a constant height was maintained between the sensors and the ground surface to improve data quality.

The electrical resistivity 0.25 m fixed-offset probe spacing data was vastly superior to the 0.50 m offset probe spaced datasets, even when using the same sample interval; making the closer probe spacing the more obvious choice for small and high-resolution surveys. However, the amount of ground covered in larger forensic search surveys using this configuration and 0.25 m grid sample intervals may make the use of this technique more problematic.

900 MHz dominant frequency GPR antennae proved more successful than 450 MHz, with a 0.025 m trace sampling interval on 0.25 m spaced survey lines. Basic 2D profile data processing with gain filters and background removal would prove sufficient for target detection although it could be worthwhile to generate 2D ‘time-slices’ if targets were more geophysically subtle in heterogeneous ground and if time allowed.

5.4.5 Determine which technique(s) could determine target depth below ground level

Only the GPR data could be used to definitively determine depth of buried forensic targets below ground level (Figs. 5.18 and 5.19). Total-field magnetic data, such as from the potassium vapour gradiometer, and the bulk electrical resistivity data could both be forward modelled to gain simple estimations of target depths if sufficient time and resources were available (e.g. Reynolds, 2011).

5.4.6 Determine if different metal types could be distinguished

Distinguishing between different buried metallic object types was difficult using the equipment utilised; Rezos *et al.* (2010), for example, used a higher specification metal detector which did allow this. The resistivity survey results did differentiate between conductive (the metal plate) and non-conductive (the brick) buried forensic targets which may be useful information for forensic search investigators. 2D forward modelling of total field magnetic data could allow relative (as opposed to *absolute*) magnetic susceptibility contrasts between the target object and the background material to be assessed, (e.g. Scott and Hunter, 2004).

Finally it was determined that the metal detector, magnetic susceptibility meter, resistivity meter (if in semi-urban environments) and a commercial GPR unit would be relatively easy for forensic search investigators to acquire (Table 5.3), and data would be relatively easy to process (Tables 5.4 and 5.5) and interpret (Table 5.6). The magnetic susceptibility equipment is not only easy to use and relatively cheap to acquire, but also, arguably, the simplest to use and to generate data, from which forensic search teams can interpret buried target locations. Datasets from the patio scenario were also very good, with low background variabilities. GPR data could be viewed in real-time and suspected burial positions marked during the field work. Resistivity data requires downloading, though 2D data profiles can be easily generated using a combination of numerical manipulation and graphical presentation software which are commercially available. The fluxgate gradiometer and magnetic (potassium-vapour) gradiometer should only be utilised by experienced operators due to the difficulty of calibration and operation.

5.5 Study limitations

5.5.1 False measurement of the buried target positions.

The probability of falsely recording a target's location in the first instance is considered negligible since these positions were measured using the tape measures which were also the markers for the survey grid. Between surveys, the start and end points of these survey lines were permanently marked with plastic pegs. During excavation, the originally-recorded target locations were confirmed.

5.5.2 Data collection error.

In the case of the particularly high-resolution surveys, some data collection points may be slightly displaced from survey lines, considering the relatively close proximity and small sample intervals, particularly for the alkali vapour magnetometer as the sample intervals were calculated based on a constant walking speed of the operator. However, considering that this technique provided a very limited number of anomalies, this potential source of error was considered insignificant. The operators were also required to maintain constant orientation of certain equipment configurations, for example: the fluxgate gradiometer required constant orientation with magnetic north and limited rotation movement of equipment. The grid orientation was designed to reduce the errors involved with this task by aligning survey lines north-south.

5.5.3 Equipment limitations

The survey equipment itself was not without its limitations. The bulk-resistivity equipment configurations, where the electrodes were separated by distances of 0.25 m and 0.50 m, give positional measurement errors of 0.125 m and 0.250 m, respectively. In the case of the 0.50 m probe separation, the equipment may therefore be influenced by the effects of targets in the two adjacent survey lines. This can result in a target-related anomaly in the data being displaced 0.25 m away from the target's true position and may therefore account for slight positional errors of anomalies locations (Fig. 5.13).

5.5.3 Data processing effects

All data were processed consistently throughout; using Microsoft Excel, GMT software and Reflex-W as illustrated. The data quality was generally very good and therefore resulting data plots did not suffer from any of the visible processing artefacts which have been reported by others, e.g. EM datasets in Dionne *et al.* (2011).

5.6 Conclusions

Using the available geophysical techniques in this investigation, the most successful detection rates for buried forensic targets in semi-urban environments were (in order of decreasing success); magnetic susceptibility, electrical resistivity (0.25 m fixed-offset probes), 900 MHz GPR and the metal detector (Fig. 5.19). Target detection success in patio environments (in order of decreasing success) were; magnetic susceptibility, magnetic gradiometry and both 450 and 900 MHz GPR (Fig. 5.19). Note that resistivity surveys were not utilised in the patio environment. It is worth noting that the magnetic susceptibility had a considerably higher success rate than the other magnetic equipment utilised, i.e. compared to the metal detector and the gradiometers, despite these techniques essentially measuring the same property of the subsurface. Differences in equipment configurations may be responsible for the differences in target detection success.

Concerns were raised over the sole use of metal detectors and GPR detection equipment for detection of buried forensic targets, as important objects such as knives and handguns in this study went undetected. It is therefore recommended that the easy-to-utilise and highly-successful magnetic susceptibility equipment should be used as a complementary tool by forensic investigators in the search for buried objects such as those used in this study. The bulk electrical resistivity technique also showed great potential due to its relatively quick acquisition time and reasonably high detection rate. Unlike GPR data processing, resistivity data processing is relatively straightforward (given available software and operator experience) and can be used to produce either 2D profiles or a map-view plot for interpretation.

Chapter 6 - Discussion

As outlined in Chapter 1, the aim of this study is to improve current forensic detection rates by investigating geophysical responses of common forensic near-surface targets using a number of geophysical techniques. In particular, GPR was used in all investigations as it has become the most common tool of choice for forensic geophysicist practitioners. Electrical resistivity techniques have also been used for comparison as previous studies (e.g. Jervis, 2011; Pringle and Jervis, 2009) have suggested its potential importance as an all-round successful tool in detecting buried forensic targets. This chapter has been organised to consider the overall effectiveness of each geophysical technique in the location of clandestine human burials, unmarked graves and non-human buried forensic targets respectively, which may provide vital evidence in a criminal or civil search.

A multi-technique approach is also considered; integrating results from different geophysical datasets, which may assist in the detection of buried targets. Other limitations on the effectiveness of each technique are also discussed, such as survey and equipment parameters, the site soil environment and the presence of non-target objects. Finally, after consideration of all the information gathered from the case studies and a review of relevant literature, a number of recommendations are made for forensic search practitioners to utilise such techniques in similar investigations.

6.1 GPR

As outlined in Chapter 2, GPR (Ground Penetrating Radar) has become the predominant tool in forensic and archaeological geophysics. This section is a discussion of the relative success of GPR in the detection of forensic targets in the context of the investigations detailed within Chapters 3, 4 and 5. In doing so, the effectiveness of survey parameters, data processing and visualisation, and finally the identification of artefacts in GPR data which pertain to physical properties of, and associated with, the targets of forensic searches are discussed.

6.1.1 2D GPR Profiles

The results of Chapter 3 suggest that both naked and wrapped cadavers are detectable for around 18 months after burial in 2D profiles for 110 – 900 MHz dominant frequency GPR (see Figs. 3.5-3.6). The buried cadavers produce a geophysical response in the form of a hyperbola of relatively high-amplitude compared to the background, with the apex indicating the approximate location of the top of the buried body. It is therefore possible to interpret the depth of the burial if the velocity of the electromagnetic pulse in the burial medium is known (see Chapters 2 & 3). Most GPR software will indicate the TWTT and/or an approximation of depth on a data display; otherwise this can be calculated using a CMP analysis or estimated if the burial medium is known. The lateral extent of the hyperbola is consistent with a distance which is slightly broader than that of the target cadaver, which is to be expected considering that the propagation of the EM pulse is not confined to the area directly beneath the antennae, but broadens with depth (see Chapter 2 for further information on theoretical background).

Beyond 18 months, a buried wrapped cadaver will continue to be detectable using 110 – 900 MHz dominant frequency antennae (see Figs. 3.7-3.8). This is presumably due to the relative preservation of the body and the material contrast of the wrapping media compared to the surrounding soil. However, any hyperbolae pertaining to a naked cadaver will be difficult to interpret from the background after 18 months. Presumably, the level of decomposition at this stage is such that decomposition fluids will attenuate the GPR signal. Additionally, the chest cavity of the cadaver, which had previously led to a high-amplitude hyperbolic response, would collapse and thus reduce the target size compared to when it not composed (see Fig. 3.1).

Lower dominant frequency (110 MHz and 225 MHz) GPR datasets were not only quicker to collect than the higher frequencies, but the data also produced less non-target hyperbolae of similar size to those pertaining to the target cadavers (*cf.* Figs. 3.5-3.8). This resulted in a more obvious hyperbola at the target location and would therefore, presumably, result in fewer false-positives during a forensic search. This is an important outcome as higher frequency antennae could improve target resolution but would result in more non-target anomalies, reduce penetration depths and take longer to acquire in the field, which comes with accompanying increased survey costs.

Potential unmarked and clandestine burials and their associated structures were identifiable in GPR 2D profiles due to a number of features. These include gaps in the otherwise uniform, horizontally-continuous radar reflectors which typify soil strata, indicating a disturbance to the soil, likely due to backfill of a burial plot (Conyers, 2006; Schultz *et al.*, 2006; Doolittle & Bellantoni, 2010). However, as has previously been noted, the soil in these burial environments were generally that of a very heterogeneous, *made ground*

nature, which meant that soil strata were not necessarily obvious in GPR 2D profiles. The most striking feature of burials were the hyperbolae produced by the burial contents – be it the so-called ‘coffin furniture’ in unmarked graveyard and cemetery burials or indeed the cadaver occupying the grave (Fig. 4.1). The appearance of these hyperbolae in 2D profiles varied which were also due to the burial style (Fig. 4.23). Very obvious hyperbola of high amplitude were observable in 225 MHz GPR profiles and were, most probably, due to a dense soil medium in contact with air in a grave. Other relatively strong reflectors were also observed from the tops of grave coffins/disturbed soil, coffin bases and brick-lined burial walls (where present), which were particularly prevalent in case study 1 (Fig. 6.1).

The strong contrast in EM properties of air and soil meant that burial vaults, in particular, which contain a large proportion of ‘empty space’, also produced very strong hyperbolae at both the top and bottom of the air gap (Fig. 6.1 and Fig.2.5). The presence of slabs, which separated vertically-stacked bodies, also produced a noticeable hyperbola due to the strong contrast between the air and the dense slab material (Fig. 6.1). Additionally, the surface of stone slabs were more resistant to degradation than wooden coffin material, as was evident from the open graves during archaeological investigations. This would mean that a smoother, generally broader surface at a right-angle of incidence to the GPR wave would reflect a higher proportion of energy by specular reflection back to the receiving antenna, and result in a high amplitude reflector (Milsom & Eriksen, 2011). Hyperbolae pertaining to coffins were less pronounced, presumably due to the smaller volume of this “air gap” and possible collapse of the weaker coffin material, as seen in some of the investigated graves. Unlike stone, wood can become waterlogged and, as discussed in Chapter 2, the main factors influencing the electric

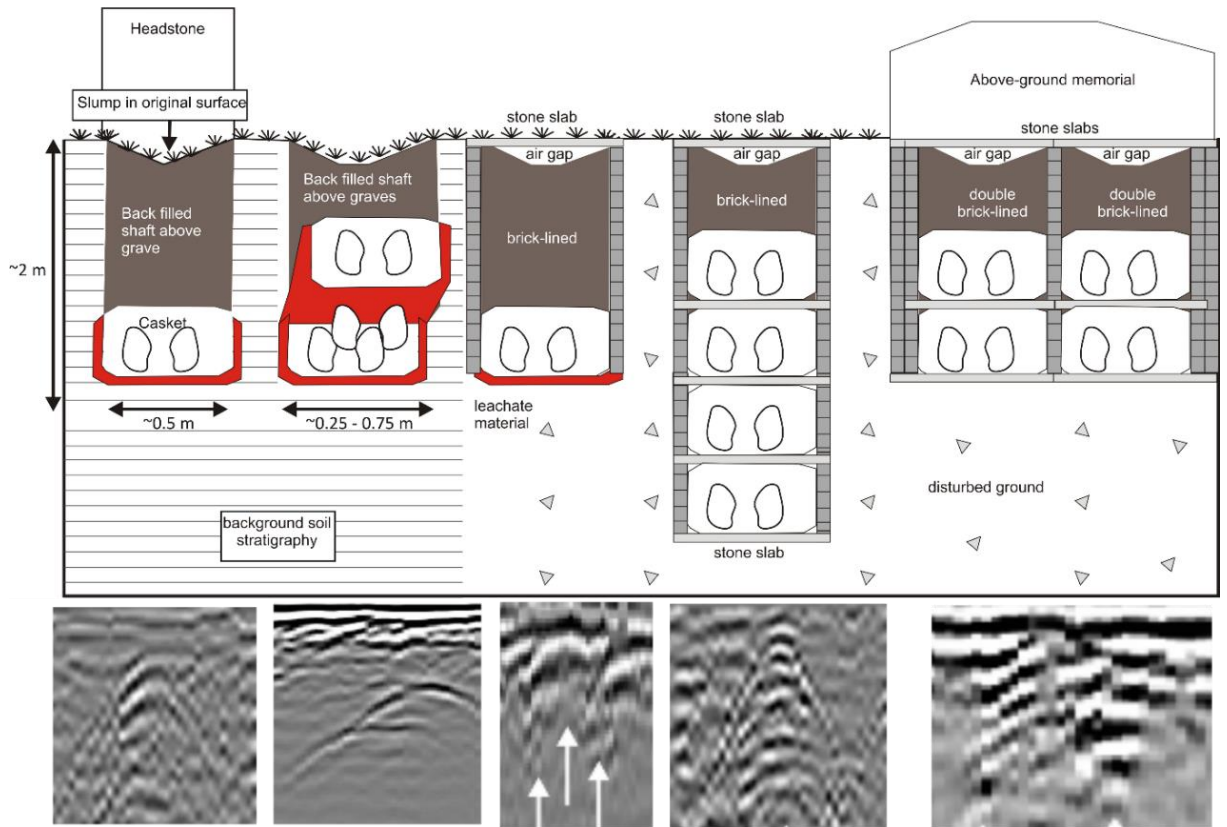


Figure 6.1. Generalised schematic of burial styles encountered in the three case studies discussed in Chapter 4 with geophysical features identified in 2D GPR profiles below. Modified from Hansen and Pringle (2011).

conductivity (σ) and electric permittivity (ϵ) of soil, and therefore the propagation of the EM GPR wave, are the fluid content and nature of this fluid (Cassidy, 2008). It would not be surprising that the contrast in physical properties between degraded, thin wooden material (note ‘coffin furniture’ and lining also varies in type, thickness and treatment) of coffins and surrounding soil are less pronounced than between a well preserved, thick stone slab and soil. Additionally, the surface of a degraded wooden coffin may produce a rough surface which would scatter a proportion of the GPR energy, reducing the amplitude of the wave reflected back to the receiving antenna (Milsom & Eriksen, 2011). Therefore, the amplitude of the reflected EM pulse from a coffin could be expected to be less identifiable in 2D profiles than from a vault.

As discovered in Chapter 5, and discussed in Chapter 2, the 900 MHz dominant frequency antennae were optimal for the detection of smaller forensic targets such as handguns. Using survey lines of 0.25 m spacing and a sampling interval of 0.025 m, it was possible to identify the majority of weapons. However, data acquisition and processing time were much longer than were required for the other techniques. The main advantages of GPR data, however, were the ability to estimate burial depth of targets and to view data in real time during acquisition.

6.1.2 GPR Timeslices

Conyers (2006) notes that GPR horizontal time-slices should be constructed from multiple 2D profiles with consideration for various site parameters, such as target depth and orientation, and the properties of the surrounding matrix in order to yield useful information. Additionally, the data processor should also have an awareness of the necessary processing steps either already undertaken or required in 2D profiles to optimise horizontal time slice data quality. In order to produce useful GPR time-slices, at least some 2D profiles should be firstly viewed in order to gain an insight into the subsurface conditions and signals which may correspond to target features (Conyers, 2006). Appropriate 2D profile data processing should then be applied in order to improve the quality of data prior to construction of horizontal time-slices.

In time-slices, radar amplitude is best plotted as an absolute value, i.e. assigned a colour/shade which is based on its deviation from a mean or zero, as opposed to its absolute numerical value. The advantage here is that hyperbolae, or other geophysical

signatures which relate to physical variations in the soil, are often characterised by a combination of alternating positive and negative amplitudes with depth. Any slight disparity in depth between two neighbouring survey lines, for example, due to surface topography or processing, could cause a feature which is laterally continuous in reality to become disguised by these alternating amplitudes in time-slices. 2D radar profiles should therefore be corrected for variations in surface topography prior to production of time-slices. This step should, ideally, have been applied early on in data processing, as traces which are offset by depth cause issues in later processing and the production of quality 2D profile data. Additionally, the method of data summation over the selected time period chosen for the creation of a time-slice can affect the quality of the data: one can choose to plot averages of trace amplitudes or an absolute summation of amplitudes over the selected time range, and in both cases this can be for actual amplitudes or those converted to an absolute, positive value which represents deviation from zero. Travel time can be used to interpret depth when the average velocity of the EM wave in the medium is calculated, be it from CMP data or analysis of hyperbolae using tools available in GPR software packages. Alternatively, a 3D cube of data can be produced, which can then be manipulated to view slices in a choice of planes and for bespoke distances/times.

When data are adequately processed, and time-slices are constructed for appropriate time-depth ranges and using an appropriate level of interpolation (since 2D profiles are not continuous in both the x and y horizontal planes), they can yield some very useful data about the physical structure of the subsurface. It then becomes possible to identify features of similar amplitude which are laterally continuous across multiple profiles and are concordant with one feature (e.g. Figs. 4.18-19). For improvement of data quality for time-slices, it was found that the use of a bandpass filter, background removal and gain function

were optimal. However, as can be interpreted from these requirements, construction of time-slices requires quite a significant amount of time and understanding about the required processing. As such, it is not a simple task, particularly for a novice, which may be an issue for search teams where time and access to specialists is limited.

However, when well-constructed, horizontal time-slices derived from 2D profiles can be used to identify the approximate location, dimensions and orientation of buried objects, and to identify those which match the approximate properties of a search target. Horizontal 2D data can also be compared with other horizontal geophysical data such as electrical resistivity, conductivity and magnetometry.

The forensic targets in these investigations (Chapters 3-5) appear in time-slices as relatively high amplitude regions, with respect to background media, which are slightly larger in lateral area than that of the targets themselves (Figs. 5.15 & 5.16). This is due to the combination of the breadth of the hyperbolae, interpolation of data between lines to produce a laterally continuous image from discrete survey lines and, in the case of cadavers, may also be an indication of the spread of decomposition fluids in the soil. The advantages of time-slice or 3D data cube presentation are that all survey lines can be simultaneously analysed for a given depth and that data can be superimposed onto a map of the survey area, thus allowing for high amplitude features to be compared to known or probable locations of non-target objects.

In Chapter 3, it was discovered that the wrapped pig cadaver was more obvious in time-slices than the naked pig due to the higher signal amplitude with respect to background and greater lateral extent of the high amplitude region. It is possible that the wrapping provided

a reflective surface which was not only smooth enough to allow specular reflection of a relatively large proportion of EM energy, but also provided a significant conductivity and permittivity contrast with the soil. Wrapped human remains may therefore be easier to locate than naked remains using GPR. After 18 months, when identification of cadavers in 2D profiles became difficult, time-slices became useful for delineating target-sized features in plan view.

In the graveyard studies (Chapter 4), the known positions of burials were identifiable in time-slices as high amplitude regions with respect to background, which had the approximate dimensions expected of a grave or vault. It was possible to identify the orientations of the burials in graveyards, which, interestingly, were not necessarily aligned in the expected directions with respect to the nearby church nor to the corresponding headstones or markers. A number of high amplitude regions of similar size, depth and orientation to known burials were identified in each case, which could respond to unmarked burials. It may be possible that several unmarked burials are a common occurrence in UK graveyards and cemeteries.

There can also be seasonal effects upon the quality of data, for example, datasets collected in winter (comparatively wetter) months, when compared to summer (comparatively dryer) months, generally showed a lower contrast in target amplitude when compared to background values. This was presumably due to the smaller contrast between the buried cadaver (and associated fluids) and that of the surrounding (wet) background soil.

Generation of time-slices was useful in the identification of metallic weapons and other targets in the study in Chapter 5. It was possible to pick out subtle features in lateral

expression of the targets which were not so obvious compared to the background, heterogeneous soil in 2D profiles. However, data acquisition and processing time were very time consuming, with detection rates being no better than for magnetic susceptibility data. Time-slices are not, however, a *photograph* of the subsurface at a particular depth, and the level of detail are determined by the resolution of the acquired data – a combination of the GPR frequency, spacing of acquisition points and their respective survey lines, and the processing steps undertaken.

The heterogeneity of the soil in the survey region should be a consideration when creating time-slices. The resulting horizontal time-slices may contain too many false positives to be of use and, perhaps, only 2D profiles should be used to identify potential target position(s) as the hyperbolae reveal more information about the nature of the reflector. 225 MHz and 450 MHz dominant frequency time-slices, though capable of resolving the pig cadavers and known graves, did contain a number of non-target anomalies, which could be an issue in true search investigations due to the large proportion of false-positives for a burial. Time-slices may instead be best used to identify possible target positions which could become the focus of 2D profile analysis.

6.2 Electrical Resistivity

In Chapter 4, a pole-pole array was used to record horizontal electrical resistivity variations in three UK graveyards. Electrode separations of 0.5 m and 1.0 m were trialled, though the 1.0 m separation data was unusable in one of the graveyards due to the over-range resistivities encountered. Where it was possible to use 1.0 m separation, however, this was found to be the optimal setup for detection of graves, which appeared as high

resistivity anomalies. As discussed in Chapter 2, high resistivities in soils are mostly influenced by a relatively low fluid content, which is to be expected due to the “voids” present in vaults and coffins. In Case Study 3, the presence of numerous animal burrows contributed to high resistivity anomalies in a large section of the survey area, which may have disguised a number of burials. However, it could also be inferred that the burrowing animal took advantage of the already-present burials, and could be used as a means of focussing an area of investigation for unmarked burials. An unforeseen outcome using electrical resistivity surveys was that a number of unmarked burials were located by the instrument electrodes themselves, encountering grassed-over horizontal stone slabs laid on top of the graves; particularly in Case Studies 2 and 3.

Plotting of map-view resistivity data was relatively simple using GMT software, and allowed interpretation of grave orientations and sizes. However, the data did not give any obvious indication of the depth of burials. Processing of data was useful for resistivity data, with removal of anomalously high resistivities and general background trends (*detrending*) proving optimal for improving data quality as it allowed subtle variations to be more easily identifiable.

For smaller forensic targets, such as buried knives or handguns, an electrode separation of 0.25 m was more favourable than 0.50 m, having a considerably higher success rate for target detection. A 0.25 m spacing of sample points was sufficient to resolve the majority of targets and data acquisition was relatively quick (30 mins for a 5 m × 5 m area).

The soil type and surface was influential on the success of resistivity surveys. Sandy loams and typical black-earth soils encountered allowed acquisition of useful resistivity data. In

Case Study 2, it was not possible to collect data over certain parts of the survey area due to the high contact resistance of the electrodes with coarse soil. Additionally, electrical resistivity data could not be acquired over the paved survey area using the available equipment due to the inability to insert the electrodes into the concrete covering.

6.3 Other trialled geophysical methods

Unsurprisingly, the magnetometry methods had some of the highest success rates in detecting the buried metallic targets. The metal detector, a routinely utilised tool by search teams, was not particularly successful in detecting the targets. Detection rates also decreased quite significantly when a ground covering of concrete was applied to the survey area. Data acquisition was, however, relatively quick (5 mins for a 5 m × 5 m area) and required no processing. The “results” were instantly useable and the equipment did produce a response at the handgun and knife locations suggesting that metal detectors may be useful for a rapid, preliminary search over a large area where little time or specialist equipment is available.

The magnetic susceptibility survey was the most successful technique in locating the buried targets of all techniques trialled. When data were plotted in plan-view, it was clear where the targets were located as magnetic susceptibility values at these locations deviated considerably from the background (Fig. 5.7). Even with the addition of the concrete patio covering, the detection rate was very good. Data acquisition time, however, was greater than using the metal detector, requiring 60 mins for acquisition of points at 0.25 m spacing, and further time was then required for plotting and visualisation of the data. However, simply constructing and visually analysing graphically-plotted individual data lines (Fig.

5.6) allowed relatively successful identification of target locations. Processing and plotting of data were no more complicated than for any of other technique used in this investigation, and equipment was relatively cheap and easy to use. Based on this study, where time is available, it would be recommended that magnetic susceptibility equipment be used in an investigation to find buried metallic targets, such as handguns or knives, in a police investigation.

Fluxgate gradiometry surveys were relatively quick to conduct (30 mins) even with a sample spacing of 0.25 m, but were not particularly successful in detecting targets, mainly due to a large proportion of the data being over range. Presumably this was due to the rather *magnetically-noisy* environment of the University campus study area. This should be a consideration for investigations in urban or semi-urban environments.

Potassium vapour gradiometry surveys were quite successful for identifying target locations using a vertical sensor separation of 1.0 m. Interestingly, target detection increased after the addition of the concrete patio covering, which may have had a dampening effect on the *magnetically-noisy* background soil environment. Data acquisition was relatively quick; around 20 mins, even with a very high sample resolution; 0.25 m survey line spacing and around 0.01 m sample interval. Despite this, the success of target detection was lower than for magnetic susceptibility equipment, which had a much lower sampling resolution. One issue often encountered with the potassium vapour gradiometry equipment was that the setup was rather difficult for the novice user, and may be difficult to navigate around uneven or overgrown topography. Data acquisition was also heavily reliant on keeping the sensors at constant height, which was physically rather strenuous

without a bespoke cart. Additionally, as with most of the other techniques used, data required processing and graphical presentation before it could be used.

6.4 Study limitations

A pervasive issue throughout all of the investigations in Chapters 3 – 5 has been the presence of anomalies or signals related to non-target features. Such anomalies can disguise signals relating to targets in the data or could simply produce a number of *false-positives* in an investigation. It is therefore important to consider how understanding of target properties and manipulation of the data through processing or the method of presentation could allow some features to be discounted as potential targets. For example, a number of strong hyperbolae were evident in the 2D GPR profiles in the graveyard investigations (Chapter 4), but not all appeared at a depth which would be expected for a grave. Time-slice generation also allowed visualisation of how a geophysical artefact appeared in map view, and considering the expected orientations, sizes and depths of burials, particular features could be identified as more likely to pertain to a burial than others.

Data resolution should also be an important consideration, whether implicit to the applied technique or in the choice of survey parameters. There are a wealth of recommendations available for the configuration and use of geophysical equipment by manufacturers and specialists based upon understandings of the theoretical limitations of techniques and results of investigations. It is important to consider whether, for example, reducing the sample spacing, thereby increasing the sampling resolution will actually make a difference to the quality of the data as there is often a trade-off between sampling resolution and

practical considerations such as acquisition time. This is particularly true of GPR, where doubling the sampling resolution tends to double the acquisition time. Instead, the survey parameters should take into account the implicit limitations of the method, based on the theory behind the technique, and considerations for the target properties. For example, for PulseEKKO 1000 GPR 225 MHz dominant frequency antennae of propagation velocity of approximately 0.07 m/ns in soil (acquired from on-site CMP analysis), the wavelength of the EM pulse is approximately 0.33 m. This equates to a maximum vertical resolution in data of around 0.08 m (see Chapter 2 for theory and PulseEKKO 1000 recommendations), which was certainly deemed adequate for detecting human burials. Sample time was also an important practical consideration during acquisition of GPR data. This refers to the time period for which the data-logger records the reflected wave and, as can be seen in the equation for EM wave velocity (Chapter 2 and Cassidy, 2009), is therefore related to the sampling depth. Calibration of the PulseEKKO 1000 equipment prior to surveying allowed a time-window to be set which would adequately record data for the expected depth region of burials, without collecting excess data from depth which would be: a) irrelevant to the investigation; and b) of poor quality due to the attenuation of the wave energy with depth.

Sampling resolution should be suitable for the implicit limitations of the technique (e.g. frequency of GPR) and sufficient to allow likely acquisition of at least one data point over the target. For buried human remains, it was discovered that for 225 MHz dominant frequency GPR antennae, a line spacing of 0.5 m and a sample spacing of 0.1 m were sufficient for sampling of burials. This was based upon the fact that the orientations of some burials were already known, allowing orientation of survey lines perpendicular to the burial orientation. However, it should be noted that in Case Study 1, there were two

prevalent grave orientations, which indicates that one survey orientation may not be optimal for all targets in an investigation.

In Chapter 2, the signal profiles for EM waves and equipotential lines of GPR and electrical resistivity are discussed. For the sake of consistency, GPR antennae were oriented with the transmitting antenna in front of the receiving antenna. For electrical resistivity surveys, pole-pole arrays were consistently used, the electrodes on the resistivity equipment were aligned perpendicular to the survey lines. However, different orientations of antennae or electrode arrays may have implications for the successes of each technique.

Deciduous trees were present in all three graveyard case studies and are common in UK graveyards (Litten, 1992). This created a two-fold problem: acquisition of data was made difficult due to the locations of trees and the uneven topography caused by roots at the ground surface; and buried and extensive root networks produced signals in GPR and resistivity data (Fig. 4.20) which other authors (e.g. Jones *et al.*, 2010) have attributed to reduced soil moisture content. In all cases, the topography of the survey areas were relatively flat and even, which required no additional manipulation of configurations or data.

Archaeological excavations in Case Studies 1 and 2 showed graveyard soils were surprisingly heterogeneous, showing significant re-use. This *made-ground* nature had a major effect on GPR and electrical resistivity surveys. For example, in Case Study 2 the relatively coarse site soil with pebbles resulted in resistivity surveys being partly unusable in delineating grave positions (Fig. 4.13). GPR survey data showed numerous hyperbolae

related to non-target features and soils were not the obvious, continuous strata which were expected in 2D profiles.

6.5 Integrated geophysical data

As discussed in Chapter 2, it has been noted by various authors that there is no single geophysical technique which can be utilised to locate any buried target. However, considering the varying successes of techniques, particularly observed in Chapter 5, a better approach may be to consider which *combination of techniques/configurations/processes* would be best applied to improve target detection. This would, of course, depend on a number of factors about the intended outcomes of the search, the target properties, the subsurface environment and the surface environment. Whether the goal of an investigation is to simply identify a target location or to gain particular information about, for example its depth, should be an important consideration in the choice of methodology. GPR data can offer a wealth of information about the subsurface, such as the relative dimensions and depths of physical objects and some information regarding relative material properties. However, the use of GPR can be limited by the soil environment, dominant frequency and configuration. It may, therefore, be useful to first acquire a rapid electrical resistivity dataset to identify areas of interest for focussing a higher frequency GPR survey for example. Datasets acquired using different techniques can also be compared to identify anomalous features which are common, and may therefore be of greater interest than those which are unique to one dataset.

This constitutes a rather qualitative approach, but future study may benefit from quantitative integration and comparison of datasets, which would form sufficient work for

a research topic in itself. The variety of mathematical and multi-physics modelling software available could mean that future searches benefit from prior construction of synthetic models of geophysical responses based on target and soil properties (see Millington *et al.*, 2011). This would allow investigators to assess the potential success of particular techniques and survey parameters, and to predict the geophysical responses of the target.

Chapter 7 – Conclusions

This thesis, along with a wealth of other data from numerous studies, can be used to guide search teams in their choice of geophysical techniques and configurations in a variety of forensic and archaeological investigations. However, there are far too many variables to be comprehensively assessed in this one research topic. Instead, it is hoped that some initial implications can be drawn from the data which could be considerations for future investigations of this type. The key implication is, despite a variety of geophysical responses from different burial styles, that it was possible to identify any of the burials using the techniques trialled. In graveyards, vaults were more obvious in the data than coffins. However, the preservation of wooden coffins and, indeed, of individuals contained within, were highly varied even within the same graveyard despite similar burial ages (Tables 4.4 and 4.5).

7.1 Key Outcomes

Due to the generally heterogeneous, clay-rich nature of UK soils, bulk-ground electrical resistivity surveys have the potential to be more successful in locating unmarked burials than GPR in certain sites. However, there are numerous considerations to be made in terms of the technique, configuration, survey parameters and processing of data with reference to the properties of the target, e.g.:

- dimensions,
- orientation,

- depth,
- soil type,
- surface topography,
- above- and below-ground survey environment (e.g. magnetic noise or obstacles to data acquisition),
- limitations of the equipment/technique (e.g. resolutions).

Such considerations should also inform the choice of GPR antennae, which also affects the choice of survey parameters. Low- to mid-frequency antennae (110 – 450 MHz) should resolve adult-sized, clandestine burials for three years after burial. Such data are relatively quick to acquire when compared to high frequency antennae, have greater penetration depths and result in fewer non-target anomalies. Although 900 MHz frequency antennae have the best resolution and were capable of delineating shallow graves, increased survey time, relative poor penetration depths and detection of numerous non-target anomalies could prove problematic for forensic searches.

GPR 2D profiles may be more useful to interpret target positions than time-slice data, but analysis of both datasets in combination could be more effective. Time-slices can be used to identify features of likely target depth, dimensions and orientation in order to set focus areas for analysis of 2D profiles and discount unlikely burials. A minimal amount of processing is recommended to improve data quality and reduce investigation time.

It is possible to interpret some information about the style of the burial (for example, grave or vault, naked or wrapped, the number of occupants, etc.) based upon the nature of the geophysical signal. High amplitude, hyperbolic reflectors approximately 1 m in breadth appear to signify burials. A single hyperbola of high amplitude tends to represent a simple, single burial (naked, wrapped or in a coffin). The higher amplitude features which have a greater vertical extent indicate stone-lined graves or vaults due to the presence of a pronounced *void* in the subsurface.

Bulk ground electrical resistivity was useful for identifying known positions of burials in graveyards, and data produced a number of discrete high-resistivity anomalies which appeared to represent the positions of unmarked burials. It would appear that a high resistivity anomaly could correspond to the *void* produced by an air-filled vault or coffin (see Chapter 2 for theory). Plan view resistivity data benefits from de-trending, which can prove valuable in reducing the effect of background variations in soil resistivity, and the method of visualisation of datasets to optimise identification of target-related features. The application of resistivity equipment was limited by the ground surface, and data was unusable in some areas due to the high contact resistance of coarse soil.

Magnetic susceptibility proved surprisingly optimal in the detection of near-surface metallic objects in both patio and non-patio environments. 900 MHz dominant frequency antennae could discern the majority of small forensic targets, but acquisition time was much greater.

In agreement with other authors in this field, there is no single effective technique for locating buried targets. The choice of technique and survey parameters should be selected after careful consideration for the target properties, soil type and environment, available survey time and access to equipment.

7.2 Recommendations for future research

7.2.1 Clandestine grave monitoring

It is recommended that monitoring of the control sites be continued using both GPR at different antennae frequencies and electrical resistivity surveys for comparison, in order to ascertain when geophysical surveys will no longer detect a clandestine burial. ‘Grave soil-water’ leachate should be collected and analysed for conductivity in order to determine when this reduces to background soil-water values (Pringle *et al.* 2015b), and ideally, its organic and inorganic constituents should be analysed to determine what is causing the variability.

The control clandestine burial study should be replicated in different depositional environments and soil types to determine the effect on the study results, which has begun to be undertaken in Colombia (Molina *et al.*, 2016). Ideally human cadavers should also be used rather than animal cadavers in future control experiments if possible, as these will be more realistic for clandestine burial research.

7.2.2 Graveyards

Known burials in graveyards and cemeteries should be surveyed so that the effect of variables concerning burial styles, contents, ages and soil environments on geophysical response can be investigated. Such research can contribute to the growing source of information which informs archaeological and forensic investigators of appropriate geophysical techniques for particular search scenarios. Geophysical surveys should also be undertaken with varying techniques (e.g. GPR, electrical resistivity and magnetics) and equipment configurations (e.g. changing resistivity electrode spacing and different radar frequency antennae) to determine optimal surveys. Initial magnetic susceptibility surveys have shown promise (Pringle *et al.*, 2015). Burial style may also be important and, if possible, it is suggested that other faith denomination burials be investigated. More investigations should be conducted where there are opportunities to *ground truth* the geophysical information.

7.2.2 Metals

Further control studies should be undertaken in order to quantify variables such as different patio constructions and varying target(s) depth below ground level to investigate the effectiveness of different techniques in such scenarios. The control studies should also be replicated in different depositional environments and soil types to determine what effect these variables have.

7.2.4 All surveys

Geophysical surveys over known target positions should be repeated using different survey and equipment parameters, for example, survey orientation and line spacings, electrical resistivity electrode spacings and varying GPR antennae frequencies in order to determine how these variations influence the success of a technique.

Numerical modelling and inversion of GPR and magnetic data should be undertaken in order to validate results as others have undertaken (e.g. Juerges *et al.*, 2010 and Millington *et al.*, 2011). Simultaneous inversion of both contemporaneous electrical resistivity and GPR datasets should be undertaken to discover whether these methods improves target detection from existing data.

References

- Acheroy, M. 2007. Mine action: status of sensor technology for close-in and remote detection of anti-personnel mines. *Near Surface Geophysics*, **5**, 43-56.
- Barker, R.D. 1989. Depth of investigation of collinear symmetrical four-electrode arrays. *Geophysical Prospecting*, **40**, 749-760.
- Bavusi, M., Rizzo, E. and Lapenna, V. 2006. Electromagnetic methods to characterize the Savoia di Lucania waste dump in southern Italy. *Environmental Geology*, **51**, 301-308.
- Bevan, B.W. 1991. The search for graves. *Geophysics*, **56**, 1310–1319.
- Bigman, D.P. 2012. The use of electromagnetic induction in locating graves and mapping cemeteries: an example from Native North America. *Archaeological Prospection*, **19**, 31-39.
- Billinger, M. S. 2009. Utilizing ground penetrating radar for the location of a potential human burial under concrete. *Canadian Society of Forensic Science Journal*, **42**, 200-209.
- Billings, S., Wright, D., 2010. Interpretation of high-resolution low-altitude helicopter magnetometer surveys over sites contaminated with unexploded ordinance. *Journal of Applied Geophysics*, **72**, 225–231.

Booth, A. and Pringle, J.K. 2016. Semblance analysis to assess GPR data from a five year study of simulated clandestine graves. *Journal of Applied Geophysics*, **125**, 37-44.

Brilis G.M., Gerlach C.L. and van Waasbergen R.J. 2000a. Remote sensing tools assist in environmental forensics. Part I. Digital tools—traditional methods. *Environmental Forensics*, **1**, 63–67.

Brilis G.M., van Waasbergen R.J., Stokely P.M. and Gerlach C.L. 2000b. Remote sensing tools assist in environmental forensics. Part II. Digital tools. *Environmental Forensics*, **1**, 1–7.

Buck, S.C. 2003. Searching for graves using geophysical technology: field tests with ground penetrating radar, magnetometry and electrical resistivity. *Journal of Forensic Sciences*, **48**, 5–11.

Buteux, S. and Cherrington, R. 2006. ‘The Excavations’, in: *St. Martin’s uncovered: investigations in the churchyard of St. Martin’s-in-the-Bull Ring, Birmingham* 2001. In: Brickley, M. and Buteux, S. (eds.), Oxbow Books, Oxford, UK, 24-89.

Butler, D.K., 2003. Implications of magnetic backgrounds for unexploded ordnance detection. *Journal of Applied Geophysics*, **54**, 111–125.

Calkin S.F., Allen R.P. and Harriman, M.P. 1995. Buried in the basement – geophysics role in a forensic investigation. *Proceedings of the symposium on the application of geophysics to engineering and environmental problems; Denver. Proceedings of the Environmental Engineers in Geophysics Society*, 397–403.

- Carter, D.O. and Tibbett, M. 2009. Cadaver decomposition and soil: processes. In: Tibbett, M. and Carter, D.O. (eds.) *Soil Analysis in Forensic Taphonomy: Chemical and Biological Effects of Buried Human Remains*. Boca Raton: CRC Press, 29–52.
- Cassidy, N.J., Eddies, R. and Dods, S. 2011. Void detection beneath reinforced concrete sections: The practical application of ground-penetrating radar and ultrasonic techniques. *Journal of Applied Geophysics*, **74**, 263–276.
- Cassidy, N.J. 2008. Processing, modelling and analysis. In: Jol, H. (Ed.), *Ground Penetrating Radar Theory and Applications*. Elsevier, 141–176.
- Chapman, P.J. 2005. Soil and the Environment. In: Holden, J. (Ed.) *An Introduction to Physical Geography and the Environment*. Pearson.
- Cheetham, P. 2005. Forensic geophysical survey. In: Hunter, J. and Cox, M. (Eds.) *Forensic Archaeology: Advances in Theory and Practice*, Abingdon: Routledge, 62–95.
- Clark, A.J. 1996. Seeing beneath the soil: prospecting methods in archaeology. 2nd Edition, Routledge Publishers, New York.
- Combrinck, M., 2001. Transient electromagnetic exploration techniques: can they be applied to the landmine discrimination problem? *African Earth Sciences*, **33**, 693–698.

Congram, D. R. 2008. A clandestine burial in Costa Rica: prospection and excavation. *Journal of Forensic Sciences*, **53**, 793-796.

Conyers, L.B. and Goodman, D. 1997. Ground-Penetrating Radar: an introduction for archaeologists.

Conyers, L.B. 2006. Ground penetrating radar techniques to discover and map historic graves. *Historical Archaeology*, **40**, 64–73.

Costello, S.B., Chapman, D.N., Rogers, C.D.F. and Metje, N. 2007. Underground asset location and condition assessment. *Tunnelling and Underground Space Technology*, **22**(5-6), 524-542.

Cox, M. and Hunter, J.R. 2005. *Forensic archaeology*. Taylor and Francis Publishers, London.

Cramp, R., Goodwin, J. and Davenport, A. 2010. *Archaeological Recording and Exhumation of Human Remains from St. James' Church, Newchapel, Staffordshire*. Stoke-on-Trent Archaeology Report **297**.

Curran, A. M., Prada, P. A. and Furton, K. G. 2010. Canine human scent identifications with post-blast debris collected from improvised explosive devices. *Forensic Science International*, **199**, 103-108.

Dabas M., Camerlynck C. and Camps P.F. 2000. Simultaneous use of electrostatic quadrupole and GPR in urban context: investigation of the basement of the Cathedral of Girona (Catalunya, Spain). *Geophysics*, **54**, 526-532.

Daniels, D.J. 2004. Ground penetrating radar. IEEE Radar, Sonar, Navigation and Avionics Series 15, 2nd edition, 723pp.

Davenport, G. C. 2001. Remote sensing applications in forensic investigations. *Historical Archaeology*, **35**, 87–100.

Davis, J.L., Heginbottom, J.A., Annan, A.P., Daniels, R.S., Berdal, B.P., Bergan, T., Duncan, K.E., Lewin, P.K., Oxford, J.S., Roberts, N. and Skehel, J.J. 2000. Ground penetrating radar surveys to locate 1918 Spanish flu victims in permafrost. *Journal of Forensic Sciences*, **45**, 68–76.

Davenport, G.C. 2001. Remote sensing applications in forensic investigations. *Historical Archaeology*, **35**, 87–100.

Davenport, G.C., Griffin, T.J., Lindemann, J.W. and Heimmer, D. 1990. Geoscientists and law enforcement officers work together in Colorado. *Geotimes*, **35**, 13–5.

Davis, J.L., Annan, A.P., 1989. Ground-penetrating radar for high-resolution mapping of soil and stratigraphy. *Geophysical Prospecting*, **37**, 531–551

Denton, J.H. 2005. The Taxatio Database. University of Sheffield. Available online at: <http://www.hrionline.ac.uk/taxatio/info>. Last date accessed: 14th July 2013.

Dionne, C. A., Schultz, J. J., Murdock II R. A and Smith, S. A. 2011. Detecting buried metallic weapons in a controlled setting using a conductivity meter. *Forensic Science International*, **208**, 18-24.

Doolittle, J. A. and Bellantoni, N. F. 2010. The search for graves with ground-penetrating radar in Connecticut. *Journal of Archaeological Science*, **37**, 941 – 949.

Dupras, T.L., Schultz, J.J., Wheeler, S.M. and Williams, L.J. 2006. Forensic recovery of human remains. CRC Press. 232pp.

Eberhardt, T.E. and Elliot, D.A. 2008. A preliminary investigation of insect colonisation and succession on remains in New Zealand. *Forensic Science International* **176**, 217–23.

Ellwood, B.B., Owsley, D.W., Ellwood, S.H. and Mercado-Allinger, P.A, 1994. Search for the grave of the hanged Texas gunfighter, William Preston Longley. *Historical Archaeology*, 28, 94–112.

Ellwood, B.B. 1990. Electrical resistivity surveys in two historical cemeteries in northeast Texas: a method for delineating unidentified burial shafts. *Historical Archaeology*, **24**, 91–98.

Environment Agency. 2004. Science project: potential groundwater pollutants from cemeteries. Available online: <http://publications.environment-agency.gov.uk/pdf/SCHO1204BIKS-e-e.pdf>. Last accessed 10th July 2013.

Fairclough, D. 2008. Proposed Extension: St. James' Church – Intrusive Report for Wormseye Ltd.

Fenning, P.J. and Donnelly, L.J. 2004. Geophysical techniques for forensic investigations. In: Pye, K., Croft, D.J. (eds), *Forensic Geoscience: Principles, Techniques and Applications*. Geological Society, London, Special Publications, **232**, 11-20.

Fiedler, S., Illich, B., Berger, J. and Graw, M. 2009. The effectiveness of ground-penetrating radar surveys in the location of unmarked burial sites in modern cemeteries. *Journal of Applied Geophysics*, **68**, 380–385.

France, D.L., Griffin, T.J., Swanburg, J.G., Lindemann, J.W., Davenport, G.C., Trammell, V., Travis, C.T., Kondratieff, B., Nelson, A., Castellano, K., Hopkins, D., Adair, T., 1997. Necrosearch revisited: further multidisciplinary approaches to the detection of clandestine graves. In: Haglund, W.D., Sorg, M.H., (Eds.), *Forensic taphonomy: the postmortem fate of human remains*, CRC Press, 497–509.

France, D.L., Griffin, T.J., Swanburg, J.G., Lindemann, J.W., Davenport, G.C., Trammell, V., Armbrust, C.T., Kondratieff, B., Nelson, A., Castellano, K., Hopkins, D., 1992. A multidisciplinary approach to the detection of clandestine graves. *Journal of Forensic Sciences*, **37**, 1445–1458.

Freeland, R.S., Miller, M.L., Yoder, R.E., Koppenjan, S.K. 2003. Forensic applications of FMCW and pulse radar. *Journal of Environmental Engineering in Geophysics*, **8**, 97–103.

Friedman, S.P. 2005. Soil properties influencing apparent electrical conductivity: a review. *Computers and Electronics in Agriculture*, **46**, 45-70.

Frohlich, B. and Lancaster, W.J. 1986. Electromagnetic surveying in current Middle Eastern archaeology – application and evaluation. *Geophysics*, **51**, 1414-1425.

Grant, I.S. and Phillips, W.R. 1990, Electromagnetism, 2nd Edition, Wiley.

Grant, F.S. and West, G.F. 1965. Interpretation theory in applied geophysics. McGraw-Hill Publishers.

Hammon, W.S. III, McMechan, G.A. and Zeng, X., 2000. Forensic GPR: finite-difference simulations of responses from buried human remains. *Journal of Applied Geophysics*, **115**, 191-204.

Hannam, J.A. and Dearing, J.A. 2008. Mapping soil magnetic properties in Bosnia and Herzegovina for landmine clearance operations. *Earth and Planetary Science Letters*, **274**, 285–294.

Hansen, J.D., Pringle, J.K. and Goodwin, J. 2014. GPR and bulk ground resistivity surveys in graveyards: locating unmarked burials in contrasting soil types, *Forensic Science International*, **237**, e14-e29.

Hansen, J.D. and Pringle, J.K. 2013. Comparison of magnetic, electrical and GPR surveys to detect buried forensic objects in semi-urban and domestic patio environments, in: Pirrie, D., Ruffell, A. and Dawson, L.A. (eds.), *Environmental and Criminal Geoforensics*, Geological Society of London Special Publication, **384**, 229-251.

Hansen, J.D. and Pringle, J.K. 2011. Geophysical investigations in UK graveyards: re-use of existing burial grounds. *Extended abstract for a presentation at the 16th European Meeting of Environmental and Engineering Geophysics of the Near Surface Geoscience Division of the EAGE, Leicester, 12th-14th September*.

Harrison M. and Donnelly L.J. 2009. Locating concealed homicide victims: developing the role of geoforensics. In: Ritz K., Dawson L. and Miller D. (eds.) *Criminal and Environmental Soil Forensics*, Springer Publishing, Dordrecht, The Netherlands, 197–219.

Hildebrand, J.A., Wiggins, S.M., Henkart, P.C. and Conyers, L.B. 2002. Comparison of seismic reflection and ground-penetrating radar imaging at the controlled archaeological test site, Champaign, Illinois. *Archaeological Prospection*, **9**, 9-21.

Holzer, T.L., Fletcher, J.B., Fuis, G.S., Ryberg, T., Brocher, T.M. and Dietel, C.M., 1996. Seismograms offer insight into Oklahoma City bombing. *Eos Transactions, American Geophysical Union*, **77**(393), 398–399.

Hunter, J. and Cox, M. 2005. Forensic archaeology: advances in theory and practice. Abingdon, Routledge Press.

Instanes, A., Lønne, A. and Sandaker, K. 2004. Location of avalanche victims with ground penetrating radar. *Cold Regions Science and Technology*, **38**, 55–61.

Jervis, J.R. and Pringle J.K. 2014. A study of the affect of seasonal climatic factors on the electrical resistivity response of three experimental graves, *Journal of Applied Geophysics*, **108**, 53-60.

Jervis, J.R. 2010. The detection of clandestine graves using electrical resistivity surveys: results from controlled experiments and a case study. Unpublished PhD dissertation, Keele University.

Jervis, J.R., Pringle, J.K. and Tuckwell, G.W. 2009a. Time-lapse resistivity surveys over simulated clandestine graves. *Forensic Science International*, **192**, 7–13.

Jervis, J.R., Pringle, J.K., Cassella, J.P. and Tuckwell, G.T. 2009b. Using soil and groundwater to understand resistivity surveys over a simulated clandestine grave. In: Ritz, K., Dawson, L. and Miller, D. (Eds.), *Criminal and Environmental Soil Forensics*, Dordrecht: Springer Press, 271-84.

Jim, K-H., Hall, M.L., Hart, A. and Pollard, S.J.T. 2008. A survey of green burial sites in England and Wales and an assessment of the feasibility of a groundwater vulnerability tool. *Environmental Technology*, **29**(1), 1-12.

Jol, H.M. 2009. Ground penetrating radar: theory and applications. *Elsevier Publications, Amsterdam, The Netherlands*, 524 pp.

Jones, G. 2008. Geophysical mapping of historical cemeteries. *Technical Briefs in Historical Archaeology*, **3**, 25-38.

Jones, G.M., Cassidy, N.J., Thomas, P.A., Plante, S. and Pringle, J.K. 2009. Imaging and Monitoring Tree-Induced Subsidence Using Electrical Resistivity Tomography. *Near Surface Geophysics*, **7**, 191-206.

Juerges A., Pringle J.K., Jervis J.R. and Masters P. 2010. Comparisons of magnetic and electrical resistivity surveys over simulated clandestine graves in contrasting burial environments. *Near Surface Geophysics*, **8**, 529-539.

Kalacska, M., Bell, L.S., Sanchez-Azofeifa, G.A. and Caelli, T. 2009. The application of remote sensing for detecting mass graves: an experimental animal case study from Costa Rica, *Journal of Forensic Sciences*, **54**, 159-166.

Kearey, P., Brooks, M. and Hill, I. 2002. An introduction to geophysical exploration. Blackwell Publishing.

Kelly 1921. *Directory of the County of Stafford*. London: Kelly's Directories Ltd.

Kenyon, J.L. 1977. Ground-penetrating radar and its application to a historical archaeological site. *Historical Archaeology*, **11**, 48–55.

Killam, E.W. 2004. *The Detection of Human Remains*. Charles C Thomas Publishers, Springfield, Illinois, USA. 268pp.

King, J.A., Bevan, B.W. and Hurry, R.J. 1993. The reliability of geophysical surveys at historic period cemeteries: an example from the Plains Cemetery, Mechanicsville, Maryland. *Historical Archaeology*, **27**, 4–16.

Koppenjan, S.K., Schultz, J.J., Ono, S. and Lee, H. 2003. The application of GPR in Florida for detecting forensic burials. Proceedings of SAGEEP Conference, San Antonio, TX, USA.

Koper, K. 2003. http://geology.about.com/od/seismo_forensics/a/kursk.htm Accessed: 25/01/2012/.

Koper, K.D., Wallace, T.C., Taylor, S.R. and Hartse, H.E. 2001. Forensic seismology and the sinking of the Kursk. *Eos Transactions, American Geophysical Union* **82**(37), 45–46.

Kvamme, K.L. 2000. Bozeman Cemetery Survey, University of Arkansas, UK.
[https://wayback.archive-
it.org/6471/20130302050120/http://www.cast.uark.edu/nadag/projects_database/Kvamme1
1/Kvamme11-r.htm](https://wayback.archive-it.org/6471/20130302050120/http://www.cast.uark.edu/nadag/projects_database/Kvamme11/Kvamme11-r.htm) Accessed: 4th March 2016.

Larson, D.O., Vass, A.A. and Wise, M. 2011. Advanced scientific methods and procedures in the forensic investigation of clandestine graves. *Journal of Contemporary Criminal Justices*, **27**, 149–182.

Lasseter, A., Jacobi, K.P., Farley, R. and Hensel, L. 2003. Cadaver dog and handler team capabilities in the recovery of buried human remains in the Southeastern United States. *Journal of Forensic Sciences*, **48**, 1–5.

Linford, N. 2004. Magnetic ghosts: Mineral magnetic measurements on Roman and Anglo-Saxon graves. *Archaeological Prospection*, **11**, 167–180.

Litten, J. 1992. The English way of death: the common funeral since 1450. Robert Hale Ltd., London.

Loke, M.H. and Barker, R.D. 1996. Rapid least-squares inversion of apparent resistivity pseudosections by a quasi-Newton method. *Geophysical Prospecting*, **44**, 131–52.

London Planning Advisory Committee, 1997, Planning for Burial Space in London : Policies for Sustainable Cemeteries in the New Millennium, London: LPAC, CBA, IBCA, Corporation of London.

Loke, M.H. and Barker, R.D. 1996. Rapid least-squares inversion of apparent resistivity pseudosections by a quasi-Newton method. *Geophysical Prospecting*, **44**, 131-152.

Lopera, O. and Milisavljević, N. 2007. Prediction of the effects of soil and target properties on the antipersonnel landmine detection performance of ground-penetrating radar: a Colombian study. *Journal of Applied Geophysics*, **63**, 13-23.

Lynam, J.T. 1970. Techniques of geophysical prospection as applied to near surface structure determination. Unpublished PhD dissertation, University of Bradford.

Manhein, M.H. 1996. Decomposition rates of deliberate burials: a case study of preservation. In: Haglund, W.D. and Sorg, M.H. (Eds.) *Forensic taphonomy: the post-mortem fate of human remains*, Boca Raton: CRC Press, 469–81.

Manrong, C., Lizhong, Y., Xiangfeng, N. and Bin, C. 2009. Application of environmental magnetism on crime detection in a highway traffic accident from Yangzhou to Guazhou, Jiansu Province, China. *Forensic Science International*, **187**, 29–33.

Marchetti, M. and Settini, A. 2011. Integrated geophysical measurements on a test site for detection of buried steel drums. *Annals of Geophysics*, **54**, 105–114.

Marchetti, M., Cafarella, L., Di Mauro, D. and Zirizzoti, A. 2002. Ground magnetometric surveys and integrated geophysical methods for solid buried waste detection: a case study. *Annals of Geophysics*, **45**, 563-573.

Matias, H.C., Monteiro Santos, F.A., Rodruiges Ferreira, F.E., Machado, C. and Luzio, R. 2006. Detection of graves using the micro-resistivity method. *Annals of Geophysics*, **49**, 1235–1244.

Meles G.A., Van der Kruk J., Greenhalgh S.A. Ernst J.R., Maurer H. and Green A.G. 2010. A new vector waveform inversion algorithm for simultaneous updating of conductivity and permittivity parameters from combination crosshole/borehole-to-surface GPR data. *Geoscience and Remote Sensing*, **48**, 3391-3407.

Mellet, J.S. 1992. Location of human remains with ground penetrating radar. In: Hanninen, P, Autio S, editors. *Proceedings of the Fourth International Conference on Ground Penetrating Radar, June 8-13; Rovaniemi, Geological Survey of Finland Special Paper 16*, 359–65.

Miller, M.L., Freeland, R.S. and Koppenjan, S.K., 2002. Searching for concealed human remains using GPR imaging of decomposition. Ninth International Conference on Ground Penetrating Radar, Santa Barbara, California, USA, April 30-May 2, 539-544.

Miller, P.S. 1996. Disturbance in the soil: finding buried bodies and other evidence using ground penetrating radar. *Journal of Forensic Sciences*, **41**, 648-652.

- Millington, T.M., Cassidy, N.J., Nuzzo, L., Crocco, L, Soldovieri, F. and Pringle, J.K. 2011. Interpreting complex, three-dimensional, near-surface GPR surveys: an integrated modelling and inversion approach. *Near Surface Geophysics*, **9**, 297-304.
- Milsom, J. and Eriksen, A. 2011. Field Geophysics. Geological Society of London Handbook, Milton Keynes, UK.: Open University Press, 4th edition, 304pp.
- Ministry of Justice 2006. Burial Law and Policy in the 21st Century: The Need for a Sensitive and Sustainable Approach. Available online:
https://www.gov.uk/government/uploads/system/uploads/attachment_data/file/162865/burial_grounds_web_whole_plus_bookmarks.pdf. Last accessed: 10th July 2013.
- Ministry of Justice. 2006. Burial law and policy in the 21st Century: The way forward. Government response to the consultation carried out by the Home Office/DCA.
<http://www.justice.gov.uk/publications/docs/burial-law-policy.pdf> Last Accessed: 27th August 2013.
- Molina, C.M., Pringle, J.K. Saumett, M., Hernandez, O, Evans, G.T. 2016. Geophysical monitoring of simulated graves with resistivity, magnetic susceptibility, conductivity and GPR in Colombia, South America. *Forensic Science International*, **261**, 106-115.
- Mualem, Y. and Friedman, S.P. 1991. Theoretical prediction of electrical conductivity in saturated and unsaturated soil. *Water Resources Research*, **27**, 2771-2777.

Munsch, M., Boulanger, D., Ulrich, P. and Bouiflane, M. 2007. Magnetic mapping for the detection and characterization of UXOs: use of multi-sensor fluxgate 3-axis magnetometers and methods of interpretation. *Journal of Applied Geophysics*, **61**, 168–183.

Murphy, J. and Cheetham, P. 2008. A comparative study into the effectiveness of geophysical techniques for the location of buried handguns. *Abstract for a presentation at the Geoscientific Equipment and Techniques at Crime Scenes*, Forensic Geoscience Group Conference, Geological Society of London, Burlington House, London, 17th December.

Murray, R.C. and Tedrow, J.C.F. 1975. Forensic geology: earth sciences and criminal investigation. Rutgers University Press, NJ, USA.

Nicholls Colton Geotechnical. A ground investigation for the Moser Centre Building, University of Keele. *Leicester: Nicholls Colton and Partners, 2005 Nov. Report No.: G06001-IR 2005.*

Nobes, D.C. 2007. Effect of soil grain size on the geophysical response of graves: clay vs silt vs sand. *Proceedings of the International Crime Science Conference (ISCS), 16-17 July, London, UK*, <http://hdl.handle.net/10092/2036> Accessed 2nd February 2012.

Nobes, D.C. 2000. The search for “Yvonne”: a case example of the delineation of a grave using near-surface geophysical methods. *Journal of Forensic Sciences*, **45**, 715–21.

- Nobes, D.C., 1999. Geophysical surveys of burial sites: a case study of the Oaro Urupa site. *Geophysics*, **64**, 357–367.
- Novo, A., Lorenzo, H., Ria, F. and Solla, M. 2011. 3D GPR in forensics: finding a clandestine grave in a mountainous environment. *Forensic Science International*, **204**, 134-8.
- Olhoeft, G.R. 1998. Electrical, magnetic and geometric properties that determine ground penetrating radar performance. Proceedings of the 78th International Conference on Ground Penetrating Radar (GPR'98), USA, 477-483.
- Owsley, D.W. 1995. Techniques for locating burials, with emphasis on the probe. *Journal of Forensic Sciences*, **40**, 735–740.
- Parker, R., Ruffell, A., Hughes, D. and Pringle, J. 2010. Geophysics and the search of freshwater bodies: a review. *Science and Justice*, **50**, 141-149.
- Pasion, L.R., Billings, S.D., Oldenburg, D.W. and Walker, S.E. 2007. Application of a library based method to time domain electromagnetic data for the identification of unexploded ordnance. *Journal of Applied Geophysics*, **61**, 279–291.
- Peel, M.C., Finlayson, B.L. and McMahon, T.A. 2007. Updated world map of the Köppen-Geiger climate classification. *Hydrological Earth Systems Science*, **11**, 1633–44.

Powell, K. 2004. Detecting human remains using near-surface geophysical instruments. *Exploration Geophysics*, **35**, 88–92.

Pringle, J.K., Wisniewski K., Giubertoni, M., Cassidy, N.J., Hansen, J.D., Linford, N.J. and Daniels, R.M. 2015. The use of magnetic susceptibility as a forensic search tool. *Forensic Science International*, **246**, 31-42.

Pringle, J.K., Cassella, J.P., Jervis, J.R., Williams, A., Cross, P., Cassidy, N.J., 2015b. Soilwater conductivity analysis to date and locate clandestine graves of homicide victims. *Journal of Forensic Sciences*, **60**, 1052-1060.

Pringle, J.K., Ruffell, A., Jervis, J.R. Donnelly, L., McKinley, J., Hansen, J., Morgan, R., Pirrie, D. and Harrison, M. 2012a. The use of geoscience methods for terrestrial forensic searches. *Earth Science Reviews*, **114**, 108-123.

Pringle, J.K., Jervis, J.R., Hansen, J.D., Cassidy, N.J., Jones, G.M and Cassella, J.P. 2012b. Geophysical monitoring of simulated clandestine graves using electrical and Ground Penetrating Radar methods: 0-3 years. *Journal of Forensic Sciences*, **57**, 1467-1486.

Pringle, J.K., Holland, C., Szkornik, K. and Harrison, M. 2012c. Establishing forensic search methodologies and geophysical surveying for the detection of clandestine graves in coastal beach environments. *Forensic Science International*, **219**, e29-e36.

Pringle, J.K., Cassella, J.P. and Jervis, J.R. 2010. Preliminary soilwater conductivity analysis to date clandestine burials of homicide victims. *Forensic Science International*, **198**, 126-133.

Pringle, J.K., Jervis, J., Cassella, J.P., Cassidy, N.J., 2008. Time-lapse geophysical investigations over a simulated urban clandestine grave. *Journal of Forensic Sciences*, **53**, 1405-17.

Pye, K. and Croft, D.J. 2004. Forensic Geoscience: Principles, Techniques and Applications. *Geology Society of London Special Publication*, **232**, 318pp.

Rebmann, A., David, E. and Sorg, M. H. 2000. *Cadaver dog handbook: forensic training and tactics for the recovery of human remains*. CRC Press, Florida, USA, 232 pp.

Redmayne, D.W. and Turbitt, T. 1990. Ground motion effects of the Lockerbie air crash impact. *Geophysical Journal International*. **101**, p.293.

Reynolds, J.M. 2011. An Introduction to Applied and Environmental Geophysics, 2nd review edition. *John Wiley and Sons*, 681pp.

Reynolds, J.M. 2004. Environmental geophysics investigations in urban areas. *First Break*, **22**, 63-69.

- Rezos, M. M., Schultz, J. J., Murdock II R.A. and Smith, S.A. 2010. Controlled research utilizing a basic all-metal detector in the search for buried firearms and miscellaneous weapons. *Forensic Science International*, **195**, 121-127.
- Rodriguez, W.C. 1997. Decomposition of buried and submerged bodies. In: Haglund, W.D. and Sorg, M.H. (Eds.), *Forensic Taphonomy: The Postmortem Fate of Human Remains*. Boca Raton: CRC Press, 459–68.
- Ruffell, A. and McAllister, S. 2015. A RAG system for the management forensic and archaeological searches of burial grounds. *International Journal of Archaeology*, **3**, 1-8.
- Ruffell, A. and McKinley, J. 2014. Forensic geomorphology, *Geomorphology*, **206**, 14-22.
- Ruffell, A., Pringle, J.K. and Forbes, S. 2014. Search protocols for hidden forensic objects beneath floors and within walls. *Forensic Science International*, **237**, 137-145.
- Ruffell, A., McCabe, A., Donnelly, C. and Sloan, B. 2009. Location and assessment of an historic (150–160 years old) mass grave using geographic and ground penetrating radar investigation, NW Ireland. *Journal of Forensic Sciences*, **54**, 382–394.
- Ruffell, A. 2010. Forensic pedology, forensic geology, forensic geoscience, geoforensics and soil forensics. *Forensic Science International*, **202**, 9-12.
- Ruffell, A. and Kulesa, B. 2009. Application of geophysical techniques in identifying illegally buried toxic waste. *Environmental Forensics*, **10**, 196-207.

Ruffell, A. and McKinley, J. 2008. *Geoforensics*. Wiley Publishers, Chichester, UK.

Ruffell, A. and McKinley, J. 2005. Forensic geoscience: applications of geology, geomorphology and geophysics to criminal investigations. *Earth Science Reviews*, **69**, 235–47.

Ruffell, A. 2005. Searching for the IRA “disappeared”: Ground Penetrating radar investigation of a churchyard burial site. *Journal of Forensic Sciences*, **50**, 1430-1435.

Rumble, J.H. 2010. Giving something back: a case study of woodland burial and human experience at Barton Glebe. Unpublished PhD Thesis, Durham University. Accessible online at: <http://etheses.dur.ac.uk/679/>. Last accessed: 10th July 2013.

Saey, T., Van Meirvenne, M., Dewilde, N., Wyffels, F., De Smedt, P., Meerschman, E., Islam, M.M. and Cockx, L. 2011. Combining multiple signals of an electromagnetic induction sensor to prospect land for metal objects. *Near Surface Geophysics*, **9**, 309–317.

Schultz, J.J. and Martin, M.M. 2012. Monitoring controlled graves representing common burial scenarios with ground penetrating radar, *Journal of Applied Geophysics*, **83**, 74–89.

Schultz, J.J. and Martin, M.M. 2011. Controlled GPR grave research: Comparison of reflection profiles between 500 and 250 MHz antennae. *Forensic Science International*, **209**, 64-69.

- Schultz, J.J. 2008. Sequential monitoring of burials containing small pig cadavers using ground-penetrating radar. *Journal of Forensic Sciences*, **53**, 279–287.
- Schultz, J. 2007. Using ground-penetrating radar to locate clandestine graves of homicide victims: forming forensic archaeology partnerships with law enforcement. *Homicide Studies*, **11**, 15-29.
- Schultz, J.J., Collins, M.E. and Falsetti, A.B. 2006. Sequential monitoring of burials containing large pig cadavers using ground-penetrating radar. *Journal of Forensic Sciences*, **51**, 607–616.
- Scott, J. and Hunter, J.R. 2004. Environmental influences on resistivity mapping for the location of clandestine graves. In: Pye, K. and Croft, D.J. (Eds.) *Forensic Geoscience: Principles, Techniques and Applications. Geological Society of London Special Publication*, **232**, 33–38.
- Smith, W.H.F. and Wessel, P. 1990. Gridding with continuous curvature splines in tension. *Geophysics*, **55**, 293–305.
- Speake, R. 1974. *The Old Road to Endon*. University of Keele: Department of Adult Education.
- Stanger, R. and Roe, D. 2007. Geophysical surveys at the West End Cemetery, Townsville: an application of three techniques. *Australian Archaeometry*, **65**, 44–50.

Stock, G. 1998. 'The 18th and early 19th century Quaker burial ground at Bathford, Bath and north-east Somerset', in Cox, M. (ed.), *Grave Concerns: Death and Burial in England 1700-1850*. York: Council for British Archaeology Research Report 113, 144-153.

Strongman, KB. 1992. Forensic applications of ground penetrating radar. In: Pilon, J. (Ed.) *Ground Penetrating Radar, Ottawa: Geological Survey of Canada Paper 90-4*, 203–211.

Sutherland, Z. 2012. *Archaeological Recording and Exhumation Project at St Luke's Church, Endon, Staffordshire NGR SJ 92812 53799*. Stoke-on-Trent Archaeology Service Report No. 344.

Taylor, G. 2002. A parish in perspective: a history of the church and parish of St. John of Jerusalem South Hackney.

Telford, W.M., Geldart, L.P. and Sheriff, R.E. 1990. Applied geophysics. Vol. 1. Cambridge University Press.

Theera-Umpon, N. 2004. Unexploded ordnance detection by measuring object symmetry via linear prediction. *IEEE Region 10 Conference proceedings*, 195-198.

Toms, C., Rogers, C. B. and Sathyavagiswaran, L. 2008. Investigations of homicides interred in concrete – The Los Angeles experience. *Journal of Forensic Sciences*, **53**, 203-207.

Tringham, N.J. 1996. Endon. In: Greenslade, M. W. (ed.) *A history of the county of Stafford: Leek and the Moorlands*. Oxford University Press: Institute of Historical Research, **7**, 176-186.

Unterberger, R.R. 1992. Ground penetrating radar finds disturbed earth over burials. EAGE Proceedings of the Fourth International Conference on Ground Penetrating Radar.

Vaughan, C. 1986. Ground penetrating radar surveys used in archaeological investigations. *Geophysics*, **51**, 595–604.

Vass, A.A., Bass, W.M., Wolt, J.D., Foss, J.E. and Ammons, J.T. 1992. Time since death determinations of human cadavers using soil solution. *Journal of Forensic Sciences*, **37**, 1236–1253.

Vaudelet, P., Schmutz, M., Pessel, M., Franceschi, M., Guérin, R., Atteia, O., Blondel, A., Ngomseu, C., Galaup, S., Rejiba, F. and Bégassat, P. 2011. Mapping of contaminant plumes with geoelectrical methods. A case study in urban context. *Journal of Applied Geophysics*, **75**, 738–751.

Watters, M. and Hunter, J.R. 2004. Geophysics and burials: field experience and software development. In: Pye, K., Crofts, D.J. (Eds.), *Forensic Geoscience: Principles, Techniques and Applications*. Geological Society of London Special Publication, **232**, pp. 21–31.

Wessel P. and Smith W.H.F. 1998. New, improved version of Generic Mapping Tools released. *Eos Transactions of the American Geophysical Union*, **79**, 579.

Witten, A., Brooks, R. and Fenner, T. 2001. The Tulsa Race Riot of 1921: a geophysical study to locate a mass grave. *Leading Edge*, **20**, 655–660.

Wright, R., Hanson, I. and Sterenberg, J. 2005. The archaeology of mass graves. In: Hunter J. and Cox, M (Eds). *Forensic archaeology: advances in theory and practice*. Oxon: Routledge Publishers, 137-158.

Zhang, Q., Al-Nuaimy, W. and Huang, Y. 2007. Interpretation of borehole magnetometer data for the detection and characterisation of unexploded bombs. *Journal of Applied Geophysics*, **61**, 206–216.

Appendices

1. Pringle, J.K., Ruffell, A., Jervis, J.R. Donnelly, L., McKinley, J., **Hansen, J.**, Morgan, R., Pirrie, D. and Harrison, M. 2012. The use of geoscience methods for terrestrial forensic searches. *Earth Science Reviews*, **114**(1-2), 108-123.
<http://dx.doi.org/10.1016/j.earscirev.2012.05.006>
2. Pringle, J.K., Jervis, J.R., **Hansen, J.D.**, Cassidy, N.J., Jones, G.M. and Cassella, J.P. 2012. Geophysical monitoring of simulated clandestine graves using electrical and Ground Penetrating Radar methods: 0-3 years. *Journal of Forensic Sciences*, **57**(6), 1467-1486.
<http://onlinelibrary.wiley.com/doi/10.1111/jfo.2012.57.issue-6/issuetoc>
3. **Hansen, J.D.** and Pringle, J.K. 2011. Geophysical investigations in UK graveyards: re-use of existing burial grounds. *Extended abstract for a presentation at the 16th European Meeting of Environmental & Engineering Geophysics of the Near Surface Geoscience Division of the EAGE, Leicester, 12th-14th September*.
4. **Hansen, J.D.** and Pringle, J.K. 2013. Comparison of magnetic, electrical and GPR surveys to detect buried forensic objects in semi-urban and domestic patio environments. Pirrie, D., Ruffell, A. & Dawson, L.A. (eds.), *Environmental & Criminal Geoforensics, Geological Society of London Special Publication*, **384**, 229-251. doi:10.1144/SP384.13
5. **Hansen, J.D.**, Pringle, J.K. and Goodwin, J. 2014. GPR and bulk ground resistivity surveys in graveyards: locating unmarked burials in contrasting soil types. *Forensic Science International*, 237, e14-e29.
<http://dx.doi.org/10/1016/j.forsciint.2014.01.009>